

A DIRECT MEASUREMENT OF THE RELATIVISTIC EFFECT OF THE  
GRAVITATION POTENTIAL ON THE RATES OF ATOMIC CLOCKS  
FLOWN IN AN AIRCRAFT

by  
Ralph Emerson Williams

PP# 76-233

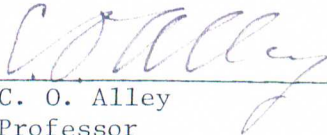
Dissertation submitted to the Faculty of the Graduate School  
of the University of Maryland in partial fulfillment  
of the requirements for the degree of  
Doctor of Philosophy  
1976

Cap. 1  
(Cap. 2 EPSL)

APPROVAL SHEET

Title of Thesis: A Direct Measurement of the Relativistic Effect of  
the Gravitational Potential on the Rates of Atomic  
Clocks Flown in an Aircraft

Name of Candidate: Ralph Emerson Williams  
Doctor of Philosophy, 1976

Thesis and Abstract Approved:   
C. O. Alley  
Professor  
Department of Physics and Astronomy

Date Approved: April 29, 1976

## ABSTRACT

Title of Thesis: A Direct Measurement of the Relativistic Effect of the Gravitational Potential on the Rates of Atomic Clocks Flown in an Aircraft

Ralph Emerson Williams, Doctor of Philosophy, 1976

Thesis directed by: C. O. Alley  
Professor  
Department of Physics and Astronomy

General relativity predicts that standard clocks placed at differing gravitational potentials will run at different rates. Although experiments confirming the gravitational redshift have been done, they involve frequency and not time, and need not appeal to general relativity for explanation. Therefore, considerable interest exists as to the result of an accurate experiment in which real macroscopic clocks are brought together for comparison before and after separation to differing potentials.

This experiment consists of flying an ensemble of atomic clocks in a military aircraft and comparing them before and after flight to another clock ensemble remaining on the ground. The ground ensemble included several Hewlett-Packard Cesium Beam clocks, three Efratom optically pumped Rubidium clocks, and two hydrogen masers. The flying ensemble included at least three Hewlett-Packard Cesium clocks and three Efratom Rubidium clocks. Five of the Cesium clocks were new models delivered with a high beam current option resulting in higher stability than standard models. The clocks were maintained under stringent environmental

controls to protect against vibration, magnetic fields, and changes in temperature, pressure, and power supply voltage.

Five main flights were made, each at approximately 30,000 feet altitude for fifteen hours. The aircraft was continuously tracked by a theodolite calibrated radar which obtained position and velocity measurements for every second of flight. This allowed an accurate calculation of a theoretical prediction to compare to experiment.

The flying clocks gained approximately 45 nanoseconds ( $45 \times 10^{-9}$  s) with respect to the ground clocks. The normalized results (measured effect divided by predicted effect) and the experimental standard deviations of the mean for each of the five flights were as follows:

$.999 \pm .016$     $.977 \pm .026$     $.963 \pm .013$     $1.002 \pm .026$     $.991 \pm .037$  .

The result for the entire experiment, with standard deviation of the mean, was  $.987 \pm .011$ . The statistically expected standard deviation of the mean based on knowledge of clock quality was approximately .015. Considering this result as well as systematic errors, a final result is established of

$$\frac{\text{Measured value}}{\text{Predicted value}} = 0.987 \pm .016 \quad .$$

## PREFACE

Absolute, true, and mathematical time, of itself, and from its own nature, flows equably without relation to anything external . . .

(Isaac Newton, Principia)

A priori it is not at all necessary that the "times" ... in different inertial frames agree with one another. One would have realized this long ago if, in the practical experience of everyday life, light did not appear (because of its high speed) as a means for the determination of absolute simultaneity.

(Albert Einstein, "Autobiographical Notes")

And time, that takes survey of all the world . . .

(Shakespeare, Henry IV, Part I)

Time Discovers Truth.

(Lucius Seneca, Moral Essays, first century A.D.)

## ACKNOWLEDGEMENTS

It should be noted that the entire experiment of which this thesis is a part was of extensive complexity with relatively few people to carry the load. Many of us consistently worked well over fifteen hours a day and were away from home with few respites for months on end. I would therefore be remiss if I neglected to list those people with whom I shared those months:

Dr. C. O. Alley - my thesis advisor, who conceived the experiment, obtained continuing funding, and was principal investigator.

Robert Reisse - my fellow graduate student who is obtaining a thesis on another aspect of the experiment.

Stephen Davis	}	- other staff members of the Quantum Electronics Group of the Department of Physics and Astronomy of the University of Maryland.
John Mullendore		
John Rayner		
Charles Steggerda		

Robert Merritts - our liaison man at the Patuxent Naval Air Test Center who was stuck with us night and day for over nine months costing him much of his spare time.

Dr. Leonard Cutler - Director of the Physics Laboratory of Hewlett-Packard. He was the original designer of the HP Cesium clocks and worked long and hard in those periods he spent with us.

I would like to list a few of the other persons who, although not as continually involved as those above, nevertheless aided the development and success of the experiment:

Dr. Gernot Winkler - Director of the Time Service Division of the U.S. Naval Observatory. He lent us most of our clocks and provided moral and political support.

Don Kaufman and Joe Soucy - of NASA Goddard Space Flight Center. They came down many times to look after the hydrogen masers lent to us.

Ron Hyatt , Joe Bourdet, Richard Lacy, Chuck Little - of Hewlett-Packard who aided in the cesium clock preparations.

The many other people, too numerous to mention, at Patuxent Naval Air Test Center who gave much of their time, often at odd hours. Harold Lowry of the tracking facility is especially thanked.

Many members of the University of Maryland Physics and Astronomy faculty, electronics shop, and main shop. Dr. Jean-Paul Richard aided with several suggestions early in the program.

Ernst Jechart - of Efratom, who lent us some of our Rubidium clocks.

My wife and the wives of those above, who probably suffered as much as we.

## TABLE OF CONTENTS

Chapter	Page
PREFACE.....	ii
ACKNOWLEDGEMENTS.....	iii
I.    INTRODUCTION.....	1
II.   CLOCKS, PACKAGING, AND ENVIRONMENTAL CONTROLS.....	11
A.   The Clocks.....	11
B.   The Cesium Clock Box.....	16
C.   The Rubidium Clock Box.....	22
D.   Other Clock Box Features.....	23
III.  DATA ACQUISITION.....	26
A.   General.....	26
B.   The Event Timer.....	26
C.   The Digital Phase Measurement.....	28
D.   The Analog Data.....	29
IV.  SOFTWARE CAPABILITY AND DATA MANIPULATION.....	32
A.   The Raw Data Files.....	32
B.   The Translated Data Files.....	33
C.   Data Plots and the Graphics Terminal.....	35
D.   Manipulation and Analysis Programs.....	37
V.   THEORY AND THE PREDICTION OF THE EFFECT.....	42
A.   The General Relativistic Effect.....	42
B.   Prediction of the Effect.....	43
C.   Range Data Accuracy.....	46



Chapter	Page
VI. STATISTICS.....	50
A. Preliminary Concepts.....	50
B. Computation of Variances.....	51
C. Projection of Phase.....	54
D. Combinations of Measurements.....	57
VII. RESULTS AND INTERPRETATIONS.....	62
A. Introduction.....	62
B. The Principal Results.....	63
C. The Other Clocks.....	66
APPENDIX A. CIRCUIT DIAGRAMS.....	83
APPENDIX B. ENVIRONMENTAL COEFFICIENTS OF THE CLOCKS.....	94
APPENDIX C. A THEOREM FOR CALCULATING VARIANCES.....	98
APPENDIX D. DATA PLOTS FOR THE FIVE FLIGHTS.....	100
APPENDIX E. LISTING OF VARIOUS PROGRAMS.....	156
BIBLIOGRAPHY.....	172

LIST OF FIGURES

Figure	Page
1. P3-C aircraft in flight.....	6
2. Pre and post flight configuration with the aircraft near the equipment trailer.....	6
3. Clock box with lid removed.....	7
4. The clock box lid.....	7
5. The Rubidium clock box.....	8
6. The clock box in position in the aircraft.....	8
7. Floor plan of the P3-C aircraft showing the equipment location.	9
8. Map showing the flight path of the aircraft.....	10
9. Schematic diagram of the clock box.....	24
10. Block diagram of the clock box.....	25
11. Signal switching diagram.....	31
12. An example of the program PHASEPLOT.....	38
13. An example of the program SRESIDUALS.....	39
14. An example of the program RESIDUALS.....	40
15. An example of the program SIGMATAU.....	41
16. The relation of range coordinates to inertial system coordinates	49
17. Sigma-tau plot for the principal Cesium clocks.....	59
18. Sigma-tau plot for the Rubidium clocks and H-maser.....	60
19. Typical form of phase data.....	61
20. Typical form of phase data over a flight.....	61
21. Typical form of phase data with slope removed.....	61

Figure	Page
22. Graph of the theoretical prediction for flight 1 (9/29).....	69
23. Graph of the theoretical prediction for flight 2 (11/11).....	70
24. Graph of the theoretical prediction for flight 3 (11/14).....	71
25. Graph of the theoretical prediction for flight 4 (11/22).....	72
26. Graph of the theoretical prediction for flight 5 (1/10).....	73
27. Summary sheet for flight 1.....	74
28. Summary sheet for flight 2.....	75
29. Summary sheet for flight 3.....	76
30. Summary sheet for flight 4.....	77
31. Summary sheet for flight 5.....	78
32. The fifteen principal measurements.....	79
33. A histogram of flying clock and ground clock shifts.....	80
34. Results using the Rubidium clocks and the travelling Cesium clocks.....	81
35. Phase Plot of "synthetic clocks" generated by a computer program.....	82

## CHAPTER I

### INTRODUCTION

One prediction of the general theory of relativity as formulated by A. Einstein is that clocks placed at different gravitational potentials will run at different rates.<sup>1</sup> A clock placed at a high altitude in a gravitational potential is predicted to run faster than a clock at a lesser altitude. Experimental efforts to confirm this prediction have principally involved red-shifted photons (the "gravitational red shift").<sup>2-13</sup> Such results are to some extent unsatisfying as they may be explained by energy conservation without appealing to general relativity (although the existence of a gravitational red shift does imply spacetime is curved).<sup>14</sup> Hence an experiment using real macroscopic clocks which are compared "side-by-side" before and after separation to differing potentials is of some interest. Considerations of such effects on real clocks in earth orbit have been considered for some time.<sup>15-18</sup> However, it is only recently that the quality of atomic clocks has made accurate aircraft experiments feasible. In fact, confirmation of this effect is now of more than theoretical interest as the increasing need for precision in navigational and time-transfer applications requires inclusion of such relativistic effects.

To this date the only previous effort at such an experiment ( using macroscopic clocks) is the "around the world" experiment of Hafele and Keating<sup>19</sup> in which a set of four Cesium beam atomic clocks was flown around the world in both directions using regularly scheduled commercial

airliners. A qualitative confirmation of the gravitational effect was obtained. The experiment described here aspires to high accuracy and credibility through improved clocks, multiple flights, stringent environmental controls, and accurate tracking of the military aircraft involved.

The experiment consisted of flying an ensemble of atomic clocks in an aircraft. Before and after flight the clocks in this ensemble were compared to clocks in a ground ensemble. (Time transfer between plane and ground was made during flight using a short pulse laser. Since this aspect of the experiment is not part of this thesis it will not be pursued here. The reader is referred to the thesis of Bob Reisse).<sup>20</sup> The remainder of this chapter consists of a very general overview of the experiment. Details will be considered later in the appropriate chapter.

The experiment was performed at the Naval Air Test Center (NATC) at Lexington Park, Maryland which is about seventy-five miles south of Washington, D.C. The aircraft made available for the experiment was a U.S. Navy P3-C Orion (figure 1). This type of aircraft is normally used in anti-submarine warfare. This specific aircraft (number 158912) is one of two P3's used for final evaluation of equipment before dispersal to the fleet. Before and after flight the P3 was parked adjacent to a large trailer on loan from the Goddard Space Flight Center, Greenbelt, Maryland. Figure 2 shows the plane, the ground trailer, and the hanger in which some lab and desk space was made available to us. The ground trailer contained much of the ground instrumentation.

Two environmental chambers, or "clock boxes", were constructed to each hold six atomic clocks. Three of these six were Hewlett-Packard Cesium Beam atomic clocks located in the main body of each clock box. The other three were optically pumped Rubidium atomic clocks contained

in a much smaller chamber attached to the lid of the main clock box. The two clock boxes were mounted on a vibration isolating system and protected the clocks from magnetic fields and changes in temperature, pressure, and power supply voltage. For each flight one box was placed in the aircraft and the other in the ground trailer. Between some flights the boxes were interchanged to aid in suppressing systematic errors. Other clocks were also associated with the experiment. Two hydrogen masers on loan from the Goddard Space Flight Center were also housed in the ground trailer. One more Hewlett-Packard Cesium clock of high quality was in the ground ensemble. Other HP Cesium clocks were usually included on the aircraft for a flight. However these units were not in environmental chambers and were not of the high quality of those Cesium clocks mentioned above. The principal Cesium clocks were obtained with a high beam current option and further modified for this experiment. This resulted in performance superior to standard Cesium clocks.

Data gathering and storage were controlled by two Data General Nova 2 minicomputers, one of which was placed in the aircraft (with associated electronics) and the other was placed in the ground trailer. Data was taken by each computer every 204 seconds before, during, and after flight. Part of this data consisted of environmental parameters (temperatures and pressures). The other part consisted of phase measurements of all clocks with respect to one clock chosen as reference. The reference clock for the ground computer was one of the ground set and the reference clock for the air computer was one of the air set. Phase measurements were made with a resolution of  $\pm 0.1$  nanosecond.

As each clock box weighed approximately 1200 pounds a part of the aircraft floor was modified to take the weight of the clock box

and two racks of equipment. The total weight was about 2000 pounds. The equipment was located on the right side of the aircraft, aft of the wing, and near the door (figure 7). Before and after flight numerous cables extended from the ground trailer into the aircraft to allow each computer system to measure all clocks available. Of course, during the actual flight these wires were removed and the ground (air) computer system measured phases of only the ground (air) clocks. This inter-comparison of clocks during flight enables a determination of which clocks, if any, changed rates during flight. Both the Cesium and Rubidium clocks are known to make small random changes in rate from time to time. Doubly shielded coaxial cable was used to carry the 5 Mhz signals whose phases were measured.

Initially there were numerous short duration test flights. Five major flights followed from September, 1975 through January, 1976. Each flight was approximately fifteen hours long with speed and altitude averaging about 250 knots and 30,000 feet respectively. The pilots were instructed to fly and make turns slowly and smoothly. The flight parameters were such that the gravitational effect was expected to be about 50 ns and the velocity effect (of opposite sign) was expected to be about -5 ns. Hence the flying clocks were expected to show a net gain of about 45 ns with respect to the ground clocks. The aircraft was purposely flown slowly to minimize the velocity effect contribution.

The aircraft was flown in a racetrack pattern inside an area restricted to military aircraft. Figure 8 shows this pattern as well as the location of the radar and theodolite stations used to track the aircraft. These were the facilities of the Chesapeake Test Range of the Naval Air Test Center. The theodolite calibrated radar data contained

position and velocity measurements for each second of flight. This data allowed the calculation of a predicted value to be compared to experiment.

The aircraft was restricted to gentle turns to keep Coriolis forces on the cesium beams in the cesium clocks to an acceptable level.





Fig. 1. P3-C aircraft in flight.

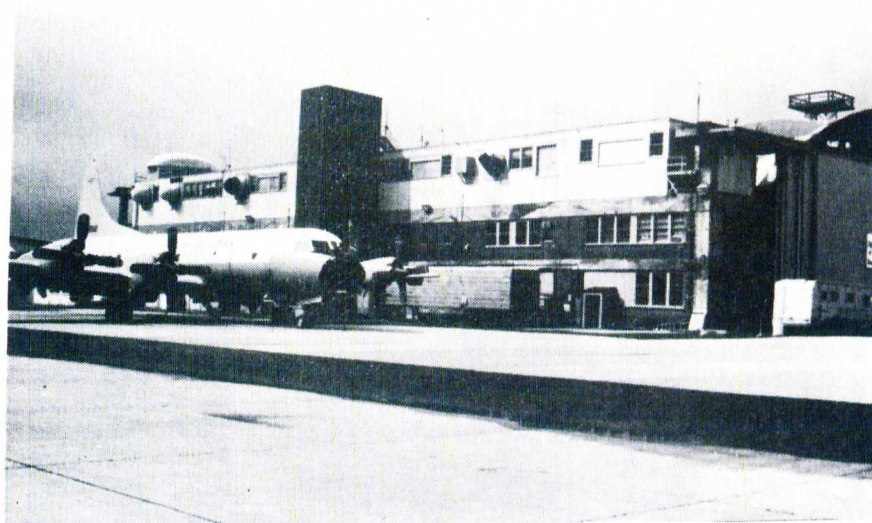


Fig. 2. Pre and post flight configuration with the aircraft near the equipment trailer.

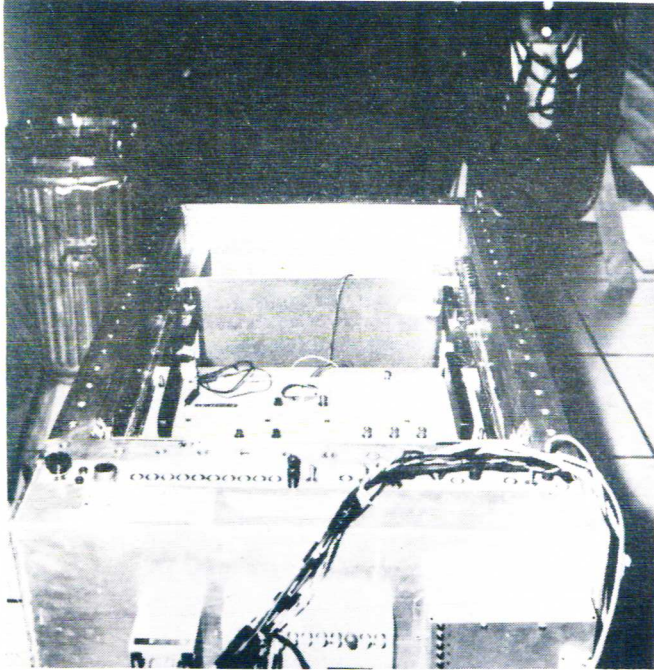


Fig. 3. Clock box with lid removed. A Cesium clock is in place in the first slot. The magnetic shield can lids have been removed.

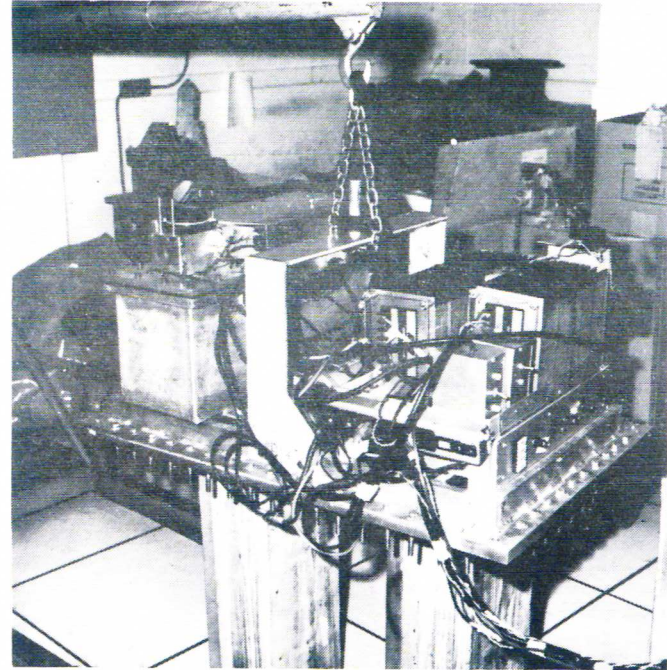


Fig. 4. The clock box lid. The smaller Rubidium clock box is placed at the left end of the lid.

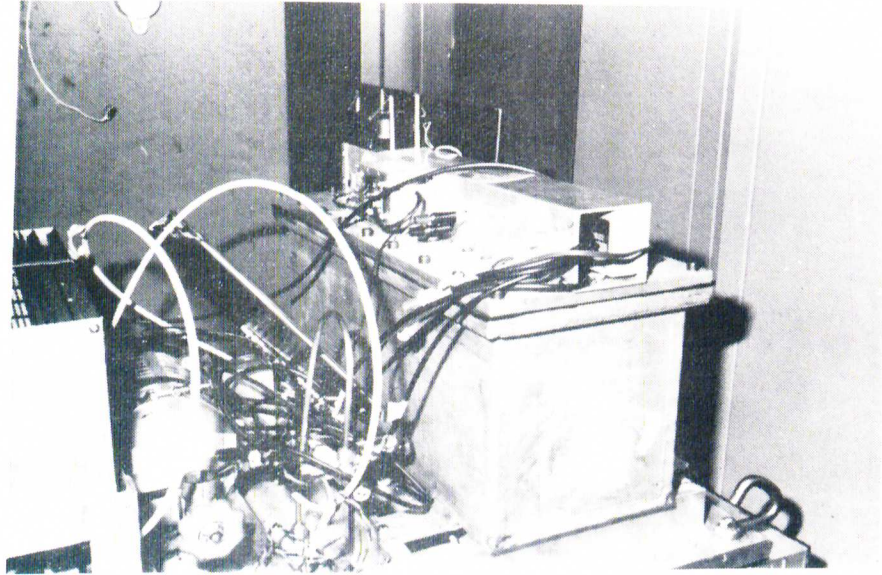


Fig. 5. The Rubidium clock box (some equipment removed for clarity).

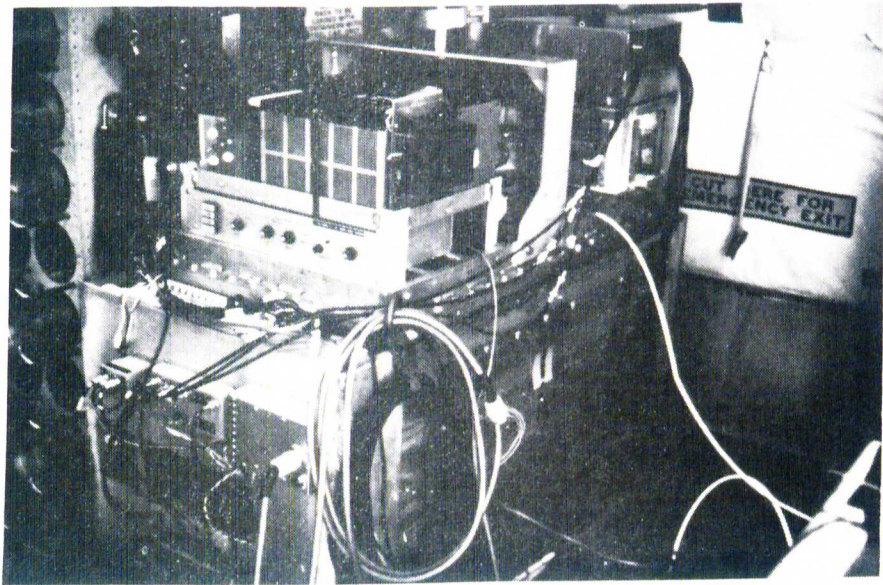


Fig. 6. The clock box in position in the aircraft. The computer rack which is normally to the right of the box has been removed.

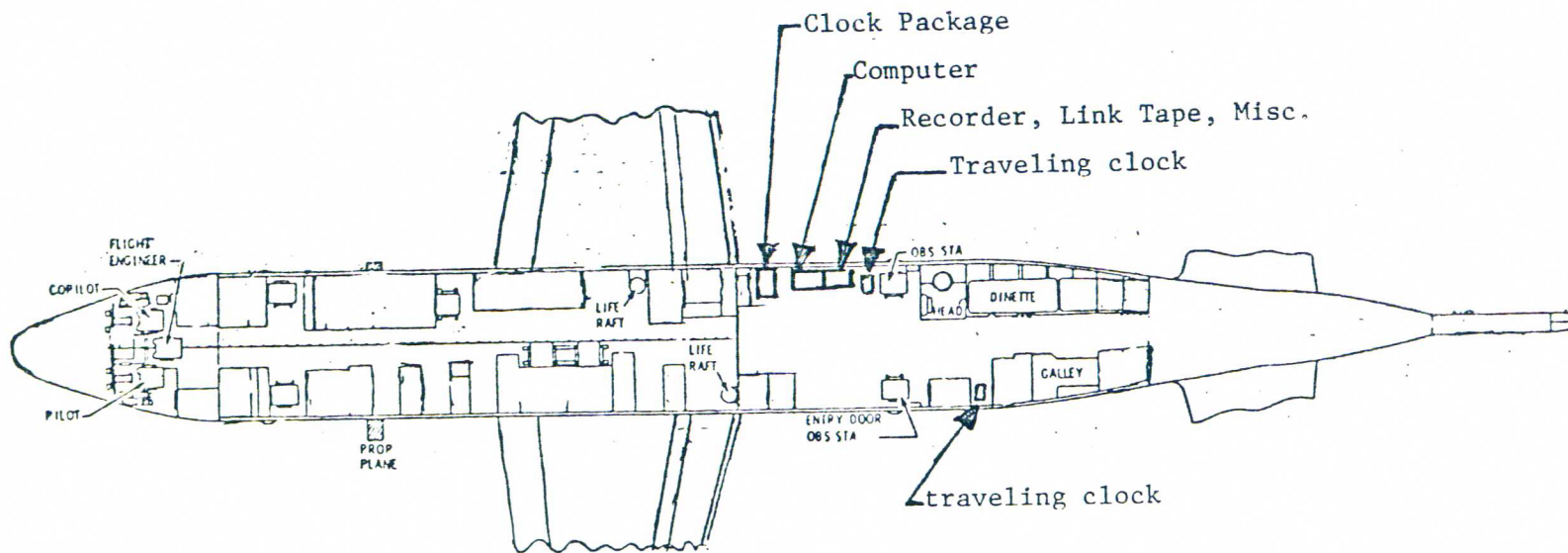


Figure 7. Floor plan of the P3-C aircraft showing the equipment location

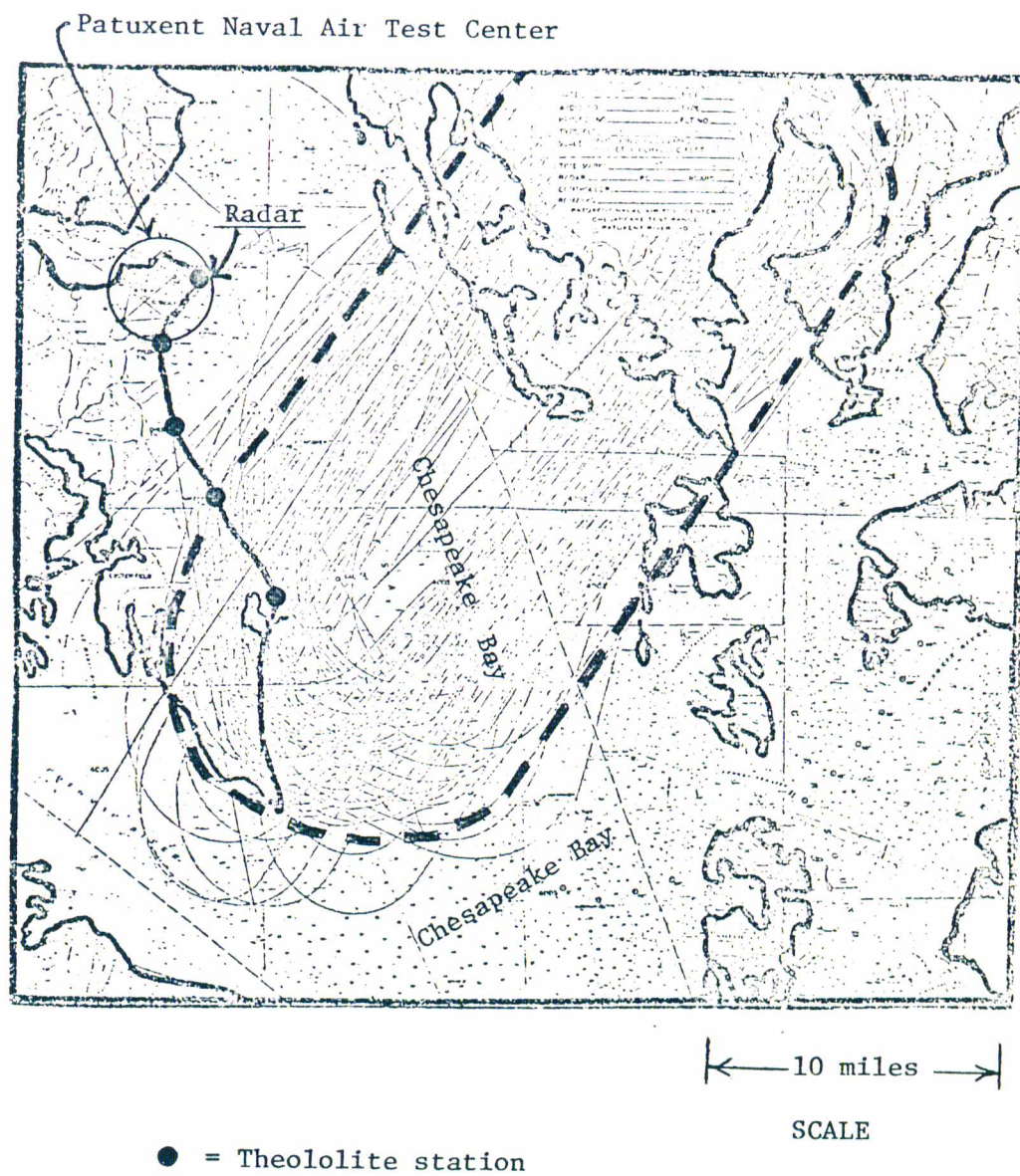


Figure 8. Map showing the flight path of the aircraft. The radar and theololite locations are also indicated. The aircraft flight path was in the clockwise direction generally inside the indicated oval area.

## CHAPTER II

### CLOCKS, PACKAGING, AND ENVIRONMENTAL CONTROLS

#### A. The Clocks

The "clocks" used in this experiment are actually atomic frequency standards which may be used as clocks by counting cycles in the output frequency or by making phase measurements of one standard with respect to another. Following general usage in such a context we will use the terms "clock" and "frequency standard" almost interchangeably.

A review of the early work leading to the development and improvement of atomic frequency standards is contained in reference 21. This work dates from the studies of Stern and Gerlach in 1921 which demonstrated the possibility of isolating atoms of selected energy states in molecular and atomic beams. It was later demonstrated by Rabi<sup>22</sup> and his co-workers that radio frequency fields could be used to excite resonances in such beams. Although many types of frequency standards were developed or studied, three principal types emerged: Cesium beam standards<sup>23-28</sup>, Rubidium gas cell standards<sup>29-30</sup>, and hydrogen masers<sup>31-34</sup>. Modern versions of each of these types was involved in this experiment. Each type will be considered separately.

##### 1. The Cesium Clocks

The Cesium clocks used in the experiment were Hewlett-Packard Cesium Beam Frequency Standards, model 5061A. These standards are approximately 9 x 19 x 18 inches and weigh 65 pounds. Earlier models comprise many if not most of the clocks in the ensemble used by many

national time service organizations, including that of the United States.

The current international definition of the second is related to the ( $F=4, m=0$ ) to ( $F=3, m=0$ ) hyperfine transition of Cesium 133. This transition frequency is 9,192,631,770 Hz. This is the atomic transition used in Cesium clocks to discipline a 5Mhz crystal oscillator. The heart of the unit is a cesium beam tube in which Cesium atoms effuse from an oven, are collimated into a beam, and pass through an inhomogeneous magnetic field which directs atoms of the chosen state down the length of the tube. These atoms pass through a Ramsey type microwave cavity (using separated oscillatory fields) where they interact with a microwave signal. Resonance microwave energy will cause atomic transitions to the other state. A second inhomogeneous magnetic field then directs such atoms to a hot wire ionizer and mass spectrometer. The result of this process is a current whose magnitude depends on how closely the impressed microwave frequency matches the atomic transition frequency. This applied microwave signal is frequency modulated at 137 Hz. If the center frequency exactly matches the transition frequency the output current will vary at twice the modulation frequency. If the center frequency is off to one side of the resonance the beam current will contain a component modulated at the fundamental frequency (137 Hz) with a phase determined by which side of the resonance the center frequency lies on. Since the impressed microwave frequency is synthesized from a 5 Mhz crystal oscillator the instrument may use the information contained in the beam current to discipline this oscillator. The result is a highly stable 5 Mhz signal. Such standards have fractional frequency stabilities over periods of days that approach parts in  $10^{13}$  or  $10^{14}$ . Since the width of

the Cesium resonance (about 360 Hz) would imply a stability of only four parts in  $10^8$ , it is seen that the electronic circuitry is outstanding in its ability to remain close to the center of the resonance.

Some of the Cesium clocks used in the experiment were standard models normally used by the U. S. Naval Observatory for time transfer applications. These clocks are sometimes called "travelling clocks". Seven of the Cesium clocks, however, were specifically selected and modified for this experiment. These Cesium standards were serial numbers 1025, 1028, 1033, 1035, 1026, 752, and 761. The first three were in clock box 1, the second three in clock box 2. Number 761 was part of the ground ensemble. The first five of these seven units were new instruments from Hewlett-Packard delivered with a high beam current option (option #004) to obtain improved stability. All seven standards were also personally modified and checked by Dr. Leonard Cutler, Director of the Physics Research Laboratory of Hewlett-Packard. One of these changes was proprietary. A second change was the modification of the feed-back servo loop to a two pole circuit which eliminated drift or steps in the crystal frequency (see Appendix A for details). This modification was principally to reduce rate changes occurring during and after vibration.

One other modification should be mentioned although it was not internal to the standard itself. One component of the Cesium standard is a "buffer amplifier" which accepts one 5 Mhz signal and delivers two buffered 5 Mhz signals. As several buffered 5 Mhz signals were desired from each standard, additional buffer amplifiers were used. Two such units were strapped to the front of the standard and powered from within the clock. The 5 Mhz output was brought to each of these units. This resulted in four buffered 5 Mhz signals being available from each clock.



These modifications were made after the first flight.

It should be mentioned that all Cesium clocks used in the experiment were the property of the Time Service Division of the U. S. Naval Observatory, directed by Dr. Gernot Winkler. They approved the above modifications.

## 2. The Rubidium Clocks

The six Rubidium clocks used in the experiment were Efratom Rubidium Frequency Standards, model FRK-H. These standards are approximately 3.9 x 3.9 x 4.4 inches and weigh 2.2 pounds. They are smaller and lighter than the Cesium standards. However their stability is worse by about a factor of ten unless great care is taken to maintain constant pressure and temperature, in which case they are worse by a factor of three or four. The units operate on a hyperfine transition of Rubidium 87 analagous to that of Cesium 133. However, these standards are not beam standards. Rather, they use an optically pumped gas cell placed in a microwave cavity. Resonance light from a Rubidium lamp enters this absorption cell containing Rubidium 87, passes through the cell, and impinges on a silicon photo detector. A microwave signal of the resonant frequency of Rubidium 87 (about 6834.68 Mhz) present in the cavity will stimulate transitions of atoms, some of which have already been "pumped" into the higher hyperfine state by the resonance light from the lamp. These transitions affect the absorption of the resonance light as it traverses the cell. This in turn affects the magnitude of the current leaving the photo detector. Thus, although the mechanism has changed, the situation is like that in the Cesium standard: The output current depends on the input microwave frequency. This frequency is frequency modulated at 127 Hz producing the same situation as that described for the Cesium standard.

The output frequency of the Rubidium standards is 10 Mhz. Since the rest of the experimental apparatus uses 5 Mhz signals, a divide-by-two circuit immediately follows each unit. A buffer amplifier is also placed on the circuit board. Hence, two buffered 5 Mhz signals are obtained from each Rubidium standard.

These units were on loan from both the U. S. Naval Observatory and the Efratom company.

### 3. The Hydrogen Maser

There were two hydrogen masers as part of the ground ensemble of clocks. These were massive units, over six feet tall and weighing several hundred pounds. They were units #NP-2 and NP-3 on loan from the Goddard Space Flight Center, Greenbelt, Maryland. These were units that had been constructed under the direction of Harry Peters. Their frequency stability over periods of a few days was approximately the same as the better Cesium clocks, or perhaps a little better.

The hydrogen maser operates on an atomic hyperfine transition of the hydrogen atom analagous to that of cesium and rubidium. This frequency is 1420,405,794.319 Hz. Hydrogen atoms in the excited hyperfine state are injected into a microwave cavity of sufficient Q to allow masing to occur. A fraction of the energy in the cavity is extracted by a coupling loop. This signal is used with a phase comparator and frequency synthesizer to lock a crystal oscillator to the transition frequency.

It has been our experience that, although the hydrogen masers are excellent standards, their reliability is less than the Cesium or Rubidium standards. This may well be because these are not commercially produced units. In any event, both masers needed occasional repair. A series of problems caused NP-2 to miss several flights. These were

usually electronics problems.

### B. The Cesium Clock Box

Pictures of the clock box appear in figures 3-6 of chapter I. Schematic and block diagrams showing the essential features of the clock box appear in figures 9 and 10. The box is constructed of aluminum plate and ribbing. It is separated from a base plate by pneumatic isolation mounts for vibration protection. This base plate is mounted on wheels so that the box may be moved about. The entire structure weighs approximately 1200 pounds. Power supplies and other electronics are located on the box lid, the front of the box, and inside of the box. The clock box is attached to the aircraft by bolting the base plate to two channels on the aircraft floor. The height of these channels is such that the box may be rolled over them with minimum clearance. The wheels then only need be lowered slightly to rest the box on the channels. In practice, the front wheels were completely removed after the box was seated.

The interior of the main box contains three Cesium standards. Other features of the clock box will be considered in the following sections which consider the environmental influences and the measures taken to protect against them.

#### 1. Magnetic Fields

The Cesium clocks are already rather well protected from magnetic fields by a triple layer magnetic shield that is part of the beam tube. We have provided further isolation by placing each clock in a magnetic shield can constructed of mu-permalloy. Openings in these cans allow

air circulation (see the next section). Measurements have shown that even with the lid of the shield can removed exterior magnetic fields are reduced by a factor of 100 near the middle of the can. Further tests were done by rotating one clock box 90 and 180 degrees in the earth's magnetic field. No effect was detected to a level of several parts in  $10^{14}$ , this being about the intrinsic quality of the clocks themselves. Measurements were made in the aircraft during flight using a Hewlett-Packard model 428B Clip-on D.C. milliammeter with a model 3529A Magnetometer probe (1 Gauss/amp). These measurements were made near the clock box in three orthogonal directions. Nothing was noted except the earth's magnetic field.

## 2. Temperature Control

Temperature control of the Cesium clock box was attempted through two stages. The first stage involved two variable speed fans which were mounted on the lower base plate to isolate their vibration from the box proper (see figure 10). A nylon skirt closes off the area between the base plate and the box proper. Lucite panels are attached to the ribbing on the rear and side of the box. The skirt and lucite panels cause the air sucked in by the two fans to be directed over the bottom, rear, and sides of the clock box. A thermistor is attached to the outside wall of the clock box. This thermistor is connected to a thermistor bridge/power controller combination (see Appendix A for circuits). This power controller delivers 0 to 29 volts dc to the two fans. Hence the rate of air flow over the bottom, rear, and sides of the box is regulated by the outside box skin temperature.

The second stage of temperature control is inside the box. The temperature of each of the three clocks is individually sensed and controlled. A constant speed dc fan (Aximax 2, model 464YS) and a heater

are associated with each clock. These units are mounted at the inside front of the clock box (see figure 10). The fans are on small spring mountings to reduce vibration. These fans are capable of moving air at 28 cfm against a pressure differential. Air is sucked in by a fan, moves over the heater, is delivered through a two inch diameter hose to the magnetic shield can of the clock in question. The air enters the can through a two inch hole in the middle of the lid and exits the can at the bottom through 40 1/4 inch holes along the bottom edge of the shield. Removal of the mechanical clock movement normally found on the front panel of the Cesium standard creates a two inch hole in the front panel allowing easy passage of air through the clock interior.

An average temperature measurement of the clock was obtained by three thermistors connected in parallel. One was directly in the input air stream, one was midway down the side of the shield near (but not touching) the shield wall, and the third was at the bottom of the can near an exit hole. These thermistors were attached to a thermistor bridge/power controller combination which supplied 0 to 29 volts to the heater winding. These windings were bifilar to reduce magnetic field generation. The heater resistance was thirty ohms resulting in a maximum power output of thirty watts to each clock. To achieve good control the temperature of the clocks were maintained somewhat above room temperature. The actual temperatures were in the range of 95 to 103°F.

To aid in temperature control of the clocks, polystyrene insulation was installed around each can. This change was made after the first flight.

The result of several measurements on the Cesium standards showed temperature coefficients between two and ten parts in  $10^{14}$  per degree Fahrenheit (see Appendix B). Hence we attempted to maintain the Cesium

clock temperatures to within  $0.1^{\circ}\text{F}$ . Generally this proved to be possible if room temperature stayed within a ten to fifteen degree range, although rapid changes of a smaller extent could cause fluctuations in the clock temperatures. Hence an effort was made to control the temperature of the area around the clock boxes. This was achieved quite well in the ground trailer in which the area containing the clocks was maintained within one or two degrees F. The plane was much more difficult. The aircraft does have an automatic temperature control system. However, it never worked well in the automatic mode until the last flights even though a large amount of effort was directed toward this problem. In fact the entire system failed during the second flight resulting in temperatures near freezing in the aircraft cabin (the Cesium clocks barely remained in their temperature control range).

The sensing and controlling elements of the plane's temperature control system were moved from their normal location near the front of the plane and placed near the clock box. When the system worked well variations of only a few degrees occurred. At other times variations of five or more degrees could occur before the system responded. This was especially true during ascent and descent when the changing cabin pressure caused changes in the convective cooling rate about the box thereby affecting the box temperature. In spite of all the above the Cesium temperatures in general were maintained to the goal of  $0.1^{\circ}\text{F}$  (see plots in Appendix D).

### 3. Pressure Control

Although pressure control was effected mainly for the Rubidium clocks, it was desired to keep all clocks at constant pressure, especially during flight when the cabin pressure would drop to 2/3 atmosphere. The main Cesium clock box and the smaller Rubidium clock box on its lid were connected by tubing and pressure controlled by the same system. A Granville-Phillips automatic pressure controller, series 216, and matching variable leak valve were used to control pressure by admitting dry nitrogen at a rate sufficient to counteract leakage. A National Semiconductor type LX3701A pressure transducer was the measuring element. These units operate using a diaphragm and piezoresistive strain sensor. Pressure was held constant to within 1 mm Hg.

Tests were performed to measure the pressure coefficients of the Cesium clocks and no effect was detected. The limit of this measurement was approximately two or three parts in  $10^{14}/\text{lb-in}^{-2}$ .

### 4. Vibration Isolation

Several aspects of this problem have been alluded to: the variable speed fans being mounted on the base plate, and the constant speed fans being on spring mountings. Thus vibration from these two sources is greatly attenuated. This section will describe the shock mount system isolating the box proper from the lower base plate.

Barry Stahl-level SLM-6 pneumatic mounts are placed at each corner of the box. Each mount is connected by pressure hose to an adjustable valve and reservoir and also to a filling stem and pressure gauge near the front of the box. The valve/reservoir units are on the back of the box. Each mount/reservoir system was normally inflated to 55 psi and the valve "tuned" to approach as close as possible to critical damping.

This resulted in a resonant frequency of three Hz with a falloff of about 12 db/octive. Although critical damping was not quite achieved, the second peak following an impulse was 1/3 to 1/4 the amplitude of the primary peak. The principal resonance of the aircraft in flight is 90 Hz from the engines. The most critical frequencies for the clocks are the 137 Hz and 127 Hz modulation frequencies of the Cesium and Rubidium clocks. Although vibration on the P3 aircraft was quite noticable in flight it did not seem to be transmitted to the box which only showed gentle swaying motions during flight. No higher frequency vibrations could be detected by touching the box.

A retaining pin was located at the very top of the box structure. A ring firmly attached to the aircraft surrounded this pin, normally not touching it, to prevent excessive movement of the box on its shock mounts. On take-off and on landing the box would jerk to the side and be abruptly stopped by the ring. This was the most violent motion transmitted to the box.

#### 5. Power Supply Variations

The clocks were electrically isolated from each other by placing each on a separate voltage regulator. A standby battery on the front of the clock box protected against brief (5 min) power failures. Longer power failures were guarded against by use of a "battery cart" between the clock box and the local AC line. Essential power could be maintained to the boxes for periods up to fifteen hours in the event of longer power failures, several of which occurred. Although the Cesium clocks were normally supplied with DC power they are capable of accepting AC power. Provision was made for doing this for repair or emergency use.



### C. The Rubidium Clock Box

The Rubidium clock box is mounted on the rear portion of the lid of the Cesium clock box (see figures 4,5,6, and 10). Inside the box are mounted the three rubidium clocks, each in a magnetic shield can, and the divide-by-two and buffer amplifier circuits. The entire box is temperature controlled as a unit by a bifilar heater winding in the lid of the box. A thermistor/thermistor-bridge/power-controller sequence regulates the temperature. The box is insulated. An exterior fan mounted on top of the box on spring mountings flows air over the top plate. In the later flights this arrangement was modified by attaching a tube causing this air to return and flow over the surface again (closed system). The speed of the air flow was regulated by the temperature of the heat transfer plate on top of the Rubidium box. This did improve performance. Following this modification the Rubidium box temperature could be maintained to better than 0.05°F. Previous to this modification large excursions were caused by rather small plane temperature excursions and were a distinct problem. The temperature and pressure coefficients of the Rubidium standards were measured and found to be approximately

Temperature:  $-3 \times 10^{-12}$  / degree F

Pressure:  $-1 \times 10^{-13}$  / mm Hg

(see Appendix B).

The Rubidium clock box shared in the pressure control and vibration isolation of the Cesium box.

#### D. Other Clock Box Features

Some features of the clock box not considered in a previous section will be discussed here.

Since the clock boxes had to be relatively pressure tight a rubber gasket was placed between the box proper and the lid. Bolts were spaced around the perimeter about 2 1/2 inches apart. These bolts were tightened with a torque wrench to 18 ft-lbs. Electrical access to the inside of the boxes was obtained by vacuum tight multi-pin or coaxial feedthrough connectors.

Environmental parameters were monitored by sensors different from the sensors used for control. These included a pressure transducer in the main Cesium clock box (National Semiconductor LM3701A) as well as one external to the box. Temperature measuring thermistors were placed in each Cesium clock shield can, the Rubidium clock box, and outside of the box. This data was accumulated by the computers. It was also available for monitoring with a voltmeter at the box itself as were other voltages not recorded by the measuring system.

Three lights of different colors exist on the front panel of the Cesium clocks indicating the condition of the clock. Photodiodes were attached to each of these lights on each clock and connected to circuitry on the outside of the box where a panel of light emitting diodes repeated the information. Hence the condition of the Cesium clocks could be discerned without opening the box. There also exists a button on the Cesium clocks for resetting. A small relay was attached to the clocks and wires brought out to buttons on the outside of the clock box to allow this function to be performed without opening the box.

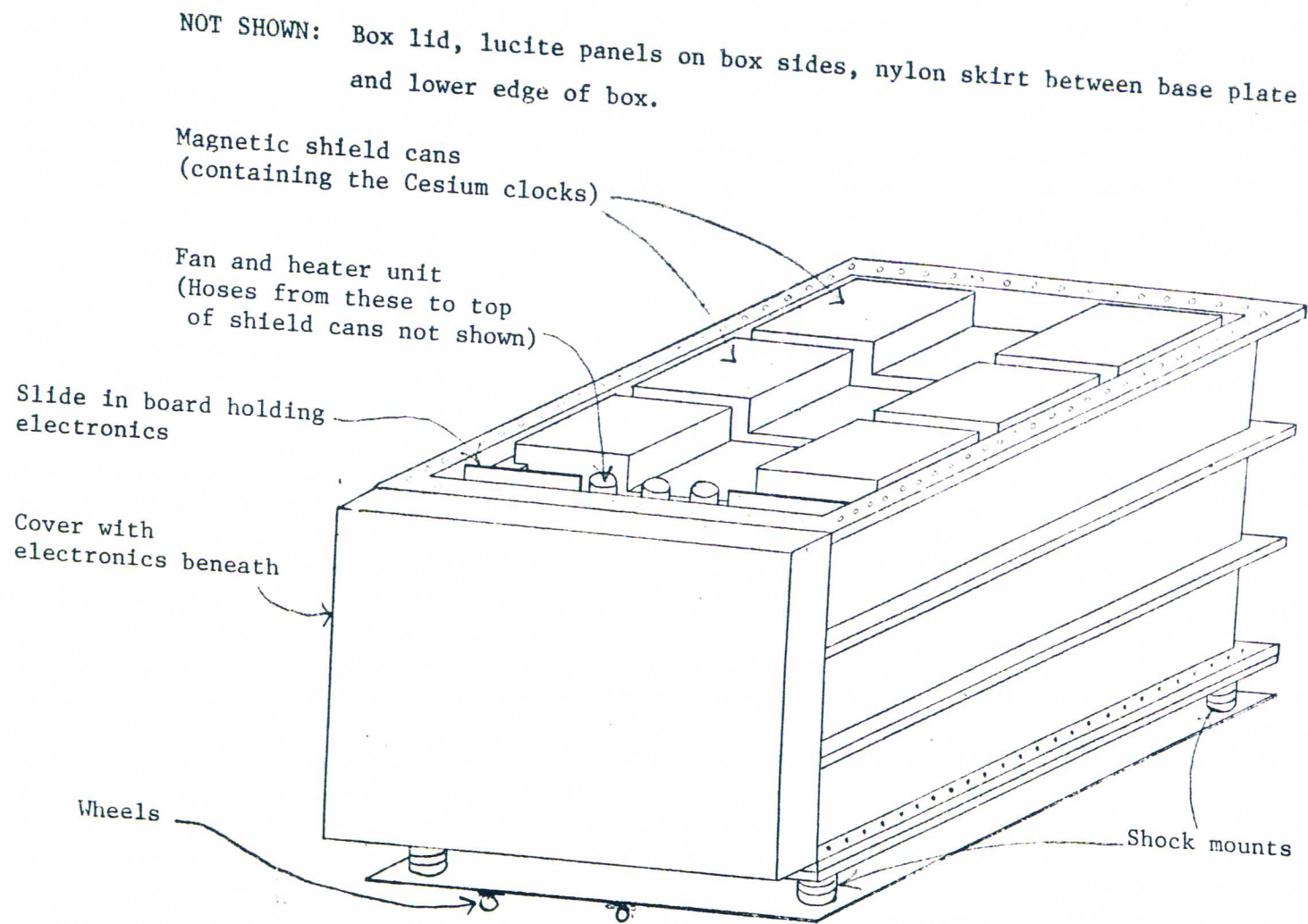
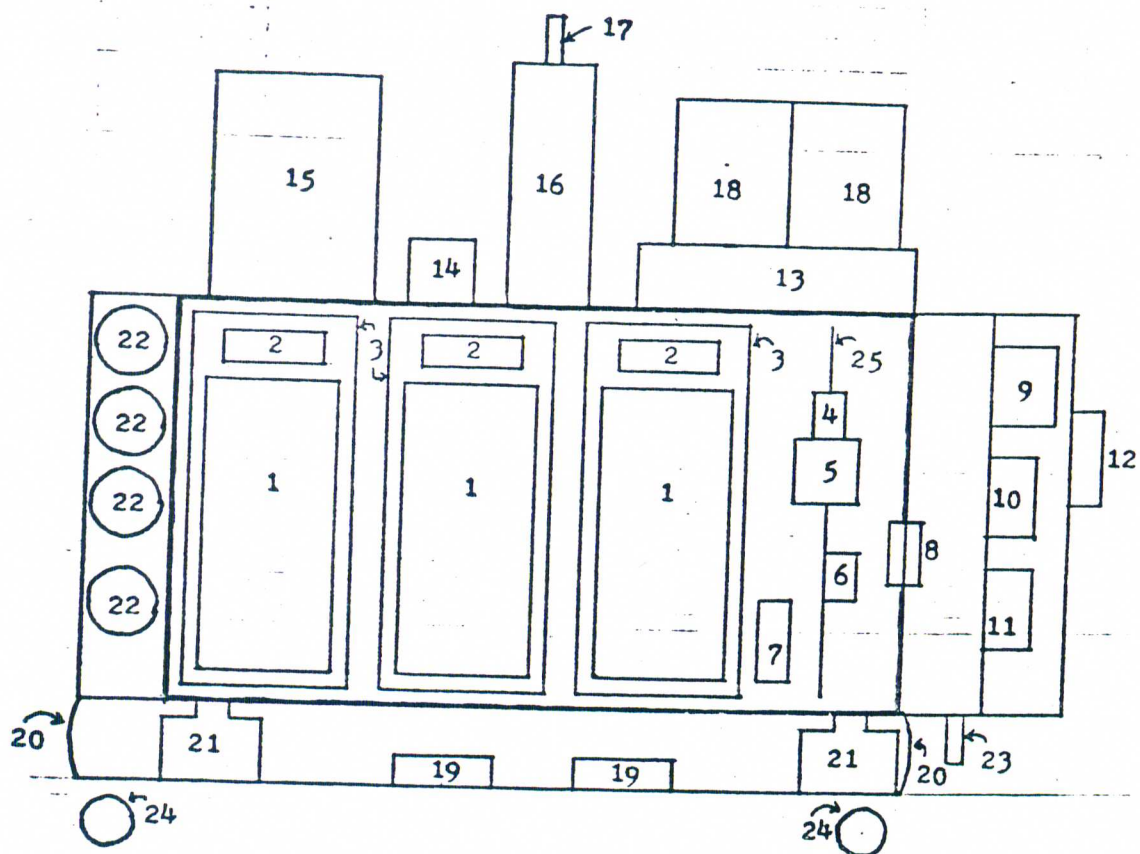


Figure 9. Schematic diagram of the clock box. The lid is not shown. Dimensions as shown are 32 x 26 x 43 inches.



- |   |   |
|---|---|
| 1. Cesium clock                                 | 13. Pressure controller                   |
| 2. Buffer amplifiers                            | 14. Pressure valve                        |
| 3. Magnetic shield cans                         | 15. Rubidium clock box                    |
| 4. Heater                                       | 16. Retaining pin support                 |
| 5. 400 Hz fans                                  | 17. Retaining pin                         |
| 6. Pressure transducer                          | 18. Power supplies                        |
| 7. Analog phase boards                          | 19. Controlled fans                       |
| 8. Feed-through area                            | 20. Nylon skirts                          |
| 9. Five minute battery                          | 21. Shock mounts                          |
| 10. Power controllers and<br>thermistor bridges | 22. Pressure chambers for<br>shock mounts |
| 11. Power supplies                              | 23. Pressure gauges for<br>shock mounts   |
| 12. R.F. switches                               | 24. Wheels                                |
|   | 25. Base mounting plate                   |

Figure 10. Block diagram of the clock box.

CHAPTER III  
DATA ACQUISITION

A. General

The phases of the clocks are measured in two ways. The primary method is the use of an "event timer" to be described below. The second method is an analog comparison using circuit boards designed and built by Charles Steggerda of the Quantum Electronics Group, Department of Physics and Astronomy, University of Maryland. Application of two 5 Mhz signals to an analog phase board results in a dc output voltage which varies between -5 and +5 volts as the phase difference between the two signals varies between 0 and 200 nanoseconds. This method is not as accurate as the event timer measurement and existed as a back-up in case of failure of the primary system. No such failure occurred.

Recall that each of the Cesium clocks has four 5 Mhz outputs (as modified for this experiment). One output from each clock goes to an analog phase board located inside the clock box. A second output of one of the three standards, the one designated as analog board reference, goes to the "reference" input of all three analog phase boards. The other outputs go to feedthrough BNC connectors on the front of the box. One of these outputs goes to the reference input of all three analog phase boards inside the Rubidium clock box.

B. The Event Timer

The heart of the primary phase measuring system is an "event timer"

built by Charles Steggerda originally for the lunar laser ranging program. This device is described completely in reference 35. It is basically a dual slope integrator in which a capacitor is charged at one rate and discharged at a second slower rate. The event timer requires a 5 Mhz time base as reference and also uses this time base to maintain an internal calendar and clock. It can measure the epoch of an event, such as the arrival of a NIM pulse<sup>†</sup>, to a precision of 0.1 nanosecond. Such a measurement will give the phase difference, measured in nanoseconds, of one 5 Mhz signal (after having passed through a discriminator to generate a NIM pulse) with respect to the reference 5 Mhz signal.

The event timer is intimately connected with the Nova 2 mini-computer which commands when a measurement is to be made and receives the result for storage or analysis. The computer console may be used to set the event timer date and time to the nearest second. If further precision is desired, the event timer may be set to the nearest tenth microsecond by supplying a one seconds tick and inserting the desired offset in microseconds from that tick.

As used in this experiment, the phase data as sent to the computer is modulo 100 nanoseconds. This is related to the fact that the 5 Mhz time base is first doubled to 10 Mhz. The event timer may be calibrated so that this "fold over" is exactly 100 ns. Experience has shown that this calibration is then stable over periods of days. The event timers were calibrated previous to each major flight. Further tests have shown that the instrument is linear to within  $\pm 0.2$  ns.

The event timer method of measuring phase differences is called the

---

<sup>†</sup> A NIM pulse is a Nuclear Instrumentation Module signal. This is an electrical pulse with nominal voltage of  $-0.7$  to  $-1$  volt and nominal rise time, fall time, and middle time of 3 nanoseconds each.

"digital phase measurement" to differentiate it from the second method using the analog phase boards which is called the "analog phase measurement".

### C. The Digital Phase Measurement

Figure 11 is a block diagram of the digital phase measuring system. There are two computers ("ground" and "air"), each with its associated event timer and electronics. There are also the two clock boxes, one on the ground and one in the plane. The system is designed so that each of the computers may access each clock box for phase measurements. Consider one of the clock boxes. The six 5 Mhz signals from the clock box (three Cesium clocks, three Rubidium clocks) are brought to the first six inputs of a electronically controlled ten-to-one R.F. switch (Trumpetor mercury wetted relay switch type CSFZ). The remaining four positions are used for any other clocks in the ensemble in question. Hence each of as many as ten signals from each clock box may be sampled in sequence. Following the ten-to-one switch is a similar one-to-one switch which determines to which computer the signals will go. Both of these R.F. switches are mounted on the front of the clock box.

At the computer location is a two-to-one switch which determines which clock box the computer is receiving signals from. A second two-to-one switch follows this one and is related to the laser time transfer technique that is not being considered in this thesis. After leaving this switch, the 5 Mhz signal in question goes to a discriminator (Ortec 436) which provides a NIM pulse to the event timer. The event timer obtains its reference signal from one of the clocks in the ensemble associated with it.

Each computer samples clock phases every 204 seconds. The computer controls the various RF switches so that it may sequence through all the

5 Mhz signals at a rate of approximately five per second. During this time, it actually makes not one but sixteen consecutive measurements of each phase. The mean of these sixteen measurements is taken to be the measurement and is stored. This technique helps to eliminate system phase noise from the measurements.

In the air computer system, the phase information is stored in the computer's memory core. It is also stored on magnetic tape (LINC Tape II) as a safety precaution. The computer can sample at the above rate for about twenty-four hours before its memory is full. The contents of the memory may be transferred by cable to the ground computer for storage.

In the ground computer system, the data, whether resulting from its own measurements or from a transfer of data from the other computer, is stored on a magnetic disk. The disk can hold all data from an entire flight as well as the programs and operating system it normally must maintain. Data may be transferred from the disk to magnetic tape for permanent storage. This was normally done every few days.

#### D. The Analog Data

The analog data consists of dc signals between -5 and +5 volts dc that come from the analog phase boards and also from the environmental measuring circuits (the pressures and temperatures). These signals leave the clock box along a cable that goes both to the computer for storage and also to a "translation box". At the computer, the signals go through an analog-to-digital converter and are sampled every 204 seconds immediately following the digital phase sampling. The "translation box" sends the signals to chart recorders and contains circuitry to isolate the computer from the recorders and also to calibrate the recorder scale for each channel. The chart recorders used are six channel



Honeywell recorders on loan from the U.S. Naval Observatory. These recorders sequence through the six input signals over a 90 second period, plotting a point every 15 seconds. The chart speed used was 6 inches per day. Two such recorders were in the ground trailer and one in the aircraft. It was therefore possible to visually monitor phases, temperatures, and pressures in real time.

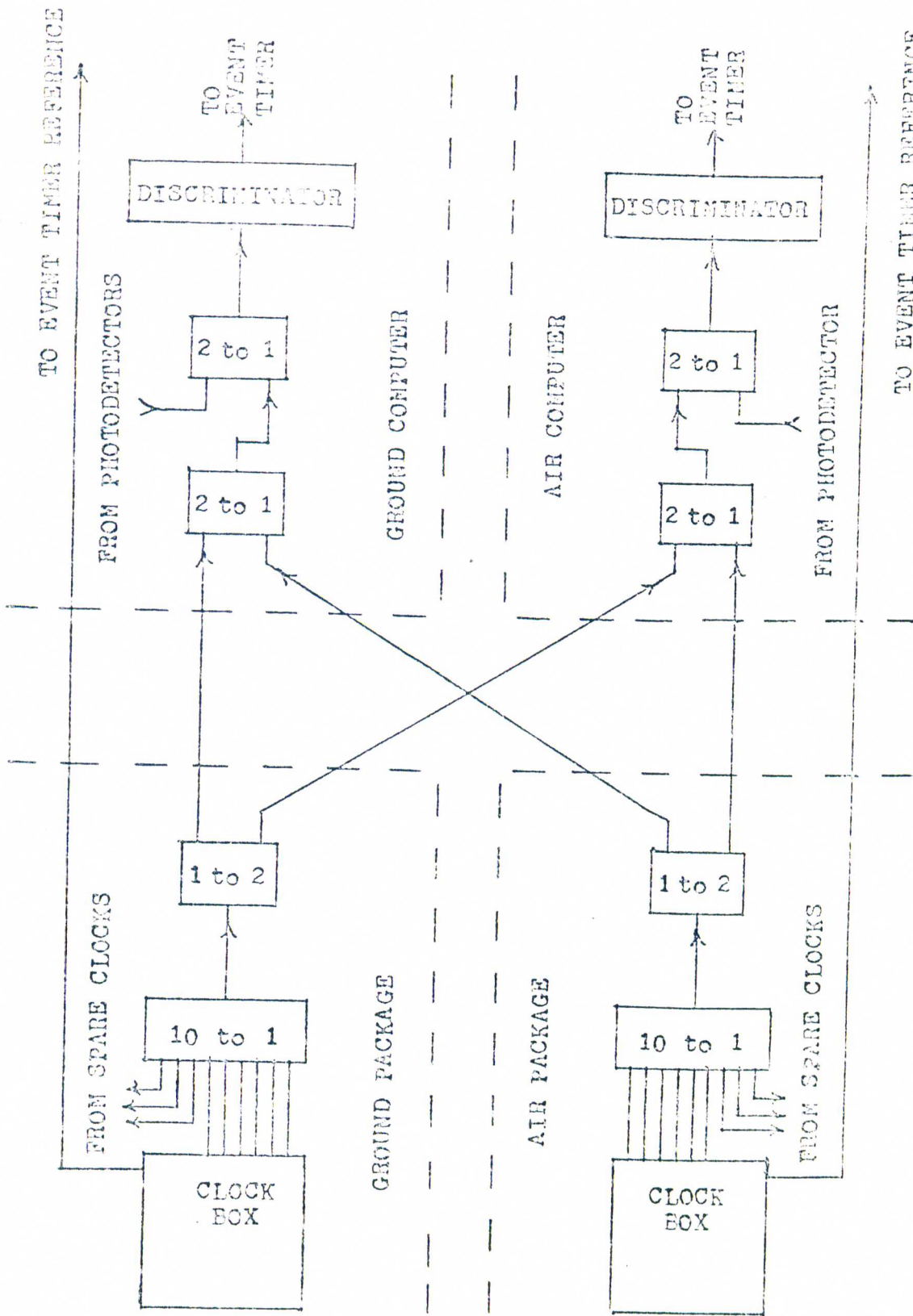


Figure 11. SIGNAL SWITCHING DIAGRAM

CHAPTER IV  
SOFTWARE CAPABILITY AND DATA MANIPULATION

A. The Raw Data Files

The data as originally taken exists as a series of "records" in a data "file". These are called "raw" data files because most of the other programs do not work on these raw files, but on "translated" files generated from them.

The records which comprise the raw data file each consist of a five word (computer word) header followed by a number of words of actual data. Each record is assigned a "record type" which is a number depending on the type of data stored in the record. Type 1 is analog data and types 6 and 7 are digital phase data from clock boxes one and two respectively. Other record types are related to the laser time-transfer operation which is not being considered in this thesis. The record header consists of the following five words:

1. The record number
2. The record type
3. The second of the half-Julian day + 22336
4. The half-Julian day
5. The number of words of data that follow the header

The format of the header is dictated by the format of the Nova 2 minicomputer and the Event Timer intimately associated with it. For example the additional constant added to the second of the half-Julian day in the third word causes that computer location to overflow at the last second of the half-Julian day. Many other features were dictated by the original use of the Event Timer for lunar laser ranging, for

example the use of Julian days for time keeping. The programs used to obtain this raw data are written in the machine language of the Nova 2 and are closely related to the characteristics of the Event Timer. This programming was the work of John Rayner of the Quantum Electronics Group of the Department of Physics and Astronomy, University of Maryland.

### B. The Translated Data Files

The "translated" data files are created from the original "raw" files and it is these new files that most of the analysis and manipulation programs work on. These new files contain only one kind of data. One such kind is the digital phase data. The program that creates this translated file consisting of digital phase data is named TRANSD.

TRANSD accomplishes the following tasks:

1. Removes "cross overs" in the phase data. Recall that the phase data existing in the raw files is modulo 100 ns. TRANSD adds or subtracts quantities of 100 so that the phase record extends continuously. For example the sequence ...98,99,0,1,2,... in a raw file would become ...98,99,100,101,102,... in the translated file.
2. Puts the time in a convenient form. The time of a reading as it exists in the raw file consists of the half-Julian day and the second of that half-Julian day (plus a constant). TRANSD converts this into a fractional Julian day (FJD) such as 4539.765482 and immediately subtracts an arbitrary but fixed constant to produce a number smaller than 100, eg. 39.765482. This procedure assures better readability and adequate

accuracy upon storage in the single precision computer word. For data extending over several days, having the time in fractional days is of obvious convenience.

3. Creates "paper" clocks. The mean of the three phase readings of the Cesium clocks in clock box 1 is stored as a separate reading, and similarly for clock box 2. These created mean clocks are often called "paper clocks".

The format of the translated data file consists of one header for the entire file followed by a number of "records" of data. Each record contains a list of phase measurements for every clock, including the two paper clocks. It also contains the time at which these readings were made. This time is modified slightly for accurate storage by the following procedure. The integer portion of the very first time in the file is subtracted from that and each succeeding time. For example, if the time of the first record is 39.765482, then .765482 is stored in the first word of the record. This same offset (39) is subtracted from each subsequent time before storage in the first word of the appropriate record. The offset (39 in this example) is stored in the file header. This procedure helps to assure adequate accuracy considering the size of the computer word. The format of the translated file header is as follows:

1. NC (the number of clocks in the original "raw" record)
2. NC+2 (the total number of clocks in the translated record)
3. N (the number of records in the entire file)
4. S (the offset of the fractional Julian day; 39 in the above example)
5. BFJD (the time of the first record: Beginning Fractional Julian Day)

6. EFJD (the time of the end record)
7. (Here follow NC+2 pairs of numbers, each pair consisting of the first and last phase reading of that clock)

As mentioned above, the first word of each record contains the time of the measurement. Then follow the phase readings in a specific order. This order is independent of what the order was in the raw files. This ordering in the translated file is as follows:

- |                      |                                 |  |  |
|----------------------|---------------------------------|--|--|
| 1. }<br>2. }<br>3. } | The Cesium clocks<br>in box 1   | 10. }<br>11. }<br>12. }                            | The Rubidium clocks<br>in box 2                          |
| 4. }<br>5. }<br>6. } | The Rubidium clocks<br>in box 1 | 13. Mean of clocks 1, 2, and 3<br>(paper clock)    | 14. Mean of clocks 7, 8, and 9<br>(paper clock)          |
| 7. }<br>8. }<br>9. } | The Cesium clocks<br>in box 2   | 15. }<br>16. }<br>17. }<br>18. }<br>19. }<br>20. } | Other clocks, with ground clocks<br>before flying clocks |

Bob Reisse has written a program (TPTRANS) that translates the environmental data (temperatures and pressures) contained in the raw files into a translated file of the same general format as that above<sup>20</sup>.

### C. Data Plots and the Graphics Terminal

A Tektronics 4013 graphics terminal and hard-copy unit were available for data plots. The usefulness of this facility can not be overstated. All plotting programs access the translated files. Several of the main plotting programs are described below.

#### 1. PHASEPLOT

PHASEPLOT is a program that plots the phase of one clock with respect to another (reference) clock. Any clock may be plotted against

any reference, including of course the two paper clocks. The scales of the plot may be specifically selected or the program will self-scale to render the entire plot on the screen. Figure 12 is an example of such a plot. This and other plots are programmed so that the numbers comprising the scales are "clean" (34.2 rather than 34.1897).

## 2. SRESIDUALS

The relatively large rate of one clock versus another will often mask features of interest in the phase data. Hence PHASEPLOT itself is rarely used in this experiment. Rather, the slope of the data is removed resulting in a plot of the difference of each data point from this slope. There are two types of slopes that may be plotted against. One is a least squares regression line fit to the data. The second is a slope line defined by the first and last point in the data file. In the latter case the option exists for using a small number of points at each end. SRESIDUALS is the program that produces the plot, called a "residual" plot. In order to run SRESIDUALS another type of file must be created containing information about the slope to be removed. The program SLOPES creates such a file for the least squares case while the program PSLOPES does this task for the "first point, last point" slope. In either case any clock or group of clocks may be specified as the reference. An example of a residuals plot appears in figure 13. The scales may be selected by the user or the program will self-scale.

## 3. RESIDUALS

RESIDUALS is a program that creates a page consisting of residual plots of every clock in the file. Such a plot is of enormous value in reviewing quickly several hours, days, or weeks of data from many clocks.

An example of such a plot appears as figure 14.

#### 4. SIGMATAU

SIGMATAU is a program that computes and displays  $\sigma(2;\tau)$  for any clock of a translated file with respect to any other clock or group of clocks. (Those unfamiliar with the meaning of a "sigma-tau" plot are referred to chapter VI.) An example appears as figure 15.

Copies of the FORTRAN listing of each of these programs appear in Appendix E.

#### D. Manipulation and Analysis Programs

Numerous other programs have been written to truncate translated files, append them, edit them, display their contents, etc. Other programs relating directly to the data analysis will be considered in chapter VII.



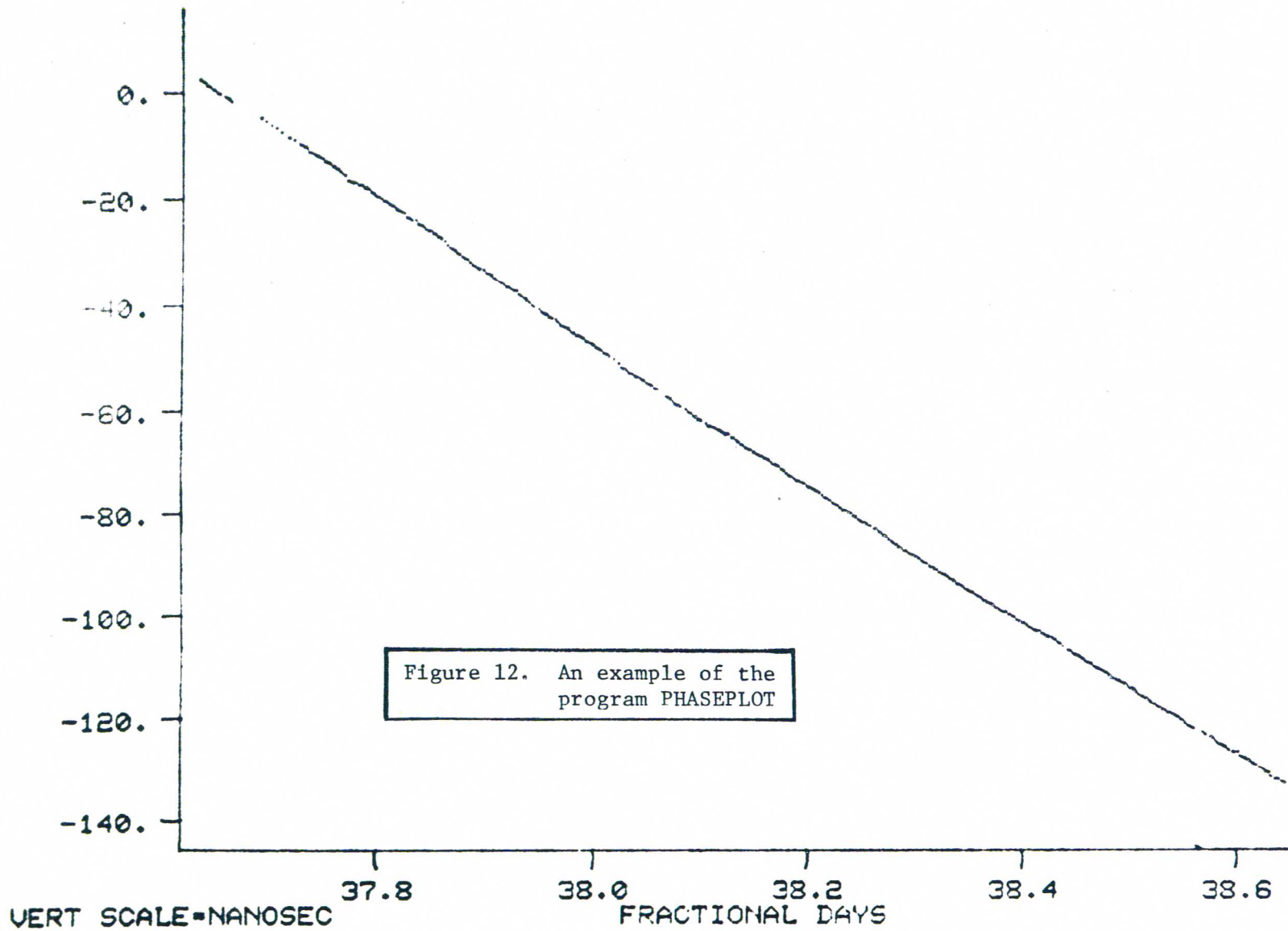


Figure 12. An example of the program PHASEPLOT

PHASE PLOT, FILE: DFGB1122  
 CLOCK 2 US PAPER REF 0,

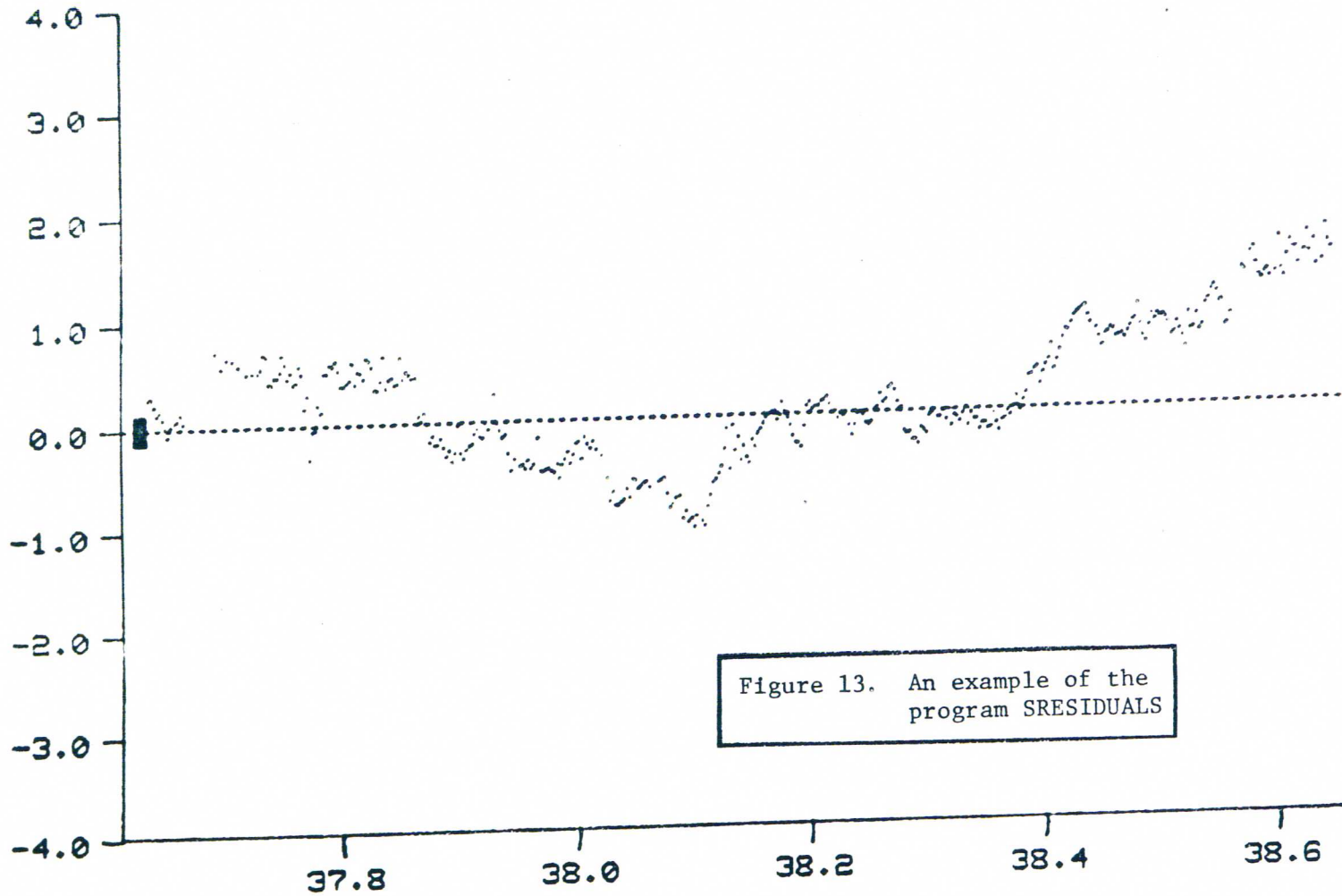


Figure 13. An example of the program SRESIDUALS

VERT SCALE= NANOSEC

FRACTIONAL DAYS

RESIDUALS, FILE: DFGB1122  
 CLOCK # 2 US PAPER REF 0,

SLOPE FILE: DSGB1122



RESIDUALS, FILE: DFGA110 FJD= 88.24078, 89.36058  
SLOPE FILE: DSGA110 SCALE= 10.00 NSEC REF CLOCK: 0,

Figure 14. An example of the program RESIDUALS.

SIGMA(2;T), FILE: DFGLONG1

TAL(SEC)	N	SIGMA	LOG SIG	SD	DEL
2040.	437	0.15E-12	-12.82	0.55E-14	5
4080.	216	0.99E-13	-13.00	0.45E-14	4
8160.	106	0.69E-13	-13.16	0.37E-14	3
16320.	51	0.51E-13	-13.29	0.42E-14	3
32640.	23	0.27E-13	-13.57	0.45E-14	3
65220.	12	0.23E-13	-13.63	0.47E-14	0
130560.	5	0.27E-13	-13.57	0.67E-14	0
261120.	2	0.19E-13	-13.73	0.24E-14	0

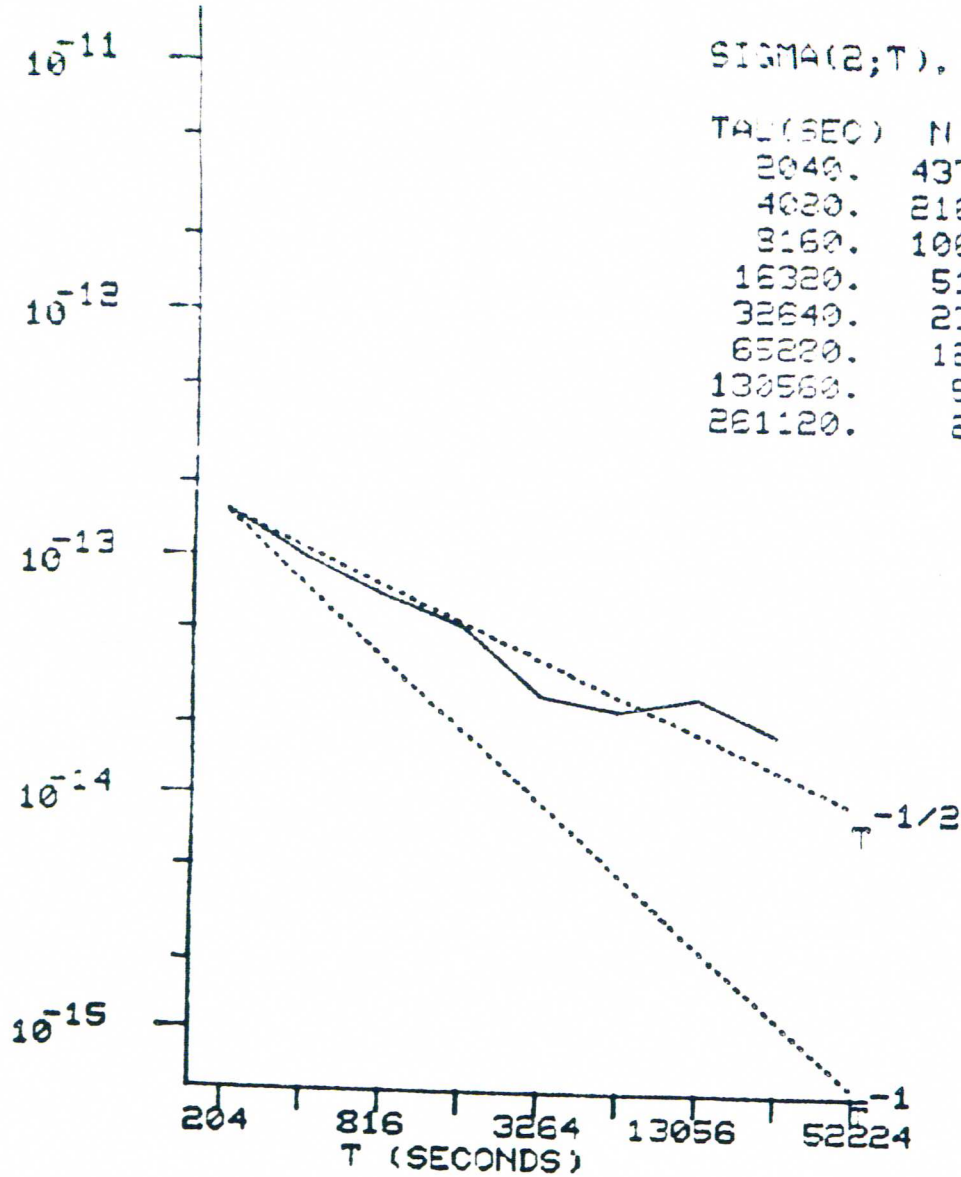


Figure 15. An example of the program SIGMATAU

CLOCK 8 VS REF: 0.

## CHAPTER V

### THEORY AND THE PREDICTION OF THE EFFECT

#### A. The General Relativistic Effect

We will not repeat here what is covered in virtually every text book on general relativity. Suffice it to say that for the metric

$$ds^2 = g_{\mu\nu} dx^\mu dx^\nu$$

(with the "zero" index being the time index) and for nearly Newtonian systems in Newtonian coordinates the metric may be approximated by

$$ds^2 = -(1 + 2\phi/c^2)c^2 dt^2 + (1 - 2\phi/c^2)(dx^2 + dy^2 + dz^2) \quad (1)$$

where  $\phi$  is the Newtonian potential ( $\phi \sim -GM/r$ ) and  $c$  is the speed of light. Hence the metric coefficients are approximately

$$g_{00} = -(1 + 2\phi/c^2) \quad \text{and} \quad g_{kk} = (1 - 2\phi/c^2) \quad .$$

Since the proper time  $d\tau$  is given by  $c^2 d\tau^2 = -ds^2$ , and since  $dx^2 = V_x^2 dt^2$  we have

$$c^2 d\tau^2 = (1 + 2\phi/c^2 - V^2/c^2)c^2 dt^2 \quad .$$

Noting that  $\phi/c^2$  for this experiment is  $\sim -7 \times 10^{-10}$  and so  $\phi/c^2 \ll 1$ , the above equation may be approximated as

$$cd\tau = (1 + \phi/c^2 - V^2/2c^2)c dt \quad . \quad (2)$$

Consider an inertial frame of reference in which time intervals,  $dt$ , are measured by clocks synchronized to a master clock at infinity, or by clocks whose rates have been adjusted to compensate for gravitational

potentials. That is, time intervals measured in this frame and using its clocks are operationally independent of the distribution of matter. This time is sometimes called "world time". Consider two observers with standard clocks and in motion in this frame. If each measures the time interval between the same two events, they measure the proper time intervals  $d\tau_1$  and  $d\tau_2$  respectively. Each of these times is related to the world time by equation 2. Hence if the two observers initially synchronize their clocks and then move apart, the accumulated time difference between their clocks will be

$$\int (d\tau_2 - d\tau_1) = \int \left( \frac{\phi_2 - \phi_1}{c^2} - \frac{v_2^2 - v_1^2}{2c^2} \right) dt \quad . \quad (3)$$

Considering the accuracy of this experiment it does not matter which time is used for the variable of integration.

#### B. Prediction of the Effect

To compute the accumulated time difference between a clock that remains on the surface of the earth and one which flies in an aircraft we will use equation 3. The inertial frame selected is a cartesian frame with origin at the center of the earth and non-rotating with respect to distant matter. The Z axis will be coincident with the axis of rotation of the earth. The coordinates of interest in this system will be the distance of a point from the origin ( $r$ ) and the latitude,  $\theta$ , of such a point. See figure 16.

Since the earth is not exactly a homogeneous sphere its gravitational potential is not exactly  $-GM/r$ . Data obtained from measurements of the orbits of artificial satellites has allowed a more exact determination

of the earth's potential. An expansion given by Allen<sup>36</sup> is:

$$\phi(r,\theta) = -(GM/r) \left[ 1 - \sum_{n=2}^{\infty} J_n \left( \frac{a}{r} \right)^n P_n(\sin\theta) \right] \quad (4)$$

$a$  = equatorial radius of the earth  
 $\theta$  = latitude  
 $P_n$  = Legendre polynomial of degree  $n$   
 $J_n$  = constants

Allen gives values for the constants  $J_2$  to  $J_{21}$ . The value of  $J_2$  is  $1.08264 \times 10^{-3}$  with the other constants being smaller by about three orders of magnitude more. It therefore seems that at the level of precision of this experiment none of these terms are important. But since the  $J_2$  term is large enough to make a minor difference it will be included in the calculation.

The  $V^2$  term in equation 3 is calculated in an inertial frame. Hence the ground clock and the plane clock will have part of their velocity due to earth rotation. It is therefore necessary to consider the reference frame in which the velocity and position of the plane are measured. This is a Cartesian frame with origin at the radar antenna tracking the aircraft. The  $z$  direction is the local vertical with positive  $z$  being upward. The  $x$ - $y$  plane is tangent to the earth's surface with positive  $x$  and  $y$  being east and north respectively. The lower case letters  $x, y, z$  and  $v_x, v_y, v_z$  will be the position and velocity components measured in this "range" frame. The origin of this frame is located at  $(r_o, \theta_o)$  as measured in the earth-centered inertial frame. Then if  $\omega$  is the angular rotation rate of the earth with respect to distant matter, the velocity,  $V$ , of an object in the earth-centered frame is related to measurements in the range frame by the relation

$$V^2(v,r,\theta) = (v_x + \omega r \cos\theta)^2 + v_y^2 + v_z^2 \quad (5)$$

(It might be noted as a point of interest that an alternative approach is to first transform into a reference frame corotating with the earth:

$$\vec{V} = \vec{v} + \vec{\omega} \times \vec{r}$$

$$v^2 = \vec{V} \cdot \vec{V} = v^2 + 2\vec{v} \cdot (\vec{\omega} \times \vec{r}) + (\vec{\omega} \times \vec{r}) \cdot (\vec{\omega} \times \vec{r})$$

which for the range coordinate system becomes

$$v^2 = v^2 + 2v_x \omega \cos\theta + \omega^2 r^2 \cos^2\theta \quad .$$

Hence the same result is obtained. This method of first transforming to a rotating system causes the  $v^2$  quantity to explicitly appear in three parts:  $v^2$  as measured in the rotating frame, the velocity dotted into a velocity due to earth rotation, and a centrifugal term.)

Since the gravitational potential is expressed in  $r$  and  $\theta$  and we measure in  $x, y, z$  it remains to transform between these systems. As may be seen in figure 16 the quantity  $z$  differs from the quantity  $r - r_0$  because of earth curvature. Study of figure 16 will reveal the relations

$$r^2 = (r_0 + z)^2 + x^2 + z^2$$

$$\tan(\theta - \theta_0) = y / (r_0 + z) \quad .$$

The value used for  $r_0$  is calculated from an expression given by Allen (ref. 34, p. 114) giving the distance from the earth's center to sea level as a function of latitude. We also allow for the height of the radar antenna above sea level. In any event, it should be noted that the result of the calculation is not sensitive to the value of  $r_0$ .

A further point of interest is the affect of the gravitational potentials of sun and moon on our results. Since the earth is free fall with respect to these bodies the effect of such potentials across the earth diameter cancels to first order<sup>37</sup>. In any event the effects are



too small to affect the accuracy of this experiment.

Using the subscripts g and p for ground and plane the previous discussion may be summarized as follows:

We calculate

$$\int \left( \frac{\phi_p - \phi_g}{c^2} - \frac{v_p^2 - v_g^2}{2c^2} \right) dt$$

where

$$\phi(r, \theta) = -(GM/r) \left[ 1 - J_2 \left( \frac{a}{r} \right)^2 P_2(\sin \theta) \right]$$

$$r_i^2 = (r_o + z_i)^2 + x_i^2 + y_i^2$$

$$\tan(\theta_i - \theta_o) = y_i / (r_o + z_i) \quad , i = g \text{ or } p$$

$$v^2 = (v_x + \omega r \cos \theta)^2 + v_y^2 + v_z^2 \quad , \text{ where } v_x = v_y = v_z = 0 \text{ for the ground clock.}$$

### C. Range Data Accuracy

It is seen that a record of  $x, y, z$  and  $v_x, v_y, v_z$  is required for calculation of a predicted effect. This data is acquired by the tracking facility of the Naval Air Test Center, the Chesapeake Test Range. Both an X and C band radar were available to track the aircraft which was equipped with transponders to facilitate tracking. Five theodolites were also available for calibration of the radar (see figure 8 at the end of chapter I showing the radar and theodolite positions with respect to the flight path). The range parameters were recorded each second of flight. A twenty-one point smoothing technique is applied to the original data. These procedures are standard practice at the Test Range. Their estimate of error is that altitude,  $z$ , will be  $\pm 100$  feet and that velocity,  $v$ , will be  $\pm 2$  knots. As an independent check on this estimate

We compared calibrated radar data with theodolite data for a seven hour period using approximately one hundred points of comparison. The mean and standard deviation of these differences were as follows:

$$\delta(\text{altitude}) = -15.5 \text{ feet} \quad \sigma = 40.6 \text{ feet}$$

$$\delta(\text{velocity}) = -.087 \text{ knots} \quad \sigma = 1.6 \text{ knots}$$

We therefore accept 100 feet and 2 knots as being realistic tolerances on these parameters. For nominal values of the flight parameters ( $z = 30,000$  ft and  $v = 250$  knots) the following errors are obtained:

$$dz/z = 100/30000 = 1/3 \%$$

$$d(v^2)/v^2 = 2dv/v = 2 \cdot 2/250 = 1.6\%$$

For a flight in which the velocity contribution is ten percent of the potential contribution an error (simple sum) is expected of:

$$.9(1/3) + .1(1.6) = .46\%$$

The range data was obtained from the tracking center on magnetic tape. Several mistakes in this data required correction. For example, there were five to ten cases each flight of repeated data which had to be eliminated. Experience using the range data has revealed a few instances in the record where the radar apparently strayed. For instance, over a twenty second period the record may show the plane suddenly climb a thousand feet at rates of over 100 ft/sec and immediately drop back down. These are periods in which the aircraft should have been in level flight. No such changes were remembered by the people on the aircraft who surely would have felt air pockets of such a nature. In any event, removal of such spurious records from the integration results in changes of only hundredths of nanoseconds out of a total of approximately 45 ns. Considering all these factors we place an uncertainty of  $\pm 0.5\%$  on the prediction calculated using the range data. This corresponds to about

.2 to .25 nanoseconds and, as will be seen later, does not seriously affect the overall accuracy obtained from the entire experiment.

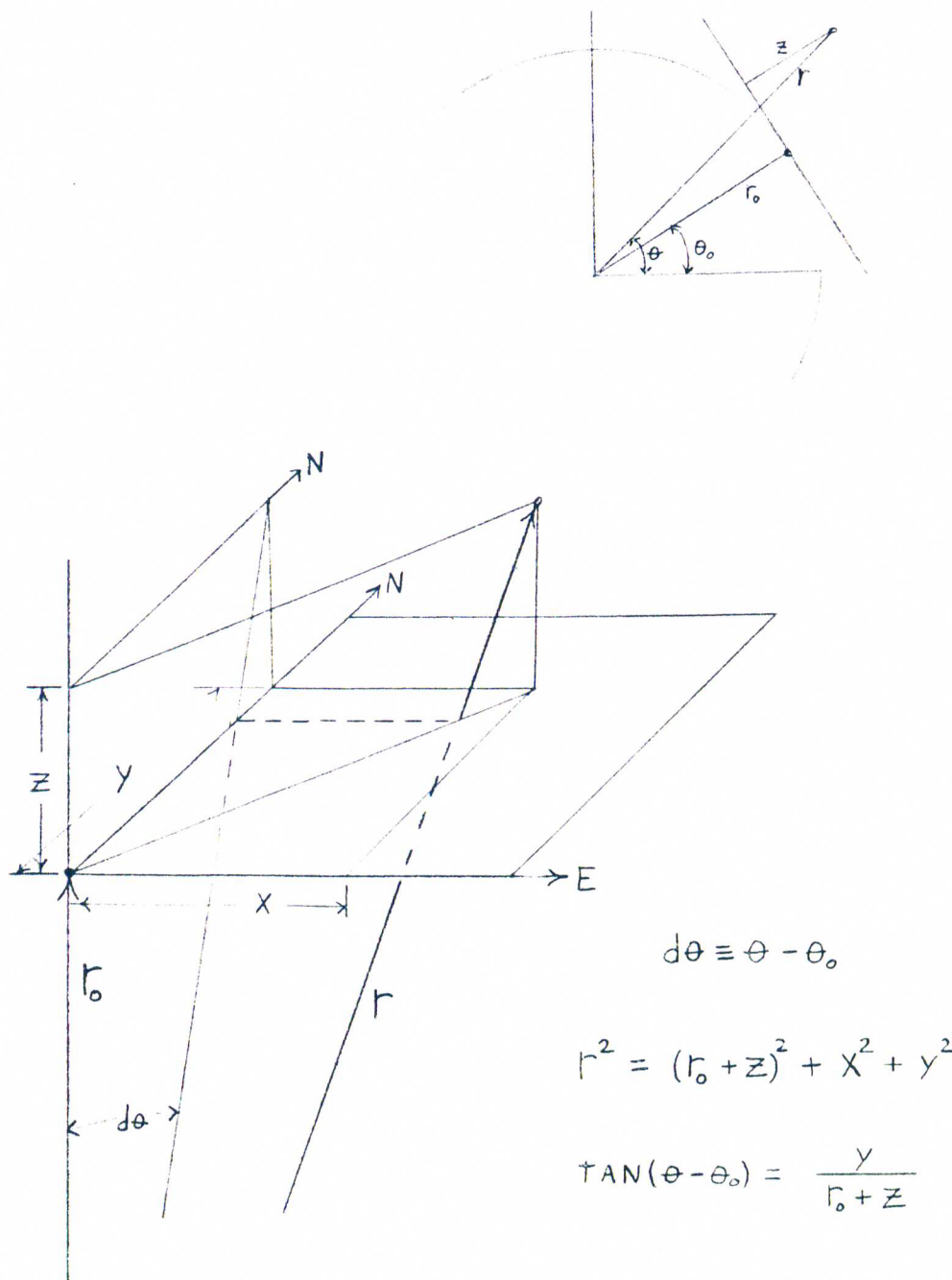


Figure 16. The relation of range coordinates to inertial system coordinates

## CHAPTER VI

### STATISTICS

#### A. Preliminary Concepts and Definitions

The subject of the statistics of atomic frequency standards has received much attention<sup>38-41</sup>. The general trend of notation used in these and other such articles is adopted for use here. The remainder of this section is a brief summary of concepts and definitions.

For a frequency standard with voltage

$$V(t) = \left( V_0 + \epsilon(t) \right) \sin(\omega_0 t + \phi(t))$$

the nominal amplitude and angular frequency are  $V_0$  and  $\omega_0$ .

It will always be assumed that  $\epsilon(t)$  and  $\dot{\phi}(t)$  are sufficiently small that the definitions to follow are meaningful. The instantaneous fractional frequency deviation is

$$y(t) = \frac{1}{\omega_0} \dot{\phi}(t)$$

and the fractional phase deviation is

$$x(t) = \frac{1}{\omega_0} \phi(t) \quad .$$

Note that  $y(t) = \dot{x}(t)$  and that  $x$  has dimensions of time ( $x$  is the phase measured in the time domain). The average frequency deviation for a period  $(t_k, t_k + \tau)$  is

$$\bar{y}_k = \frac{1}{\tau} \int_{t_k}^{t_k + \tau} y(t) dt = \frac{1}{\tau} [x(t_k + \tau) - x(t_k)]$$

One measure of frequency stability is the "Allan Variance"<sup>37</sup>

defined by

$$\sigma^2(\tau) = \left\langle \frac{1}{2} (\bar{y}_{k+1} - \bar{y}_k)^2 \right\rangle \quad (1)$$

where  $\langle \rangle$  denotes an infinite time average and  $t_{k+1} = t_k + \tau$ .

Lacking data records of infinite length, the expression used in actual practice for the Allan variance is

$$\begin{aligned}\sigma^2(\tau) &= \frac{1}{N} \sum_{k=1}^N \frac{1}{2} (y_{k+1} - y_k)^2 \\ &= \frac{1}{N} \sum_k \frac{1}{2\tau^2} (x_{k+2} - 2x_{k+1} + x_k)^2\end{aligned}\quad (2)$$

Reference 39 discusses the accuracy expected in using (2) instead of (1).

We will also make use of  $S_y(f)$ , the one-sided (power) spectral density of  $y(t)$ . For white frequency noise  $S_y$  is a constant,

$$S_y(f) = h_0 \quad .$$

There is the relation

$$S_x(\omega) = \frac{1}{\omega^2} S_{\dot{x}}(\omega) = \frac{1}{\omega^2} S_y(\omega) \quad .$$

If  $R_x(\tau)$  is the autocorrelation function

$$R_x(\tau) = \lim_{T \rightarrow \infty} \frac{1}{T} \int_{-\tau}^{\tau} x(t) \cdot x(t+\tau) dt = \langle x(t) \cdot x(t+\tau) \rangle$$

then  $R_x(\tau)$  and  $S_x(\omega)$  are Fourier transforms of each other:

$$R_x(\tau) = \frac{1}{2\pi} \int_{-\infty}^{\infty} S_x(\omega) e^{-i\omega\tau} d\omega \quad (S_x(\omega) \text{ two-sided here})$$

### B. Computation of Variances

Since  $x(t)$  is the phase in the time domain we are often interested in the variance of quantities that are essentially phase differences; quantities of the form

$$x_2 - x_1 \quad \text{or} \quad x_3 - \frac{1}{2}(x_2 + x_1) \quad , \quad \text{where } x_i = x(t_i) \quad .$$

A useful theorem for calculating such variances is the following:

If  $D$  is a linear combination of phases

$$D = \sum_{i=1}^N \alpha_i x_i \quad , \text{ where } \alpha_i \text{ are coefficients}$$

and  $\sum \alpha_i = 0$       and  $\langle D \rangle = 0$

then for pure white frequency noise ( $h_0$  defined on previous page)

$$\sigma^2(D) = -\frac{h_0}{2} \sum_{\substack{i>j \\ i>j}}^N \alpha_i \alpha_j (t_i - t_j) \quad , \text{ where } i>j \Rightarrow t_i > t_j .$$

This result is proved in Appendix C. The condition that the sum of the coefficients be zero assures that only phase differences are being considered. As an example of this result consider the difference between the phase values of two standards at time  $t_1$  and  $t_2$  and assume a mean slope has been removed so that the condition that  $\langle x_2 - x_1 \rangle = 0$  is satisfied. Application of the above theorem reveals that the variance of the quantity  $x_2 - x_1$  is

$$\sigma^2(x_2 - x_1) = \frac{h_0}{2} (t_2 - t_1) \quad .$$

This theorem may also be used to relate the Allan variance to the constant  $h_0$ . The result is

$$\sigma^2 = \frac{h_0}{2\tau} \tag{1}$$

indicating that if only white frequency noise exists a plot of the Allan variance,  $\sigma(\tau)$ , against the time interval,  $\tau$ , will decrease as  $\tau^{-1/2}$ . This is one way of experimentally determining the value of  $h_0$  for actual atomic clocks. Such a determination has been made for the principal Cesium standards used in this experiment (the six standards in clock boxes). Of course, care must be taken that an unfortunate choice of

reference clock does not bias the determination. Experience with data taken both during the actual flight and also during a ten day run, and often using the paper clocks, has shown that a typical value for the clocks used in this experiment is

$$\sqrt{h_0/2} = 7 \times 10^{-12} .$$

This is for a single clock versus a single clock. The constant is given in this form since this form appears often in calculating the standard deviation of quantities.

Figure 17 is a plot of such "sigma-tau" data for the ten day run. It is presented as being typical of clock performance. The dashed line labeled system resolution results from a measurement of the reference clock against itself. The top plot (the worst one) is of Cesium clock #752 which did not have the high beam current option. The "confidence" appearing at the top of the figure is a theoretical expectation based on the number of measurements (see reference 39). Its meaning is as follows: let  $\sigma_\infty^2$  and  $\sigma_n^2$  be the Allan variances for an infinite and finite (n points) sequence of data (equations 1 and 2). Then define  $\delta$  to be

$$\delta = \frac{\sigma_\infty - \sigma_n}{\sigma_\infty} .$$

Then the "confidence" is  $\sigma(\delta)$  expressed as a percent ( $100 \times \sigma(\delta)$  ).

Figure 18 is a similar plot for the Rubidium clocks using a Cesium as reference. The wide lines appearing on this figure are the same as those on figure 17 to facilitate comparison. A plot for the hydrogen maser is also on figure 18. However since the masers are roughly the same quality as the cesium standards for these time periods, such a measurement of maser against Cesium standard is not very meaningful.



### C. Projection of Phase

If the phase difference,  $x(t)$ , between two frequency standards is known for the period  $(t_1, t_2)$  a plot of such data would appear as in figure 19. The question arises as to the best method of estimating the phase at a later time,  $t_3$ . The criteria for this choice is that the chosen method shall have the least variance of the quantity  $x_3 - \hat{x}_3$ , where  $x_3$  is the phase the clock actually produces at  $t_3$  and  $\hat{x}_3$  is the estimated value. Dr. Leonard Cutler has considered three methods of phase projection and calculated the associated variances<sup>42</sup>. The three methods are as follows:

1. Two point projection - projects along a line defined by the first and last points,  $x_1$  and  $x_2$ :

$$\hat{x}_3 = x_2 + \frac{x_2 - x_1}{t_2 - t_1} (t_3 - t_2)$$

2. Linear regression slope projected from last point - projects along a line extending from the last point,  $x_2$ , and having the same slope as the linear regression line fit to the data:

$$\hat{x}_3 = x_2 + A(t_3 - t_2) \quad , \text{ where the regression line is } x = At + B$$

3. Pure linear regression - projects along the linear regression line fit to the data:

$$\hat{x}_3 = At_3 + B$$

If  $N$  is the number of samples used in the linear regression line and if

$$\alpha = \frac{t_3 - t_2}{t_2 - t_1} = \frac{\text{prediction time}}{\text{calibration time}}$$

and

$$\delta = x_3 - \hat{x}_3$$

then the results of Dr. Cutler's calculations are as follows:

Method	$\delta$	$\sigma^2(\delta)$
1	$x_3 - x_2 - \alpha(x_2 - x_1)$	$\frac{h_0}{2} (1+\alpha)(t_3 - t_2)$
2	$x_3 - x_2 - A(t_3 - t_2)$	$\frac{h_0}{2} \left[ 1 + \alpha \frac{6(N^2+1)}{5N(N+1)} \right] (t_3 - t_2)$
3	$x_3 - At_3 - B$	$\frac{h_0}{2} \left[ \frac{(2N-1)(N-2)}{15N(N+1)\alpha} + \frac{6(N^2+1)}{5(N^2+N)} (1+\alpha) \right] (t_3 - t_2)$

Note that the two point projection is the best (has the least variance) and that the least squares method is the worst. In fact the variance in the latter case can be large even when  $\alpha \ll 1$ ! It is plausible that the two point method is best since it gives the average frequency over the interval, ie.

$$\bar{y} = \frac{1}{t_2 - t_1} \int_{t_1}^{t_2} y(t) dt = \frac{1}{t_2 - t_1} \int_{t_1}^{t_2} \dot{x}(t) dt = \frac{x_2 - x_1}{t_2 - t_1}$$

Thus we will use the two point method in projecting phase. In actual practice we use the average of a small number of points ( $\sim 5$ ) at the beginning and end of the phase record to aid in the suppression of phase noise.

The phase data that results from a flight will have the form of figure 20. That is, a clock that is flown is compared to a ground clock before flight (the period  $t_1$  to  $t_2$ ) and after flight ( $t_3$  to  $t_4$ ). Upon returning from flight the clock is expected to have gained time (with respect to the ground clock) because of the potential effect and therefore will show a step as indicated in figure 20. The preflight record may be projected forward to a time,  $t$ , and the postflight record

projected backward to the same time,  $t$ . The difference between these two projected phases,  $\Delta x(t)$  is the time gained by the clock. We call this number the "shift". In the graphs to be presented the slope of the preflight file has often been removed to enhance the readability. This results in a graph of the form of figure 21. Use of the two point projection method gives

$$\Delta x(t) = \left[ x_3 - \frac{x_4 - x_3}{t_4 - t_3} (t_3 - t) \right] - \left[ x_2 + \frac{x_2 - x_1}{t_2 - t_1} (t - t_2) \right]$$

The variance of this quantity may be calculated using the theorem described earlier. This result, first calculated by Dr. Cutler, is as follows:

$$\sigma^2(\Delta x) = \frac{h_o}{2} \left[ \alpha_f^2 (t_2 - t_1) + \alpha_r^2 (t_4 - t_3) + t_3 - t_2 \right] \quad (2)$$

where

$$\alpha_f = \frac{t - t_2}{t_2 - t_1} \quad \text{and} \quad \alpha_r = \frac{t_3 - t}{t_4 - t_3} .$$

A minimum of  $\sigma^2(\Delta x)$  exists at the time

$$t_o = \frac{t_2 t_4 - t_3 t_1}{t_2 - t_1 + t_4 - t_3}$$

resulting in

$$\Delta x(t_o) = \frac{x_3 - x_2 - \beta(x_4 - x_1)}{1 - \beta} \quad (3)$$

$$\sigma^2(\Delta x)_{t_o} = \frac{h_o}{2} \left[ \frac{1}{1 - \beta} \right] (t_3 - t_2) , \quad \beta \equiv \frac{t_3 - t_2}{t_4 - t_1} \quad (4)$$

#### D. Combinations of Measurements

In an actual flight there are several flying clocks and several ground clocks. The "shift",  $\Delta x$ , between each of these clocks and the reference clock can be obtained. Let  $\Delta x_{fi}$  be the shift of the  $i^{\text{th}}$  flying clock with respect to the reference, and  $\Delta x_{gj}$  the shift of the  $j^{\text{th}}$  ground clock with respect to the same reference. Let the number of flying and ground clocks be  $N$  and  $M$  respectively. The mean shift of the air and ground ensembles are as follows:

$$\begin{aligned} \text{Air:} \quad \Delta x_f &= \frac{1}{N} \sum_{i=1}^N \Delta x_{fi} \\ \text{Ground:} \quad \Delta x_g &= \frac{1}{M} \sum_{j=1}^M \Delta x_{gj} \end{aligned} \tag{5}$$

The quantity  $\Delta x_g$  will not be exactly zero because of the intrinsic statistical variations of the clocks. Each of the above two quantities depends on the choice of reference clock. However their difference does not. Hence the ensemble shifts may be combined to obtain the overall shift for the flight of

$$\Delta x = \Delta x_f - \Delta x_g \tag{6}$$

independent of which clock is being used as reference. Note that this result may also be interpreted as the mean of  $N$  measurements of single flying clocks versus the ground ensemble:

$$\Delta x = \frac{1}{N} \sum_{i=1}^N \left[ \Delta x_{fi} - \left( \frac{1}{M} \sum_{j=1}^M \Delta x_{gj} \right) \right]$$

If  $\sigma_f^2$  and  $\sigma_g^2$  are the variances of the  $\Delta x_{fi}$  and the  $\Delta x_{gj}$  respectively, then the formal variance of  $\Delta x$  is

$$\sigma^2(\Delta x) = \frac{\sigma_f^2}{N} + \frac{\sigma_g^2}{M} \quad (7)$$

and this expression is also independent of the choice of reference.

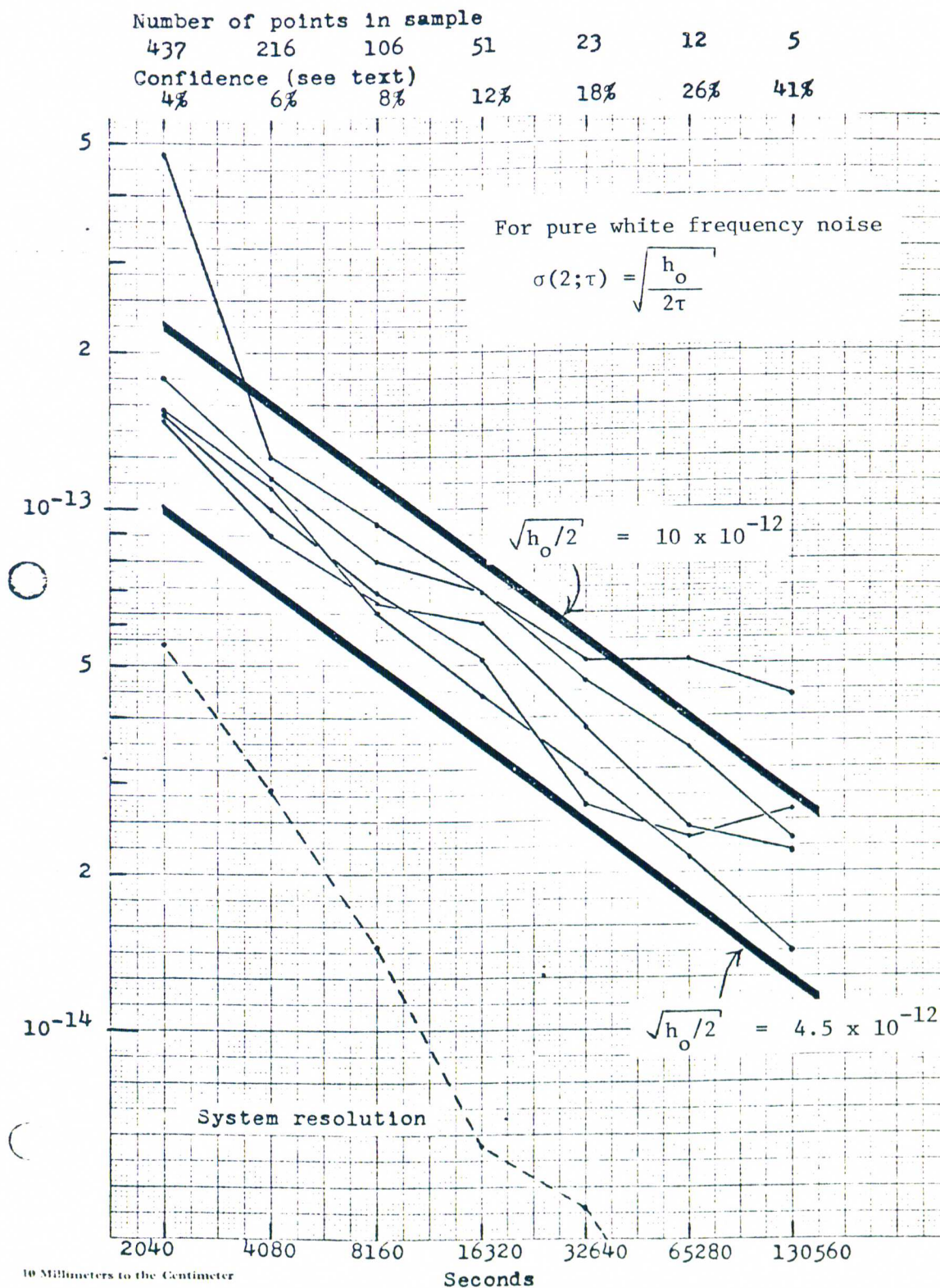


Figure 17. Sigma-tau plot for the principal Cesium clocks.  
The reference is one single Cesium clock.

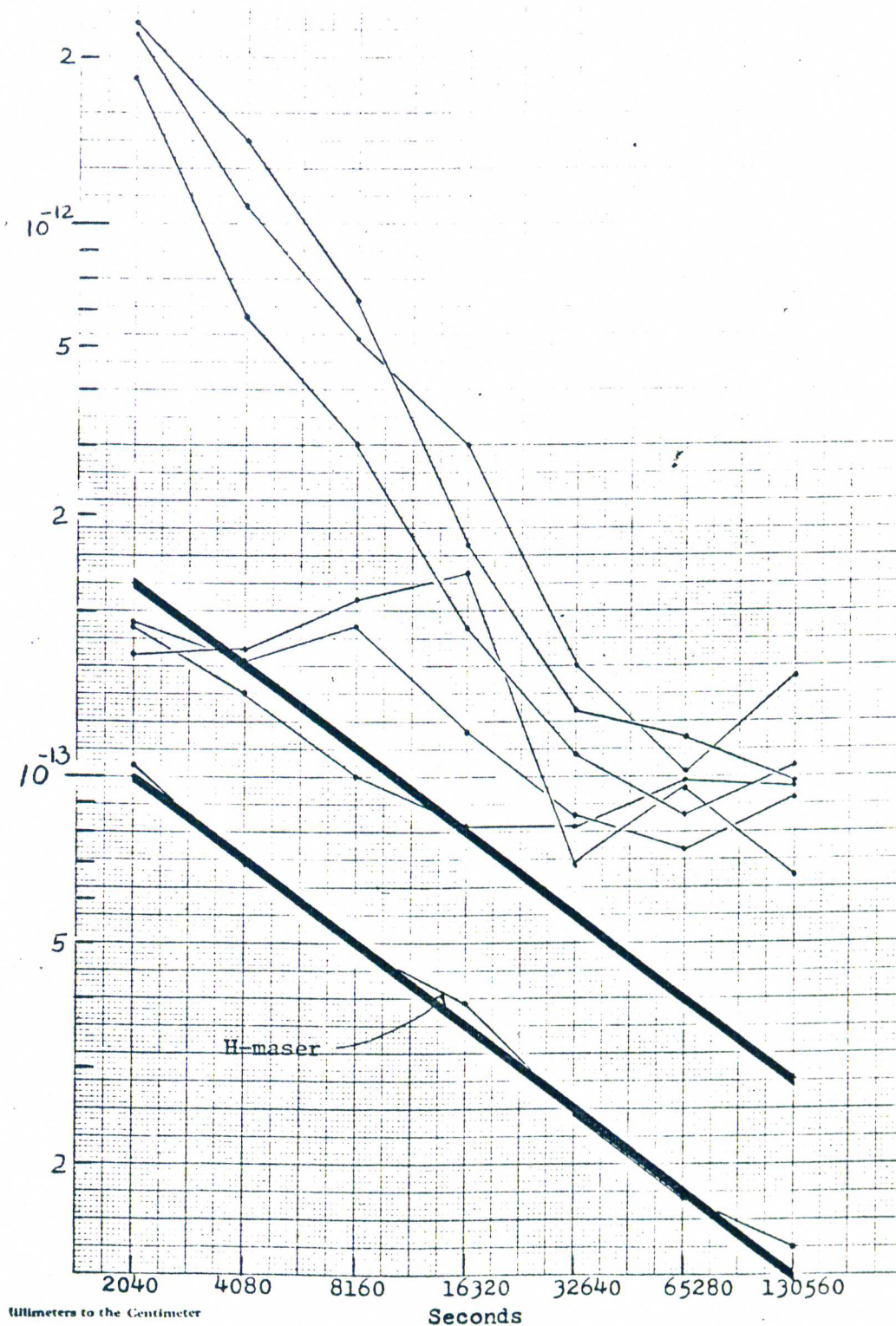


Figure 18. Sigma-tau plot for the Rubidium clocks and H-maser. The broad lines are the same as in figure 17 to facilitate comparison. The H-maser plot is largely covered by the lower broad line. The number of samples is the same as the previous graph.



Figure 19. Typical form of phase data.

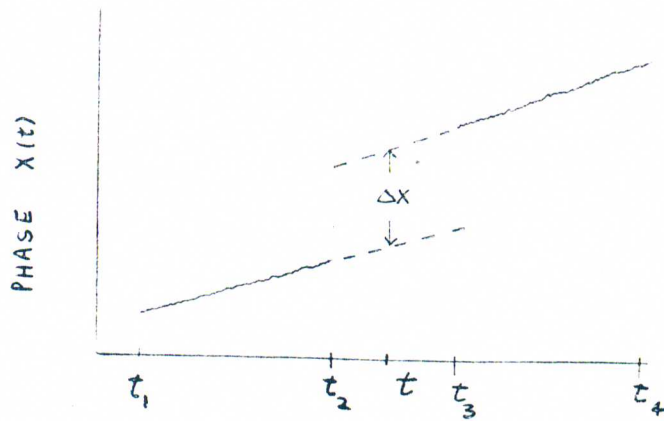


Figure 20. Typical form of phase data over a flight.

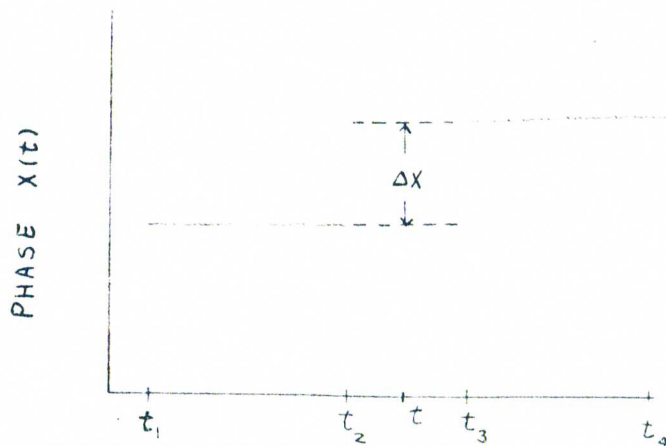


Figure 21. Typical form of phase data with slope removed.



CHAPTER VII  
RESULTS AND INTERPRETATIONS

A. Introduction

The shifts,  $\Delta x$ , as described in the previous chapter, are computed by a computer program named SHIFT. SHIFT will calculate the  $\Delta x_{fi}$  of each clock with respect to any designated choice of ground clock ensemble. Inspection of the plotted data from each flight enabled a determination as to which clocks behaved well enough to include in the ground set for the purpose of this calculation.

SHIFT calculates the  $\Delta x_{fi}$  at the time of minimum uncertainty (as described in the previous chapter) and also at the first and last times of the flight period. The latter numbers then give some idea of the amount that a particular  $\Delta x_{fi}$  varies depending on the time at which it is calculated. The program is also capable of using an intermediate time given to it by the operator. This feature is useful when examination of the inflight intercomparison phase data reveals that one of the clocks has clearly changed rates at a particular time. This time is then a good choice for use in calculating the  $\Delta x_{fi}$ .

The rate of a clock with respect to the ground ensemble sometimes appears to make a small rate change during the preflight or postflight period. In such cases SHIFT is also run using only the portion of that file between the flight and the apparent rate change. For the two-point projection method, this procedure is identical to correcting for the rate shift and using the full extent of data. It should be noted that apparent rate changes are not always "real". For example a clock modeling program by L. Cutler resulted in the traces shown in figure 35 (page 82). One

trace appears to make a distinct rate change, but it is only an artifact of the statistical process. The above procedures have been used to generate two sets of  $\Delta x_{fi}$ . The first set is a "selected" set in which the  $\Delta x_{fi}$  have been calculated at the optimum time, or at a time when a rate change during flight was deduced to have occurred, and/or using a lesser extent of the pre- or postflight file when rate changes apparently occurred in them. In short, the selected set of  $\Delta x_{fi}$  rest on a large amount of subjective, but hopefully fair and unbiased, human judgement.

The second set of  $\Delta x_{fi}$  is called the "mean" set. These are generated by considering all runs of SHIFT made for various lengths of the pre- and postflight files, extracting the minimum and maximum shift of these values, and then taking the mean of those two numbers.

It is gratifying to note that the result for the entire experiment is virtually identical using either of the two sets.

### B. The Principal Results

Figures 22-26 (pages 69-73) show the results of the theoretical prediction based on the range data. The wiggles in the lines are due both to earth rotation and winds, both of which add and subtract as the plane travels through a complete orbit. Figures 27-31 (pages 74-78) are summary sheets for each of the five major flights. They contain information about the shifts,  $\Delta x_{fi}$ , of each of the three principal flying Cesium clocks in the clock box with respect to the chosen ground ensemble. Also shown are the normalized values (measured value divided by predicted value) of these shifts. The overall result of the flight, the average of these three numbers, is also indicated. The indicated standard deviation (SD) is the straight-forward standard deviation of the three numbers. The standard deviation of the mean is calculated using equation 7 of chapter VI and therefore includes the variations of clocks in the ground set as well.

The two dashed lines in each figure represent the  $\pm .5\%$  uncertainty in the calculated prediction. We summarize here the results of those five flights, giving a triplet of numbers consisting of the normalized shift, standard deviation, and standard deviation of the mean:

<u>Flight</u>	<u>Mean Shifts</u>			<u>Selected Shifts</u>		
1 ( 9/29)	.999	.021	.016	1.013	.013	.013
2 (11/11)	.977	.044	.026	.986	.063	.037
3 (11/14)	.963	.020	.013	.963	.019	.012
4 (11/22)	1.002	.008	.026	.986	.012	.027
5 ( 1/10)	.991	.063	.037	.979	.043	.026

Referring again to figures 27-31, the dark points refer to  $\Delta x_{fi}$  from the mean set and the open circles refer to  $\Delta x_{fi}$  from the selected set. The error bars displayed on the flight result (the average of the three measurements) are a wide bar for the standard deviation (SD) and a narrow bar for the standard deviation of the mean (SDM) as described above. The error bars attached to the three individual measurements are as follows: the right (narrow) error bars indicate the minimum and maximum shifts as described earlier. The left (wide) error bars show the standard deviation expected on statistical grounds. This standard deviation is calculated by first using equation 4 of chapter VI to calculate  $\sigma(\Delta x_{fi})$ , this value being for two individual clocks. Since the shift values reported here are being calculated with respect to the entire ground ensemble of M clocks, one must make the modification:

$$\sigma_M = \frac{\sigma}{\sqrt{2}} \left[ 1 + \frac{1}{M} \right]^{1/2}$$

It is this value that is plotted as the wide error bars.

Since flight duration and other parameters were reasonably similar for each of the five flights it is possible to calculate an "average"

statistically expected standard deviation. Using the average parameters from the flights results in a value (equation 4, chapter VI) for  $\sigma(\Delta x_{fi})$  of approximately 2 ns for a single clock versus a single clock. Assuming three flying clocks and an average of four good ground clocks for a flight results in an expectation for  $\sigma(\Delta x)$  of (equation 7, chapter VI):

$$\sigma(\Delta x) = \left( \frac{2^2}{3} + \frac{2^2}{4} \right)^{1/2} = 1.53 \text{ ns} .$$

Using 45 ns as an approximation to the  $\Delta x$  for each flight, an uncertainty of 3.4% is therefore expected for each flight ( $1.53/45 = .034$ ) on the basis of knowledge of clock performance.

A result for the entire experiment may be obtained by taking the fifteen principal measurements (three measurements of a flying box Cesium clock against the ground ensemble, for each of five flights) and averaging them after they have been normalized by dividing by the predicted value for each flight. Those results are as follows (normalized shift, standard deviation, standard deviation of the mean):

Mean result:	.987,	.035,	.011
Selected result:	.986,	.035,	.010

Again, the statistically expected standard deviation of the mean may be calculated by using the above value of 2 ns as the expected uncertainty for single clock against single clock. In this case there are essentially fifteen flying clocks (three per flight for five flights). The corresponding "number" of ground clocks is twenty-one. Hence by calculating

$$\sigma(\Delta x) = \left( \frac{2^2}{15} + \frac{2^2}{21} \right)^{1/2} = .68 \text{ ns}$$

and  $.68\text{ns}/45\text{ns} = .015$

it is seen that an uncertainty of approximately 1.5% is to be expected for the entire experiment. This compares to the experimentally obtained result of 1.1%. The fifteen normalized results appear in figure 32.

A histogram of flying clock and ground clock normalized shifts ( $\Delta x_{fi}$  and  $\Delta x_{gj}$ ), with respect to the ground ensemble appears in figure 33.

The errors (standard deviation of the mean) discussed above involve only clock performance. Other errors are yet to be considered. One of these is the  $\pm 0.5\%$  uncertainty attached to the calculated prediction. Since this uncertainty is clearly independent of the clock uncertainties, the two may be added in quadrature. This increases the above mentioned experimental and statistically expected standard deviations of the mean by .001 (normalized value) in each case. Hence the experimental SDM and statistically expected SDM are increased to .012 and .016 respectively. Considering all of the above, and the environmental protection afforded the clocks, a final result is given as

$$\frac{\text{Measured value}}{\text{Predicted value}} = .987 \pm .016$$

### C. The Other Clocks

The previous results were obtained using only the Cesium clocks inside of clock boxes, the masers, and Cesium clock #761 in the ground ensemble. This is because all other clocks were not of sufficient quality to include in an accurate measurement. We will consider these other clocks in this section. Data plots of all clocks in the experiment for each flight are available for inspection in appendix D.

Examination of these plots reveal that the flying Rubidium clocks distinctly changed rates both at the beginning and at the end of flight.

This occurred for each flying Rubidium clock for each flight. It is strongly suspected that this was caused by the "banging" of the clock box against its retaining ring on take-off and landing, and also by the larger-than-normal vibration occurring when the aircraft is moving at high speed on the ground. It may also be noted that in many cases the inflight Rubidium phase record is rather erratic. This may be due to vibration as the Rubidium clocks are known to be more vibration sensitive than the Cesium clocks. In general, rate changes are not necessarily fatal to a measurement because the inter-comparison data allows such rate changes to be identified and corrected for. However, when such rate changes take place both at the very beginning and end of flight, as they do here, then such a procedure is guaranteed to result in a value near that of the Cesium clocks used for the identification of the rate changes.

Similar remarks also apply to the "travelling" Cesium clocks also included on flights. Vibration was a problem with these standards both because they were not well isolated (being placed on foam cushions on the aircraft floor) from vibration, and also because they lacked the second order feed-back loop discussed in chapter II.

A program (SHIFT1) does exist for making corrected shift measurements involving multiple rate changes. The preflight data is projected to the time of the first rate change and the postflight data is projected back to the time of the last rate change. A set of "good" flying clocks is then used to determine the rates between these two times. The rate of this "good" ensemble can be determined from the pre\_ and postflight data. This information is then used by the program to compute a corrected  $\Delta x_{fi}$  for the clock in question. The results for the Rubidium and

travelling Cesium clocks are presented in figure 34. It is stressed that for the above reasons these results are in no way independent.

FT1

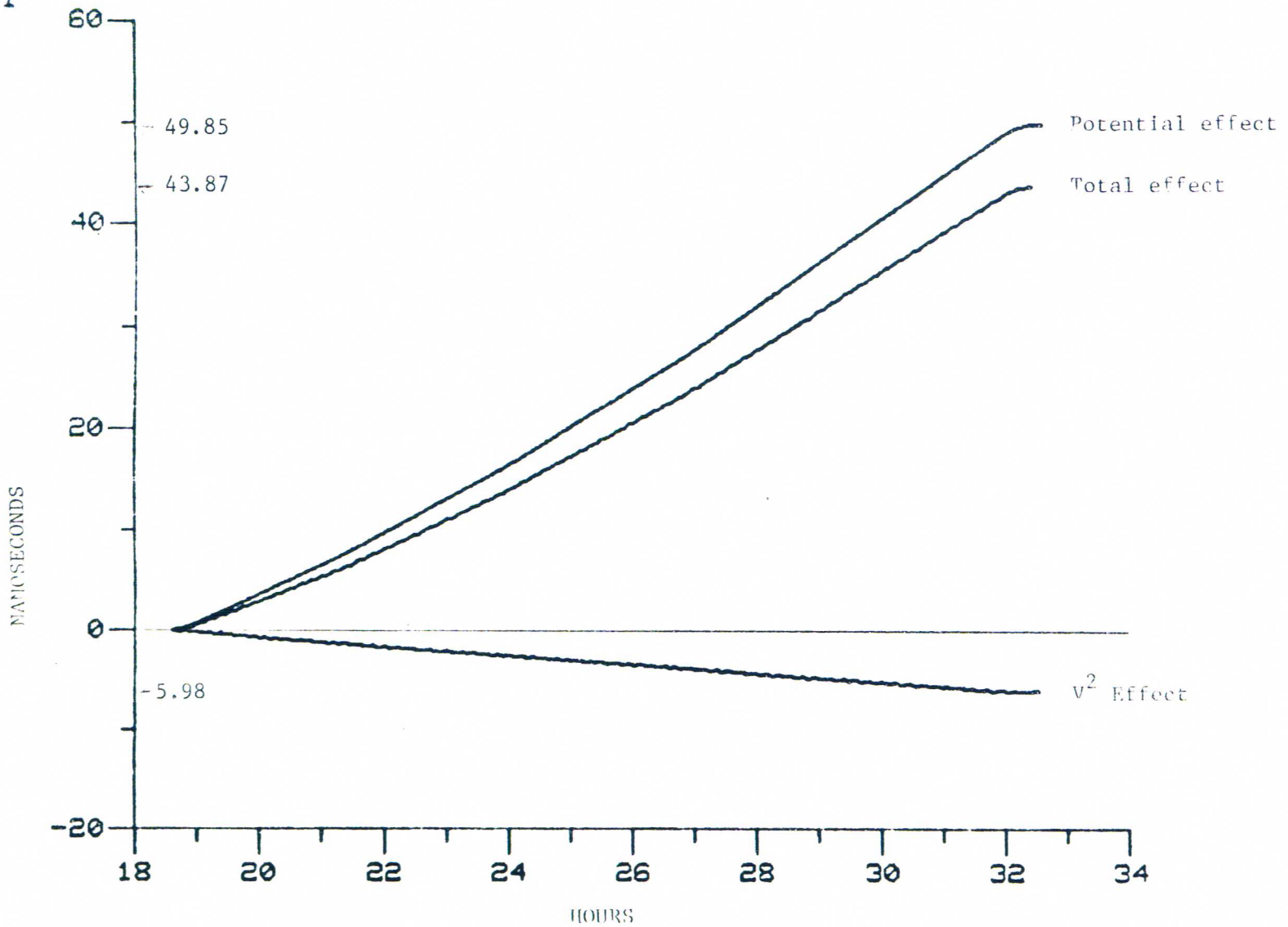


Figure 22. Graph of the theoretical prediction for flight 1 (9/29).



FT2

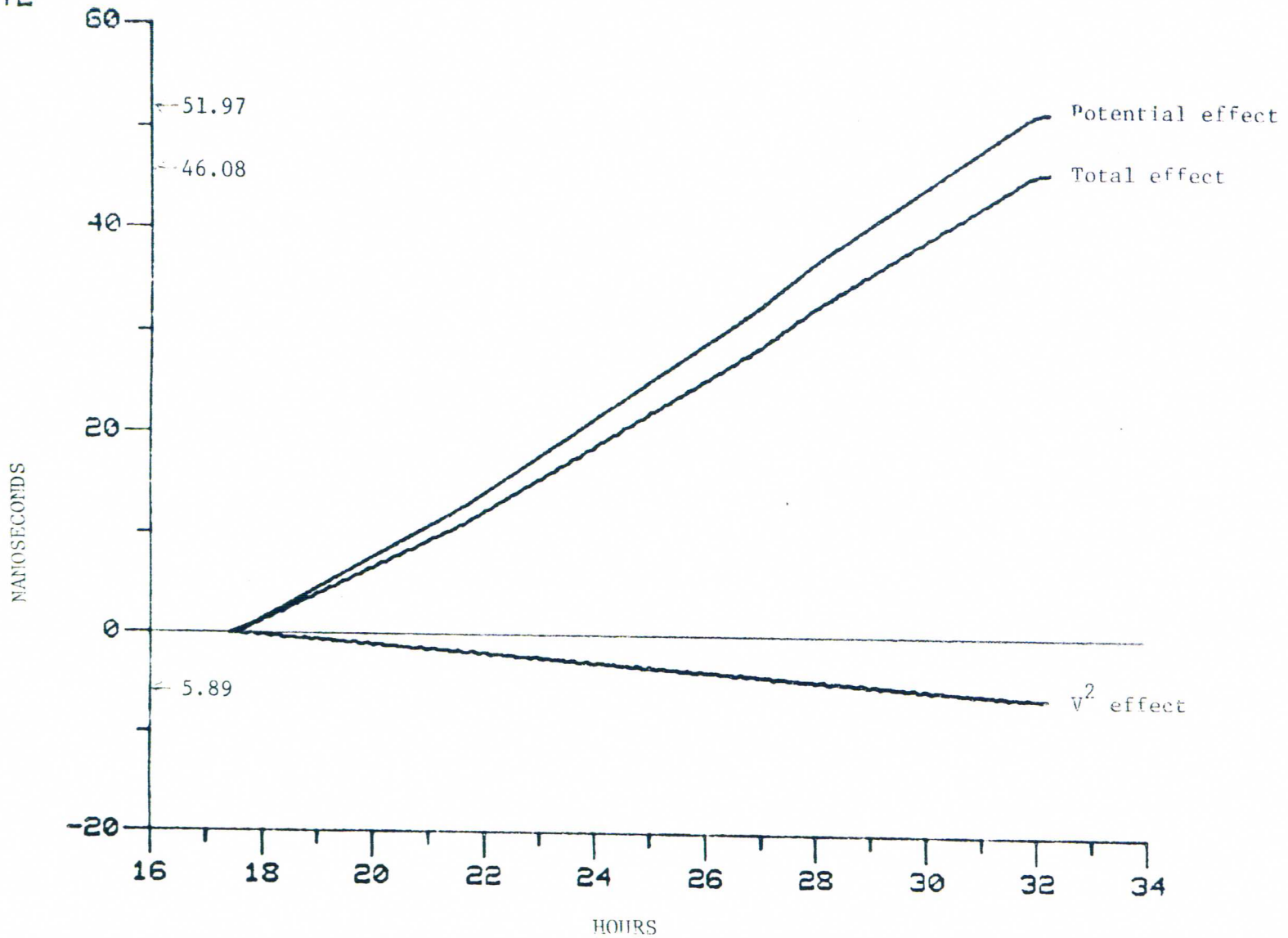


Figure 23. Graph of the theoretical prediction for flight 2 (11/11).

FT3

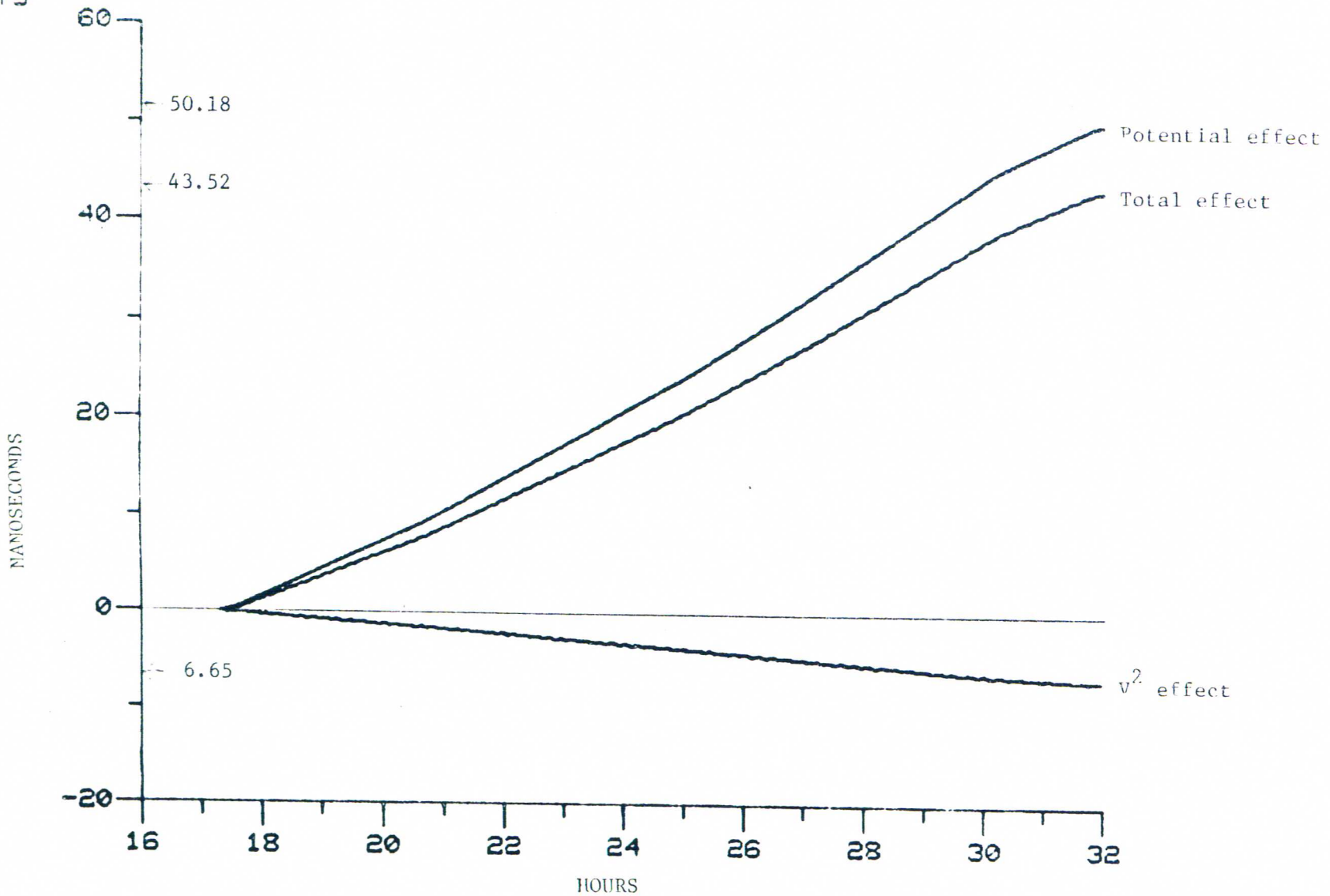


Figure 24. Graph of the theoretical prediction for flight 3 (11/14).

FT4

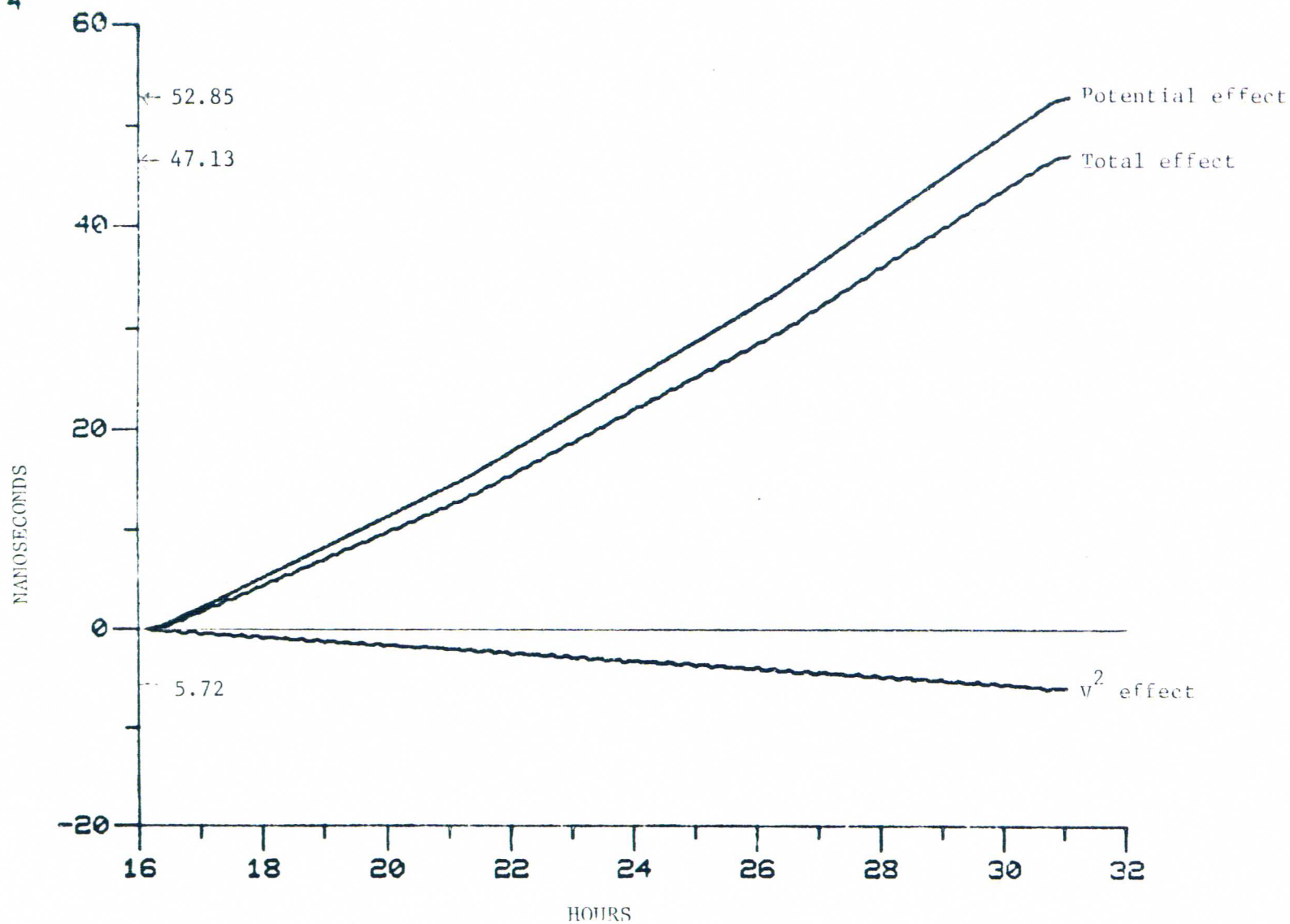


Figure 25. Graph of the theoretical prediction for flight 4 (11/22).

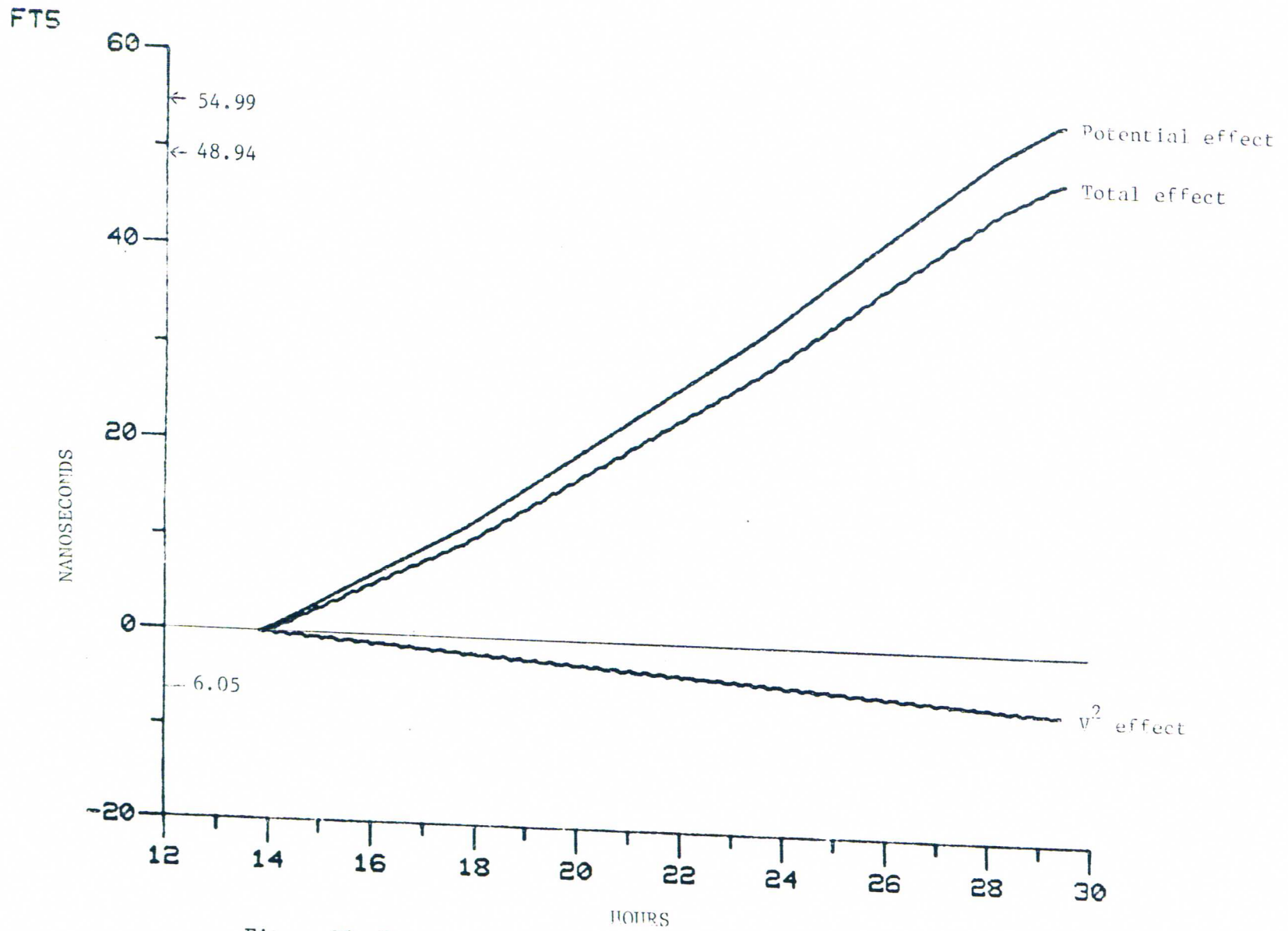
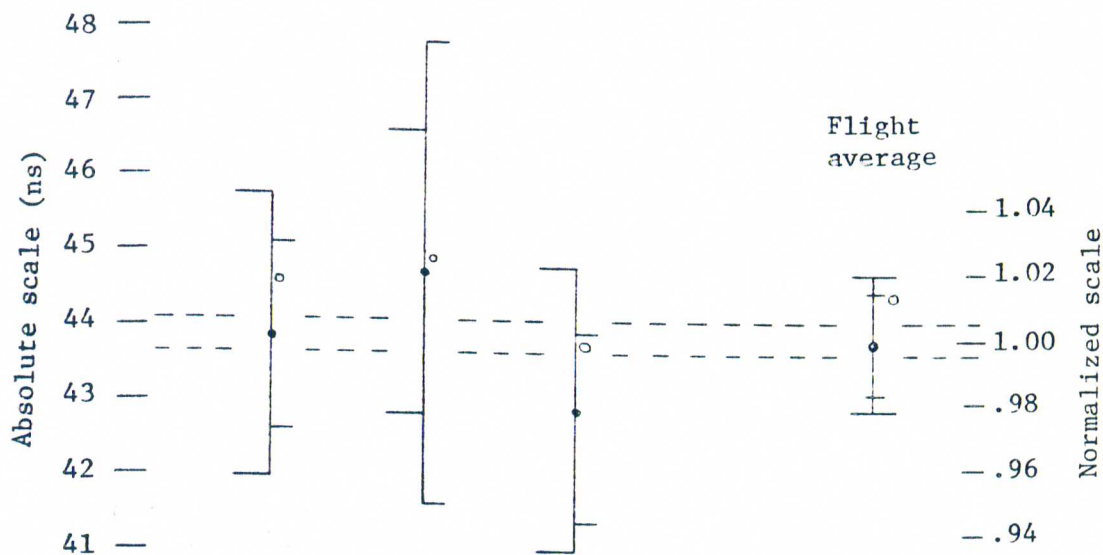


Figure 26. Graph of the theoretical prediction for flight 5 (1/10).



FLIGHT #1  
9/29

$$\text{PREDICTION} = 49.849 - 5.977 = 43.87 \text{ ns}$$

SHIFT VALUES:	<u>Cs 1</u>	<u>Cs 2</u>	<u>Cs 3</u>	<u>Mean, SD, SDM</u>
Mean method				
Absolute	43.86	44.71	42.88	43.82, .916
Normalized	1.000	1.019	.977	.999, .021, .016
Selected method				
Absolute	44.64	44.89	43.77	44.43, .588
Normalized	1.018	1.023	.998	1.013, .013, .013

Figure 27. Summary sheet for flight 1. The dashed lines represent the  $\pm 0.5\%$  uncertainty in the predicted value. The solid dots show the "mean" values, the open circles show the "selected" values.

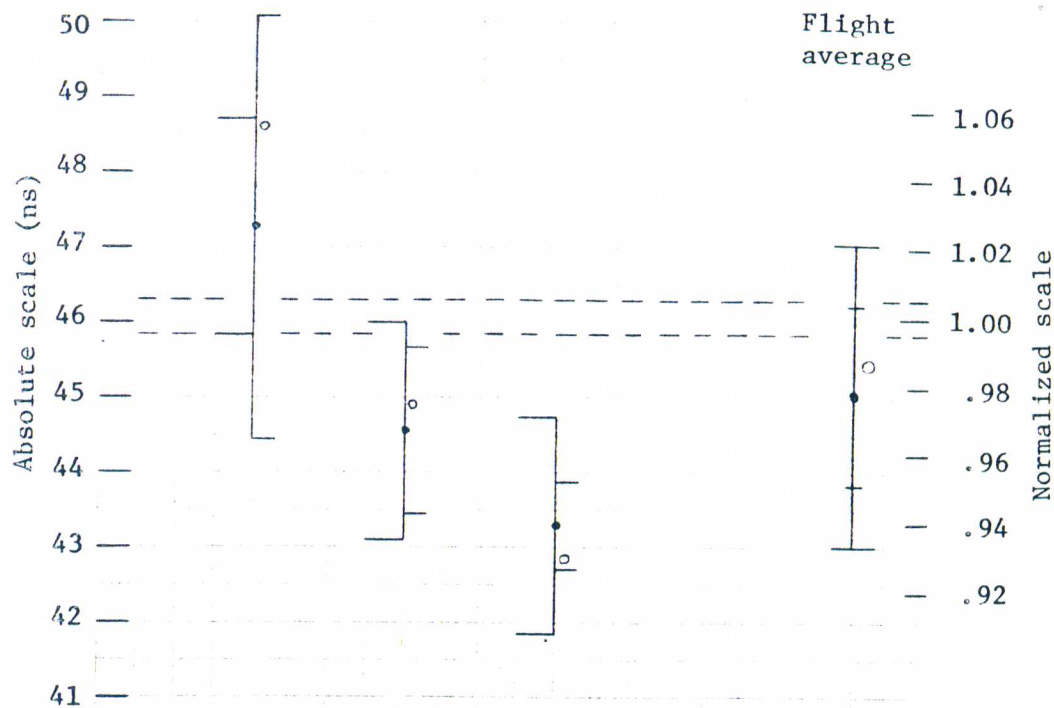
Right (narrow) error bars = Max and min of possible interpretation

Left (wide) error bars = Statistically expected variation

Error bars on the flight average: Wide = standard deviation

Narrow = standard deviation of the mean

See text for details.



FLIGHT #2  
11/11

$$\text{PREDICTION} = 51.969 - 5.890 = 46.08 \text{ ns}$$

SHIFT VALUES:	<u>Cs 7</u>	<u>Cs 8</u>	<u>Cs 9</u>	<u>Mean, SD, SDM</u>
Mean method				
Absolute	47.27	44.56	43.30	45.04, 2.03
Normalized	1.026	.967	.940	.977, .044, .026
Selected method				
Absolute	48.61	44.89	42.85	45.45, 2.92
Normalized	1.055	.974	.930	.986, .063, .037

Figure 28. Summary sheet for flight 2. The dashed lines represent the  $\pm 0.5\%$  uncertainty in the predicted value. The solid dots show the "mean" values, the open circles show the "selected" values.

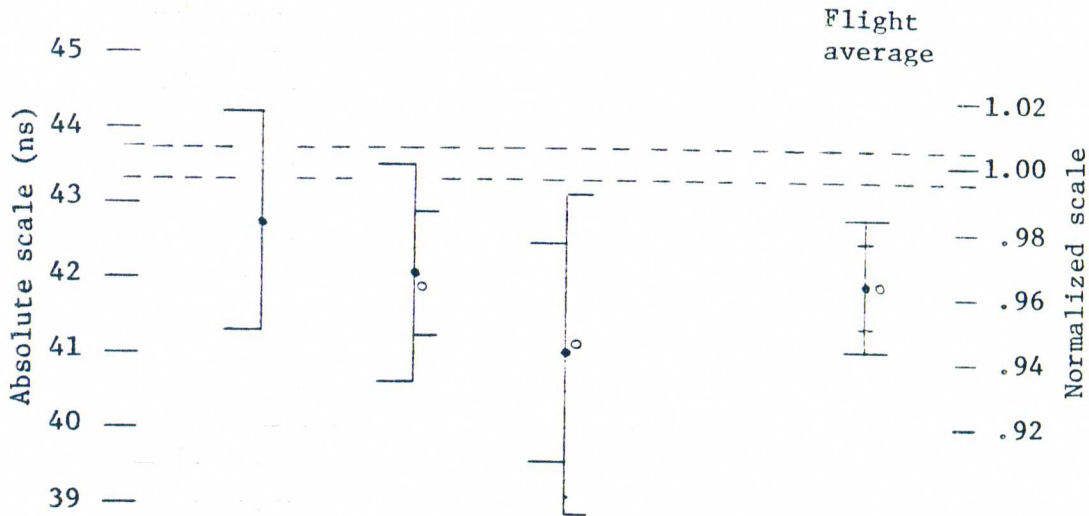
Right (narrow) error bars = Max and min of possible interpretation

Left (wide) error bars = Statistically expected variation

Error bars on the flight average: Wide = standard deviation

Narrow = standard deviation of the mean

See text for details.



FLIGHT #3  
11/14

$$\text{PREDICTION} = 50.176 - 6.653 = 43.52 \text{ ns}$$

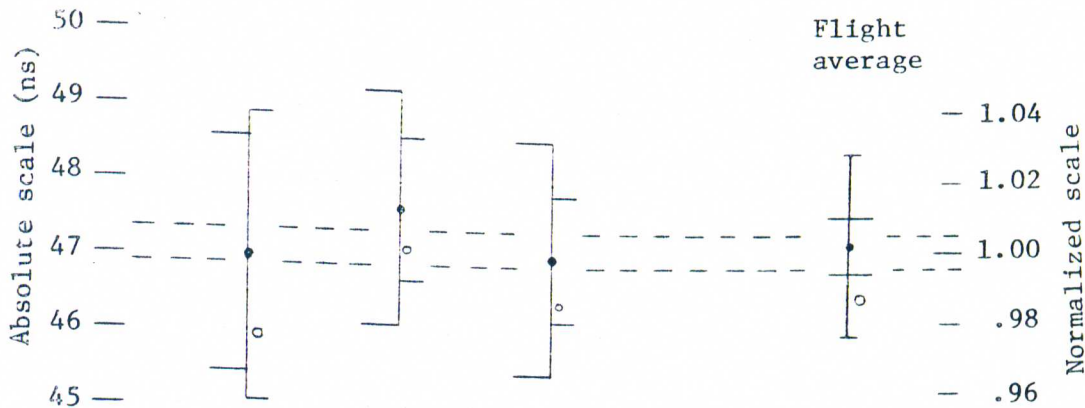
SHIFT VALUES:	<u>Cs 7</u>	<u>Cs 8</u>	<u>Cs 9</u>	<u>Mean, SD, SDM</u>
Mean method				
Absolute	42.74	42.06	40.99	41.93, .882
Normalized	.982	.966	.942	.963, .020, .013
Selected method				
Absolute	42.74	41.88	41.13	41.92, .806
Normalized	.982	.962	.945	.963, .019, .012

Figure 29. Summary sheet for flight 3. The dashed lines represent the  $\pm 0.5\%$  uncertainty in the predicted value. The solid dots show the "mean" values, the open circles show the "selected" values.

Right (narrow) error bars = Max and min of possible interpretation.  
Left (wide) error bars = Statistically expected variation.

Error bars on the flight average: Wide = standard deviation  
Narrow = standard deviation of the mean

See text for details.



FLIGHT #4  
11/22

$$\text{PREDICTION} = 52.846 - 5.719 = 47.13 \text{ ns}$$

SHIFT VALUES:	<u>Cs 1</u>	<u>Cs 2</u>	<u>Cs 3</u>	<u>Mean, SD, SDM</u>
Mean method				
Absolute	46.99	47.65	47.01	47.22, .375
Normalized	.997	1.011	.998	1.002, .008, .026
Selected method				
Absolute	45.95	47.12	46.41	46.49, .589
Normalized	.975	1.000	.985	.986, .012, .027

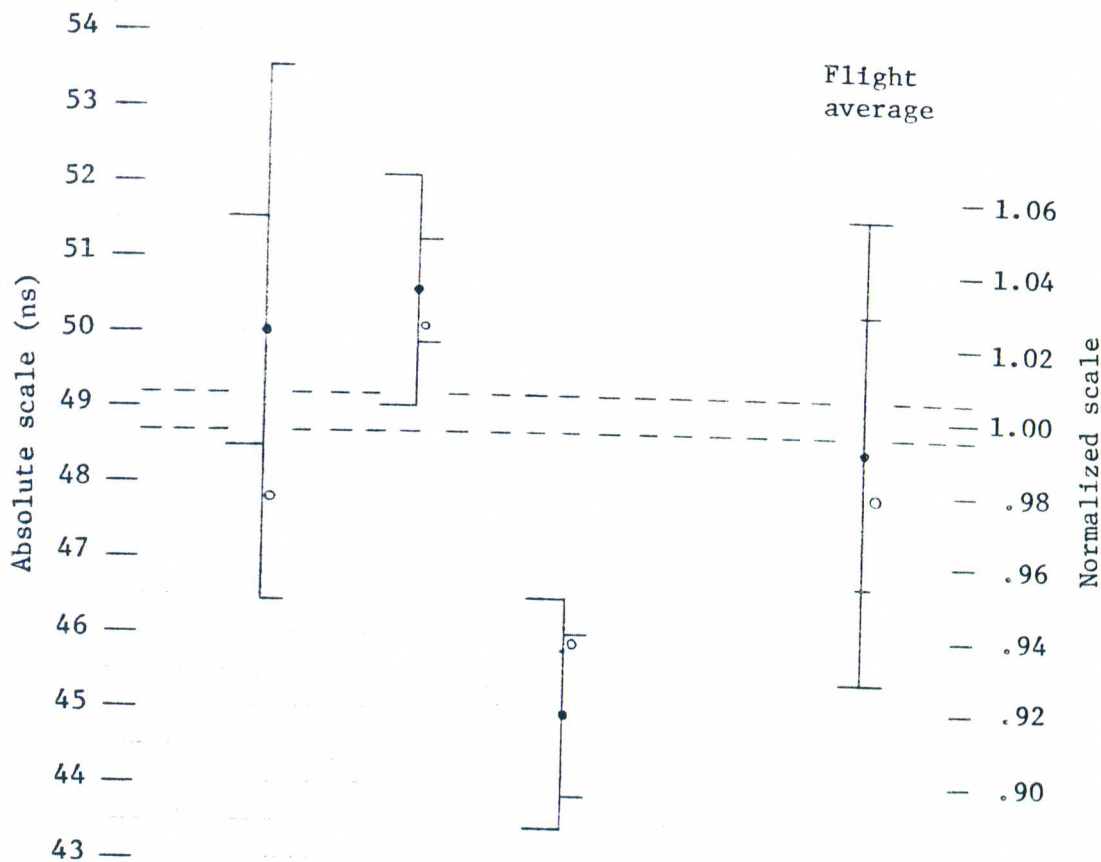
Figure 30. Summary sheet for flight 4. The dashed lines represent the  $\pm 0.5\%$  uncertainty in the predicted value. The solid dots show the "mean" values, the open circles show the "selected" values.

Right (narrow) error bars = Max and min of possible interpretation.  
Left (wide) error bars = Statistically expected variation.

Error bars on the flight average: Wide = standard deviation  
Narrow = standard deviation of the mean

See text for details.





FLIGHT #5  
1/10

$$\text{PREDICTION} = 54.996 - 6.053 = 48.94 \text{ ns}$$

SHIFT VALUES:	<u>Cs 1</u>	<u>Cs 2</u>	<u>Cs 3</u>	<u>Mean, SD, SDM</u>
Mean method				
Absolute	50.00	50.58	44.95	48.51, 3.10
Normalized	1.022	1.033	.918	.991, .063, .037
Selected method				
Absolute	47.81	50.07	45.90	47.93, 2.09
Normalized	.977	1.023	.938	.979, .043, .026

Figure 31. Summary sheet for flight 5. The dashed lines represent the  $\pm 0.5\%$  uncertainty in the predicted value. The solid dots show the "mean" values, the open circles show the "selected" values.

Right (narrow) error bars = Max and min of possible interpretation.  
Left (wide) error bars = Statistically expected variation.

Error bars on the flight average: Wide = standard deviation  
Narrow = standard deviation of the mean

See text for details.

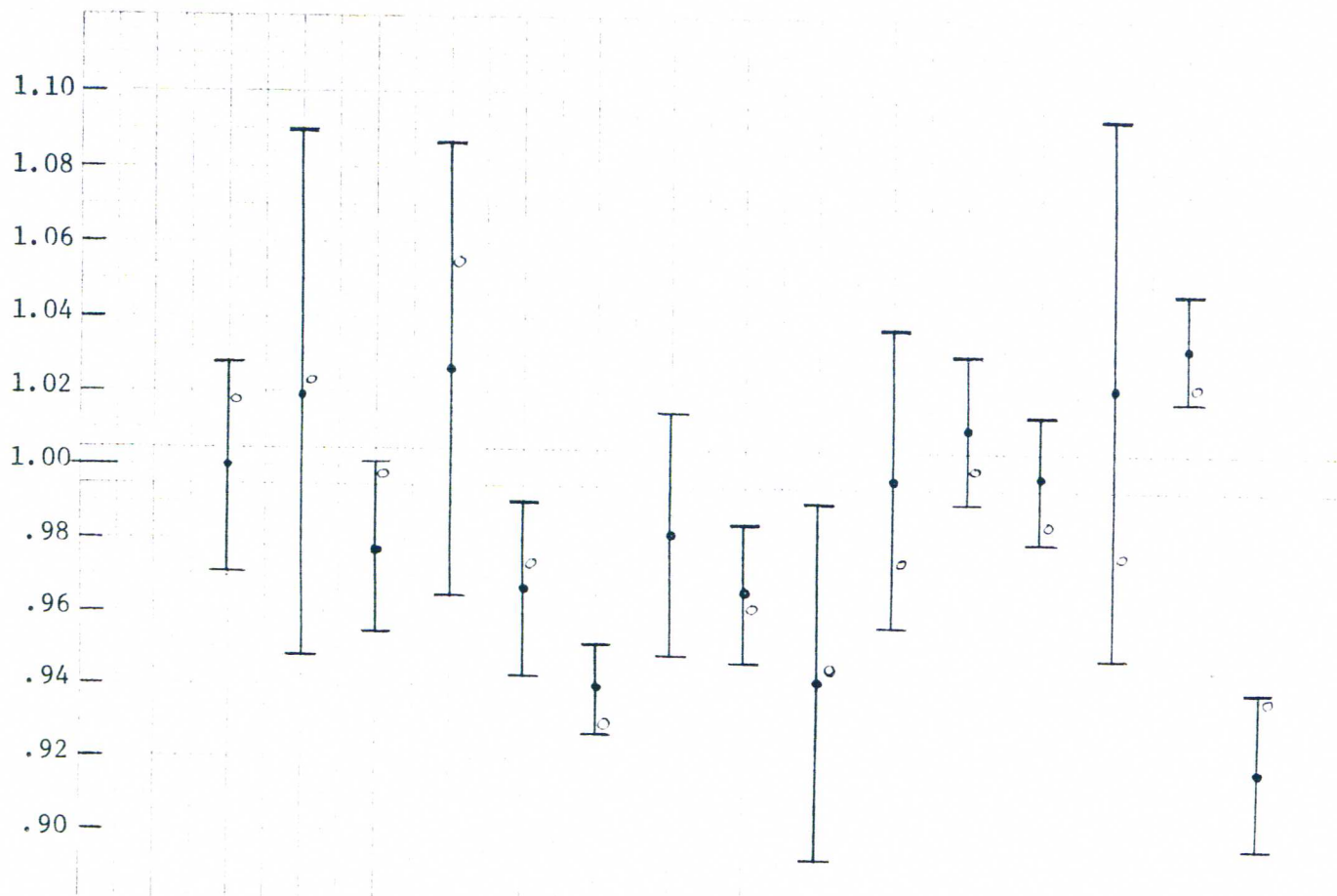


Figure 32. The fifteen principal measurements. The solid dots are the "mean" values and the open circles are the "selected" values. The error bars are the maximum and minimum as described in the text. Each value is a single flying Cesium clock with respect to a ground ensemble of clocks. The lines across the middle of the figure represent the  $\pm 0.5\%$  confidence of the prediction.

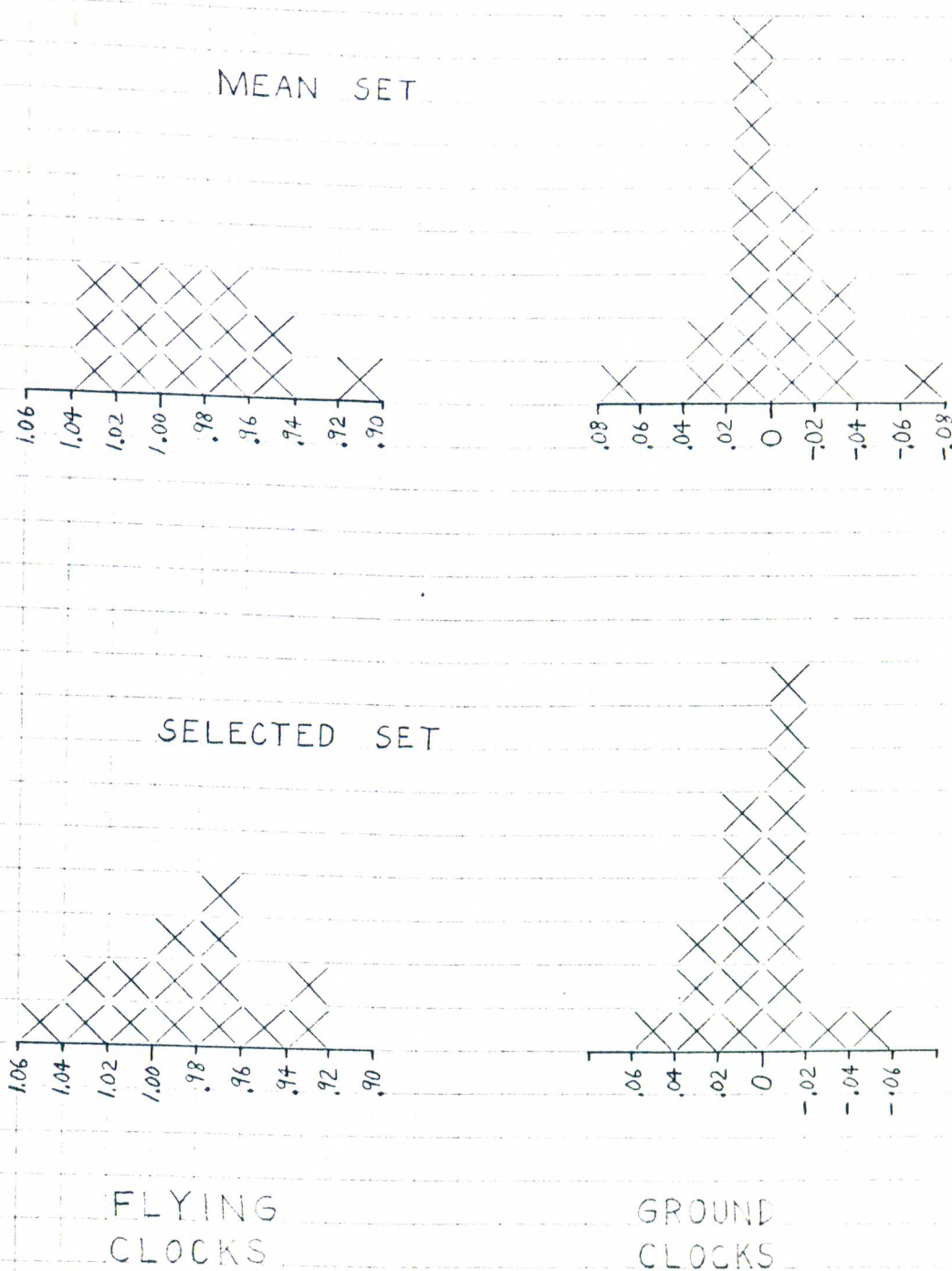


Figure 33. A histogram of flying clock and ground clock shifts. Represented are the normalized values (measured shift divided by predicted shift); hence flying clocks will have shifts near one, and ground clocks near zero.

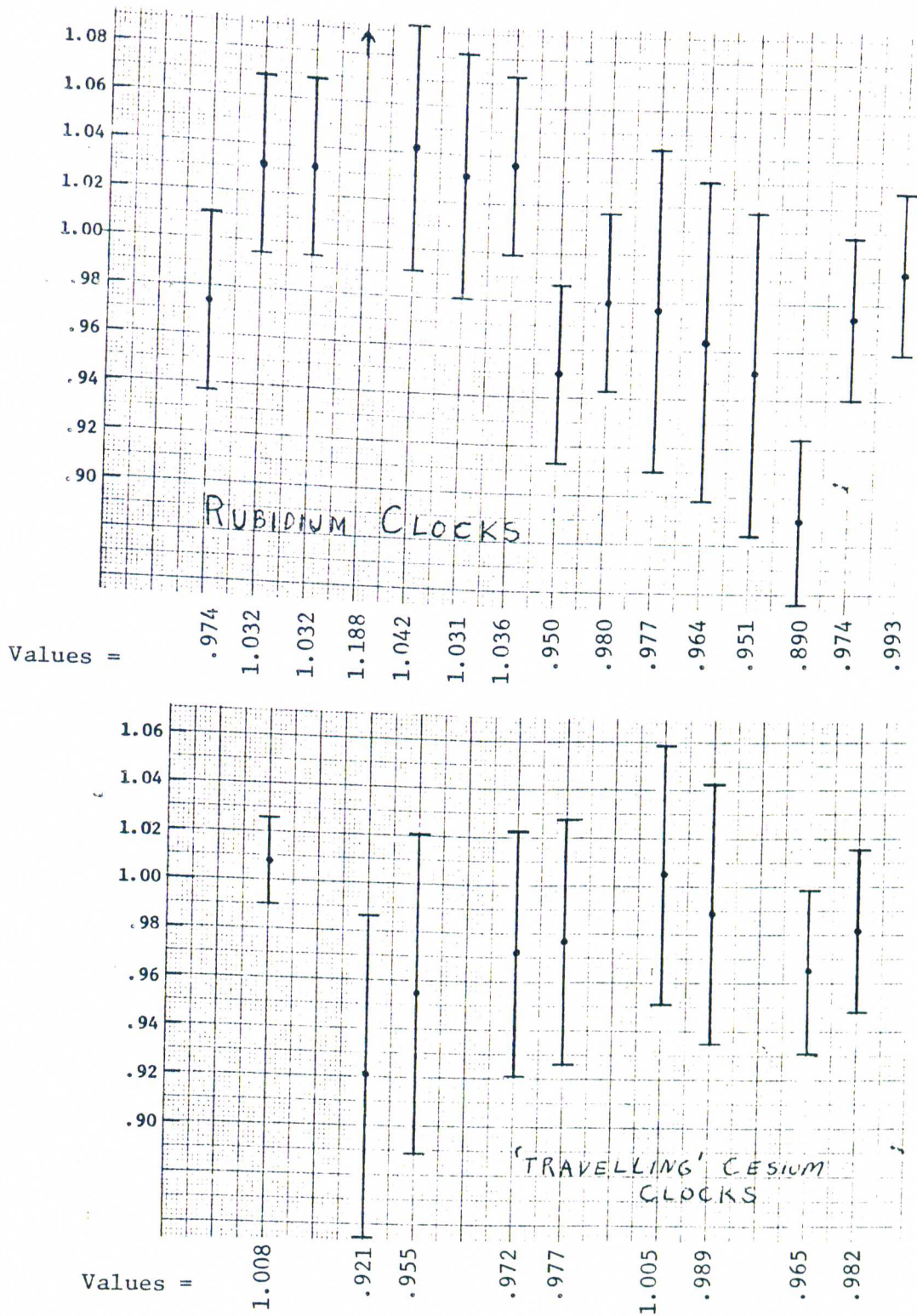
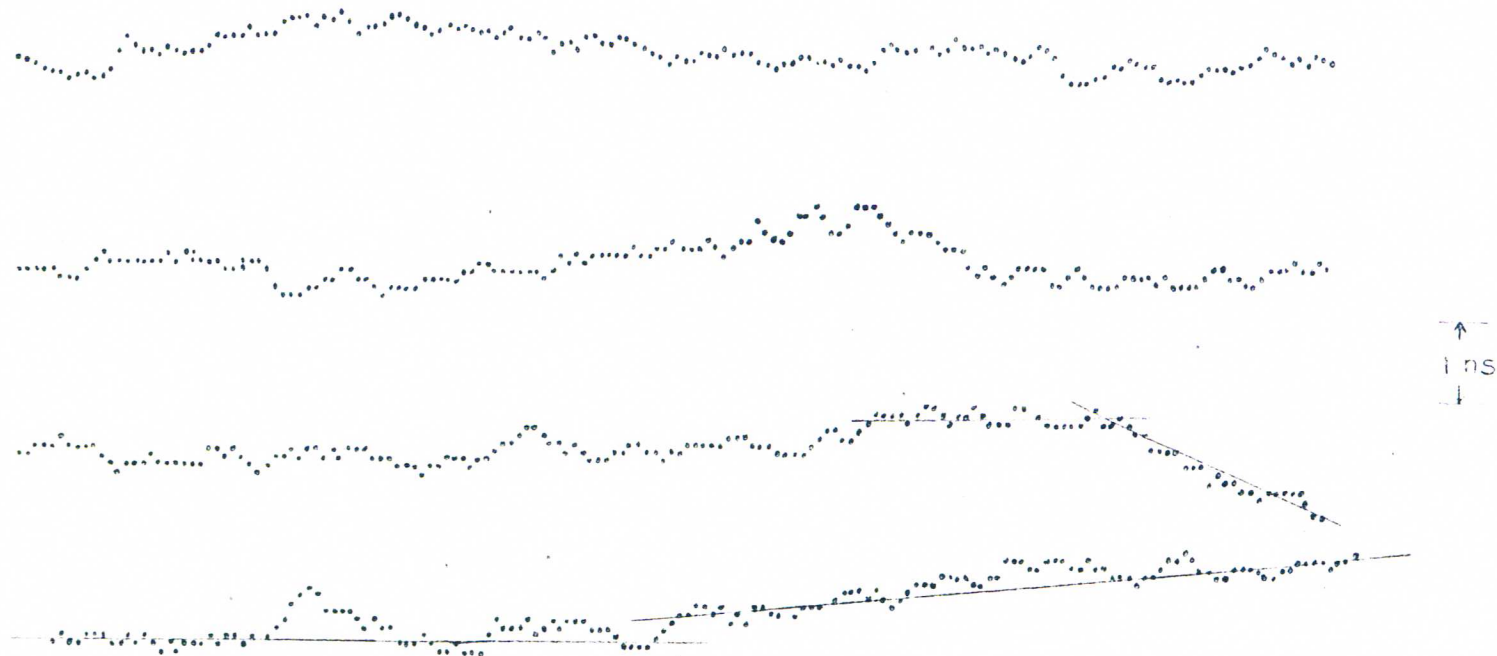


Figure 34. Results using the Rubidium clocks and the travelling Cesium clocks. These measurements were obtained by using the principal Cesium clocks to correct for rate changes at the first and last of flight; hence they are in no way independent.



DATA LENGTH = 15 HOURS

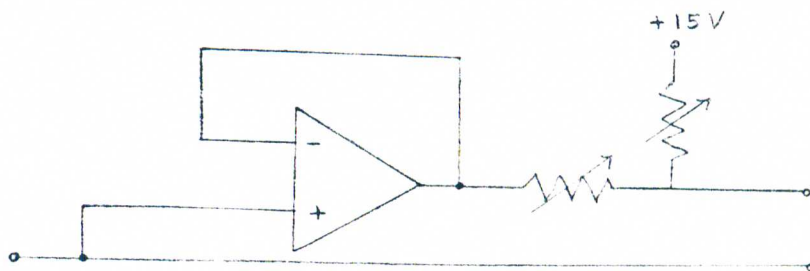
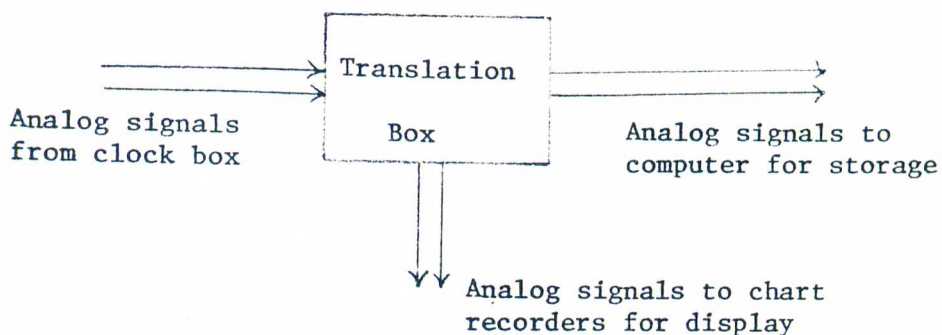
Figure 35. Phase plot of "synthetic clocks" generated by a computer program. The lines in the lower two plots indicate what could be construed as a rate change. No such rate change occurs in the generating program. The point is therefore illustrated that the normal statistical process can mimic rate changes. These results are from Dr. L. Cutler.

APPENDIX A.  
CIRCUIT DIAGRAMS

This Appendix contains circuit diagrams of some components of the experimental system. Other circuits may be found in the thesis of Robert Reisse<sup>20</sup>. Also included in this section is a reproduction of the notes made by Dr. Leonard Cutler concerning the circuit change he made in the servo loop in the Cesium clocks.

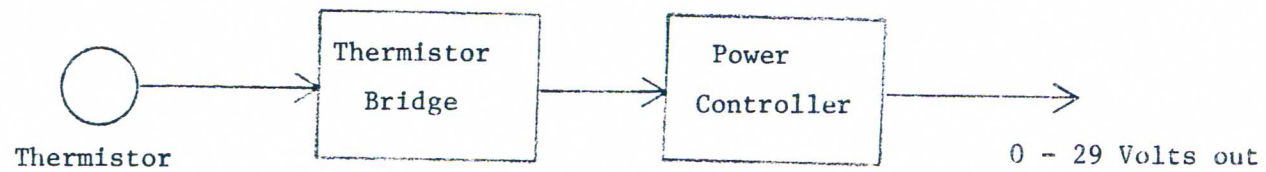
### The Translation Box

The translation box is inserted between the clock box and the computer where it may divert analog signals to chart recorders. The input is buffered so that the electrical loading of the computer is not affected. The circuitry also contains adjustments to calibrate the chart recorder.



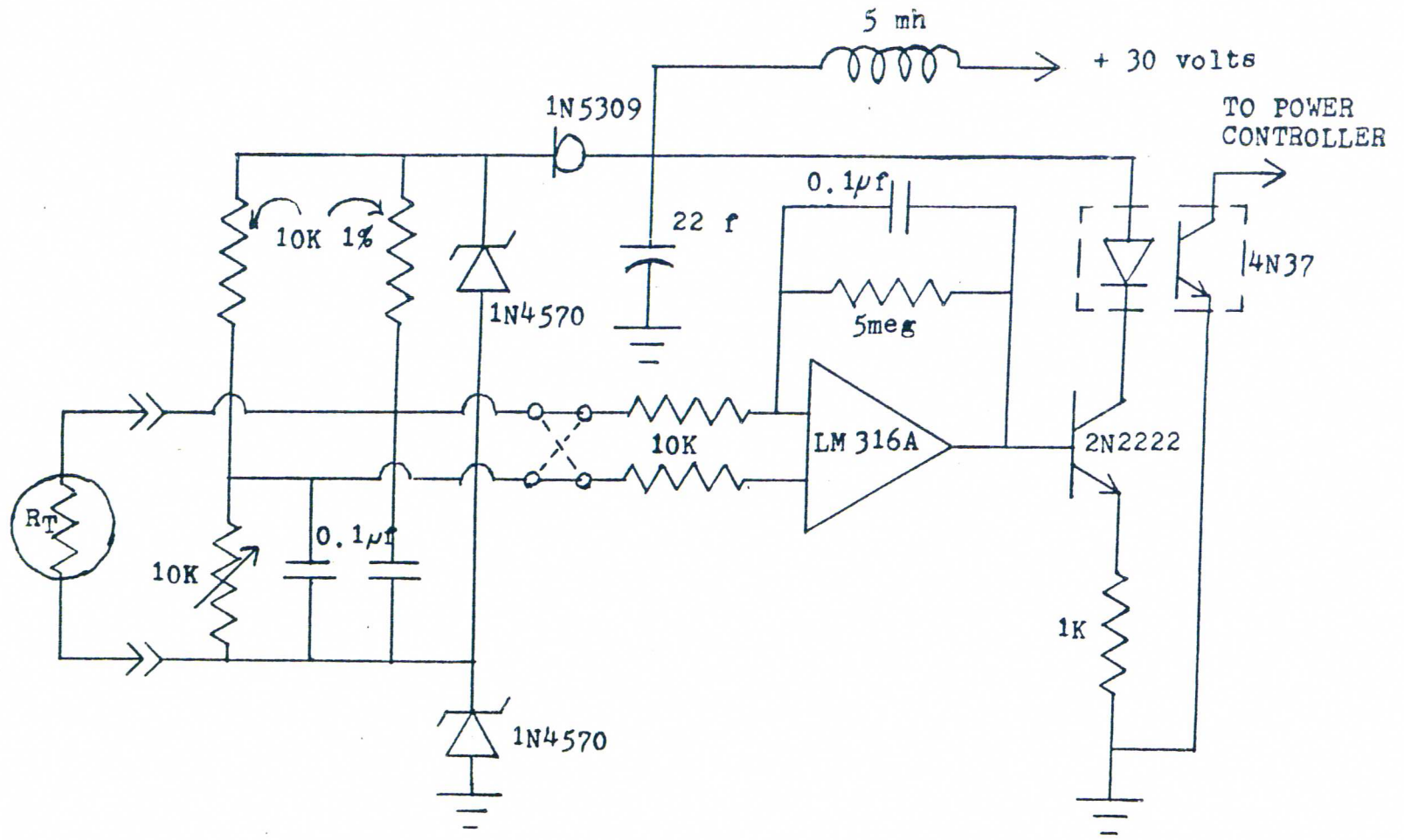
Circuit diagram of one channel of the translation box.

The incoming  $-5$  to  $+5$  volt signal is converted to a  $0$  to  $1$  ma current to drive the Honeywell six channel chart recorders.

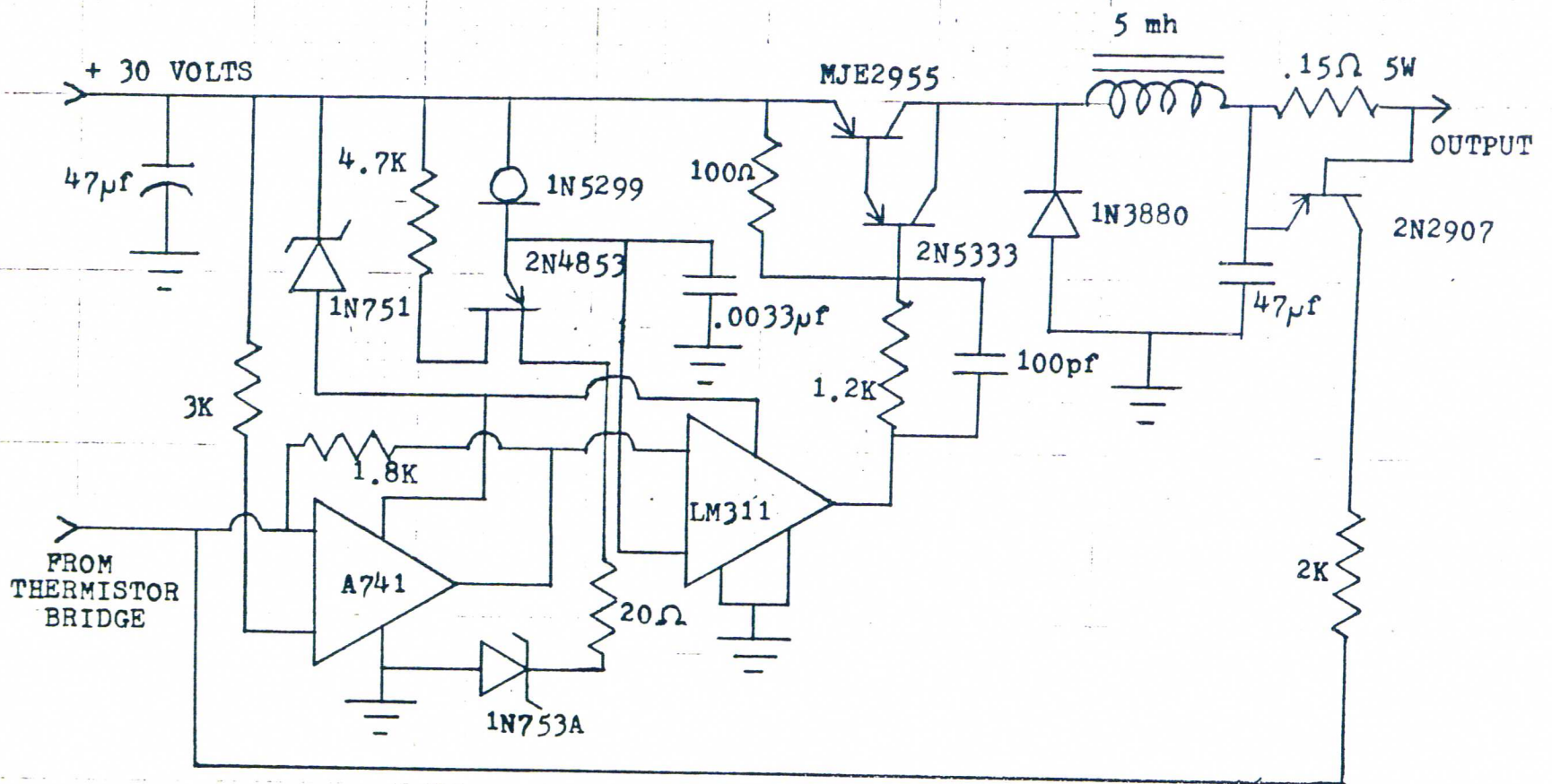


This is the scheme used to control the box heaters and the variable speed fans. Circuit diagrams of the thermistor bridge and power controller are on the next two pages.



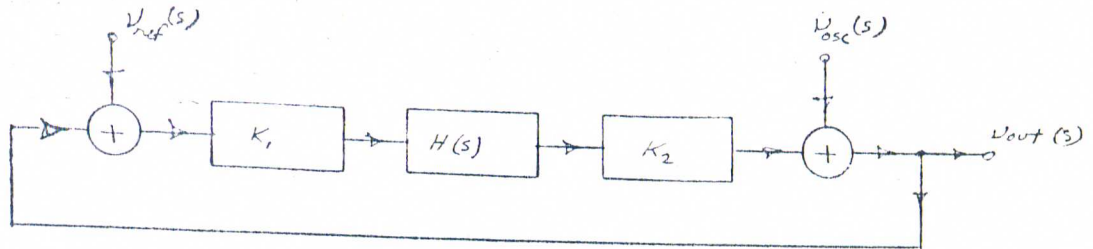


THERMISTOR BRIDGE



POWER CONTROLLER

- 1 -  
CESIUM CLOCK SERVO LOOP ANALYSIS



$k_1$  represents the gain from the cesium tube comparison to the synchronous detector output in volts per unit of fractional error.

$k_2$  represents the control gain of the oscillator in fractional frequency change per volt.

$H(s)$  is the transfer function of the filter following synchronous detection.

$v_{ref}(s)$  is the cesium reference frequency

$v_{osc}(s)$  is the oscillator free running frequency.

$v_{out}(s)$  is the output frequency.

In the clocks we have  $k_1 = 3.2 \times 10^8$  volts

$k_2 = 5 \times 10^{-9}$ /volt

$H(s) \approx \frac{2s + 1}{1.6 s^2}$  (to a good approximation for our second order loop)

the closed loop output frequency is

$$v_{out}(s) = \frac{v_{osc}(s)}{1 + k_1 k_2 H(s)} = \frac{v_{ref}(s) k_1 k_2 H(s)}{1 + k_1 k_2 H(s)}$$

Putting in the actual values we have

$$v_{\text{out}}(s) = \frac{s^2 v_{\text{osc}}(s)}{(s+1)^2} = \frac{(2s+1) v_{\text{ref}}(s)}{(s+1)^2}$$

The time domain response of  $v_{\text{out}}$  to a unit step in  $v_{\text{ref}}$  is

$$v_{\text{out}}(t) = 1 - (1-t)e^{-t} \quad (\text{unit step in } v_{\text{ref}})$$

This is plotted in the figure following the next page.

The response of  $v_{\text{out}}$  to a unit step in  $v_{\text{osc}}$  is

$$v_{\text{out}}(t) = (1-t)e^{-t} \quad (\text{unit step in } v_{\text{osc}})$$

This is plotted in the figure following the figure mentioned above.

The response of  $v_{\text{out}}$  to a unit ramp in  $v_{\text{osc}}$  is

$$v_{\text{out}}(t) = te^{-t} \quad (\text{unit ramp in } v_{\text{osc}})$$

This is plotted in the figure following those above.

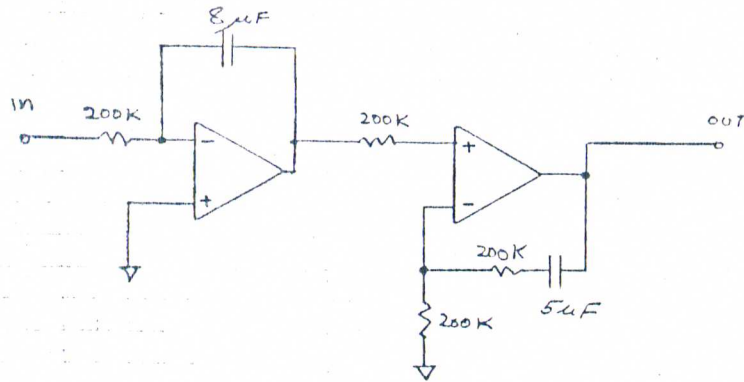
Note that the response to the unit ramp vanishes as  $t \rightarrow \infty$ .

This means that linear drift in the oscillator causes no frequency error or accumulated time error. The same thing is true for the response to a unit step. Therefore, if the oscillator moves around in an arbitrary way during some time interval, there will be no time error contributed provided

1. The oscillator has at worst linear drift before and after the interval, and
2. The servo loop is not overloaded by the oscillator excursions.

This is the important benefit gained by the second order loop.

A simplified schematic of the circuitry to realize  $H(s)$  for the second order loop is shown below:



$$H(s) = \frac{V_{out}}{V_{in}} \approx \frac{2s+1}{1.6s^2}$$

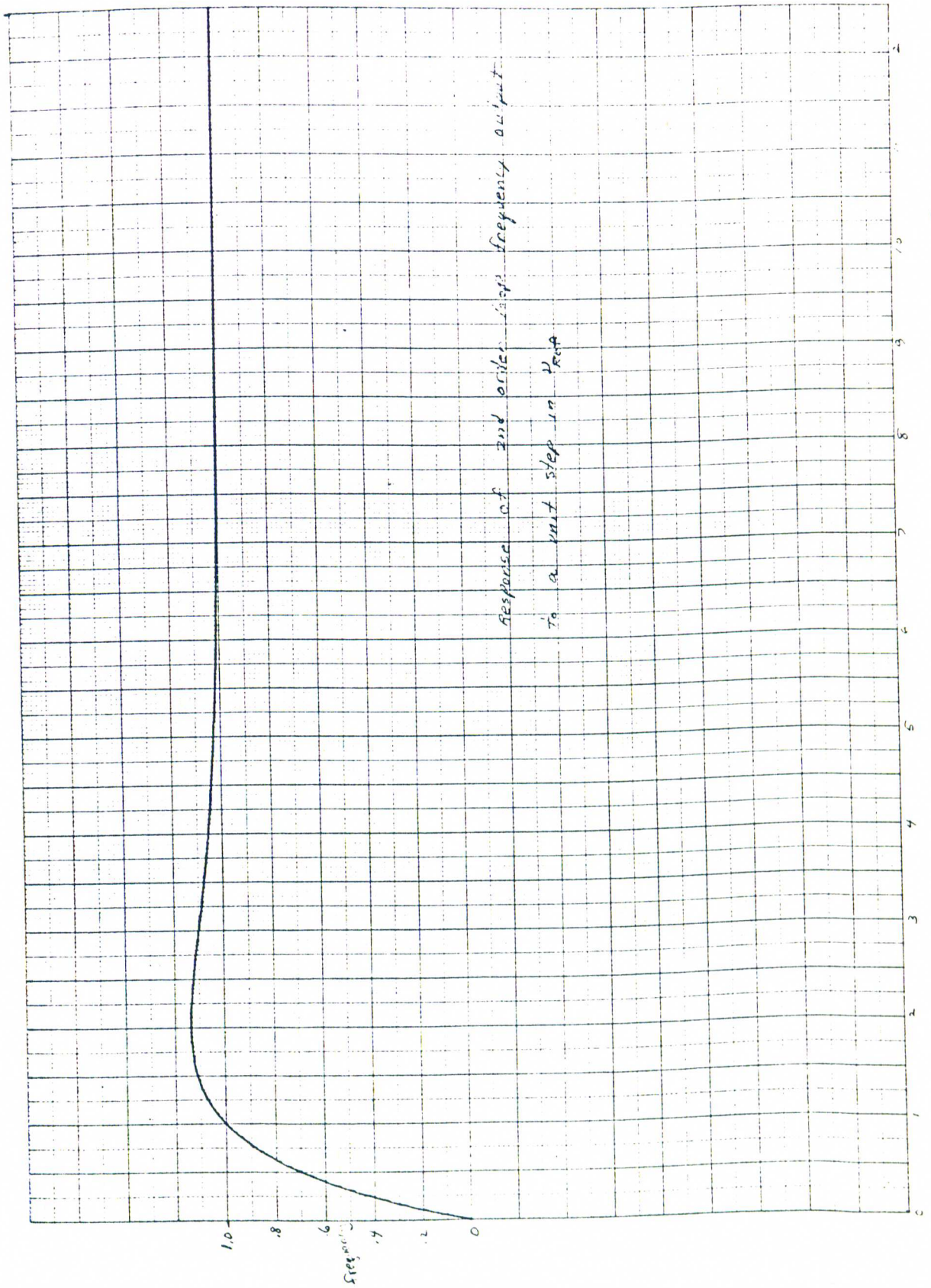


Fig 1

Time - seconds

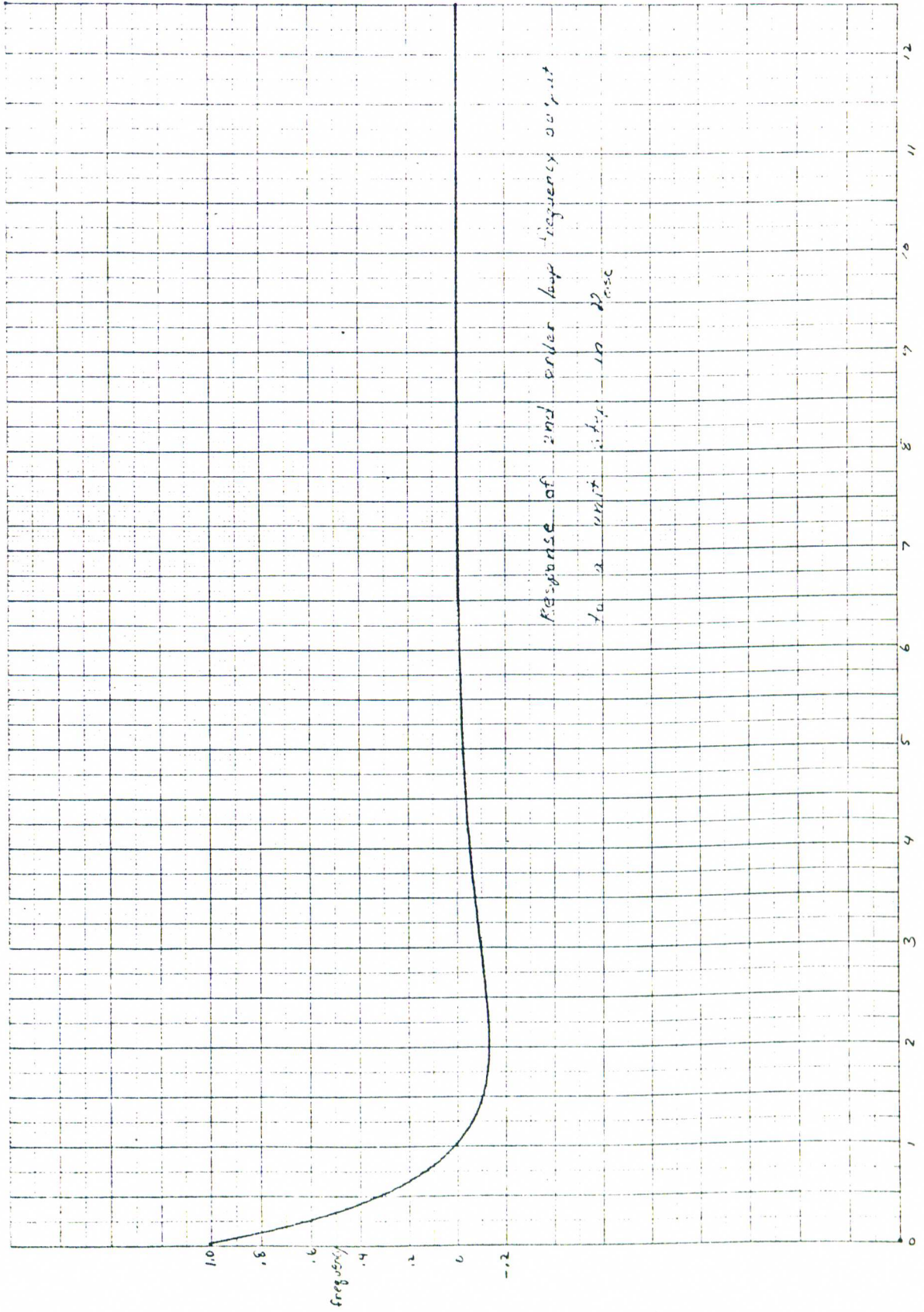
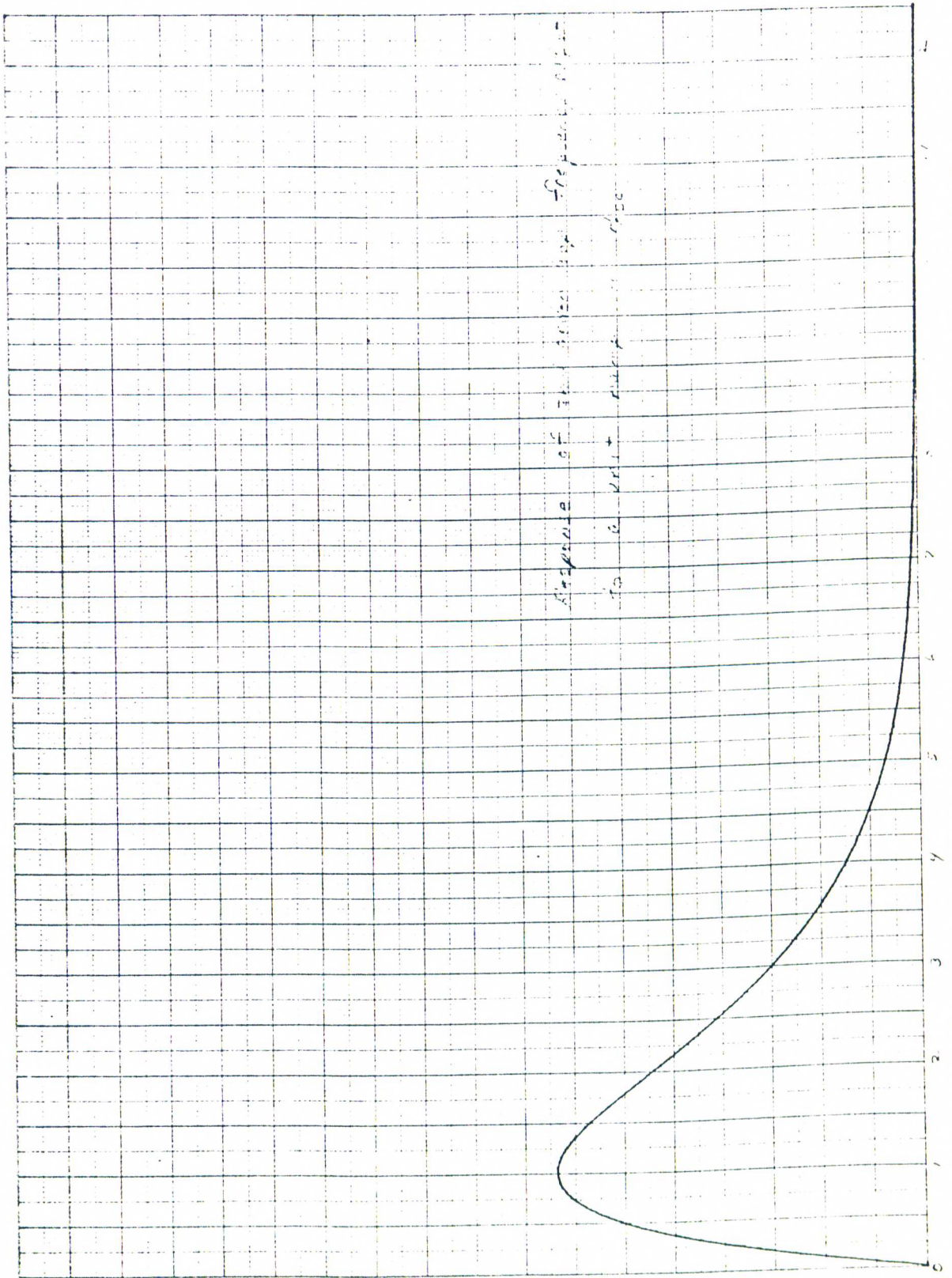


Fig. 1

KE 10 X 10 TO THE CENTIMETER 18 X 25 CM  
KEUFFEL & ESSER CO. MADE IN U.S.A.

461510



Graph of  $f(x) = 2.5 - 0.5x^2$   
to 6 digit accuracy

Time Series



## APPENDIX B.

### ENVIRONMENTAL COEFFICIENTS OF THE CLOCKS

Summarized in this Appendix are the results of various environmental tests on the Cesium and Rubidium clocks.

#### MAGNETIC TESTS:

A rotation of one clock box  $90^{\circ}$  and  $180^{\circ}$  in the earth's magnetic field showed no effect on clock rates. Of course, this was with the clocks inside their magnetic shield cans and so is not a measurement on the clocks themselves. The limit of this measurement was approximately three or four parts in  $10^{14}$  for a variation of about 1/3 gauss.

#### PRESSURE TESTS:

These tests were performed by changing the pressure in the clock box by several lbs/in<sup>2</sup>. No effect was detected on the Cesium clocks to the level of several parts in  $10^{14}$ . Tests on the Rubidium clocks showed pressure coefficients between  $-0.8 \times 10^{-13}$  and  $-1.0 \times 10^{-13}$ /mm Hg. This is a rather large coefficient and the effects on the clock rates are dramatic--see the graph on the next pages.

#### TEMPERATURE TESTS:

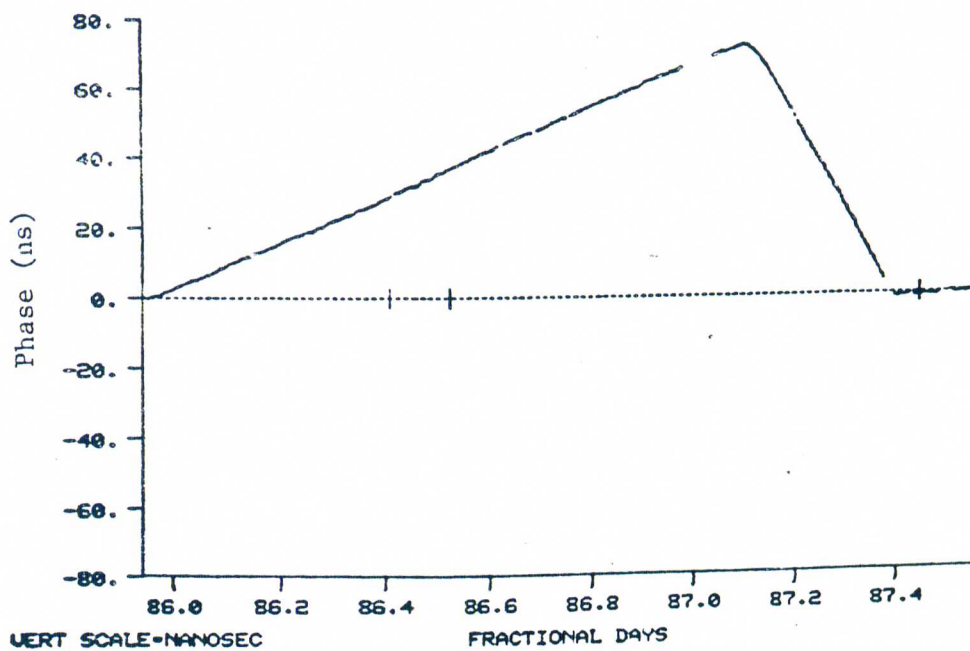
Temperature tests were performed by changing the set points of the clock temperature controllers. This allowed changes in temperature of five or more degrees. The temperature coefficients of the Rubidium clocks varied between  $-2.7 \times 10^{-12}$  and  $-3.0 \times 10^{-12}$ /°F.

The temperature coefficients of the Cesium clocks are known to vary depending on clock position and other factors. The coefficients that we have measured with the clocks in their normal positions in the clock boxes are as follows:

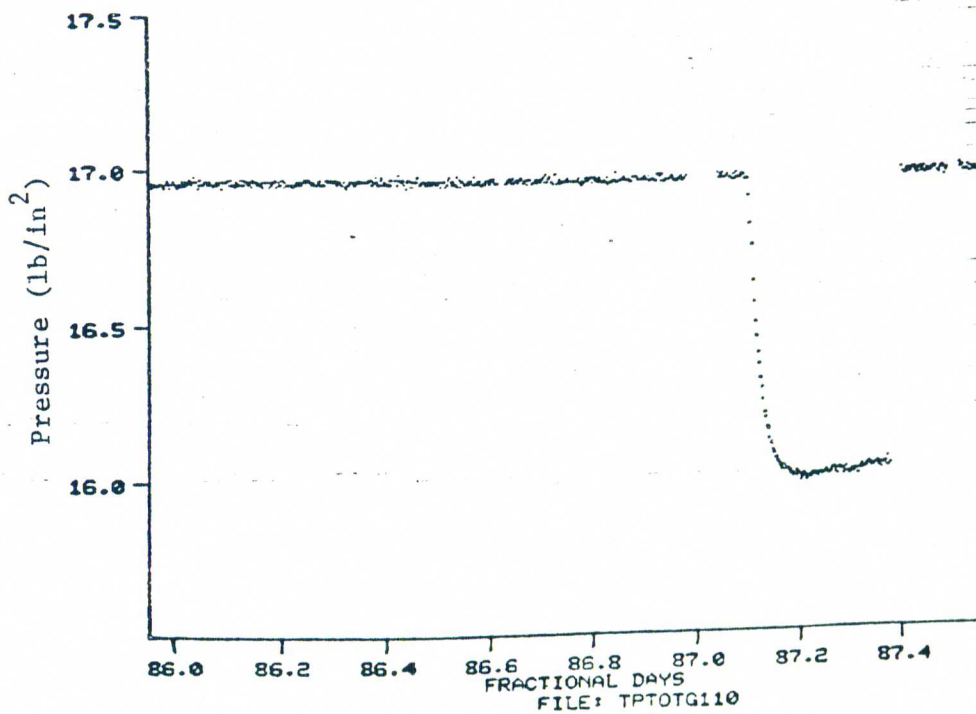
<u>Clock</u>	<u>Coefficient ( /<sup>o</sup>F)</u>
1 (#1033)	$-3.8 \times 10^{-14}$
2 (#1028)	$-4.0 \times 10^{-14}$
3 (#1025)	$-3.3 \times 10^{-14}$
7 (# 752)	$-2.0 \times 10^{-13}$
8 (#1026)	$-1.7 \times 10^{-14}$
9 (#1035)	$-7.1 \times 10^{-14}$

The coefficients of #752 and #1035 were also measured by Hewlett-Packard under other conditions. Those results were as follows:

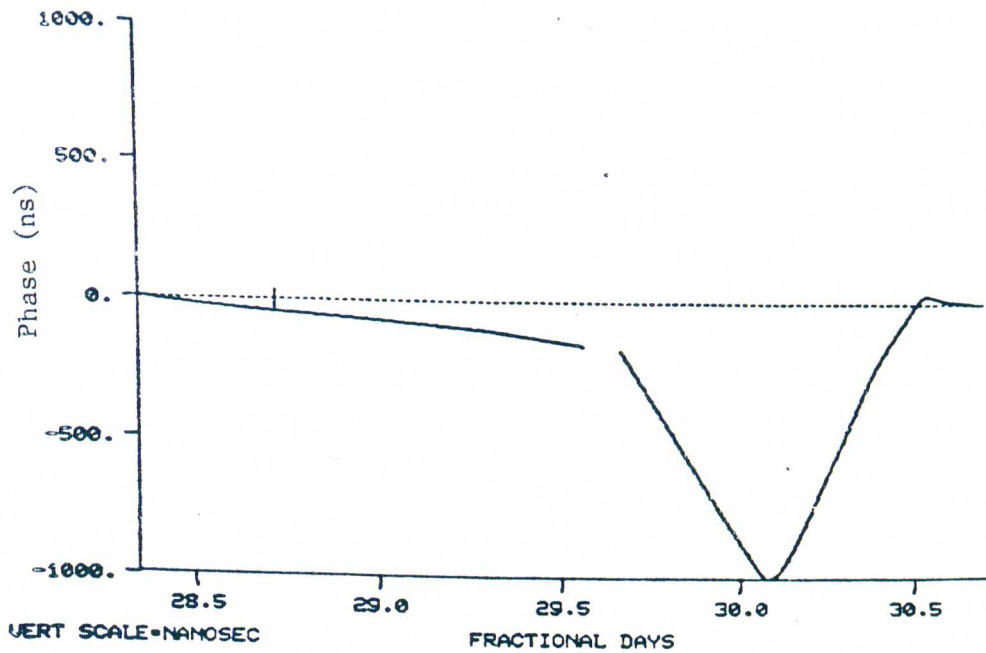
	<u>Upright, panels on</u>	<u>On side, panels off</u>
#752	$-5 \times 10^{-14} / ^{\circ}\text{F}$	$-4.1 \times 10^{-14} / ^{\circ}\text{F}$
#1035	$-1.9 \times 10^{-14} / ^{\circ}\text{F}$	$-0.8 \times 10^{-14} / ^{\circ}\text{F}$ .



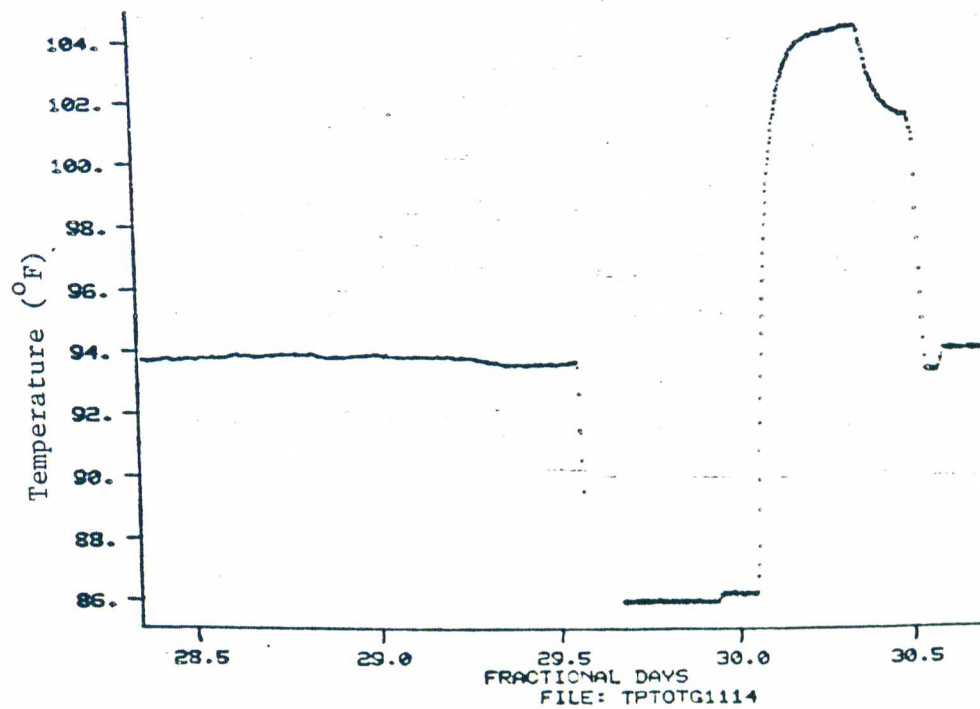
RESIDUALS, FILE: DFGB110 SLOPE FILE: GPSGB110  
CLOCK # 12 US PAPER REF 7, 8, 9, 15, 17.



A typical Rubidium clock rate change due to pressure.



RESIDUALS, FILE: DFGB1114 SLOPE FILE: GPSGB1114  
 CLOCK # 4 US PAPER REF 1, 2, 3,15,16,



A typical Rubidium clock rate change due to temperature.

APPENDIX C

A THEOREM FOR CALCULATING VARIANCES

In this appendix we prove the theorem mentioned in chapter VI. That is, if  $D$  is a linear combination of phases measured in the time domain

$$D = \sum a_i x_i \quad x_i = x(t_i) = \frac{\phi(t_i)}{\omega_0}$$

$$\alpha_i = \text{a constant}$$

$$i > j \Rightarrow t_i > t_j$$

and  $\sum \alpha_i = 0$  and  $\langle D \rangle = 0$ ,

then

$$\sigma^2(D) = -\frac{h_0}{2} \sum_{i>j} \alpha_i \alpha_j (t_i - t_j)$$

where  $h_0$  is the spectral distribution function as defined in chapter VI. The condition that the sum of the constants be zero assures that the quantity considered is essentially a phase difference.

PROOF:

$$\begin{aligned} \sigma^2(D) &= \langle D^2 \rangle - \langle D \rangle^2 = \langle (\sum \alpha_i x_i) \rangle \\ &= \left\langle \sum_i \alpha_i^2 x_i^2 + 2 \sum_{i>j} \alpha_i \alpha_j x_i x_j \right\rangle \\ &= \left\langle \sum_i \alpha_i^2 R_x(0) + 2 \sum_{i>j} \alpha_i \alpha_j R_x(t_i - t_j) \right\rangle \end{aligned} \quad (1)$$

where  $R_x(\tau)$  is the autocorrelation function

$$R_x(\tau) = \lim_{T \rightarrow \infty} \int_{-T}^T x(t)x(t+\tau) dt = \langle x(t)x(t+\tau) \rangle .$$

Since  $\sum \alpha_i = 0$ , we have

$$0 = \left( \sum_i \alpha_i \right) \cdot \left( \sum_j \alpha_j \right) = \sum_i \alpha_i^2 + 2 \sum_{i>j} \alpha_i \alpha_j$$

Therefore equation 1 may be written

$$\sigma^2(D) = - \sum_{i>j} 2\alpha_i \alpha_j \left[ R_x(0) - R_x(t_i - t_j) \right] \quad (2)$$

Recall from the summary in chapter VI that there are the relations

$$R_x(\tau) = \frac{1}{2\pi} \int_{-\infty}^{\infty} S_x(\omega) e^{-i\omega\tau} d\omega$$

and

$$S_y(\omega) = S_x(\omega) = \omega^2 S_x(\omega) .$$

Hence we have

$$R_x(\tau) = \frac{1}{2\pi} \int_{-\infty}^{\infty} \frac{S_y(\omega)}{\omega^2} e^{-i\omega\tau} d\omega$$

which for pure white frequency noise,  $S_y(\omega) = h_o$ , becomes

$$R_x(\tau) = \frac{h_o}{4\pi} \int_{-\infty}^{\infty} \frac{e^{-i\omega\tau}}{2} d\omega$$

the extra factor of 2 appearing because  $S_y(\omega)$  is the one-sided spectral distribution function. Thus

$$\left[ R_x(0) - R_x(\tau) \right] = \frac{h_o}{4\pi} \int_{-\infty}^{\infty} \frac{1 - e^{-i\omega\tau}}{\omega^2} d\omega = \frac{h_o}{4\pi} (\pi\tau) = \frac{h_o}{4} \tau$$

where the principal value of the integral has been evaluated. Inserting this result in equation 2 gives the required expression:

$$\sigma^2(D) = - \frac{h_o}{2} \sum_{i>j} \alpha_i \alpha_j (t_i - t_j) .$$

APPENDIX D  
DATA PLOTS FOR THE FIVE FLIGHTS

This appendix contains data plots and environmental plots concerning all clocks for all major flights. The clocks are referred to by number in these plots, the general sequence of this numbering system being discussed in chapter II. We list here a summary of the numbering scheme:

For all flights:

- |                  |                  |                              |
|------------------|------------------|------------------------------|
| 1 = Cesium #1033 | 7 = Cesium # 752 | 13 = Mean of<br>clocks 1,2,3 |
| 2 = Cesium #1028 | 8 = Cesium #1026 |                              |
| 3 = Cesium #1025 | 9 = Cesium #1035 | 14 = Mean of<br>clocks 7,8,9 |
| 4 = Rubidium     | 10 = Rubidium    |                              |
| 5 = Rubidium     | 11 = Rubidium    |                              |
| 6 = Rubidium     | 12 = Rubidium    |                              |

Clocks 1 through 6 were in box #1 which flew on flights 1,4, and 5.

Clocks 7 through 12 were in box #2 which flew on flights 2 and 3.

Other clocks:

The identity of other clocks varied from flight to flight. The identification is summarized here:

<u>Clock #</u>	<u>Flight 1</u>	<u>Flight 2</u>	<u>Flight 3</u>	<u>Flight 4</u>	<u>Flight 5</u>
15	NP2	NP2	NP2	NP2	NP2
16	NP3	Cs 761	Cs 761	NP3	NP3
17	Cs 761	Cs 444	Cs 444	Cs 761	Cs 761
18	Extra	Cs 862	Cs 862	Cs 052	Cs 871
19		Cs 871	Cs 871	Cs 871	Cs 862
20				Cs 862	

The units NP2 and NP3 are the two hydrogen masers.

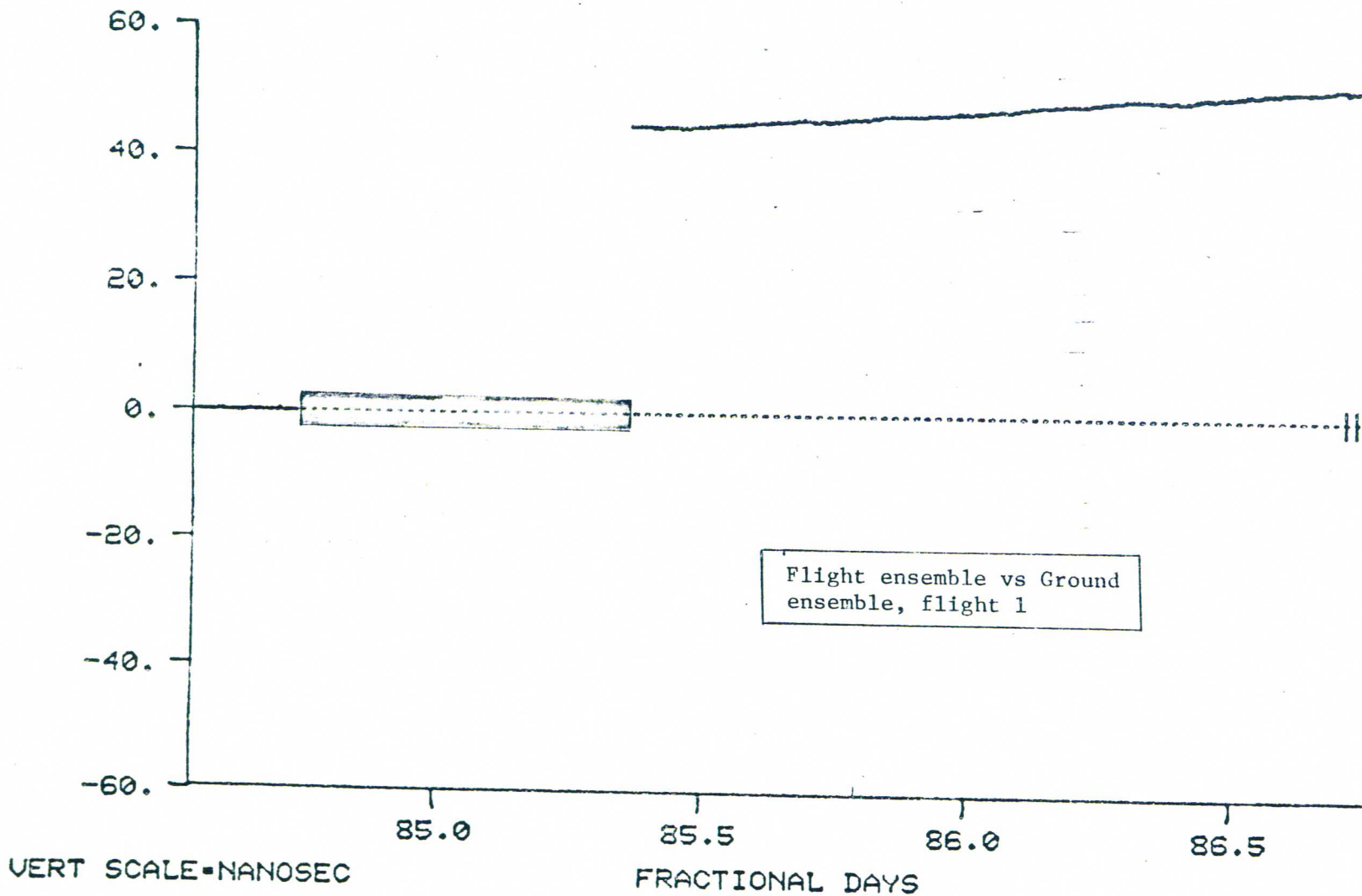
The plots in this appendix are arranged in the following order:

<u>PLOT</u>	<u>PAGE</u>
One graph from each flight of the flying ensemble (the three Cesium clocks) versus the ground ensemble.....	102-106
One environmental summary sheet from each flight.....	107-111
One summary sheet from each flight showing the phase record of the ground Cesium and H-maser clocks versus the ground ensemble.....	112-116
Three pages per flight, each page showing the phase record of one flying Cesium clock as measured by the ground ensemble and as measured by the air ensemble....	117-131
Similar plots to the above, but for the flying "travelling" Cesium clocks.....	132-140
Similar plots to the above, but for the flying Rubidium clocks.....	141-155

Depending on the type of phase plot (air or ground), there may or may not be phase data for the inflight period. If there is data, the inflight period is indicated by a vertical line at the beginning and end of the inflight period. If there is not data, a solid bar appears on the axis for the inflight period. In both cases this "inflight period" is really the period between the times that the cables carrying signals from the plane to the ground are removed or reconnected. Hence the "inflight period" appearing on the plots includes engine warmup, taxi, etc.

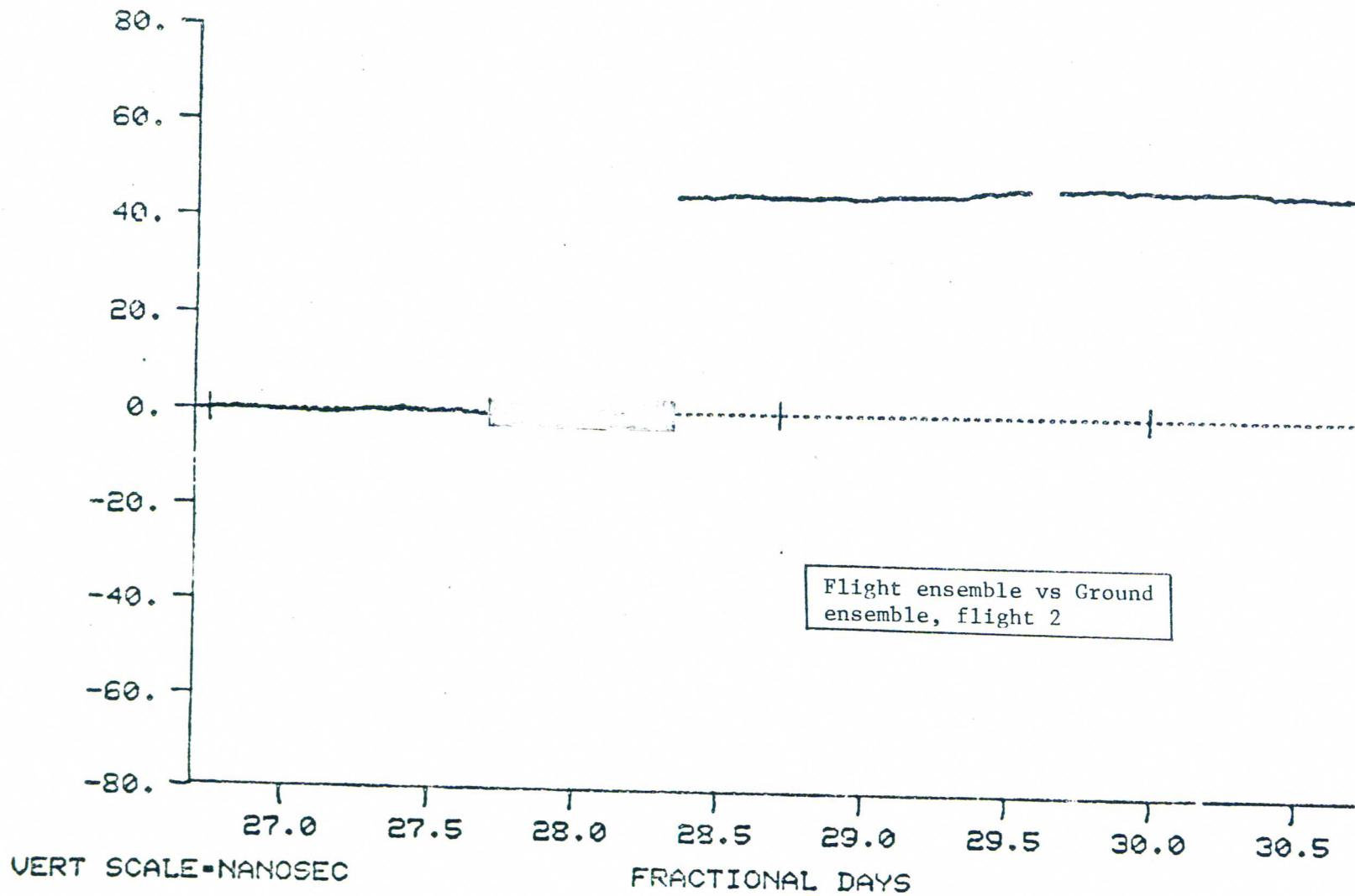
The arrows appearing on the Cesium clock plots indicate the end points used by various runs of the program SHIFT (see chapter VII). Since the program works on all clocks from a given flight at the same time, arrows dictated by a possible rate change in one clock appear on all clocks.





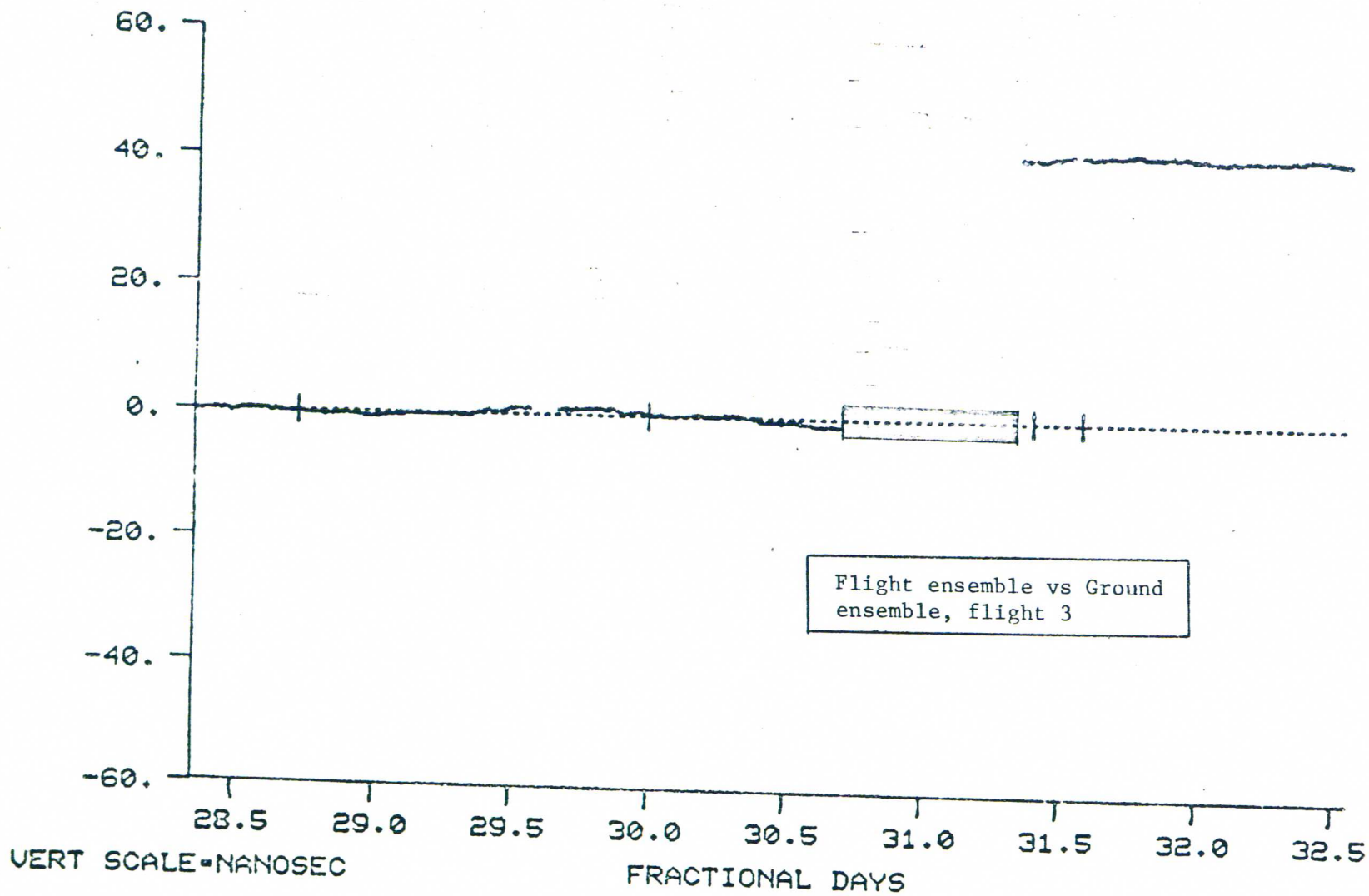
RESIDUALS, FILE: DFTOTG929 SLOPE FILE: GDSQB929  
 CLOCK # 13 US PAPER REF 7, 8, 9, 15, 16, 17,

$$\cong \frac{1}{3} (\#1 + \#2 + \#3)$$



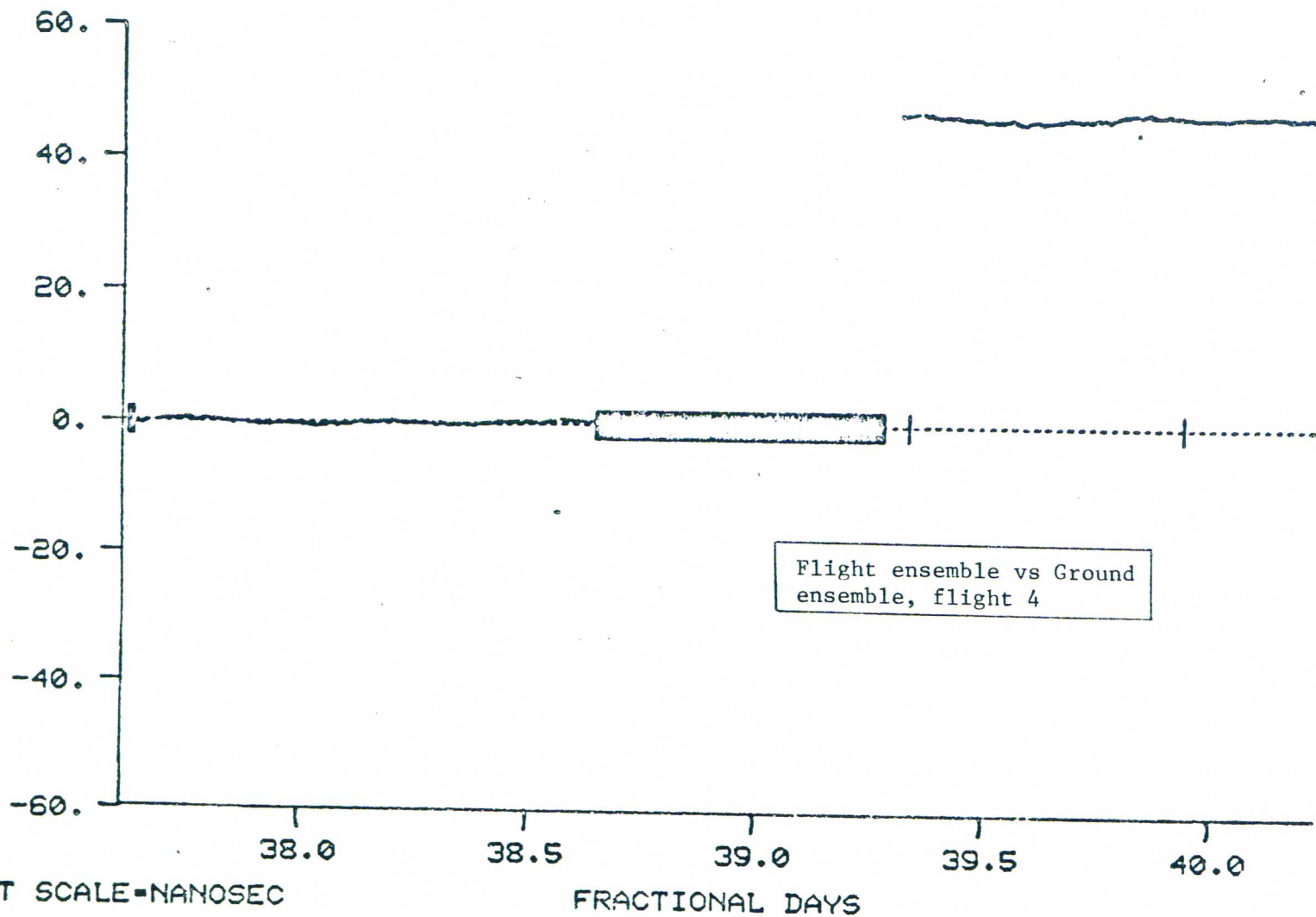
RESIDUALS, FILE: DFTOTG1111 SLOPE FILE: GDSGB1111  
 CLOCK # 14 US PAPER REF 1, 2, 3, 16,

$$\equiv \frac{1}{3} (\#7 + \#8 + \#9)$$



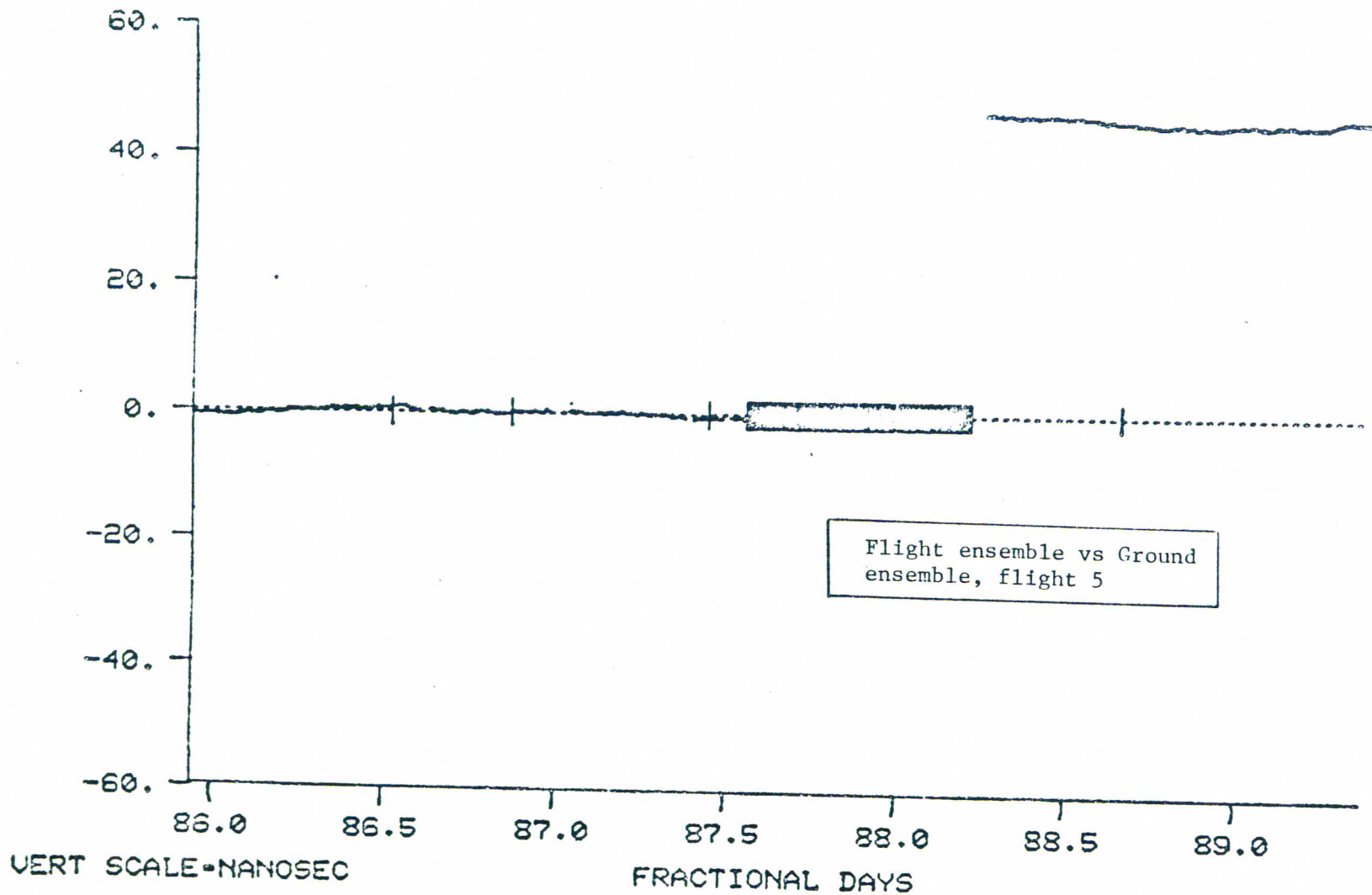
RESIDUALS, FILE: DFTOTG1114 SLOPE FILE: GDSGB1114  
 CLOCK # 14 US PAPER REF 1, 2, 3, 15, 16,

$$\equiv \frac{1}{3} (\#7 + \#8 + \#9)$$

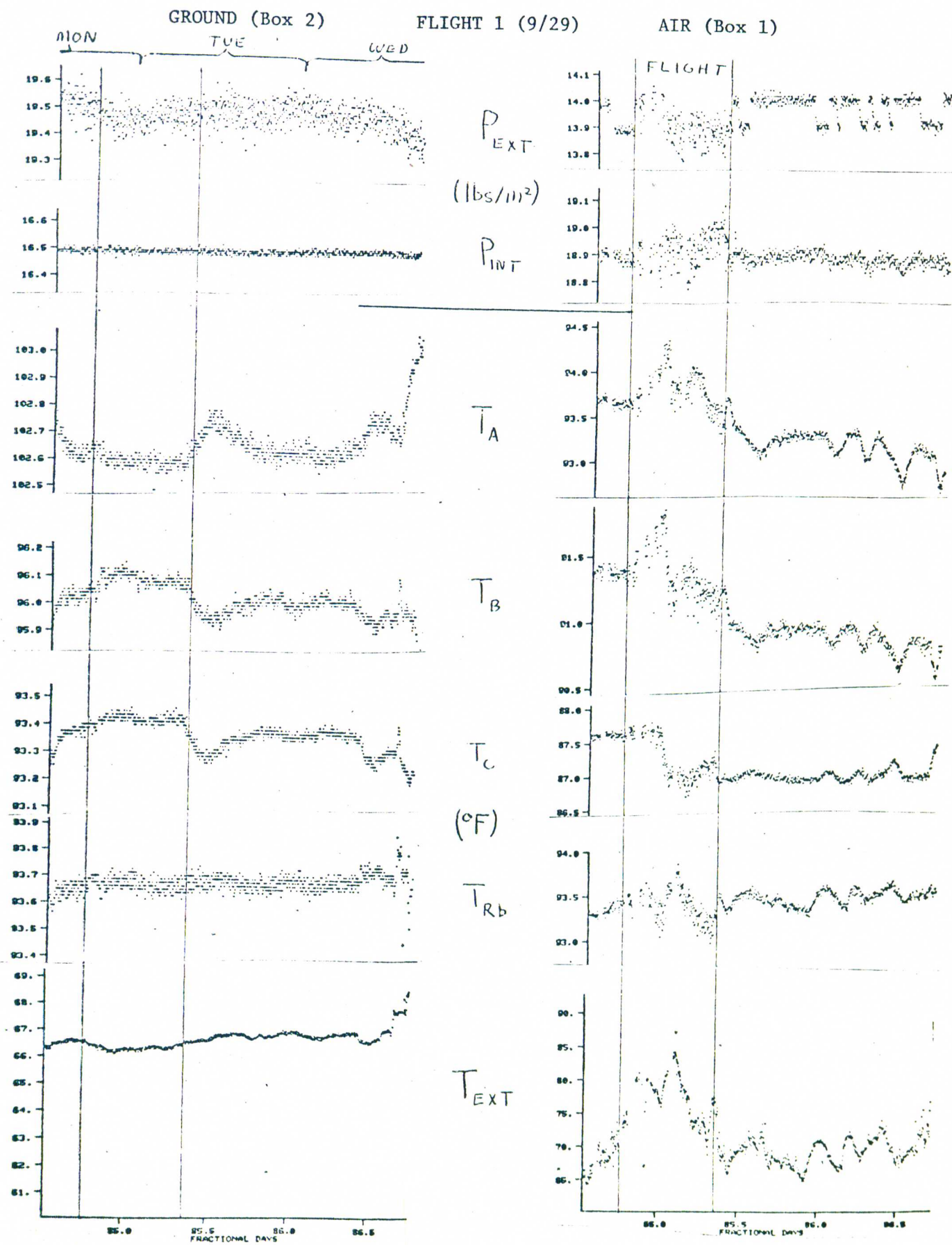


RESIDUALS, FILE: DFTOTG1122 SLOPE FILE: GDSGB1122  
 CLOCK # 13 US PAPER REF 7, 8, 9, 17,

$$\equiv \frac{1}{3}(1+2+3)$$



RESIDUALS, FILE: DFTOTG110 SLOPE FILE: GDSGB110  
 CLOCK # 13 US PAPER REF 7, 8, 9, 15, 17,  
 $\equiv \frac{1}{3}(1+2+3)$

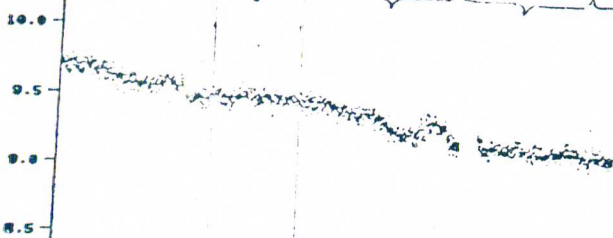


GROUND (Box 1)

FLIGHT 2 (11/11)

AIR (Box 2)

TUES WED THUR FRI



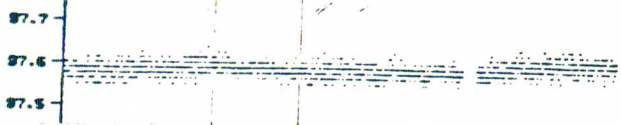
$P_{EXT}$   
(lbs/in<sup>2</sup>)



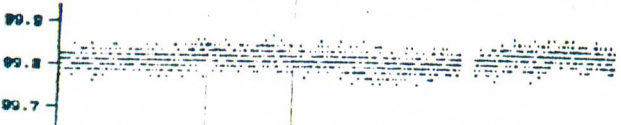
$P_{INT}$



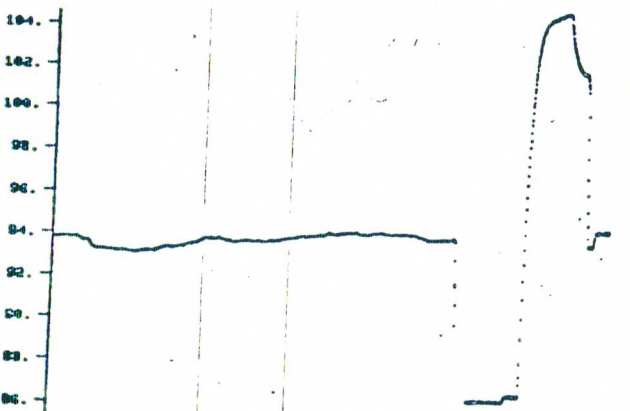
$T_A$



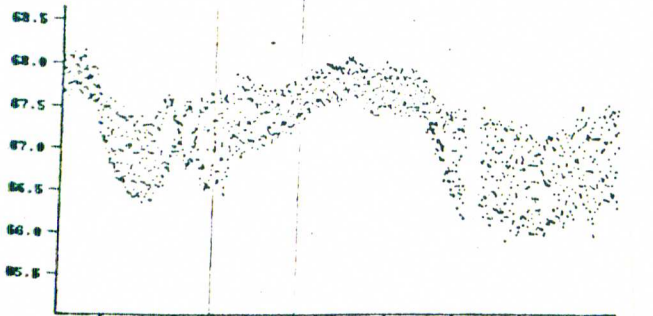
$T_B$



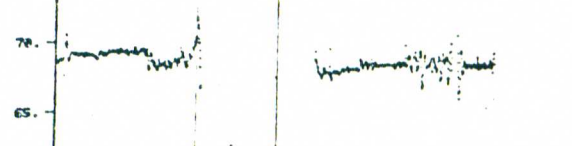
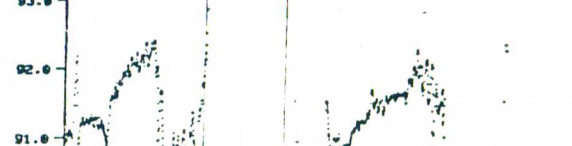
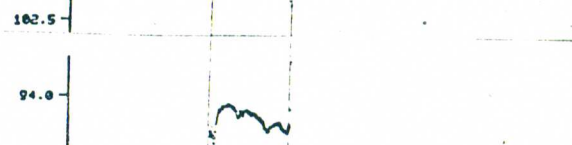
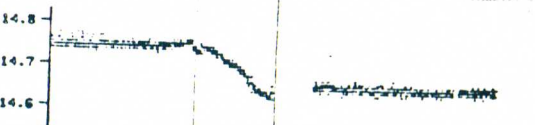
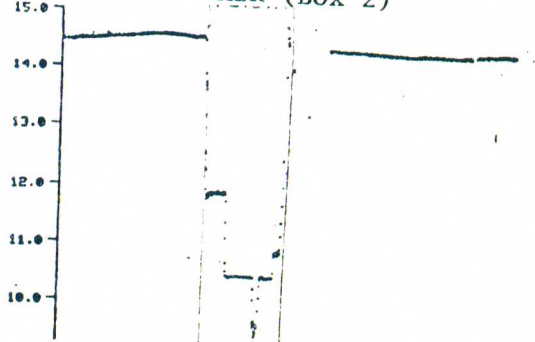
$T_C$

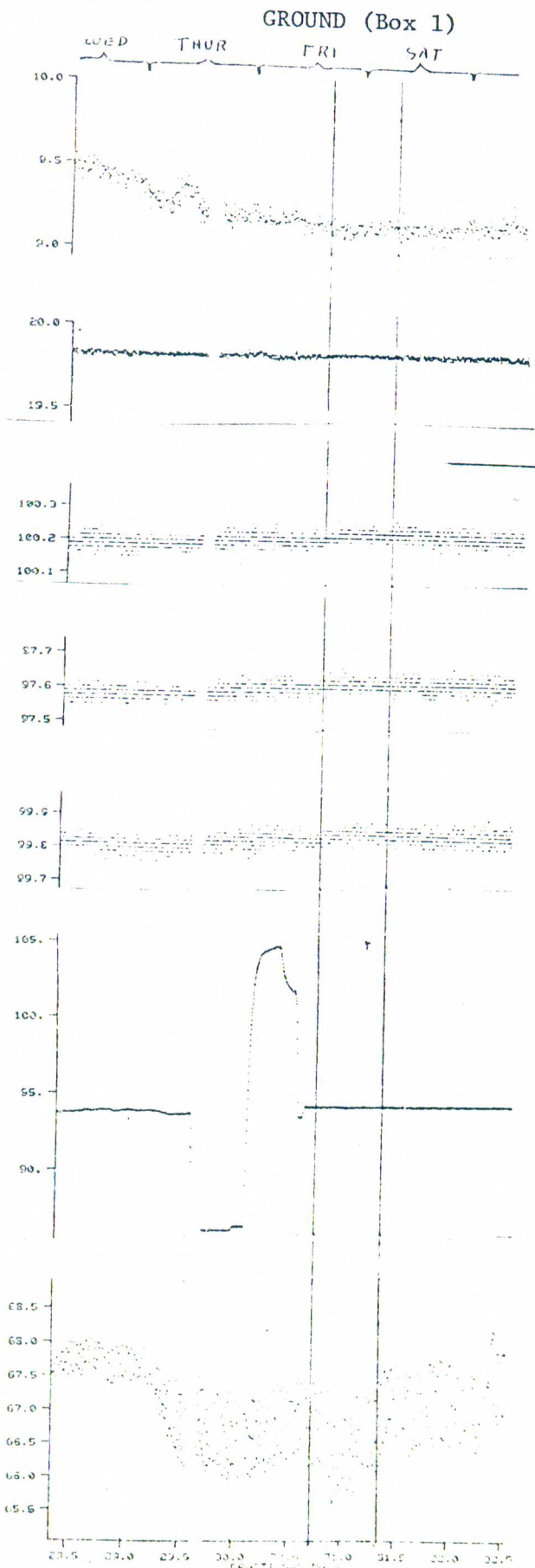


(°F)  
 $T_{RB}$



$T_{EXT}$





FLIGHT 3 (11/14)

AIR (Box 2)

$P_{EXT}$   
(lbs/in<sup>2</sup>)

$P_{INT}$

$T_A$

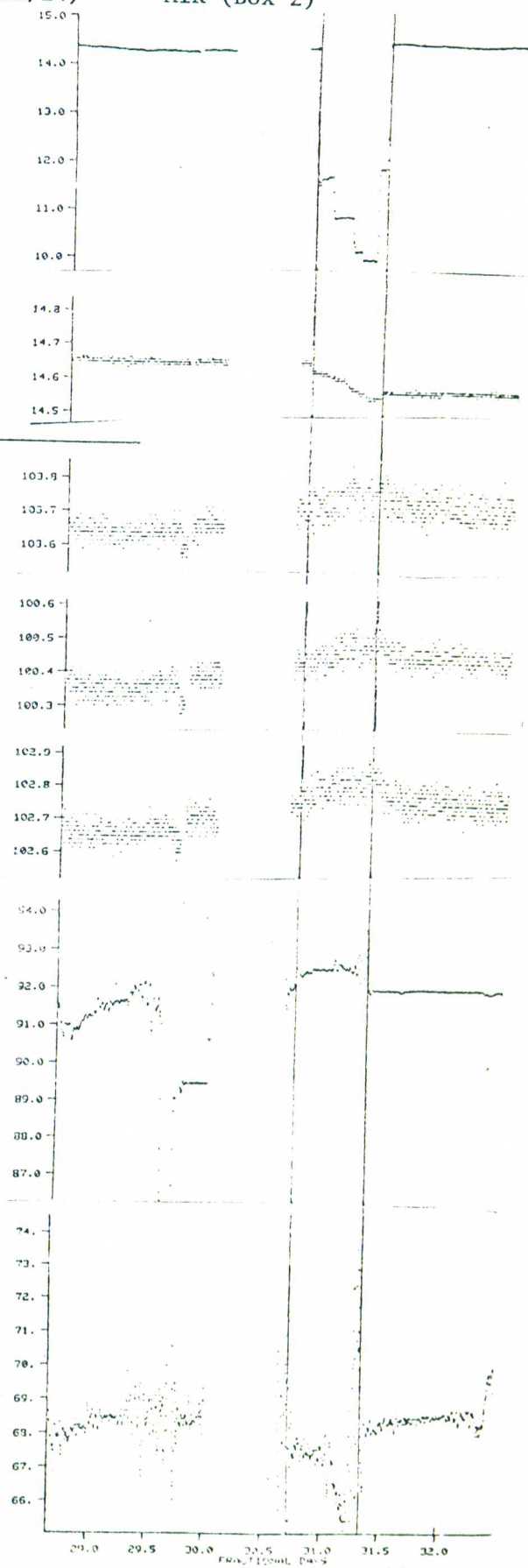
$T_B$

$T_C$

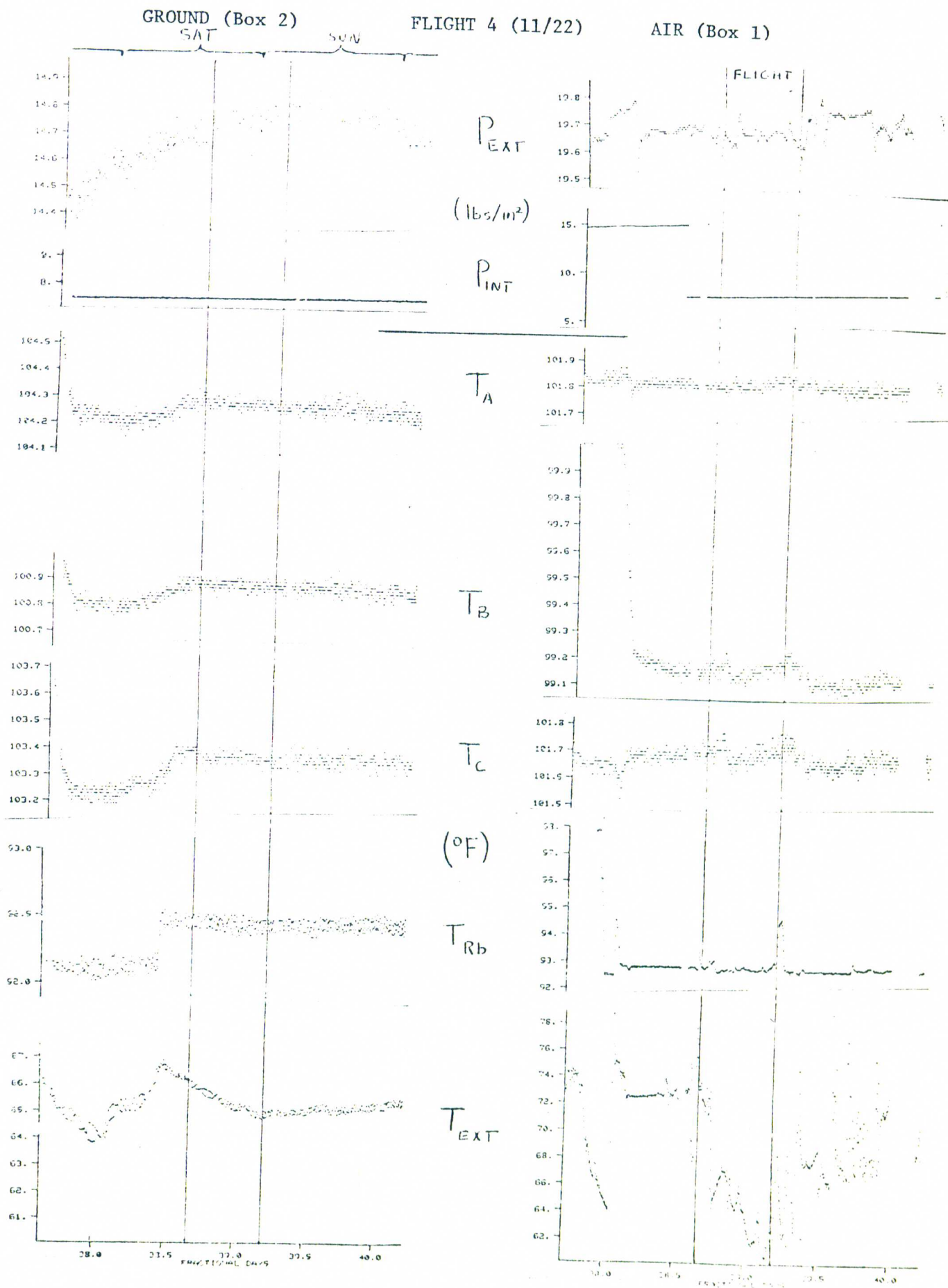
(°F)

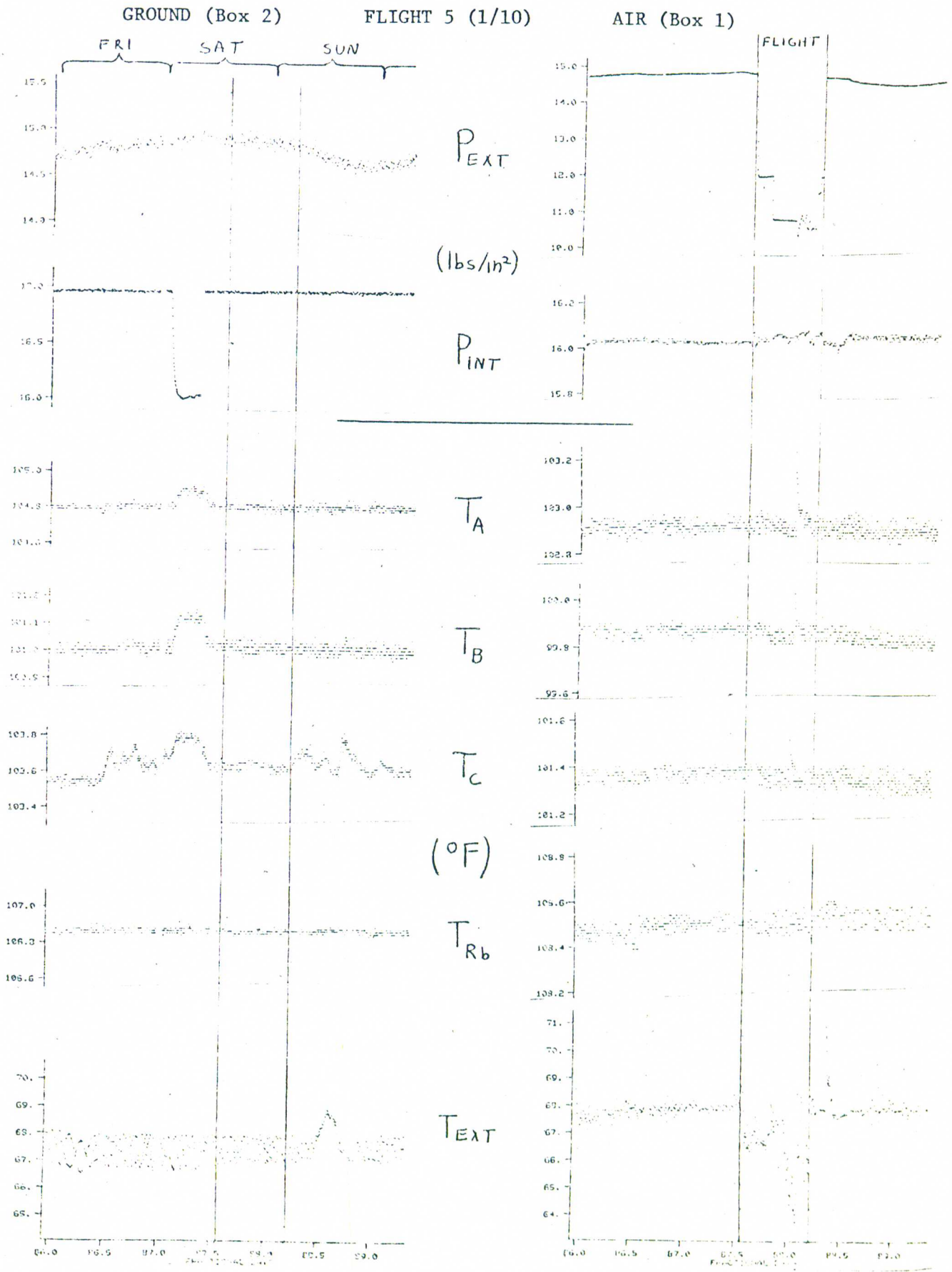
$T_{RB}$

$T_{EXT}$

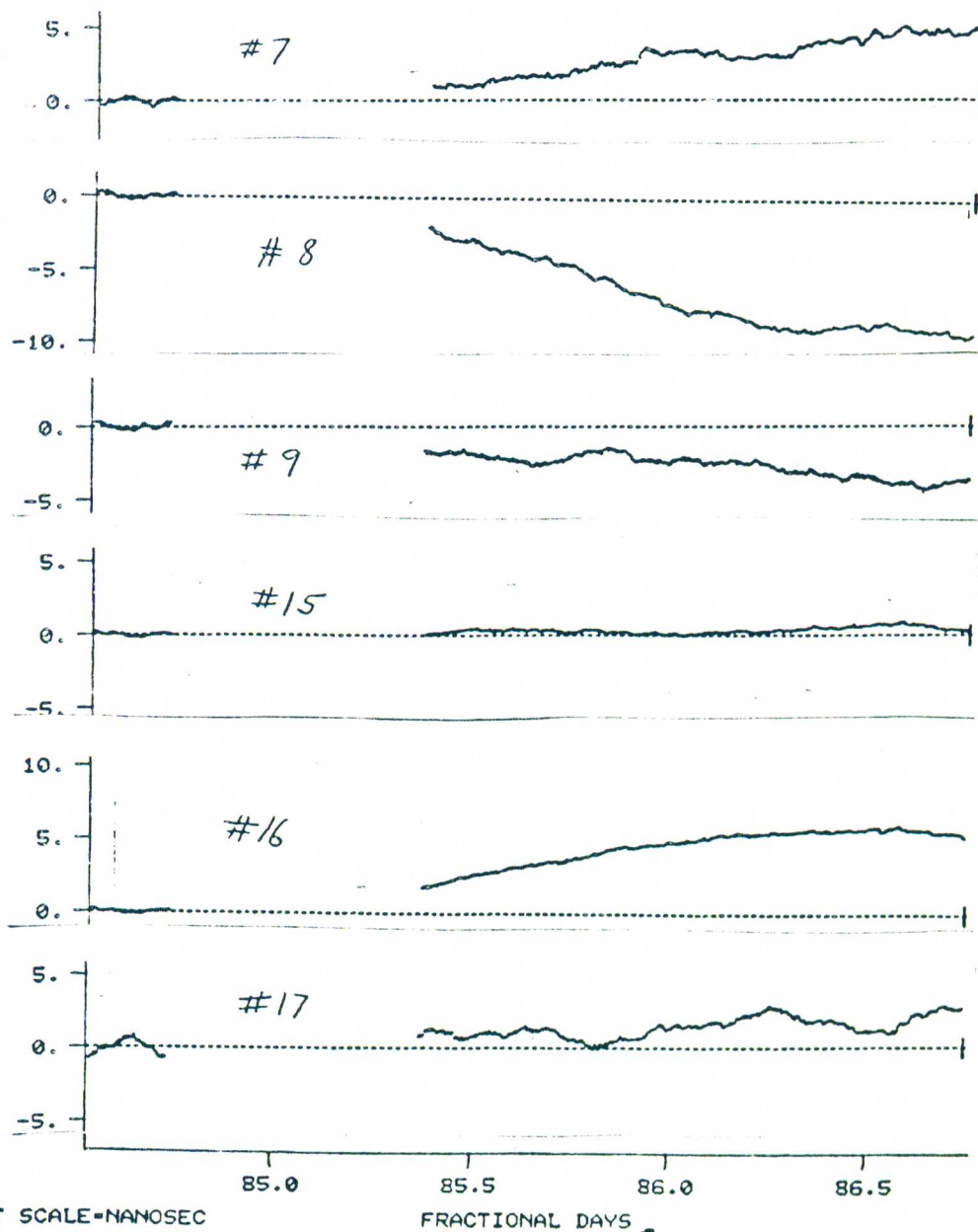






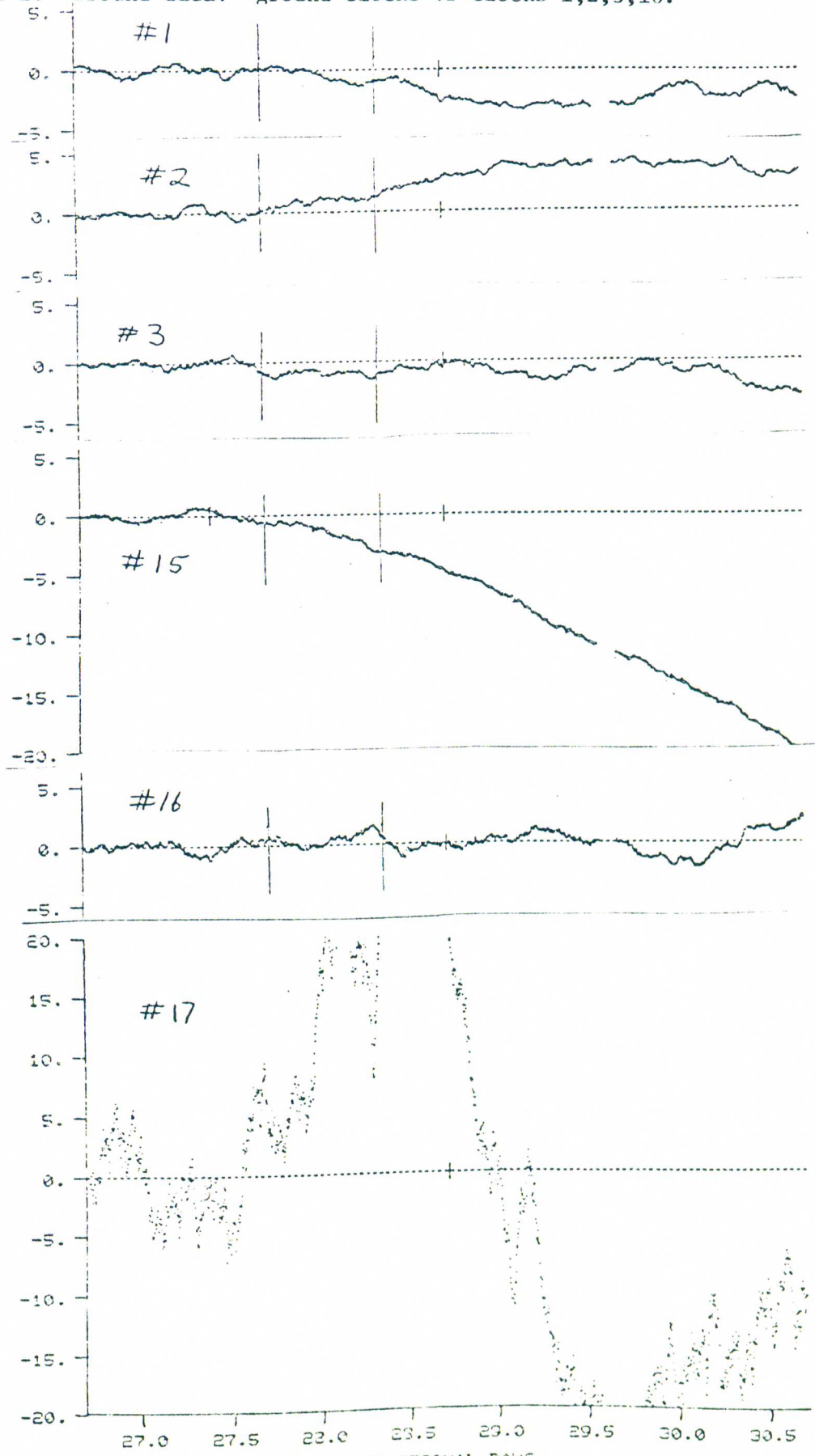


FLIGHT 1. Ground data: Ground clocks vs clocks 7,8,9,15,16,17



RESIDUALS, FILE: DFTOTG929 SLOPE FILE: GDSGB929  
 PAPER REF 7, 8, 9,15,16,17,

FLIGHT 2. Ground data: ground clocks vs clocks 1,2,3,16.

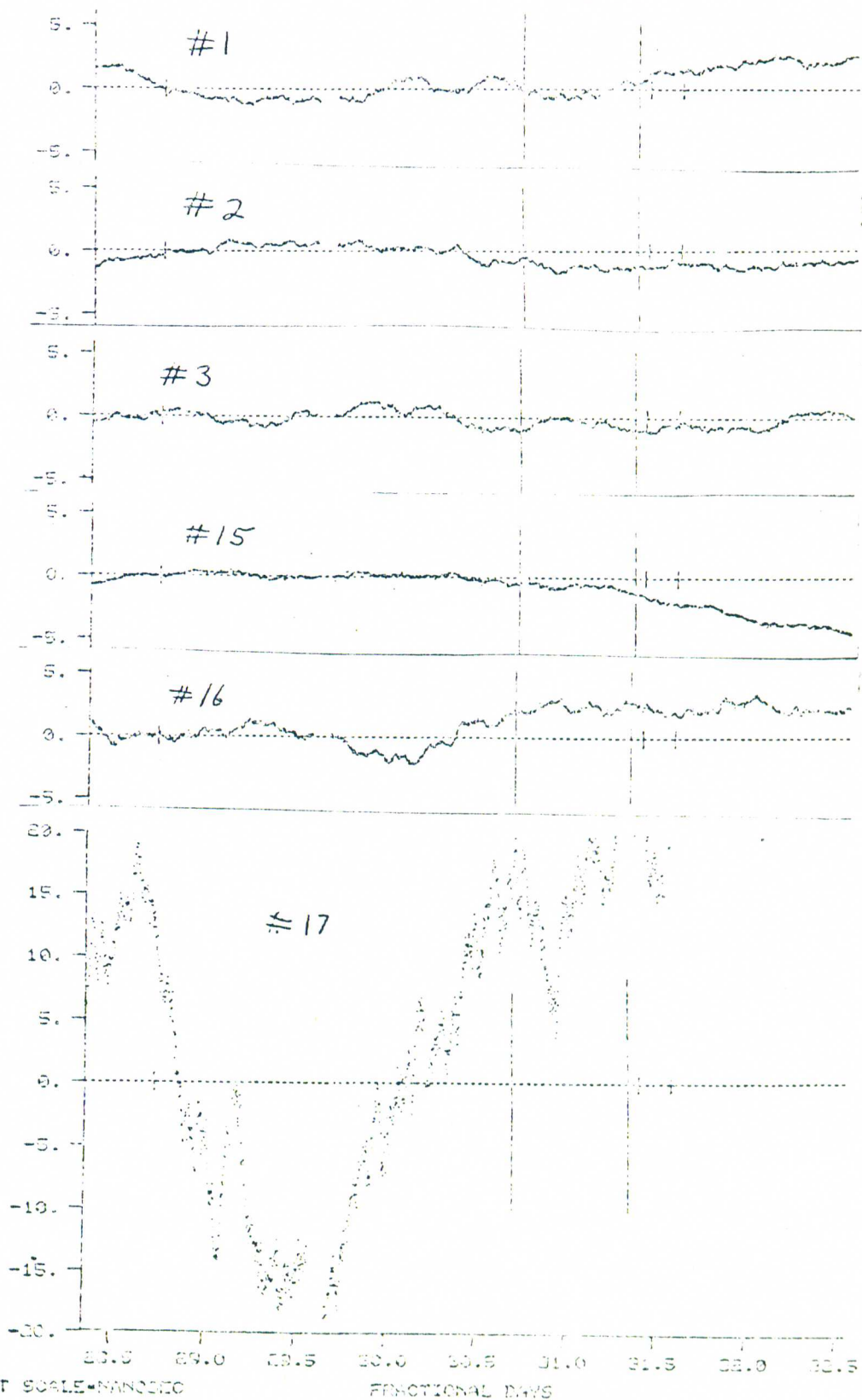


VERT SCALE= NANOSEC

FRACTIONAL DAYS

RESIDUALS FILE: RESOTG1111 SLOPE FILE: GDSOR1111

## FLIGHT 3. Ground data: Ground clocks vs clocks 1,2,3,15,16

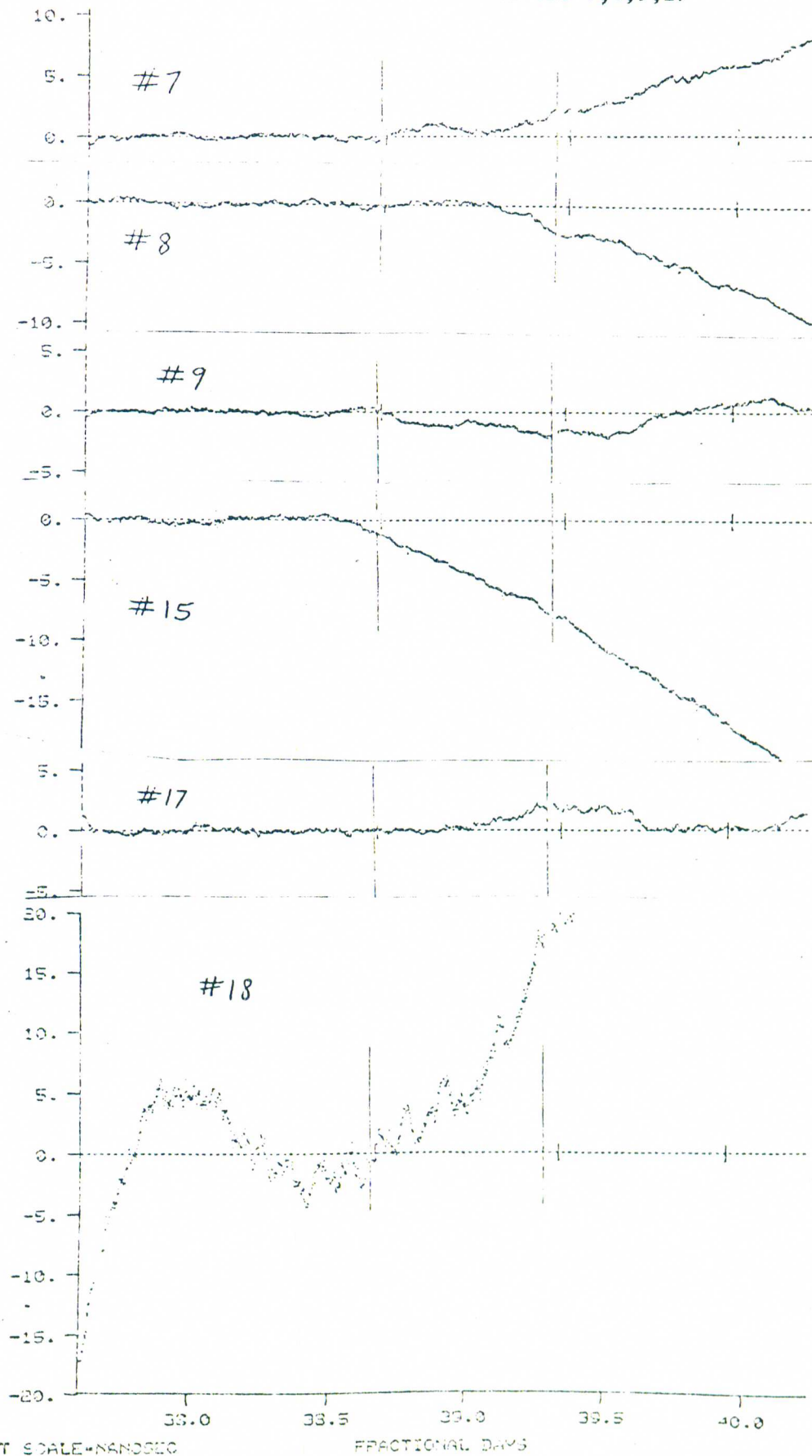


VERT SCALE - NANOS

FRACTIONAL DAYS

RESTINALS. FILE: DITOF01114 SLOPE FILE: GFSOP1114  
 PAPER REF: 1, 2, 3, 15, 16

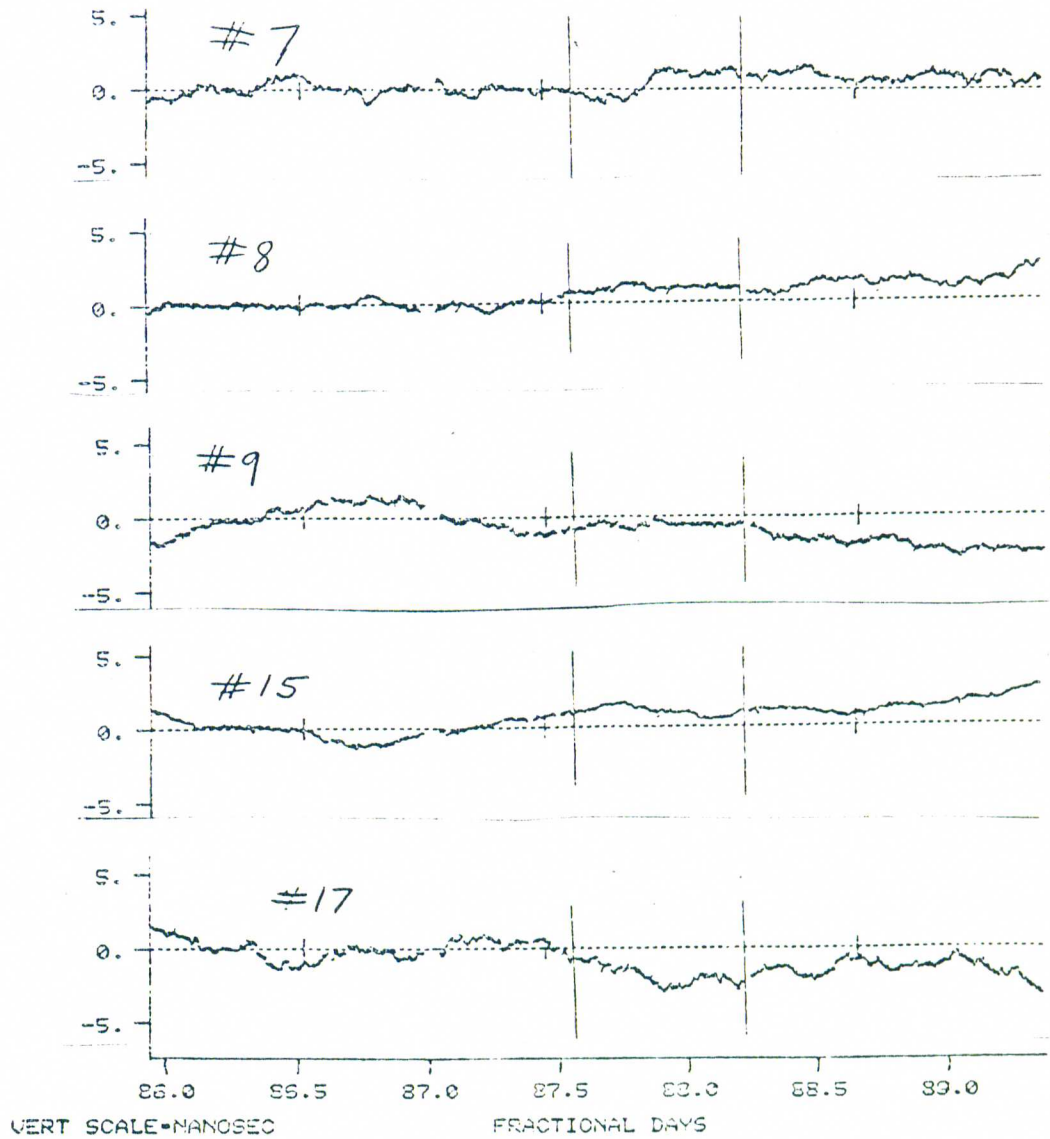
## FLIGHT 4. Ground data: Ground clocks vs clocks 7,8,9,17



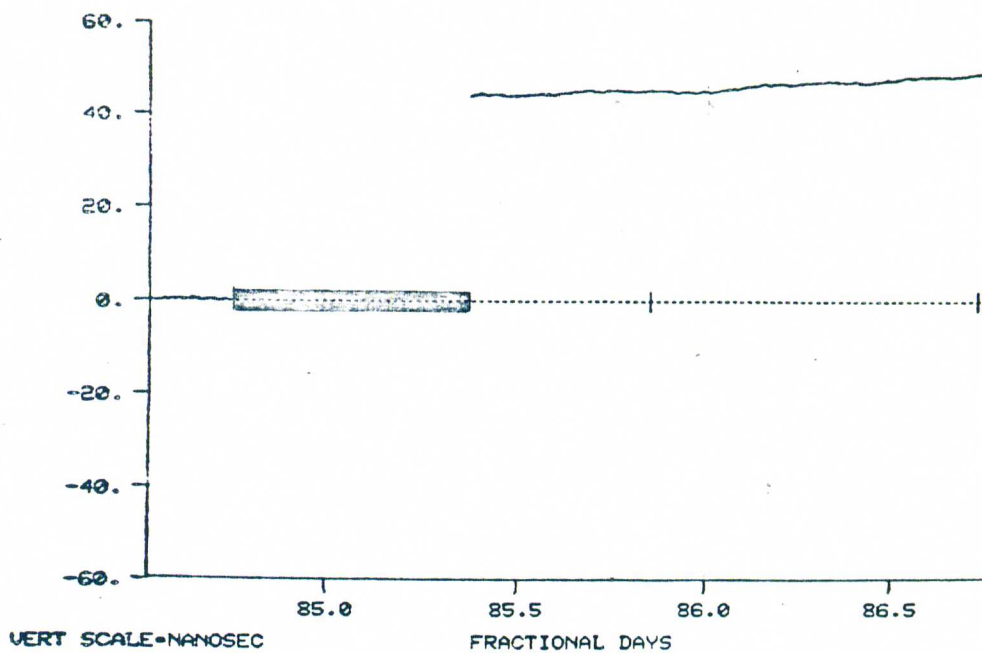
VERT SCALE-NANOSSEC

FRACTIONAL DAYS

FLIGHT 5. Ground data: Ground clocks vs clocks 7,8,9,15,17.

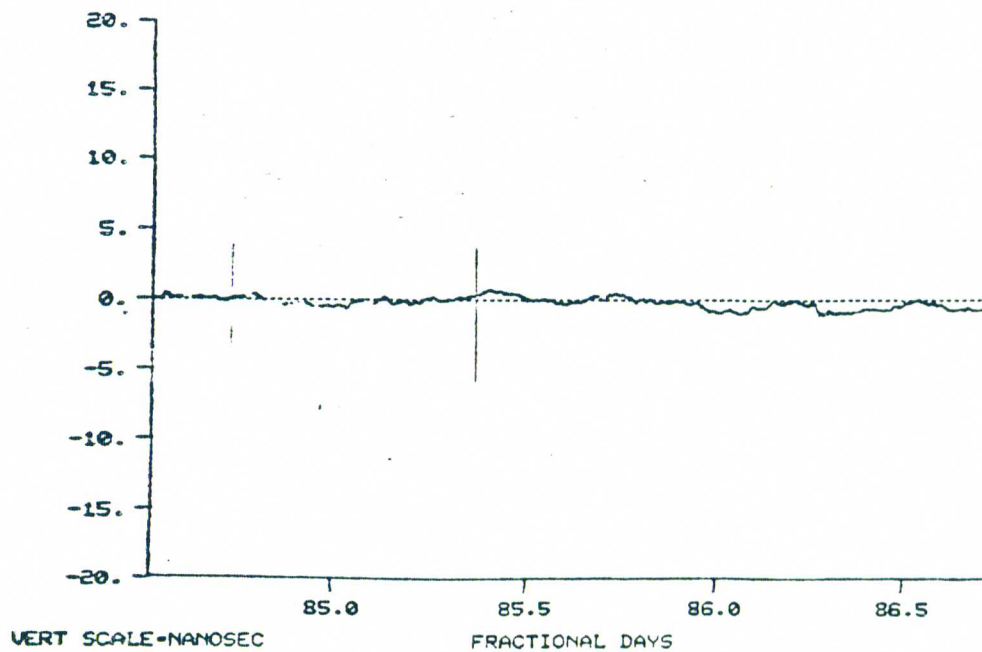


RESIDUALS, FILE: DFTOTG110 SLOPE FILE: GDSGB110  
 PAPER REF 7, 8, 9, 15, 17,



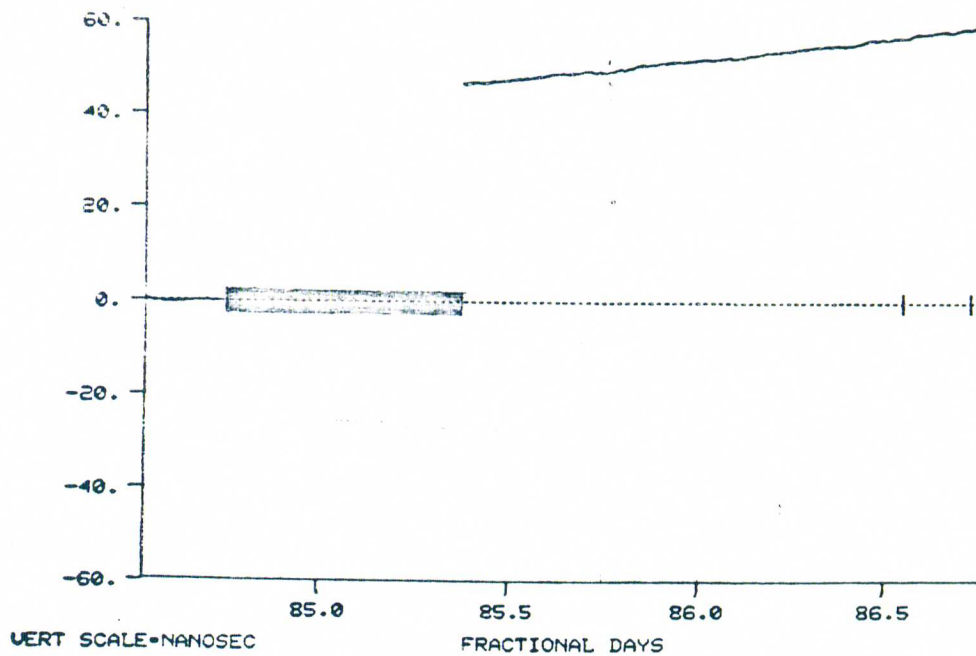
RESIDUALS, FILE: DFTOTG929 SLOPE FILE: GPSGB929  
CLOCK # 1 US PAPER REF 7, 8, 9,15,16,17,

Cesium clock 1  
Flight 1



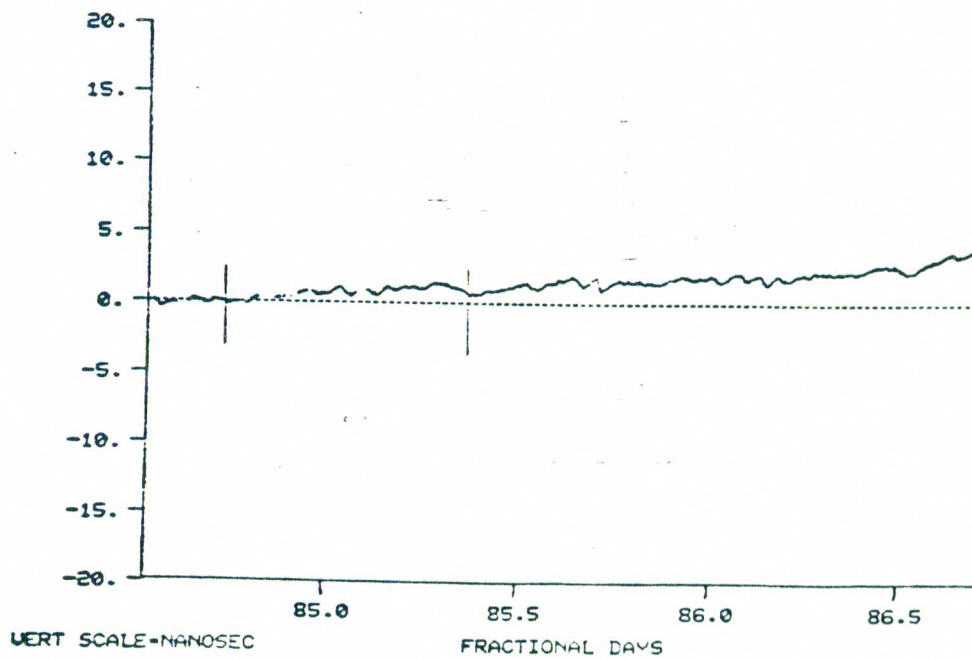
RESIDUALS, FILE: DFTOTA929 SLOPE FILE: PSAB929  
CLOCK # 1 US PAPER REF 1, 2, 3,



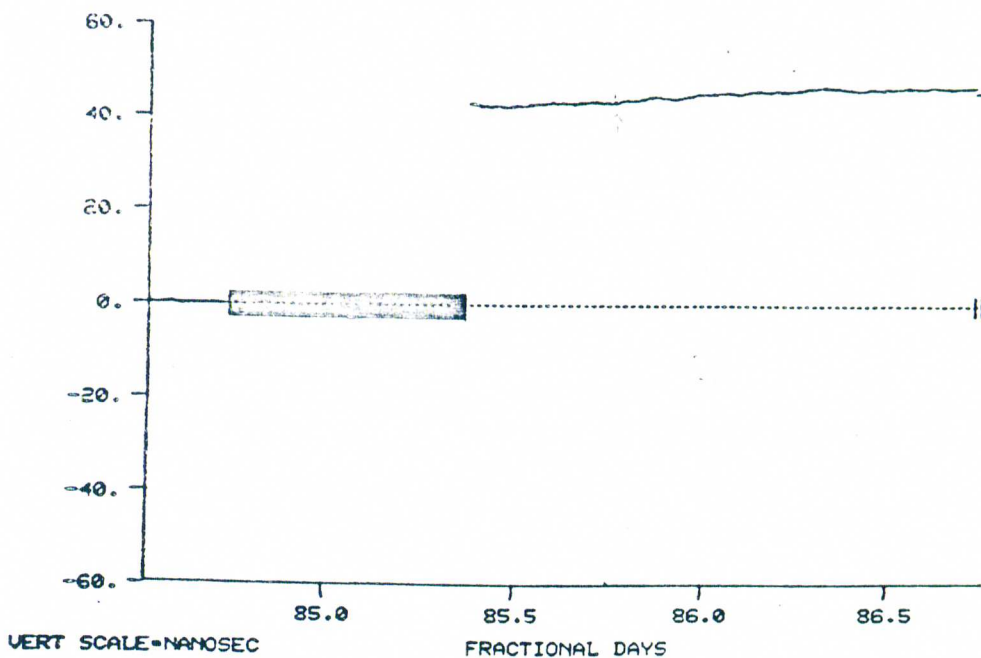


RESIDUALS, FILE: DFTOTG929 SLOPE FILE: GPSGB929  
 CLOCK # 2 US PAPER REF 7, 8, 9, 15, 16, 17,

Cesium clock 2  
 Flight 1

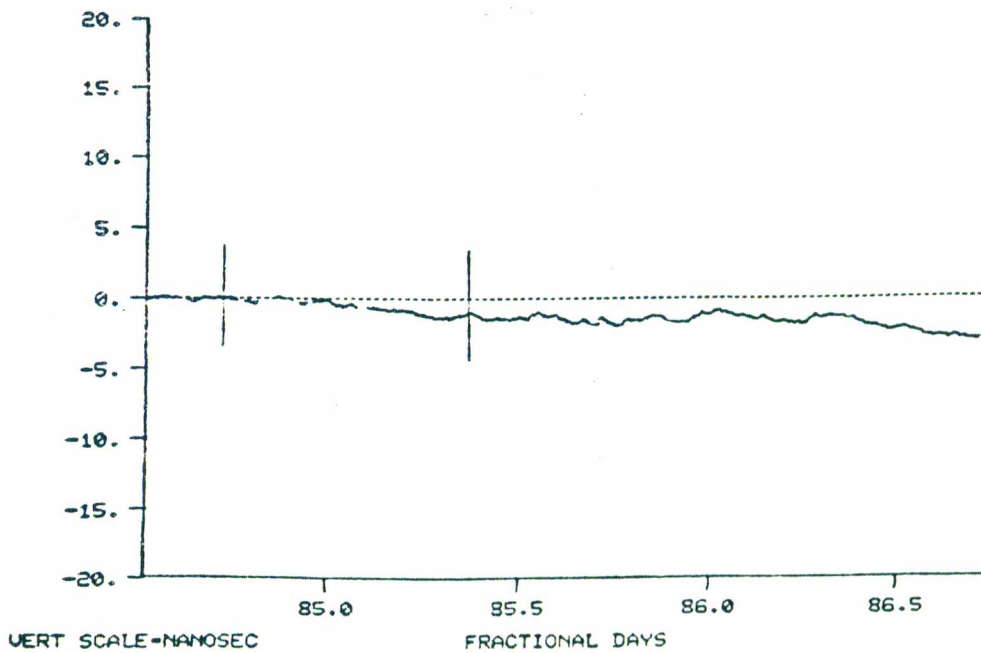


RESIDUALS, FILE: DFTOTA929 SLOPE FILE: PSAB929  
 CLOCK # 2 US PAPER REF 1, 2, 3,

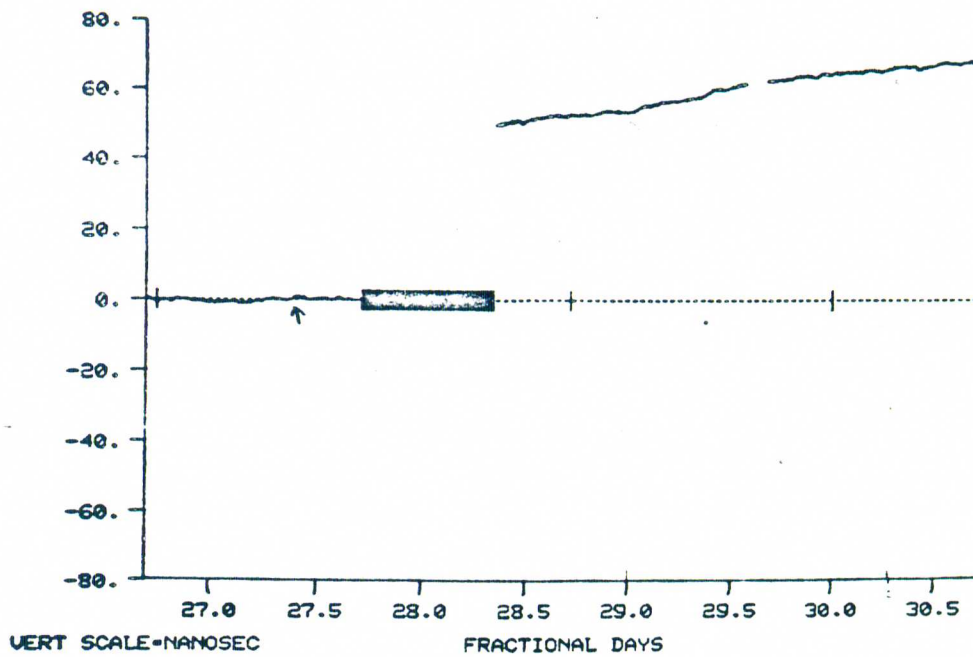


RESIDUALS, FILE: DFTOTG929 SLOPE FILE: GPSGB929  
 CLOCK # 3 US PAPER REF 7, 8, 9,15,16,17,

Cesium clock 3  
 Flight 1

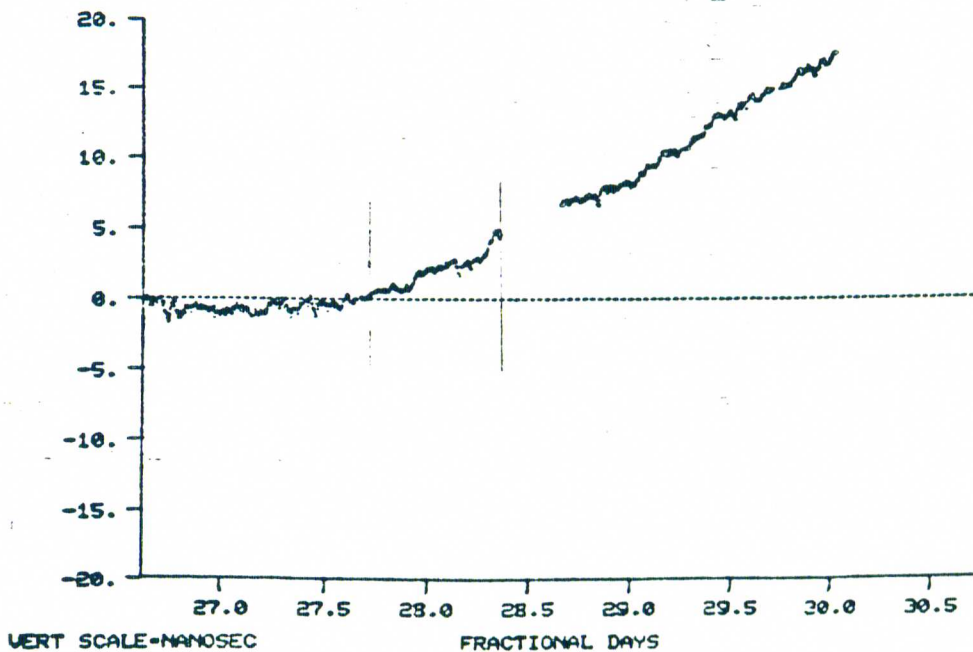


RESIDUALS, FILE: DFTOTA929 SLOPE FILE: PSAB929  
 CLOCK # 3 US PAPER REF 1, 2, 3,

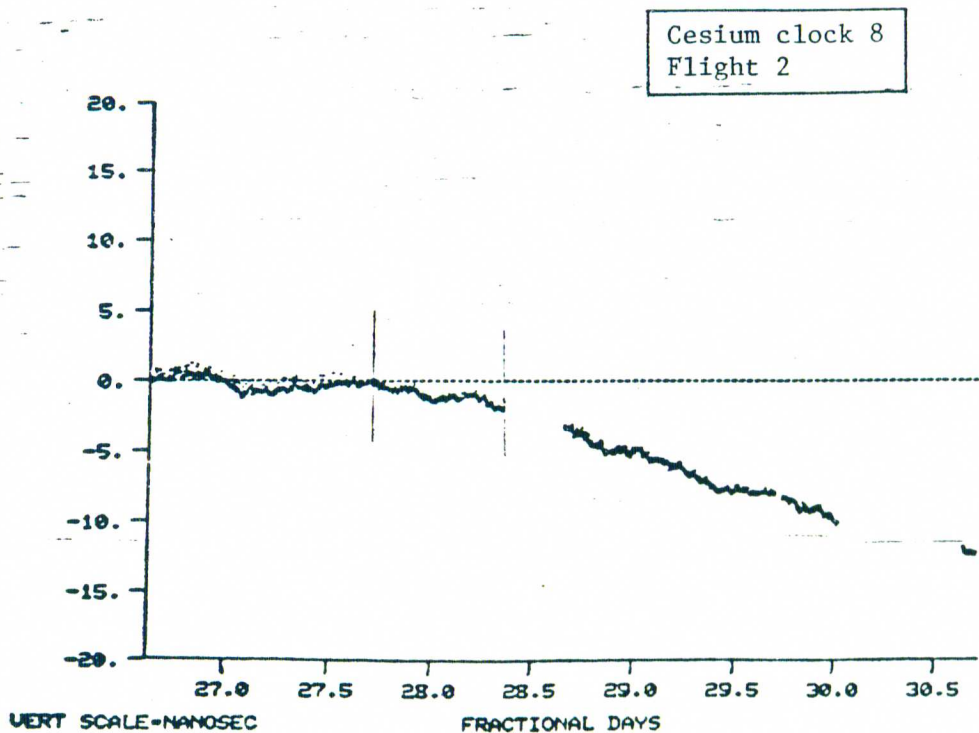
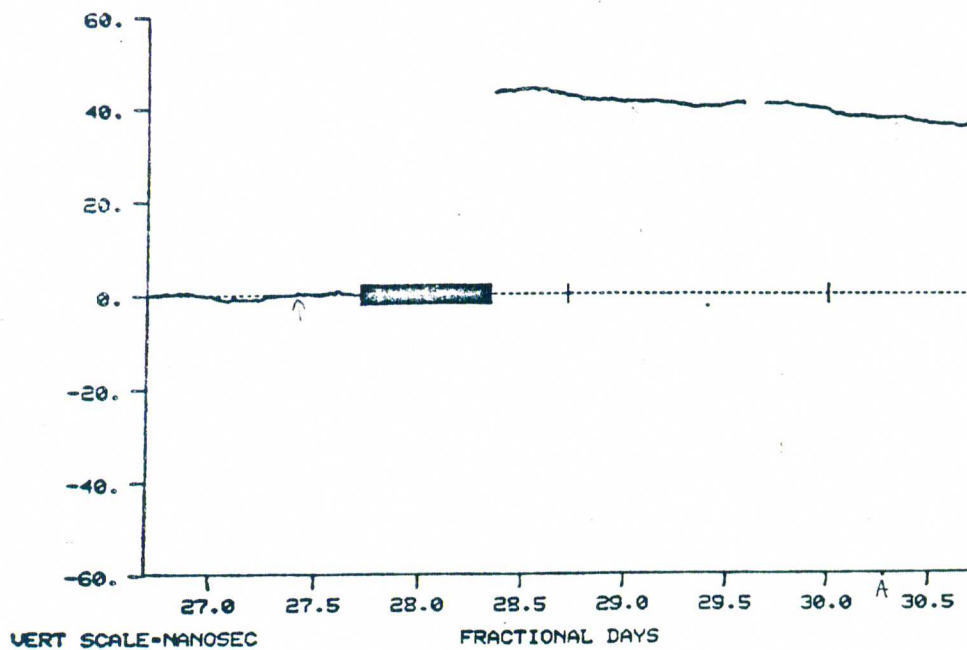


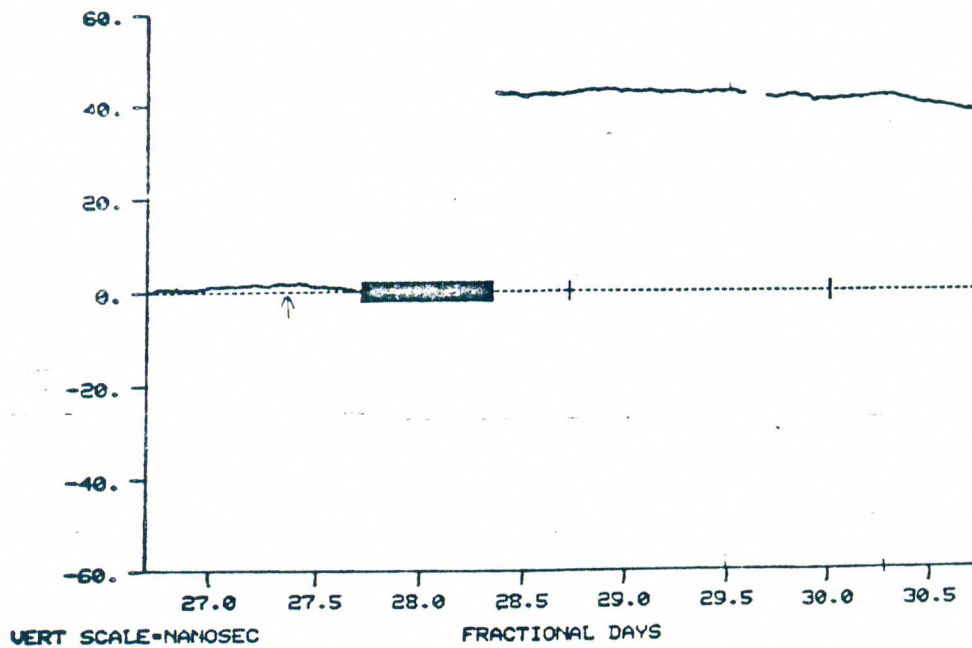
RESIDUALS, FILE: DFTOTG1111 SLOPE FILE: GPSGB1111  
CLOCK # 7 US PAPER REF 1, 2, 3, 16,

Cesium clock 7  
Flight 2

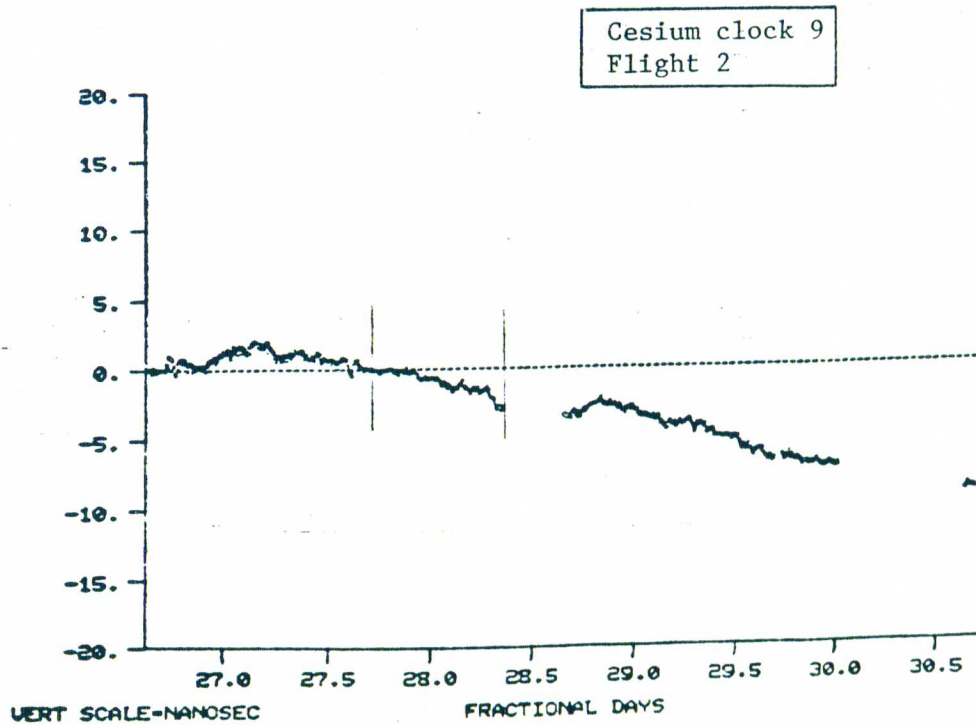


RESIDUALS, FILE: DFTOTA1111 SLOPE FILE: GPSAB1111  
CLOCK # 7 US PAPER REF 7, 8, 9,

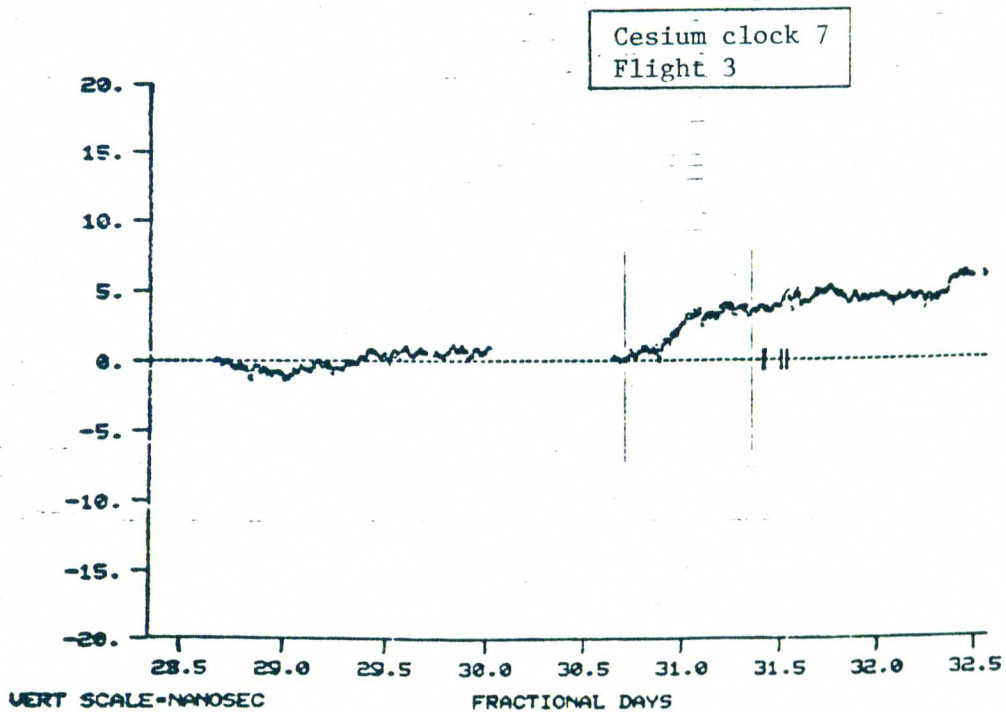
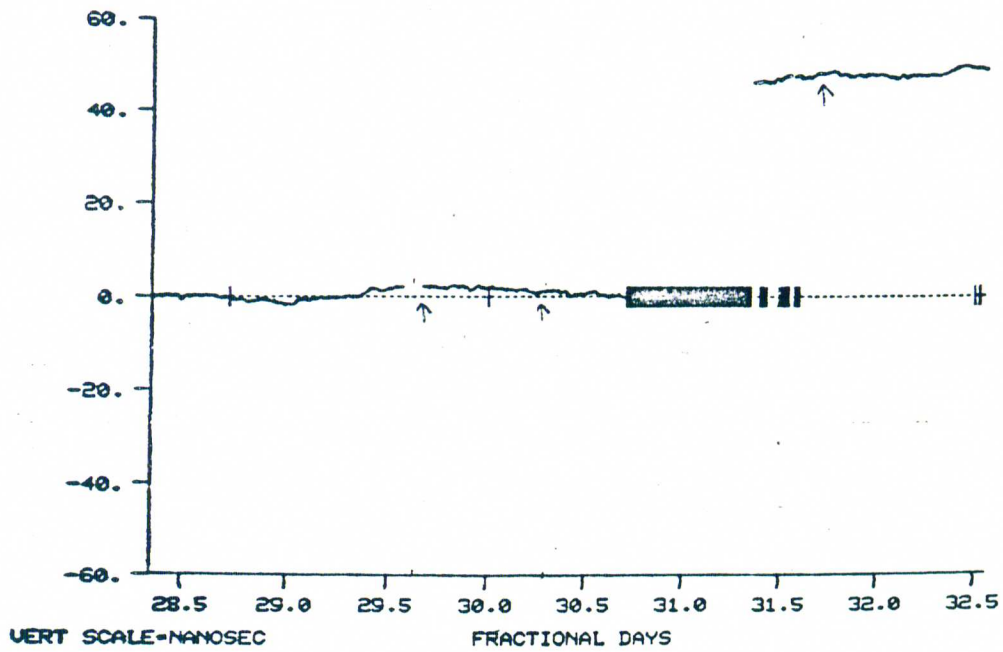


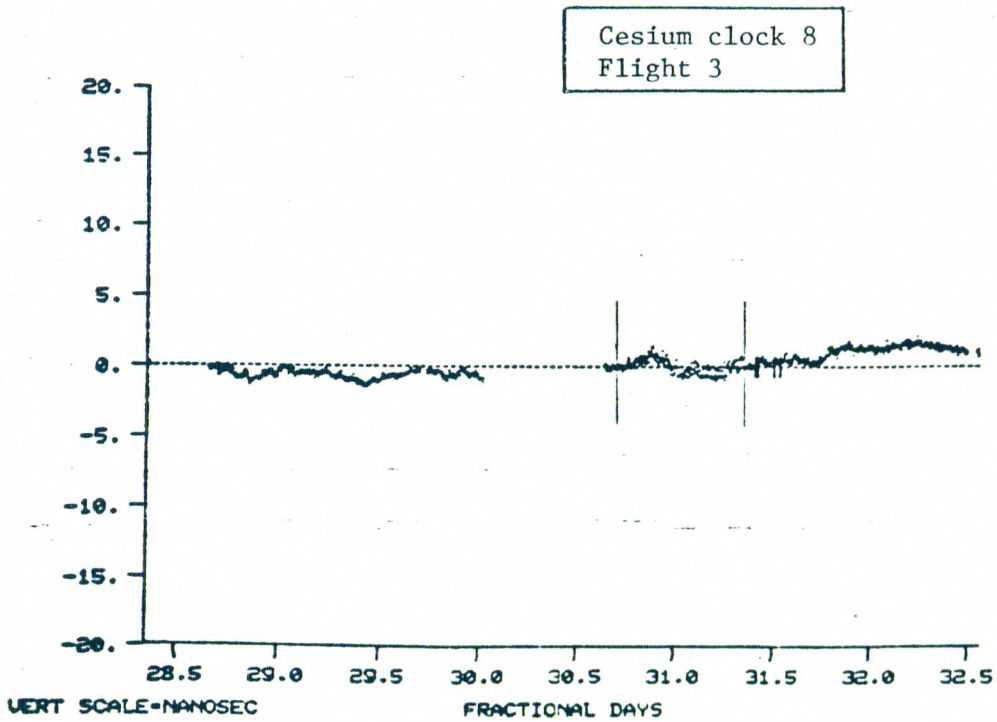
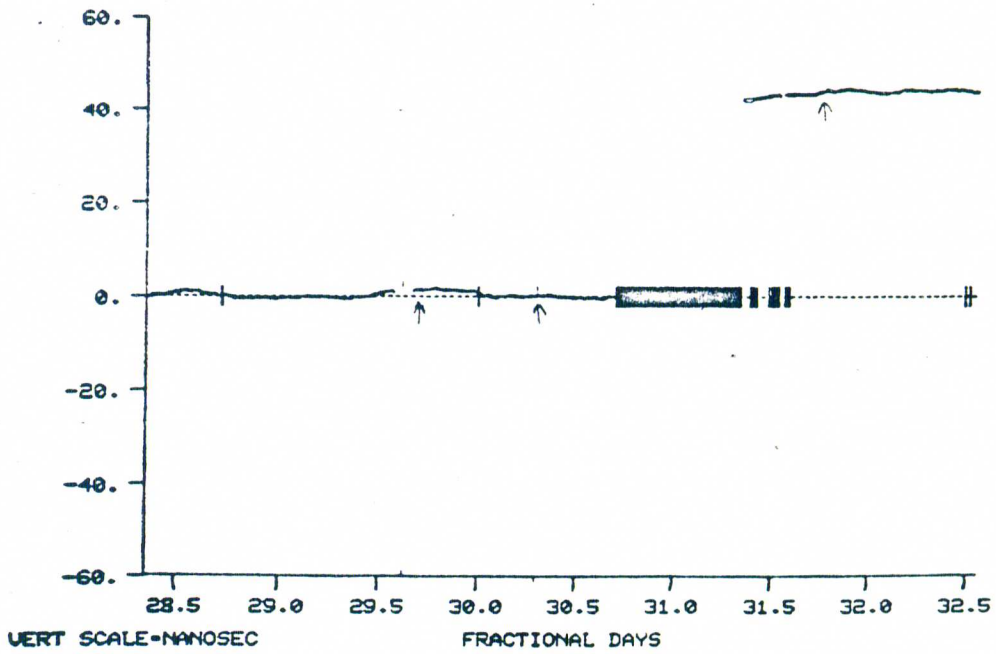


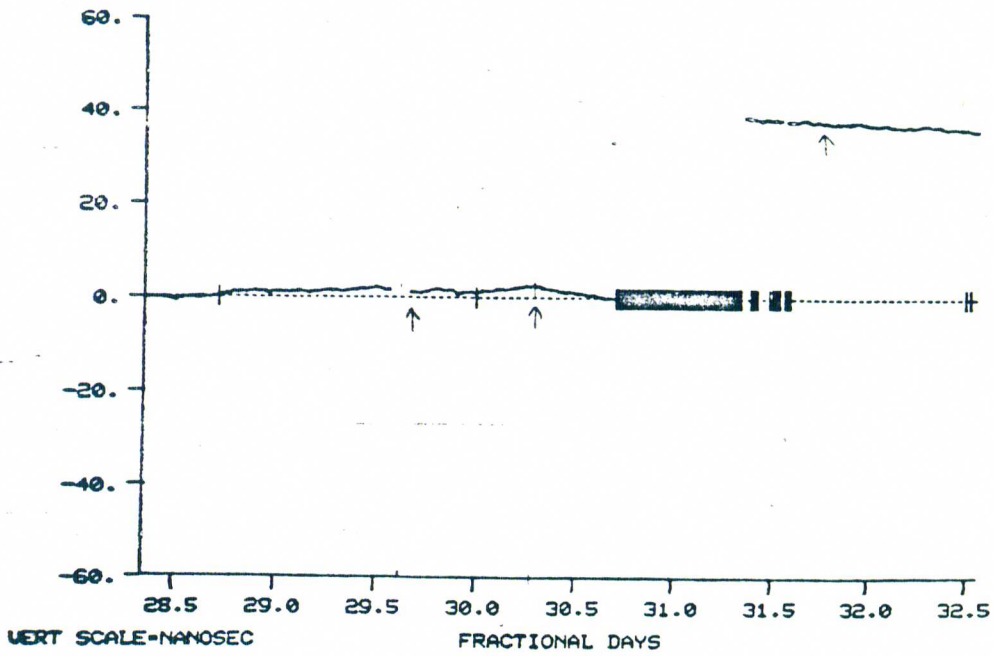
RESIDUALS, FILE: DFTOTG1111 SLOPE FILE: GPSGB1111  
 CLOCK # 9 US PAPER REF 1, 2, 3, 16.



RESIDUALS, FILE: DFTOTA1111 SLOPE FILE: GPSAB1111  
 CLOCK # 9 US PAPER REF 7, 8, 9.

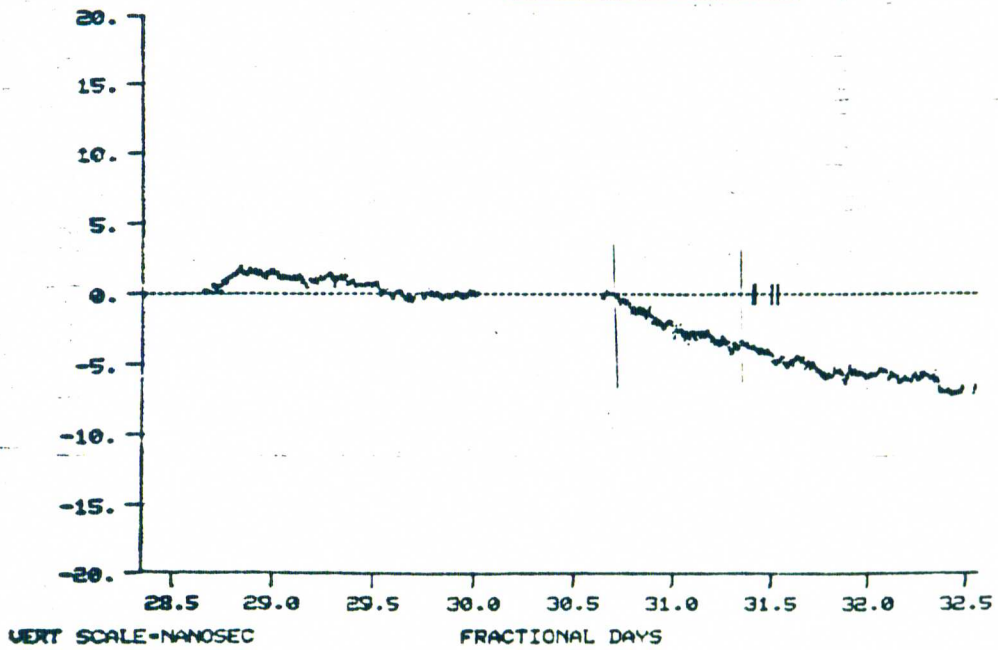






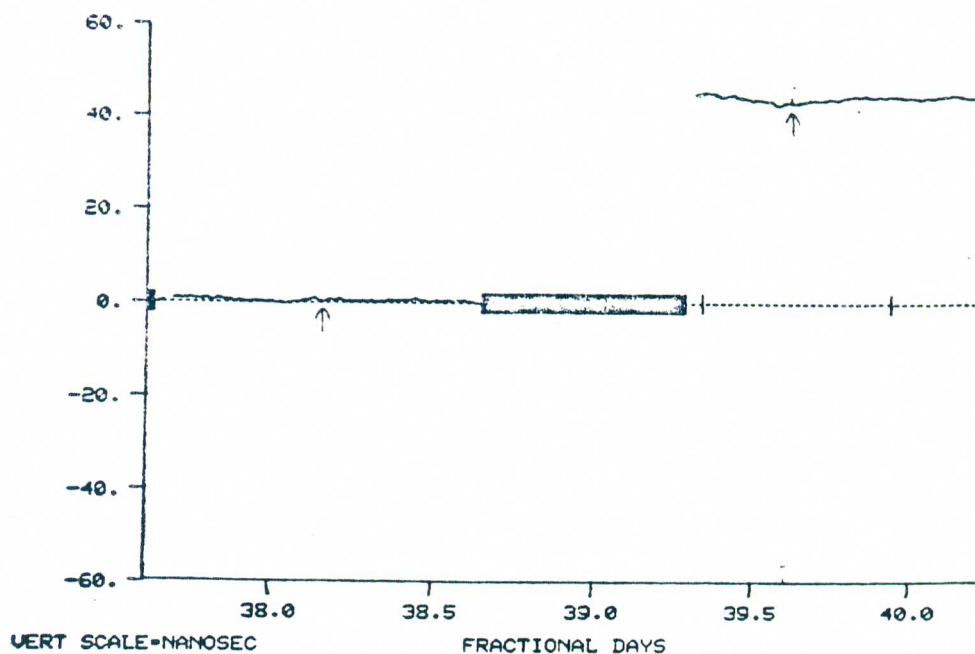
RESIDUALS, FILE: DFTOTG1114 SLOPE FILE: GPSGB1114  
 CLOCK \* 9 US PAPER REF 1, 2, 3,15,16.

Cesium clock 9  
 Flight 3

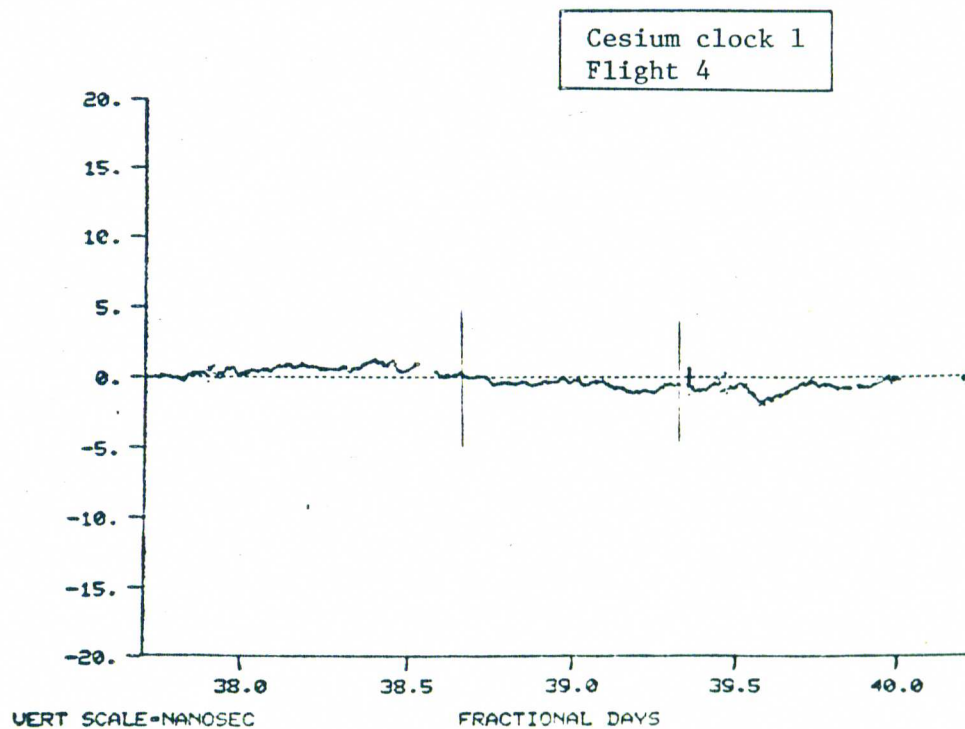


RESIDUALS, FILE: DFTOTA1114 SLOPE FILE: PSAB1114  
 CLOCK \* 9 US PAPER REF 7, 8, 9,

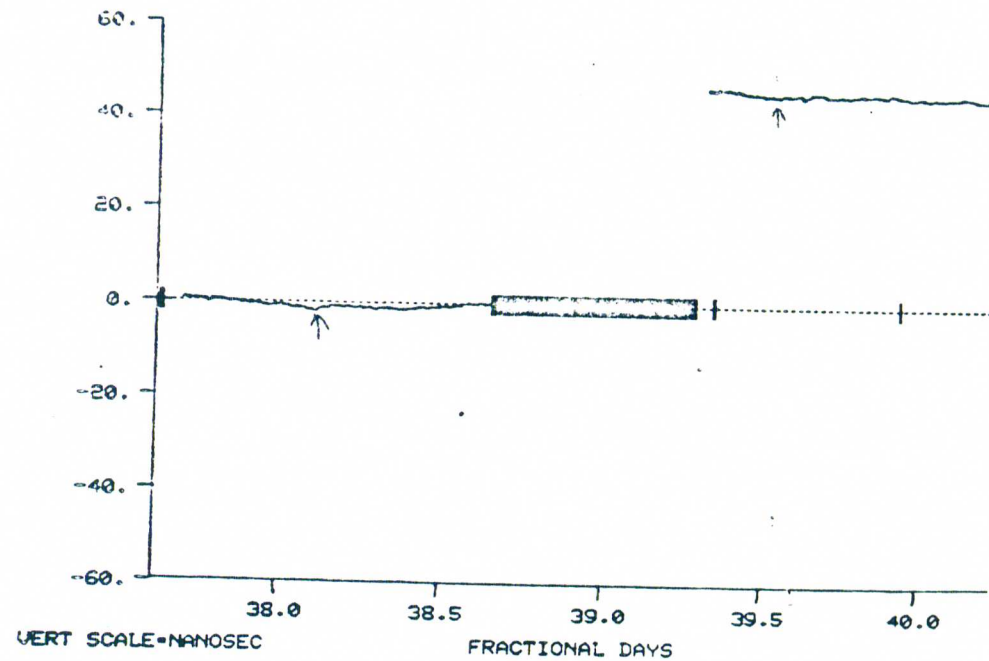




RESIDUALS, FILE: DFTOTG1122 SLOPE FILE: GP5GB1122  
 CLOCK # 1 US PAPER REF 7, 8, 9, 17,

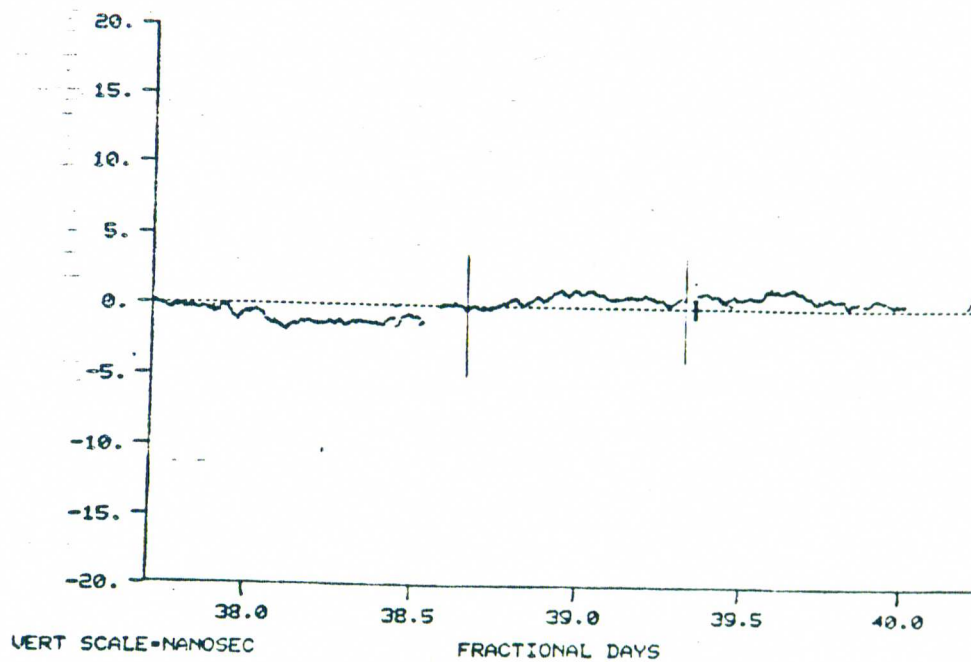


RESIDUALS, FILE: DFTOTA1122 SLOPE FILE: PSAB1122  
 CLOCK # 1 US PAPER REF 1, 2, 3,

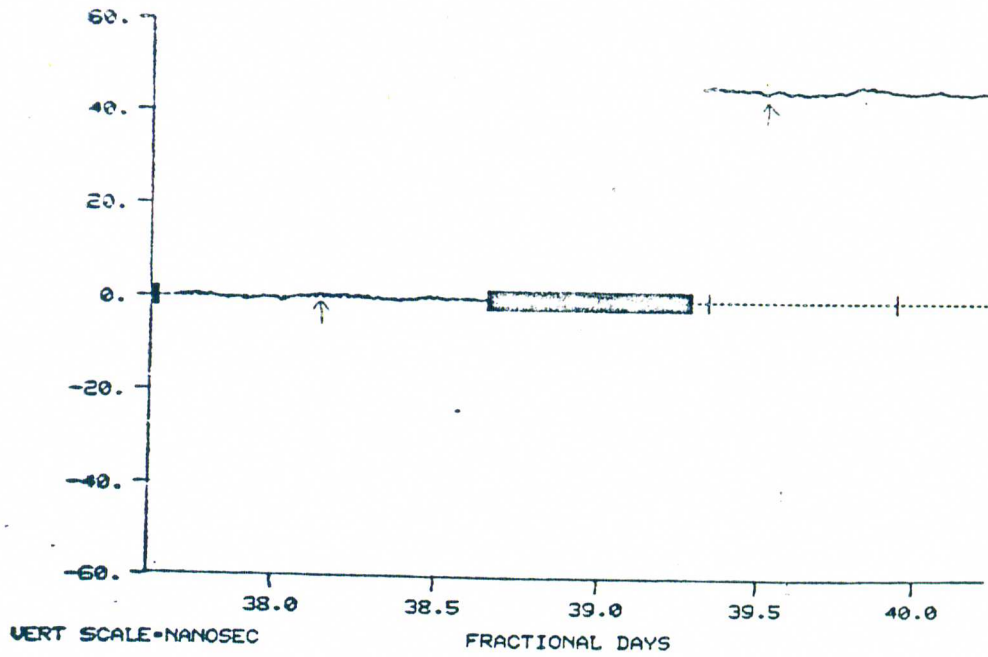


RESIDUALS, FILE: DFTOTG1122 SLOPE FILE: GPSGB1122  
 CLOCK # 2 US PAPER REF 7, 8, 9, 17,

Cesium clock 2  
 Flight 4

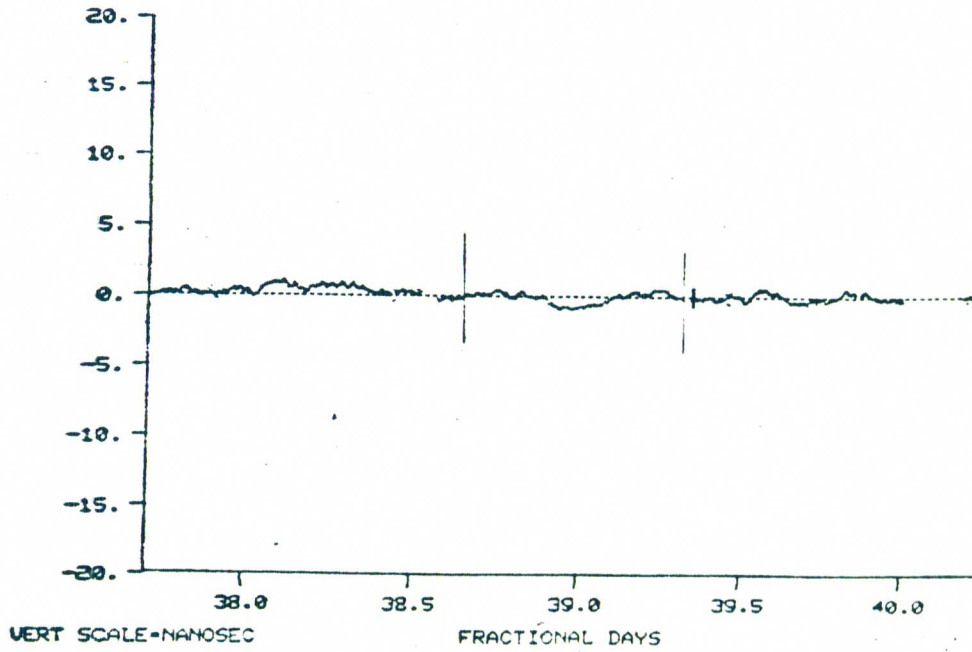


RESIDUALS, FILE: DFTOTA1122 SLOPE FILE: PSAB1122  
 CLOCK # 2 US PAPER REF 1, 2, 3,

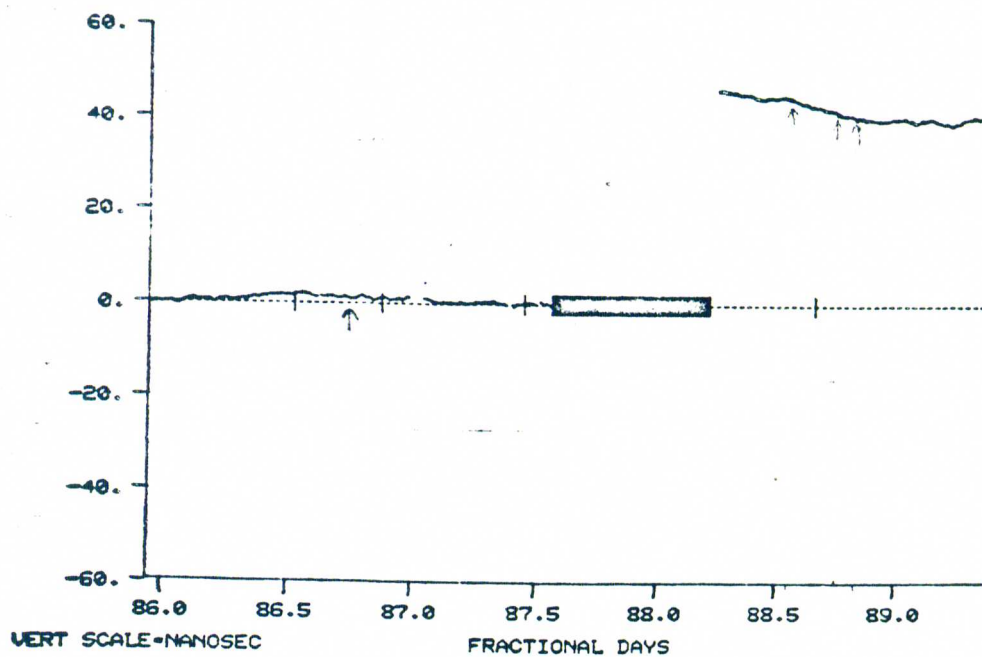


RESIDUALS, FILE: DFTOTG1122 SLOPE FILE: GPSGB1122  
CLOCK # 3 US PAPER REF 7, 8, 9, 17,

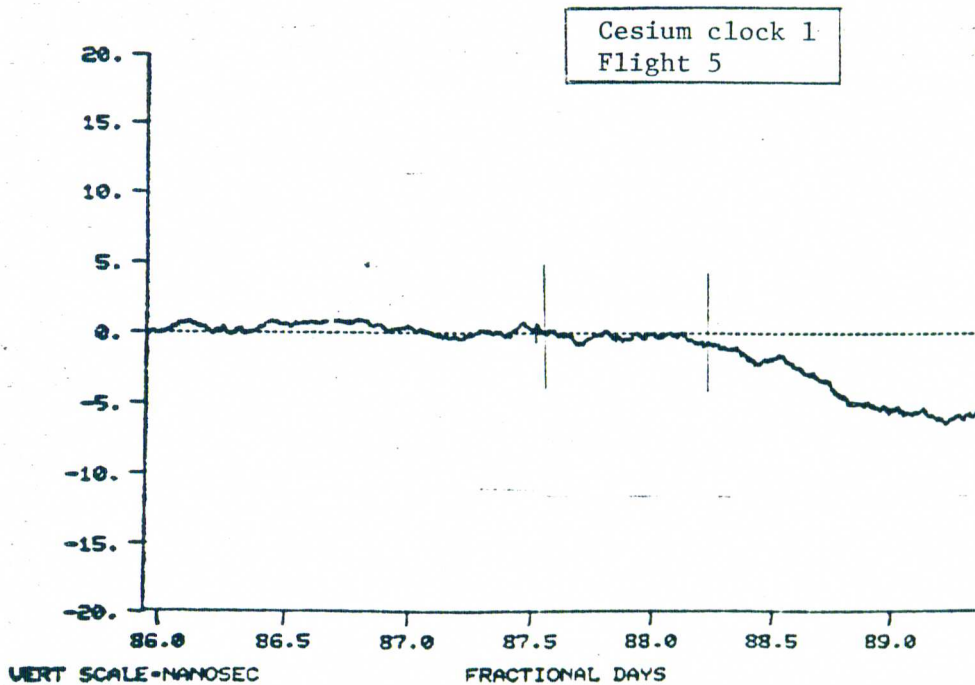
Cesium clock 3  
Flight 4



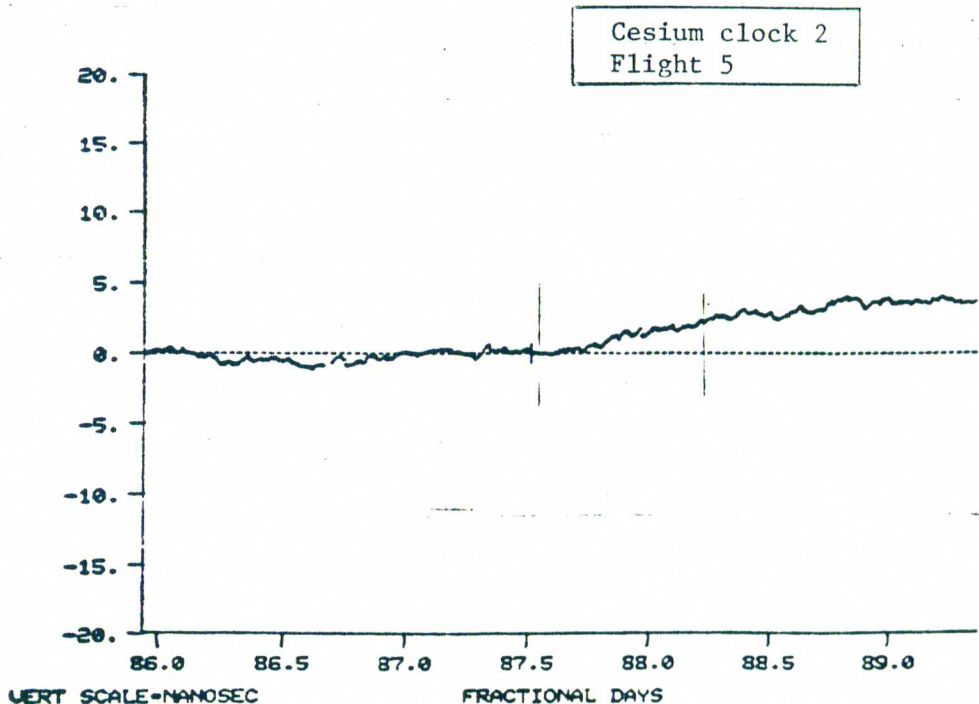
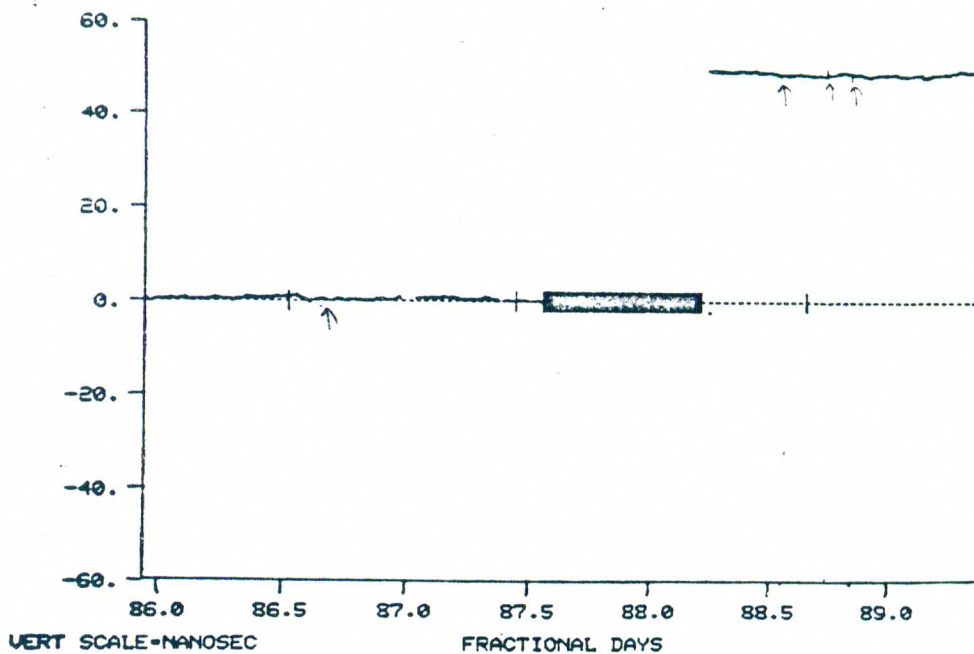
RESIDUALS, FILE: DFTOTA1122 SLOPE FILE: PSAB1122  
CLOCK # 3 US PAPER REF 1, 2, 3,

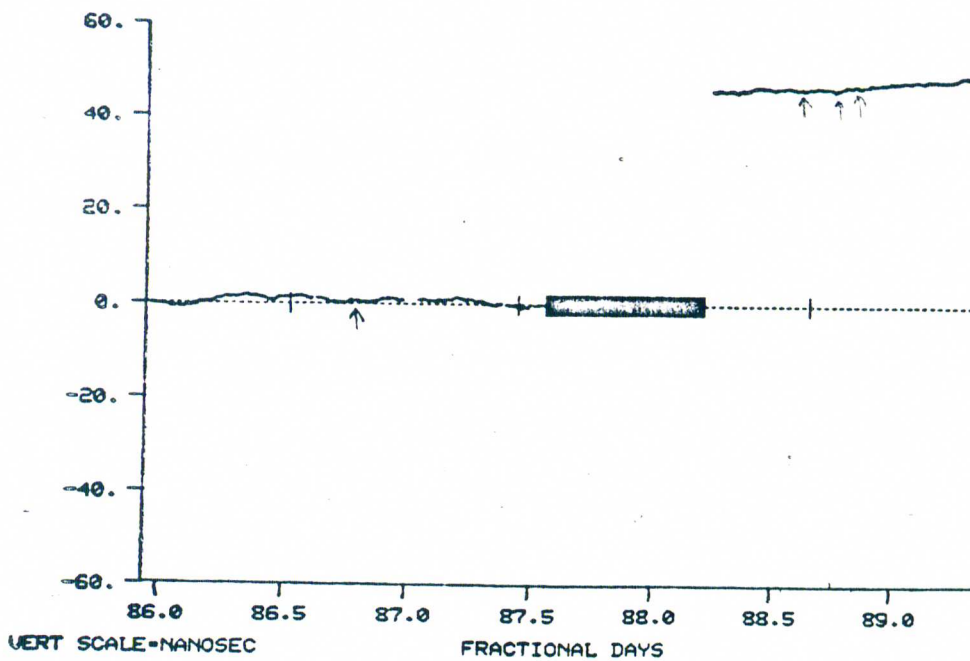


RESIDUALS, FILE: DFTOTG110 SLOPE FILE: GPSGB110  
 CLOCK # 1 US PAPER REF 7, 8, 9, 15, 17,



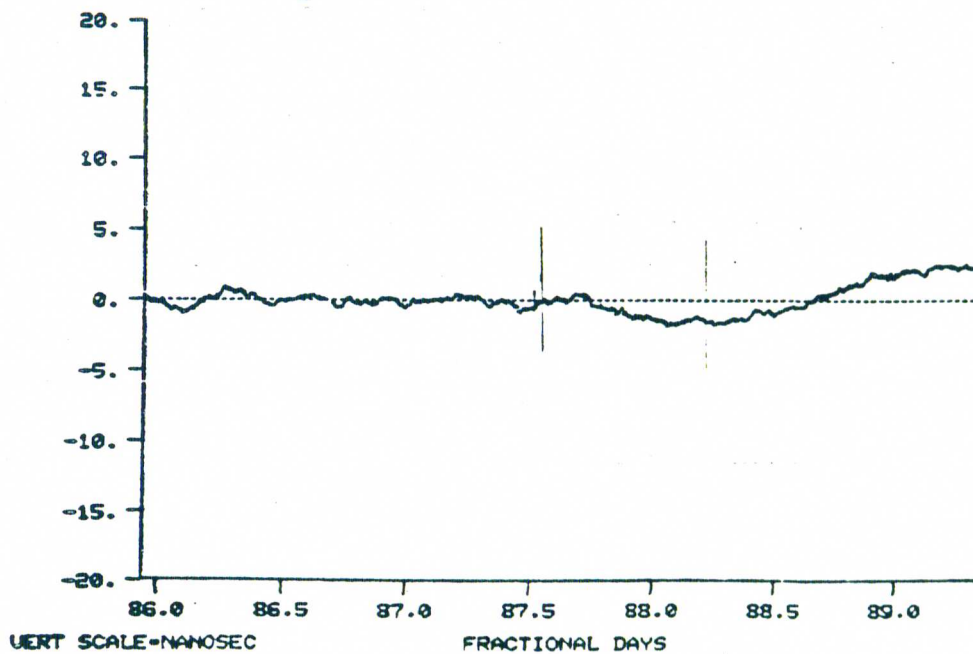
RESIDUALS, FILE: DFTOTA110 SLOPE FILE: GPSAB110  
 CLOCK # 1 US PAPER REF 1, 2, 3,



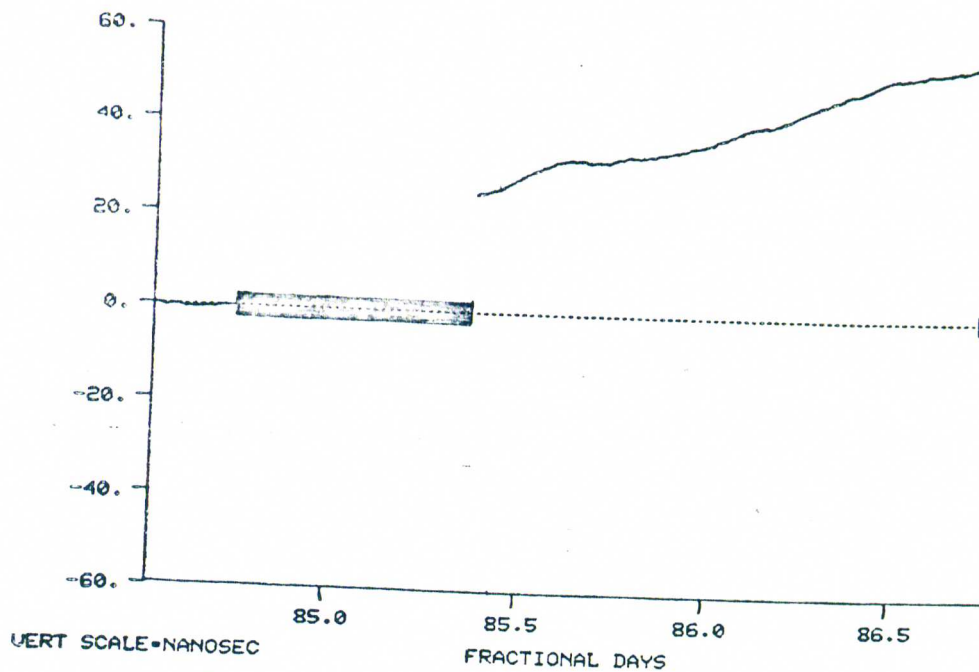


RESIDUALS, FILE: DFTOTG110 SLOPE FILE: GPSGB110  
 CLOCK # 3 US PAPER REF 7, 8, 9, 15, 17,

Cesium clock 3  
 Flight 5

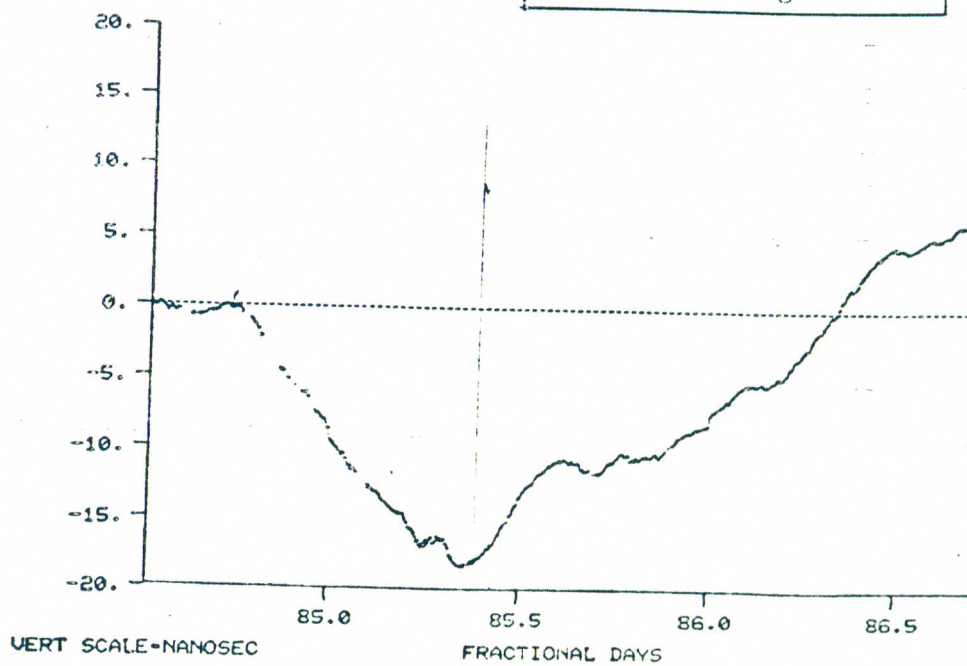


RESIDUALS, FILE: DFTOTA110 SLOPE FILE: GPSAB110  
 CLOCK # 3 US PAPER REF 1, 2, 3,

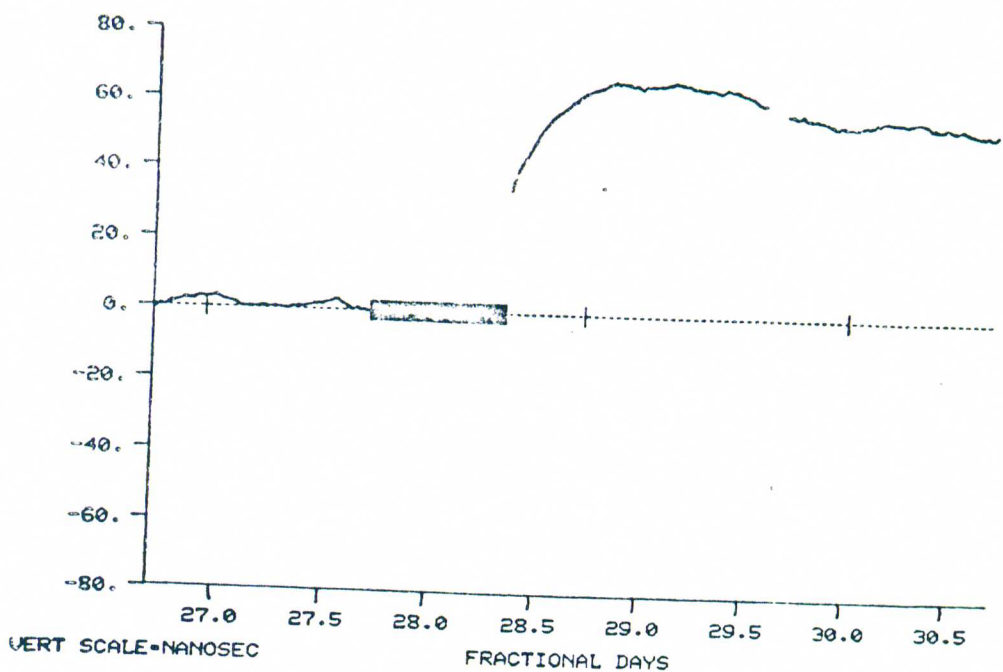


RESIDUALS, FILE: DFTOTG929 SLOPE FILE: GPSGB929  
 CLOCK # 18 US PAPER REF 7, 8, 9, 15, 16, 17,

"Travelling" Cesium clock  
 Clock #18 Flight 1

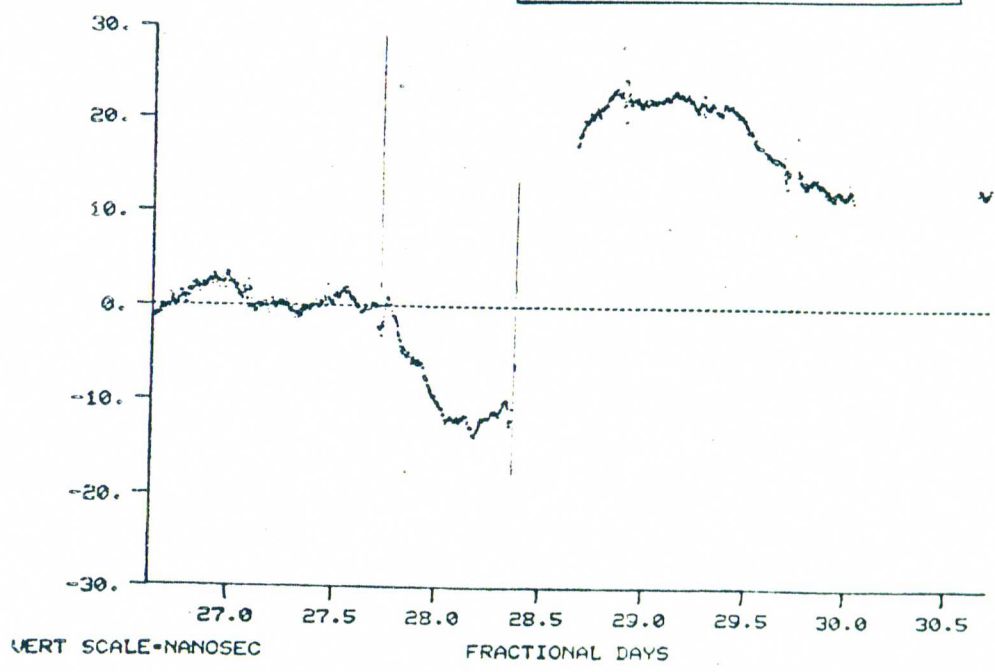


RESIDUALS, FILE: DFTOTAG29 SLOPE FILE: 31PSAB929  
 CLOCK # 18 US PAPER REF 1, 3,



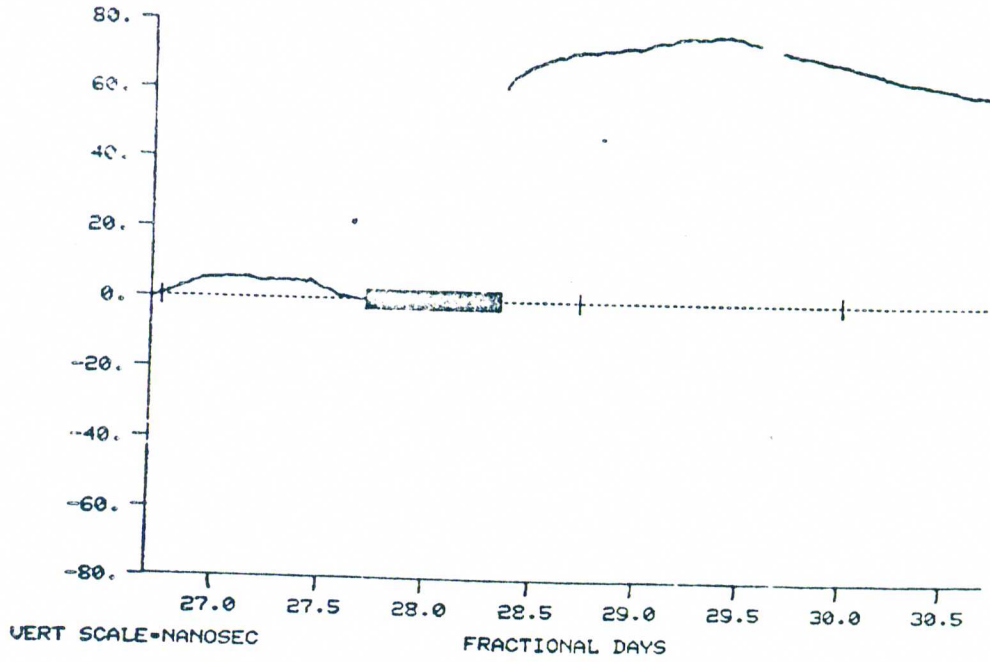
RESIDUALS, FILE: DFTOTG1111 SLOPE FILE: GPSGB1111  
 CLOCK # 18 US PAPER REF 1, 2, 3, 16,

"Travelling" Cesium clock  
 Clock #18 Flight 2



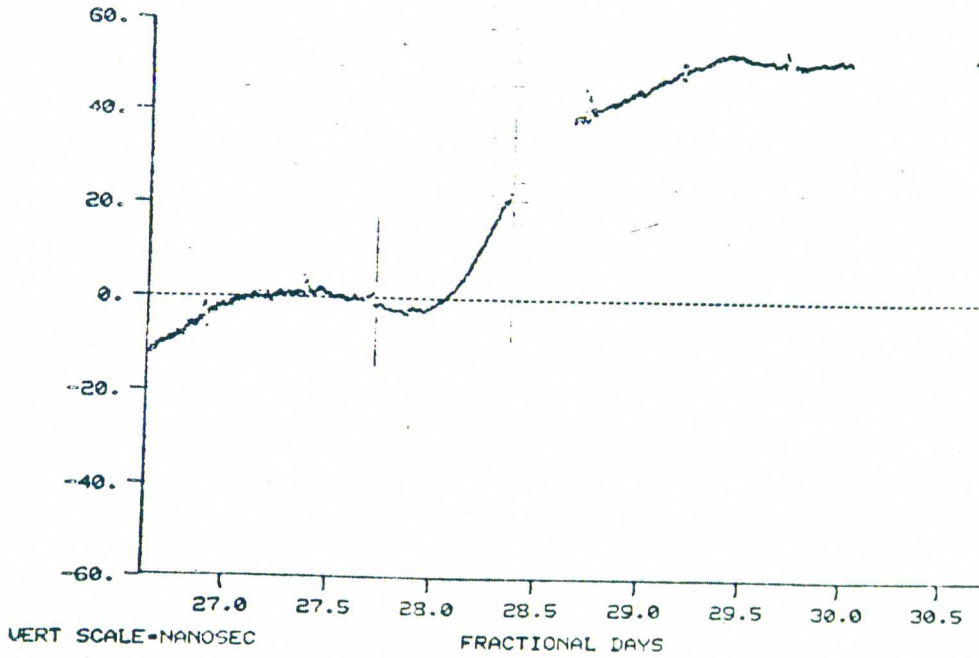
RESIDUALS, FILE: DFTOTA1111 SLOPE FILE: PSAB1111A  
 CLOCK # 18 US PAPER REF 8, 9,



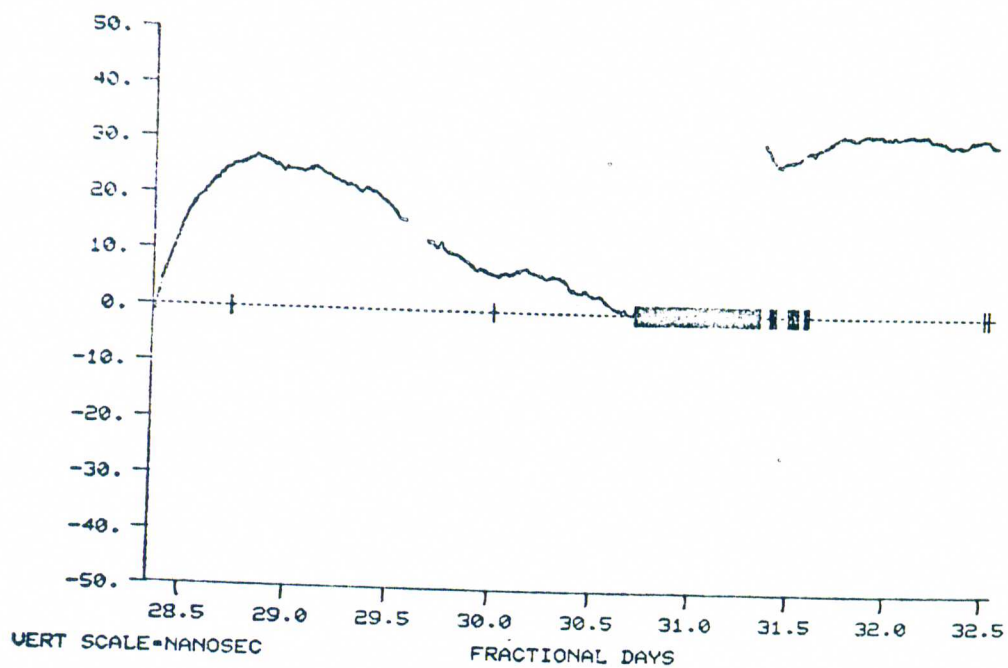


RESIDUALS, FILE: DFTOTG1111 SLOPE FILE: GPSGB1111  
 CLOCK # 19 US PAPER REF 1, 2, 3, 16,

"Travelling" Cesium clock  
 Clock #19 Flight 2

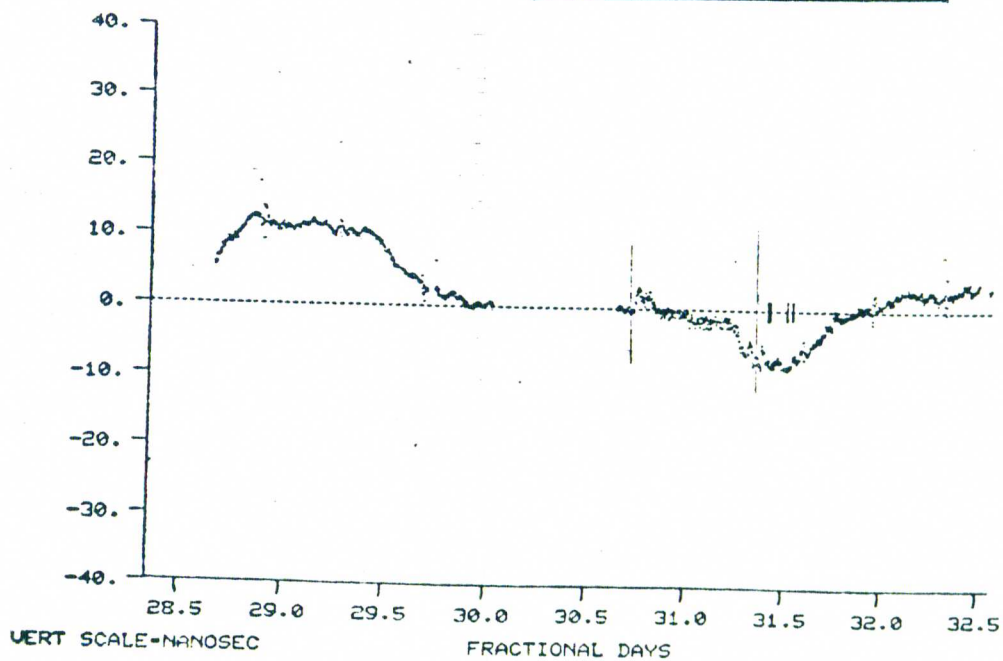


RESIDUALS, FILE: DFTOTA1111 SLOPE FILE: PSAB1111A  
 CLOCK # 19 US PAPER REF 8, 9,

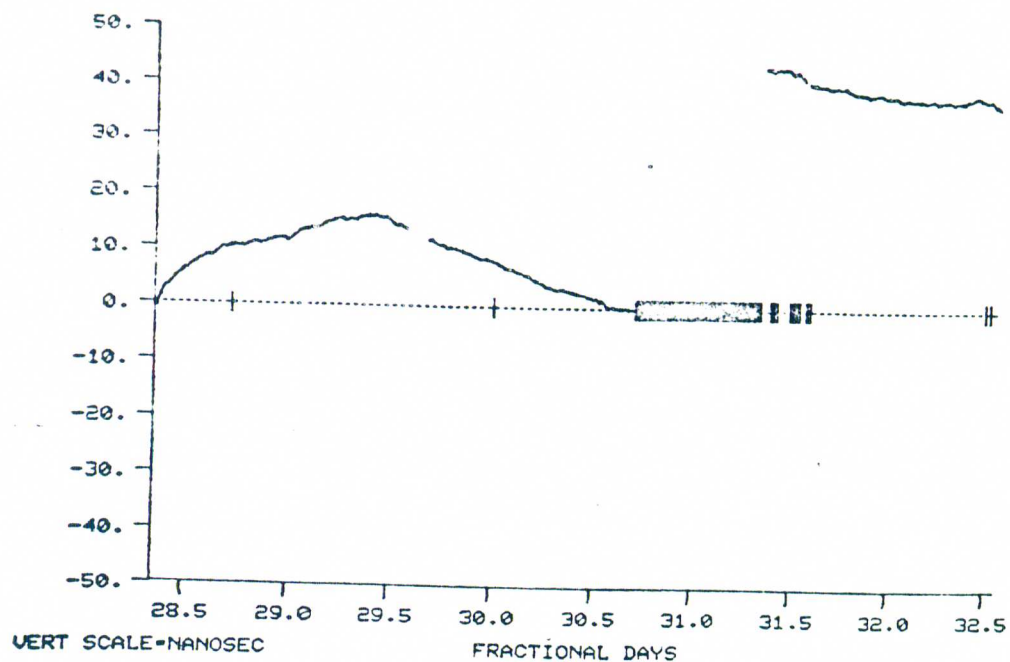


RESIDUALS, FILE: DFTOTG1114 SLOPE FILE: GPSGB1114  
 CLOCK # 18 US PAPER REF 1, 2, 3, 15, 16,

"Travelling" Cesium clock  
 Clock #18 Flight 3

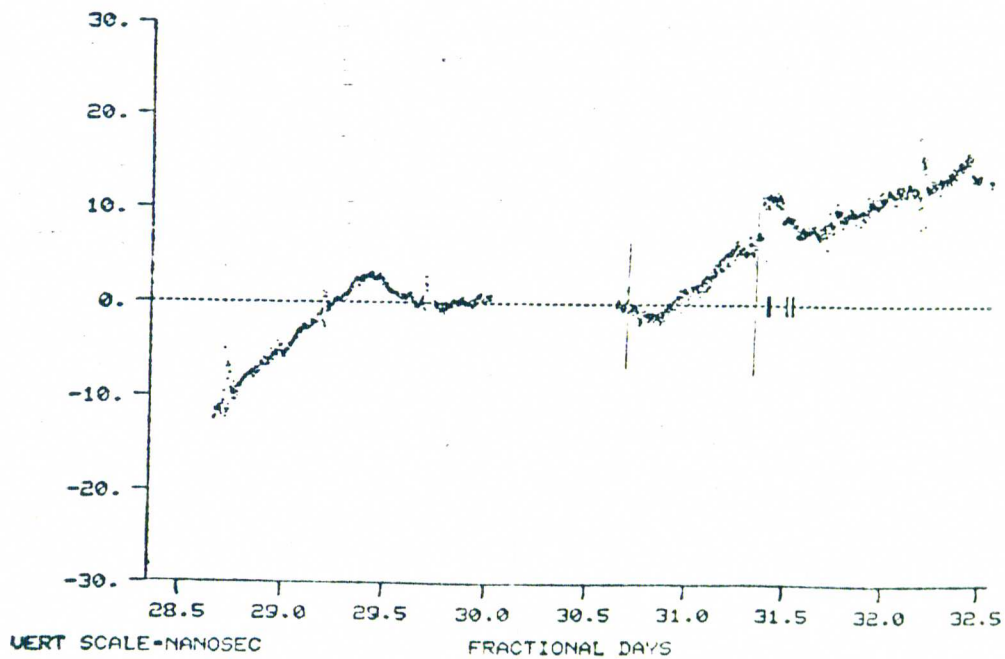


RESIDUALS, FILE: DFTOTA1114 SLOPE FILE: PSAB1114A  
 CLOCK # 18 US PAPER REF 8,

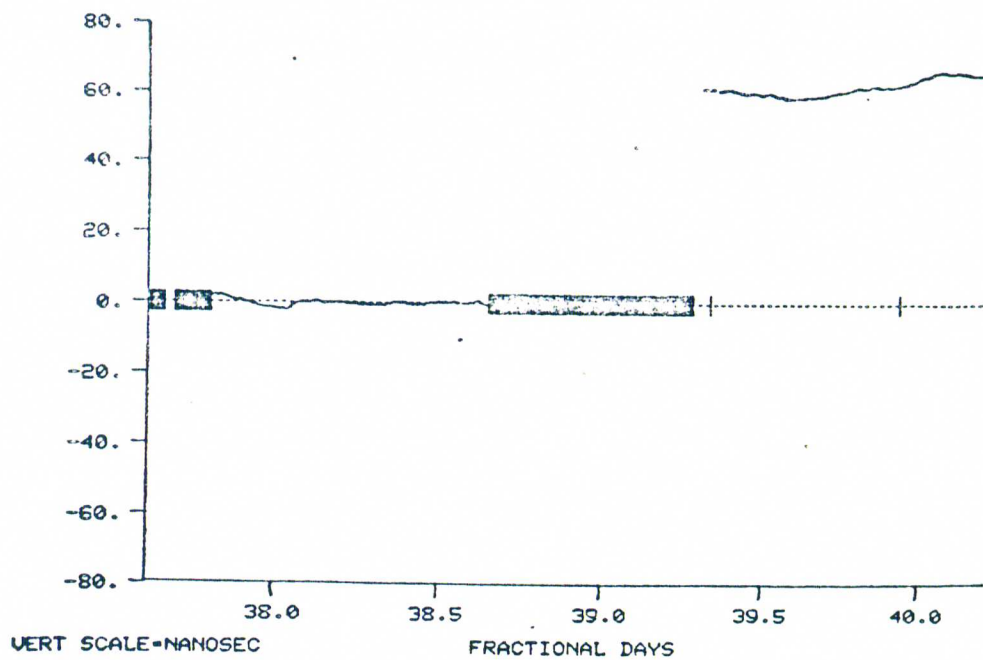


RESIDUALS, FILE: DFTOTG1114 SLOPE FILE: GPSGB1114  
 CLOCK # 19 US PAPER REF 1, 2, 3, 15, 16,

"Travelling" Cesium clock  
 Clock #19 Flight 3

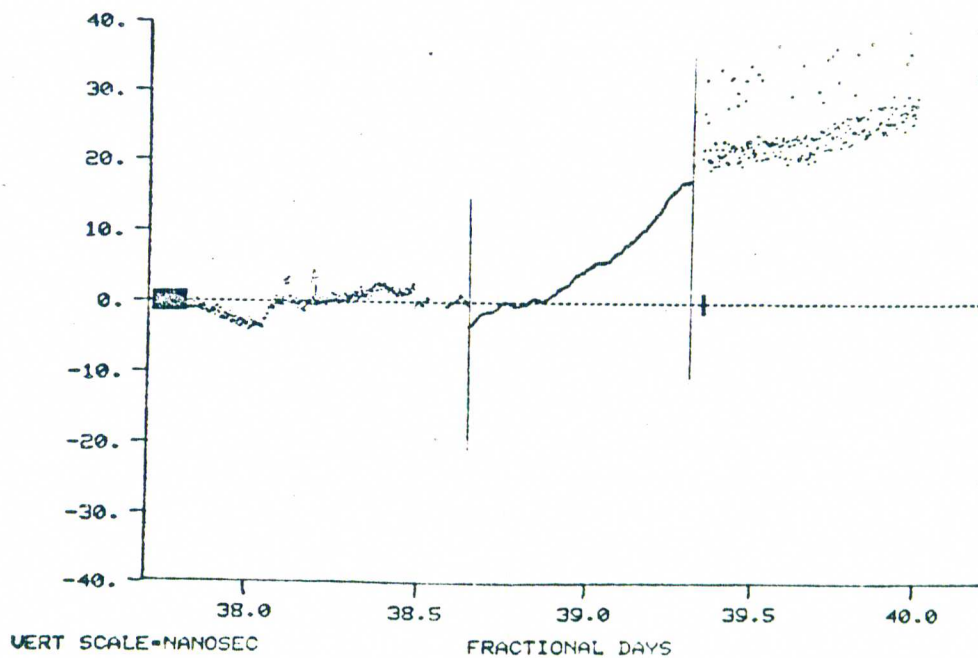


RESIDUALS, FILE: DFTOTA1114 SLOPE FILE: PSAB1114A  
 CLOCK # 19 US PAPER REF 8,

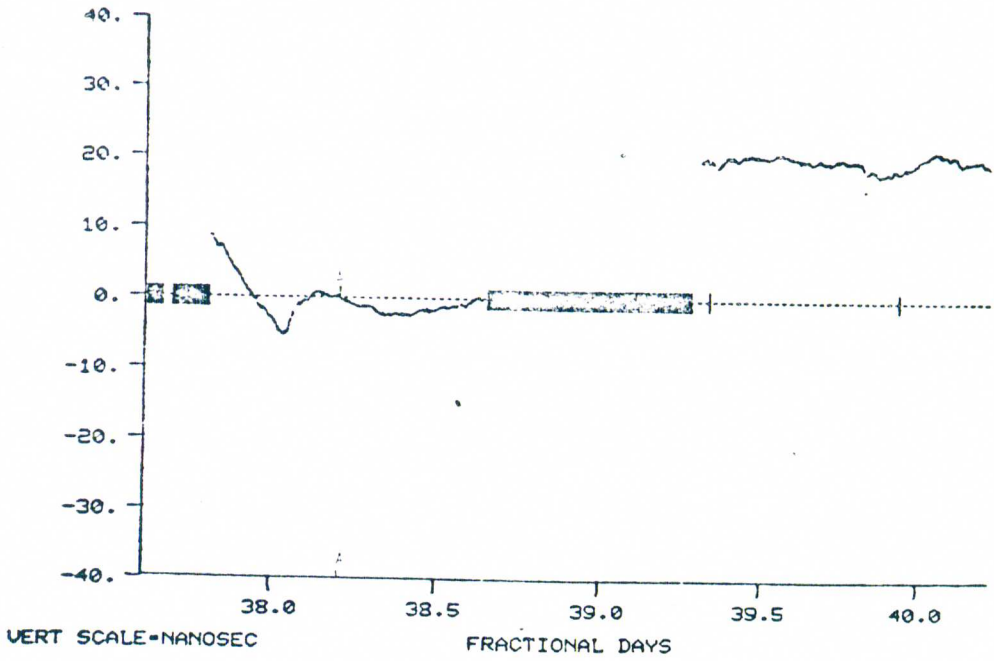


RESIDUALS, FILE: DFTOTG1122 SLOPE FILE: GPSGB1122A  
 CLOCK # 19 US PAPER REF 7, 8, 9, 17.

"Travelling" Cesium clock  
 Clock #19 Flight 4

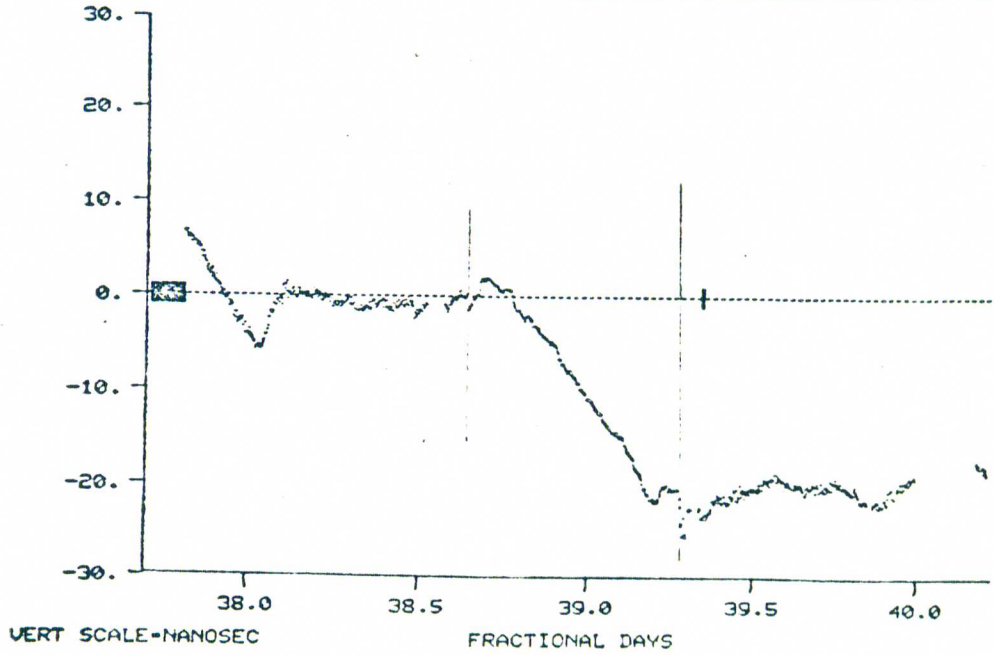


RESIDUALS, FILE: DFTOTA1122 SLOPE FILE: GPSAB1122A  
 CLOCK # 19 US PAPER REF 1, 2, 3.

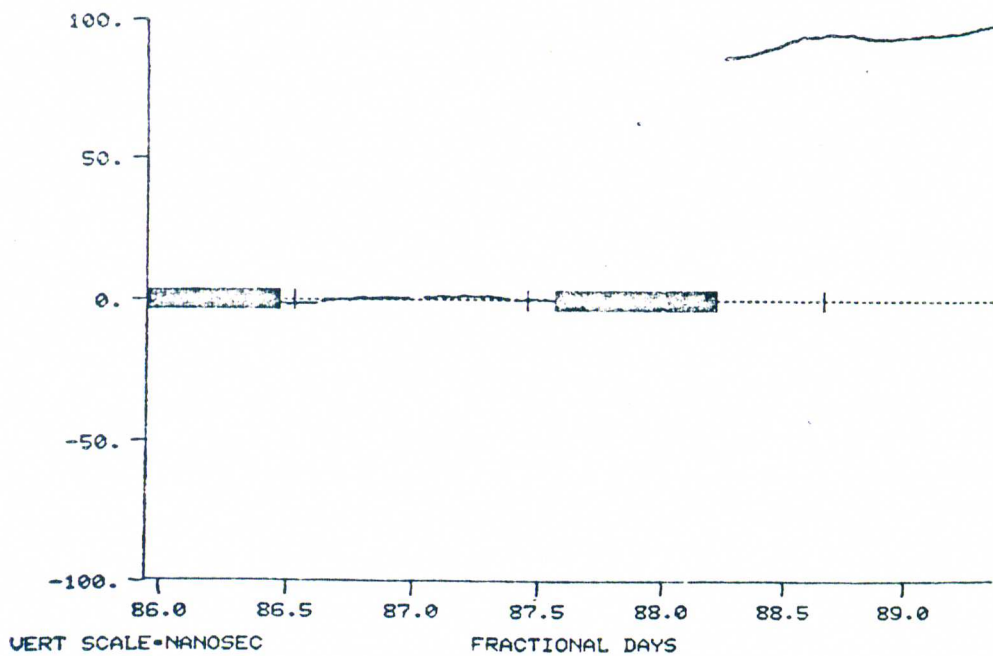


RESIDUALS, FILE: DFTOTG1122 SLOPE FILE: GPSGB1122A  
CLOCK # 20 US PAPER REF 7, 8, 9,17,

"Travelling" Cesium clock  
Clock #20 Flight 4

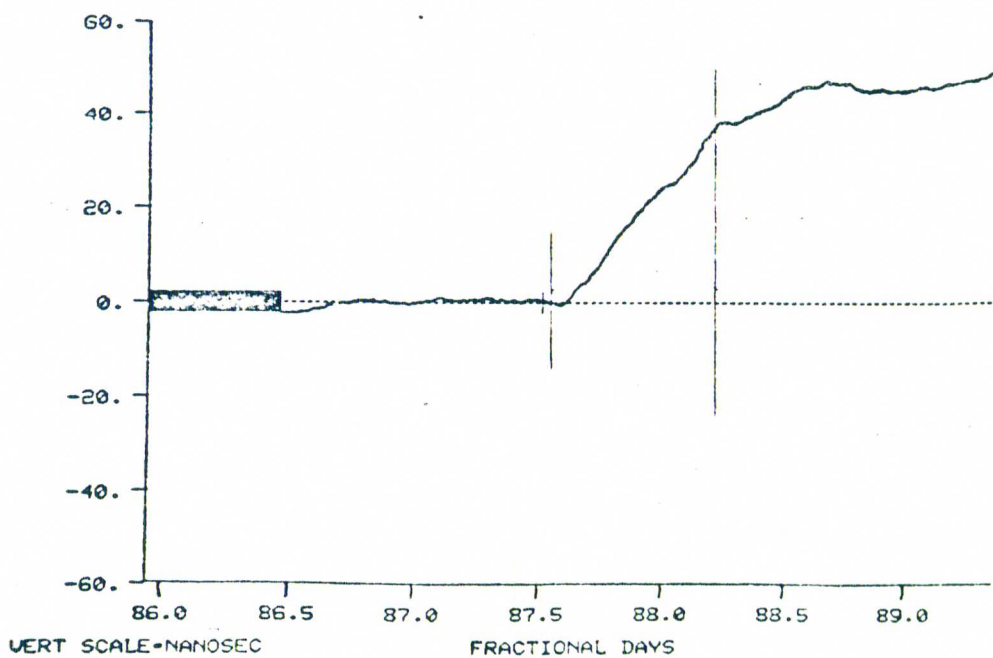


RESIDUALS, FILE: DFTOTA1122 SLOPE FILE: GPSAB1122A  
CLOCK # 20 US PAPER REF 1, 2, 3,

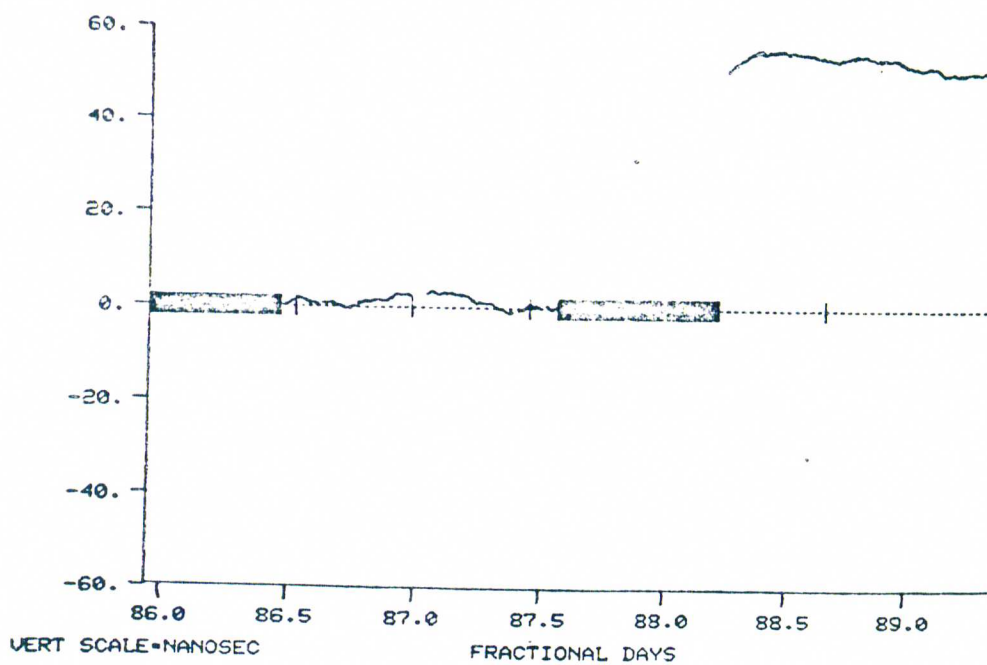


RESIDUALS, FILE: DFTOTG110 SLOPE FILE: GPSGB110A  
 CLOCK # 18 US PAPER REF 7, 8, 9, 15, 17,

"Travelling" Cesium clock  
 Clock #18 Flight 5

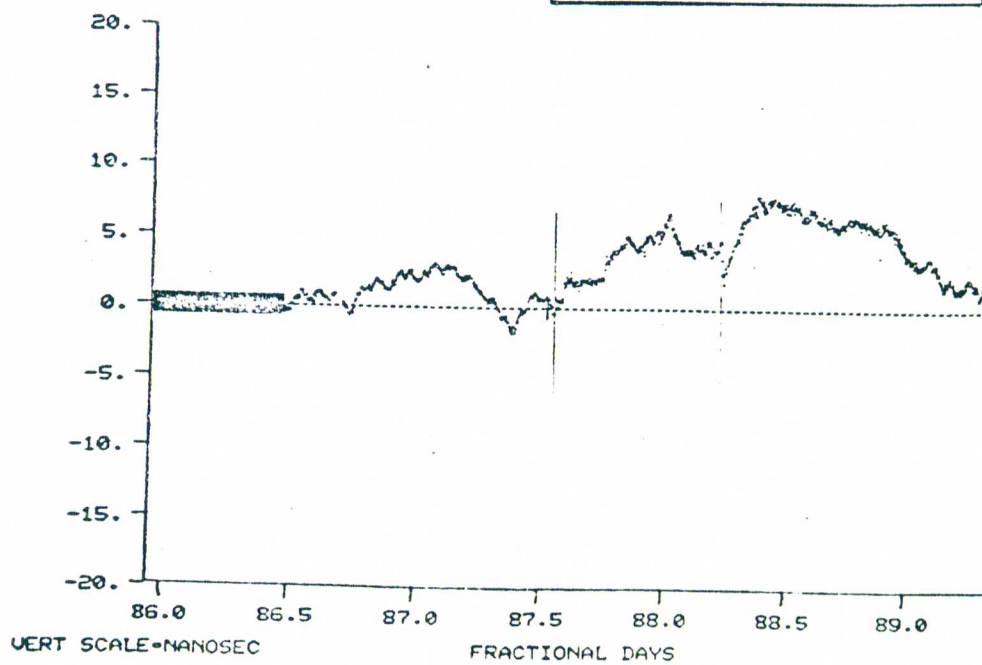


RESIDUALS, FILE: DFTOTA110 SLOPE FILE: GPSAB110A  
 CLOCK # 18 US PAPER REF 2, 3,

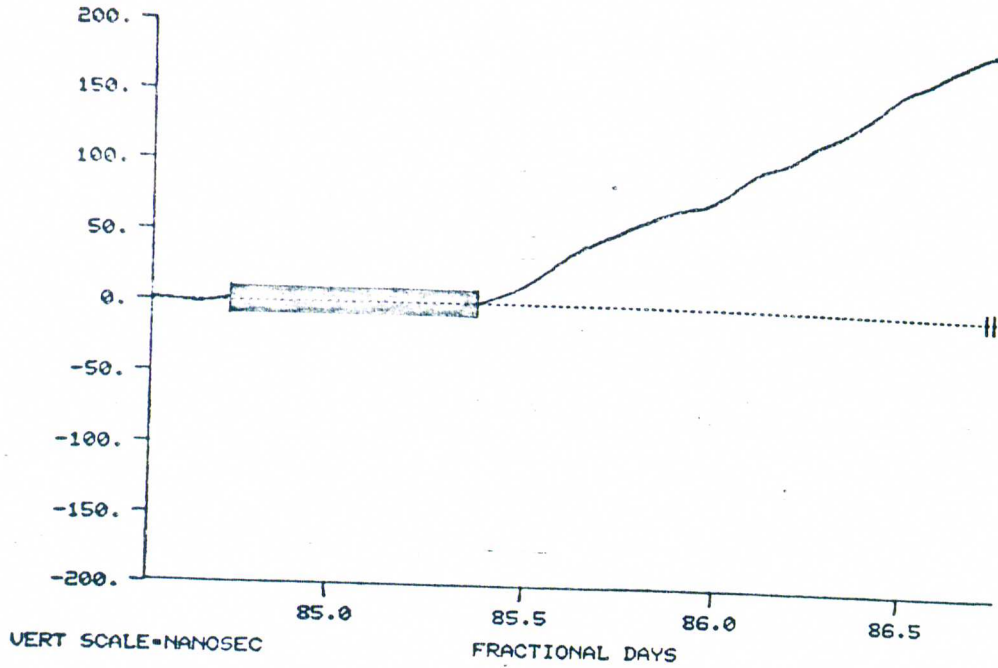


RESIDUALS, FILE: DFTOTG110 SLOPE FILE: GPSGB110A  
 CLOCK # 19 US PAPER REF 7, 8, 9,15,17,

"Travelling" Cesium clock  
 Clock #19 Flight 5

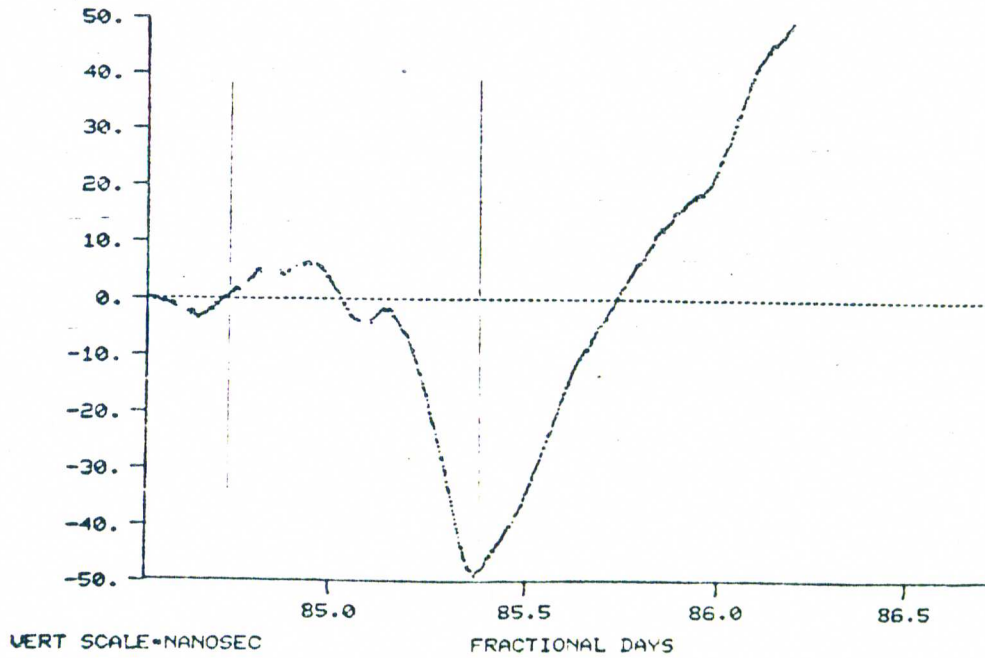


RESIDUALS, FILE: DFTOTA110 SLOPE FILE: GPSAR110A  
 CLOCK # 19 US PAPER REF 2, 3,



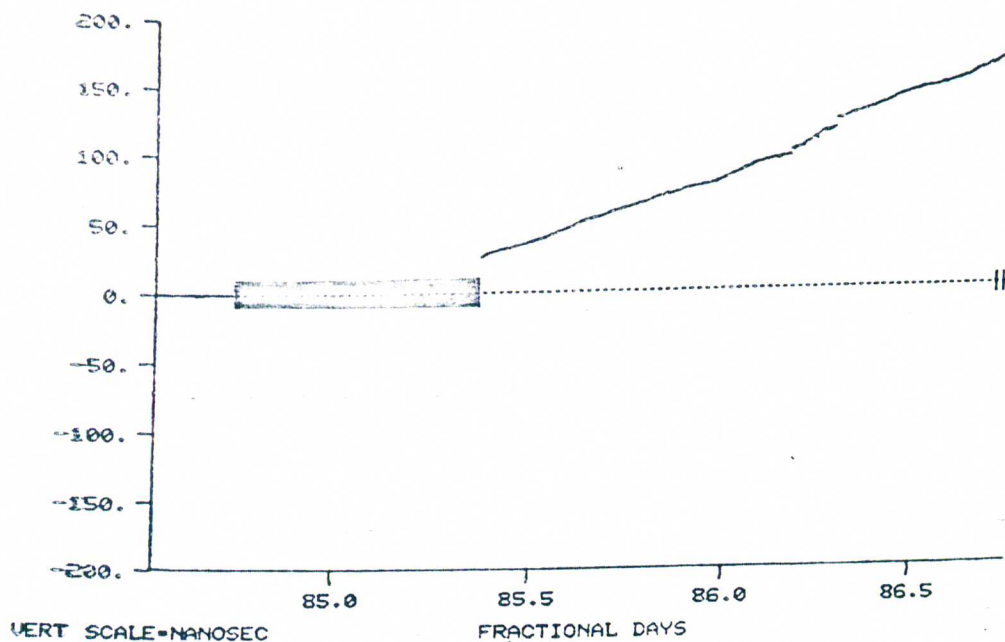
RESIDUALS, FILE: DFTOTG929 SLOPE FILE: GDSGB929  
CLOCK # 4 US PAPER REF 7, 8, 9, 15, 16, 17,

Rubidium clock 4  
Flight 1



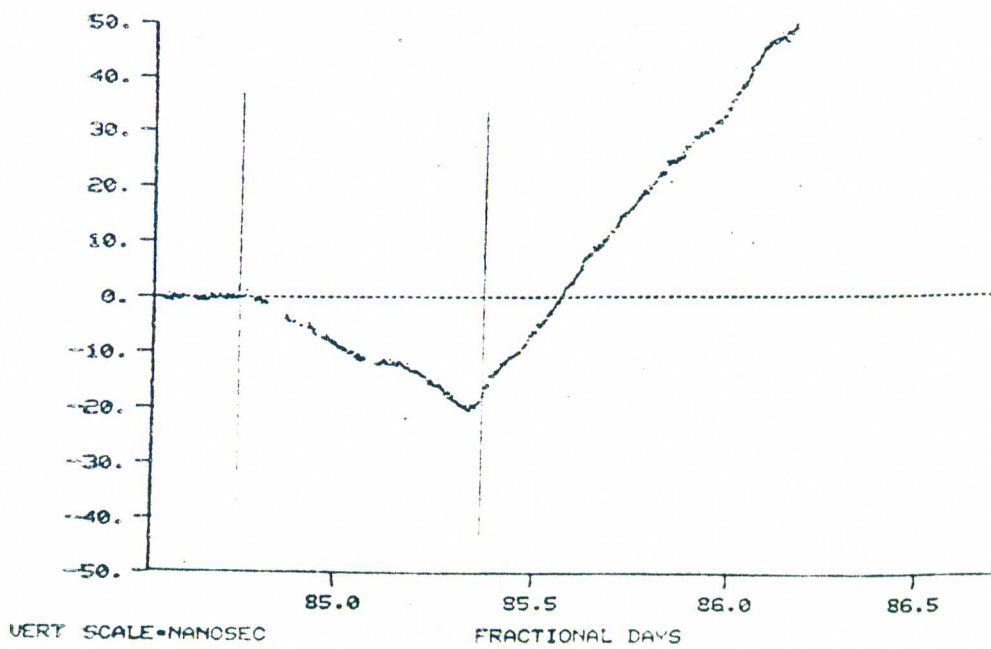
RESIDUALS, FILE: DFTOTAG29 SLOPE FILE: 31PSAB929  
CLOCK # 4 US PAPER REF 1, 3,



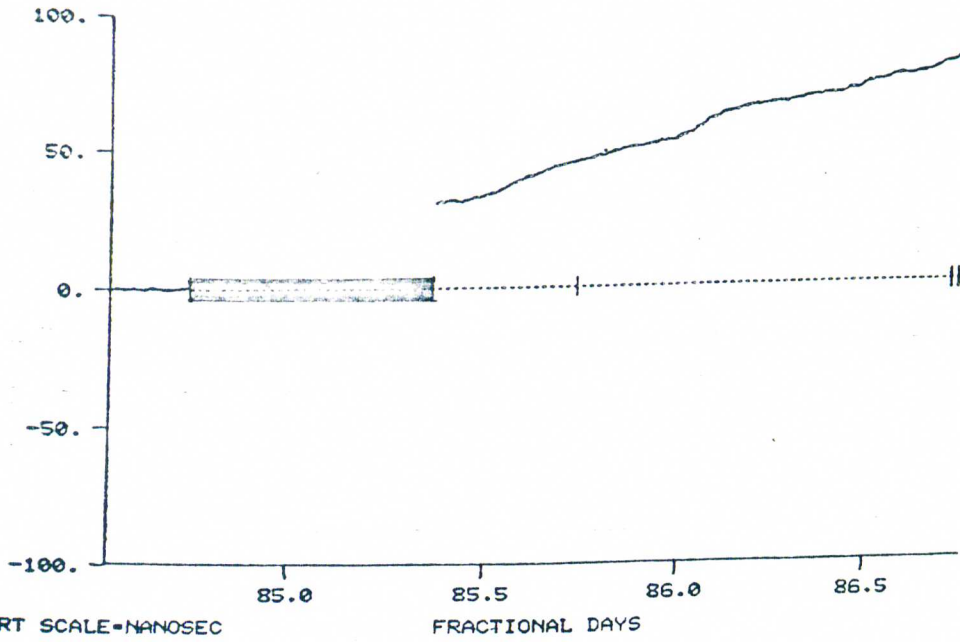


RESIDUALS, FILE: DFTOTG929 SLOPE FILE: GDSGB929  
 CLOCK # 5 US PAPER REF 7, 8, 9, 15, 16, 17,

Rubidium clock 5  
 Flight 1

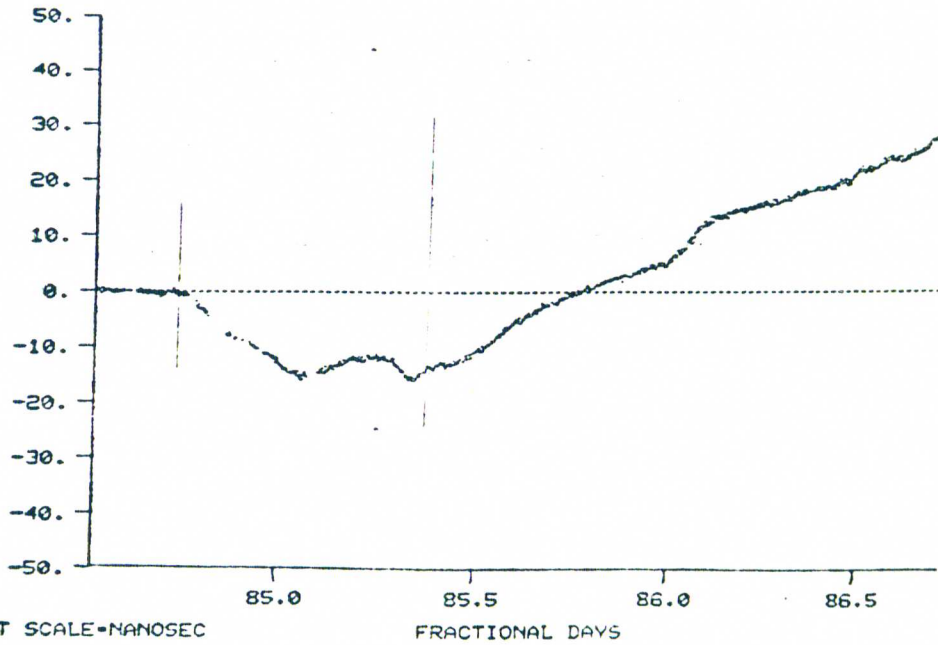


RESIDUALS, FILE: DFTOTG929 SLOPE FILE: 31PSAB929  
 CLOCK # 5 US PAPER REF 1, 3,

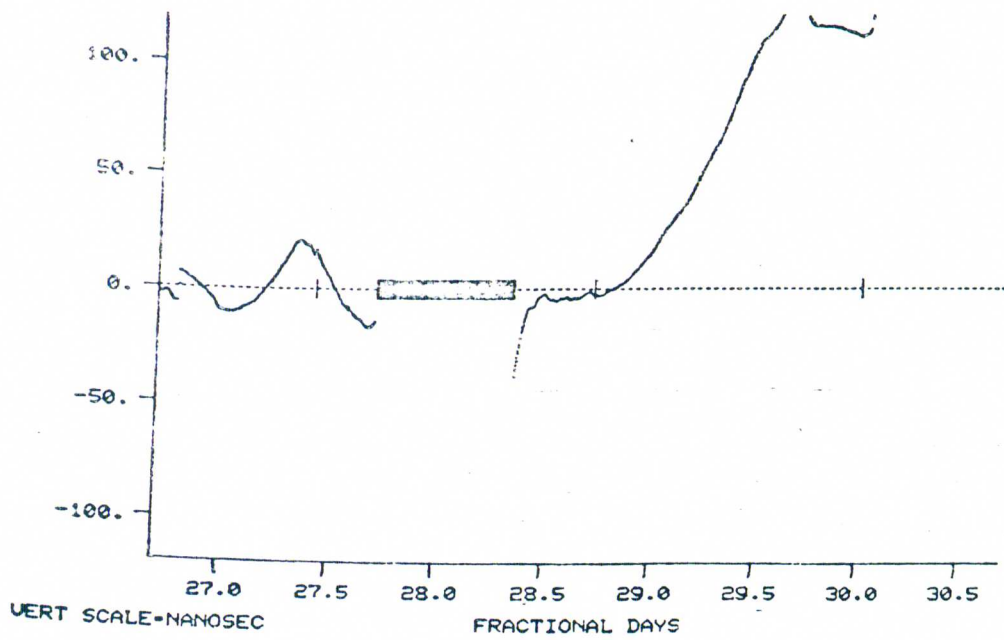


RESIDUALS, FILE: DFTOTG929 SLOPE FILE: GDSGB929  
CLOCK # 6 US PAPER REF 7, 8, 9, 15, 16, 17,

Rubidium clock 6  
Flight 1

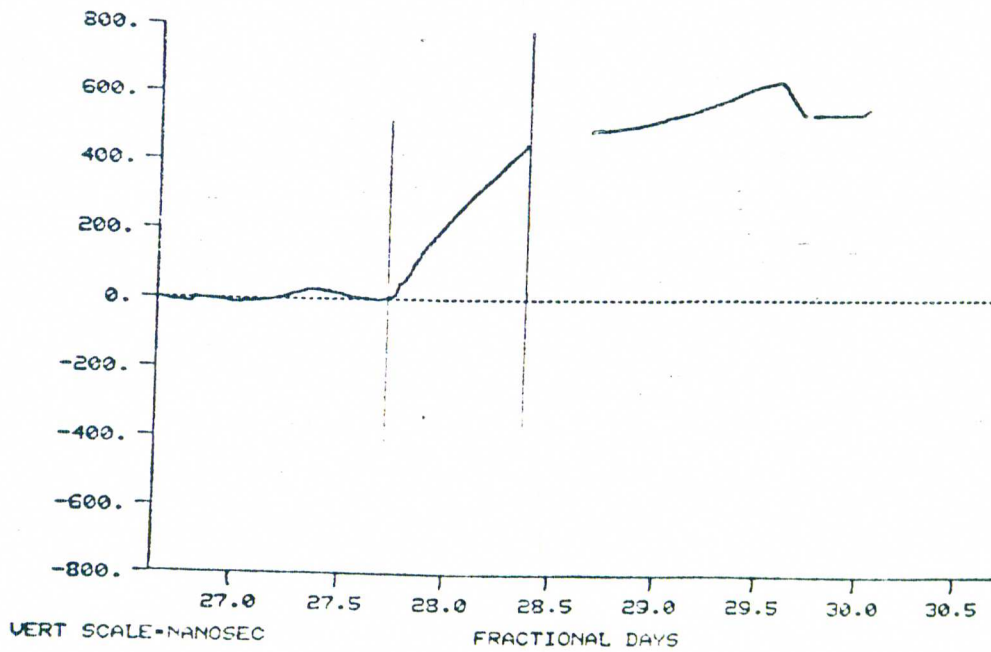


RESIDUALS, FILE: DFTOTA929 SLOPE FILE: 31PSAB929  
CLOCK # 6 US PAPER REF 1, 3,

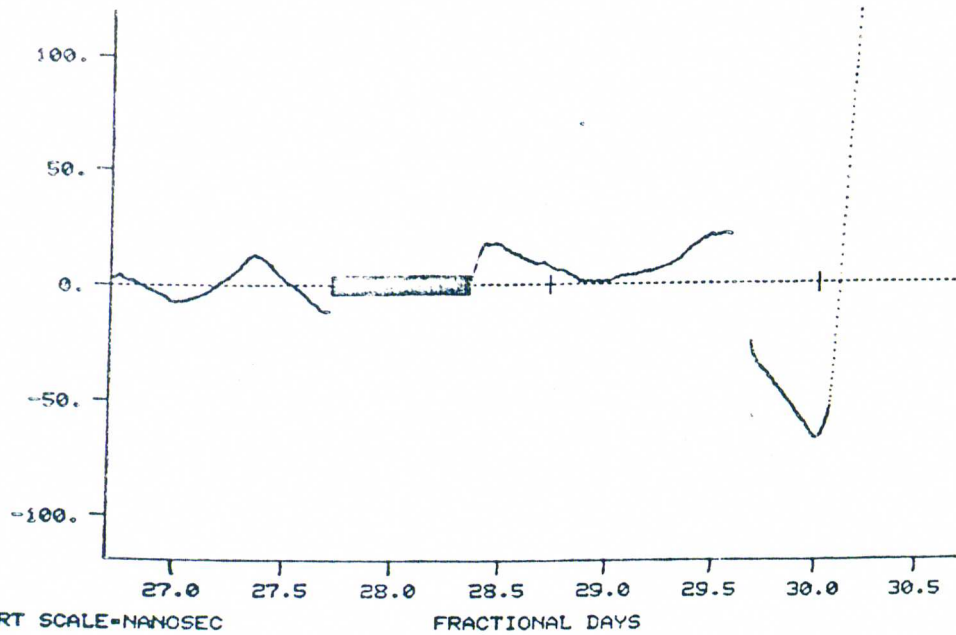


RESIDUALS, FILE: DFTOTG1111 SLOPE FILE: GDSGB1111  
 CLOCK # 10 US PAPER REF 1, 2, 3, 16,

Rubidium clock 10  
 Flight 2

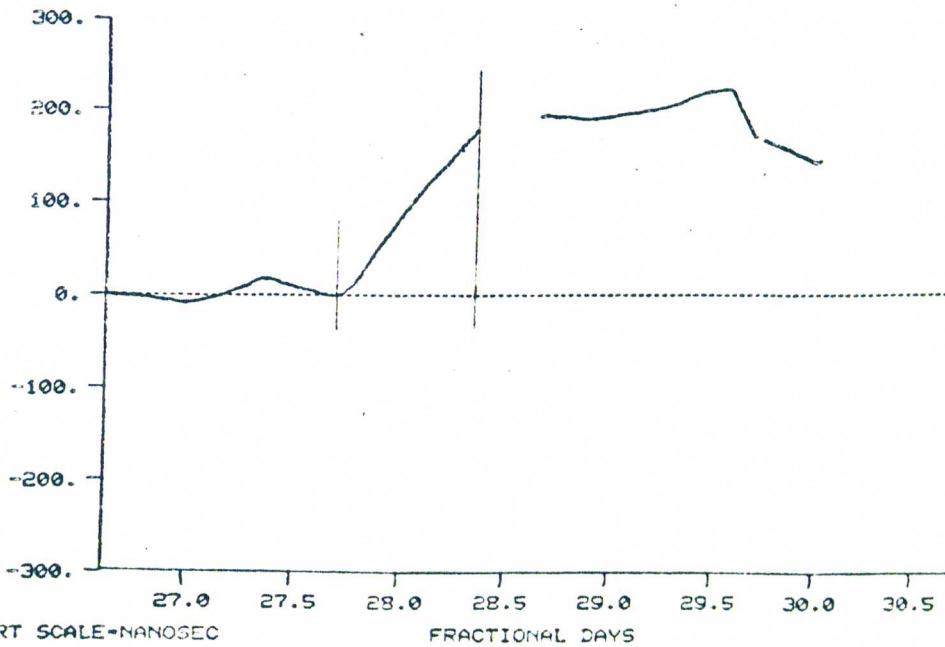


RESIDUALS, FILE: DFTOTA1111 SLOPE FILE: PSAB1111  
 CLOCK # 10 US PAPER REF 8, 9,

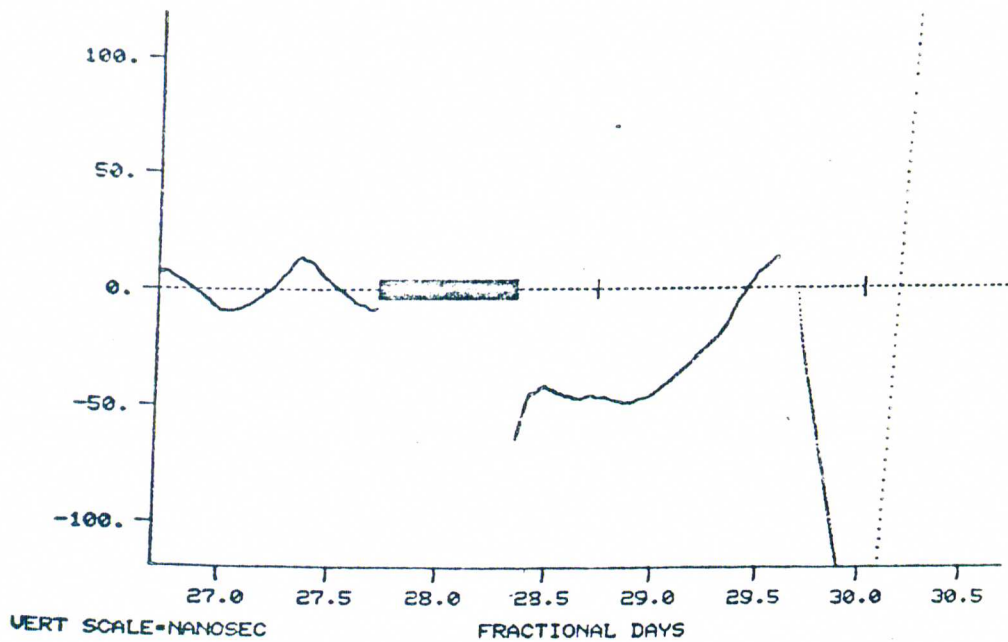


RESIDUALS, FILE: DFTOTG1111 SLOPE FILE: GDSGB1111  
CLOCK # 11 US PAPER REF 1, 2, 3,16,

Rubidium clock 11  
Flight 2

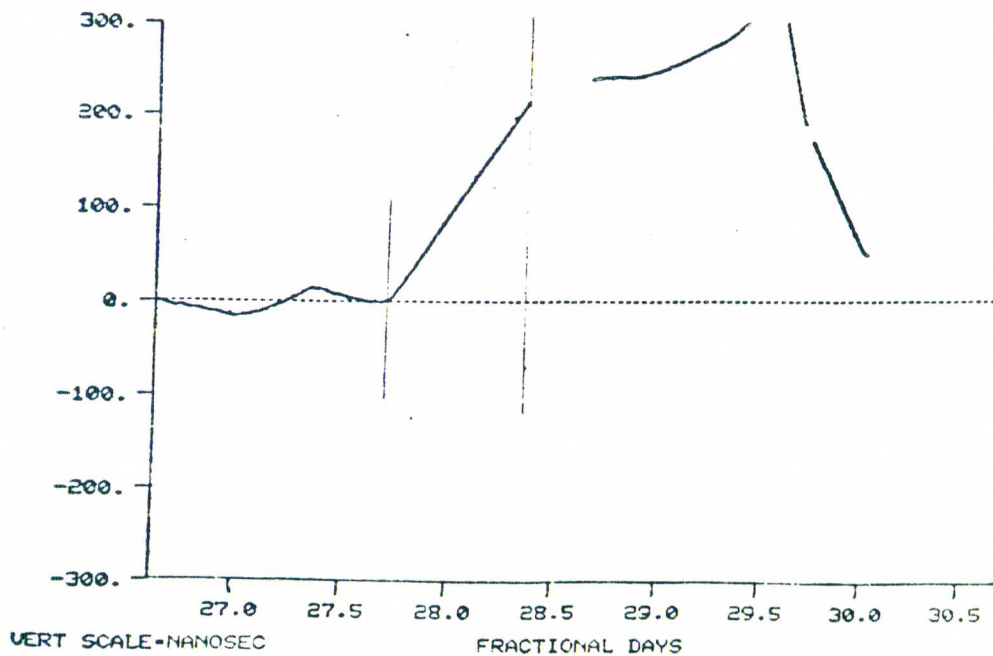


RESIDUALS, FILE: DFTOTA1111 SLOPE FILE: PSAB1111  
CLOCK # 11 US PAPER REF 8, 9,

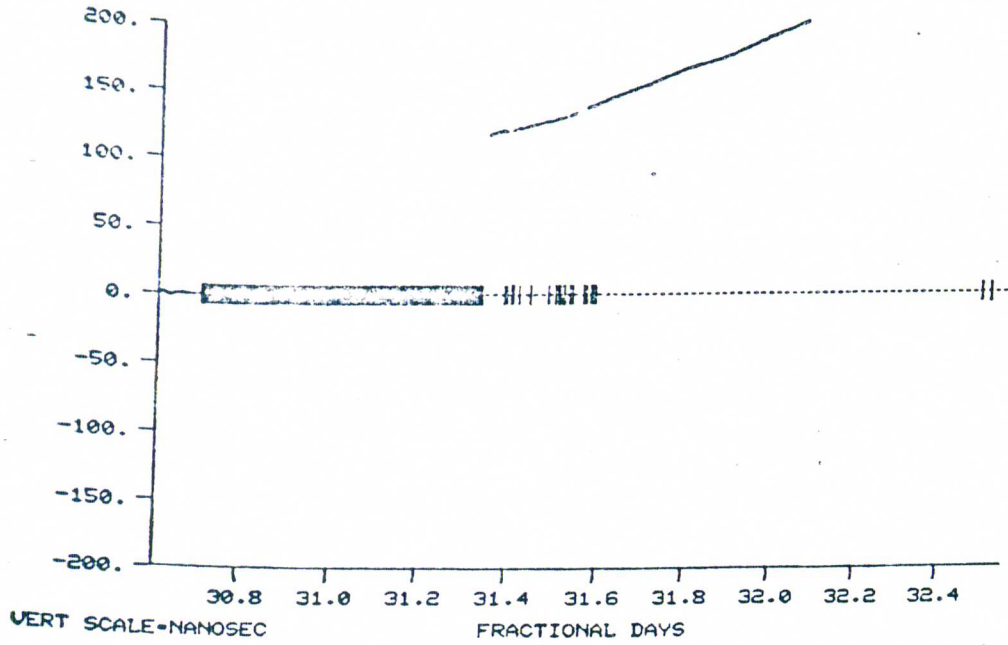


RESIDUALS, FILE: DFTOTG1111 SLOPE FILE: GDSGB1111  
 CLOCK # 12 US PAPER REF 1, 2, 3, 16,

Rubidium clock 12  
 Flight 2

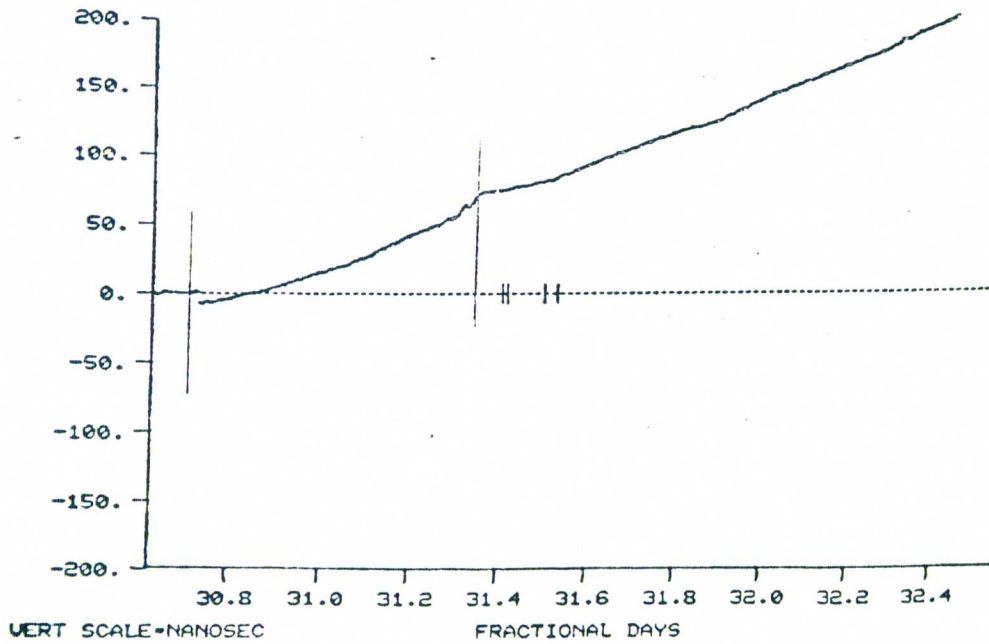


RESIDUALS, FILE: DFTOTA1111 SLOPE FILE: PSAB1111  
 CLOCK # 12 US PAPER REF 8, 9,

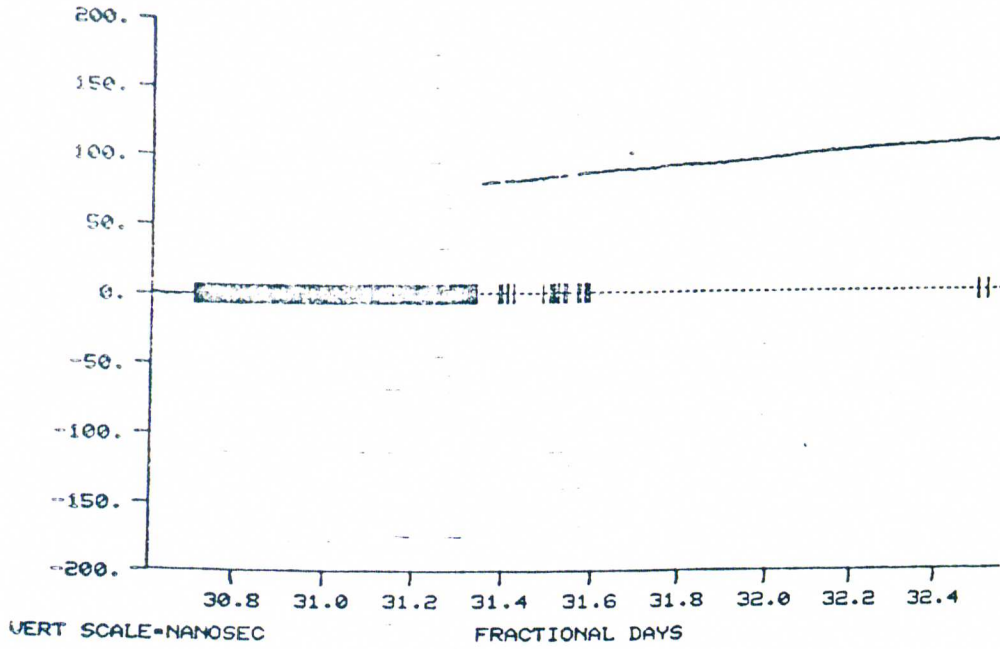


RESIDUALS, FILE: RBTOTG1114 SLOPE FILE: RBDSGB1114  
 CLOCK # 10 US PAPER REF 1, 2, 3,15,16,

Rubidium clock 10  
 Flight 3

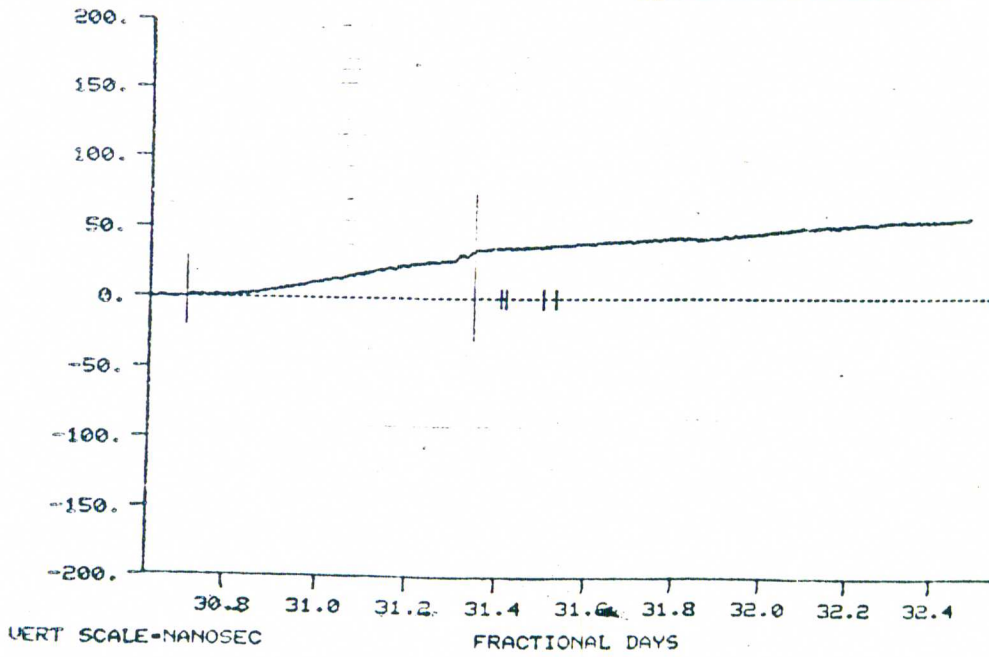


RESIDUALS, FILE: RBTOTA1114 SLOPE FILE: RBPSAB1114  
 CLOCK # 10 US PAPER REF 8,

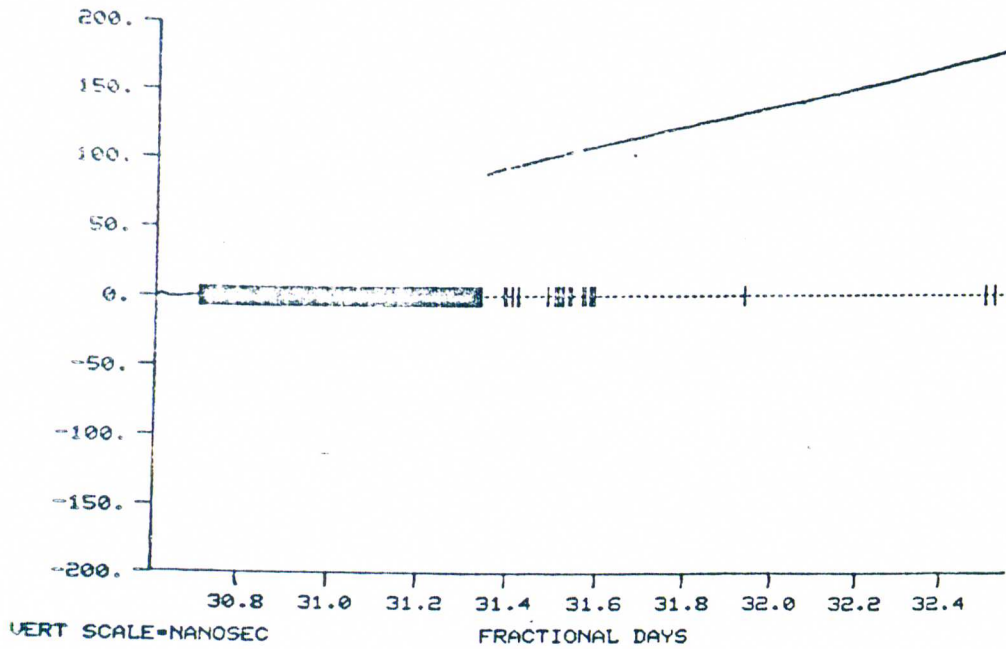


RESIDUALS, FILE: RBTOTG1114 SLOPE FILE: RBDSGB1114  
 CLOCK # 11 US PAPER REF 1, 2, 3, 15, 16,

Rubidium clock 11  
 Flight 3

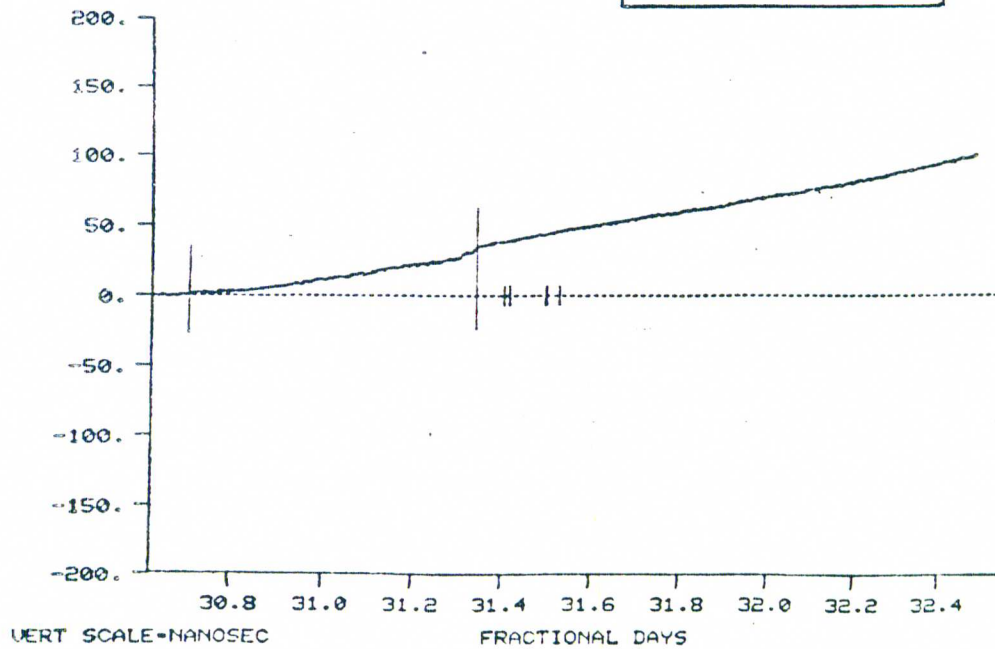


RESIDUALS, FILE: RBTOTA1114 SLOPE FILE: RBPSAB1114  
 CLOCK # 11 US PAPER REF 8,



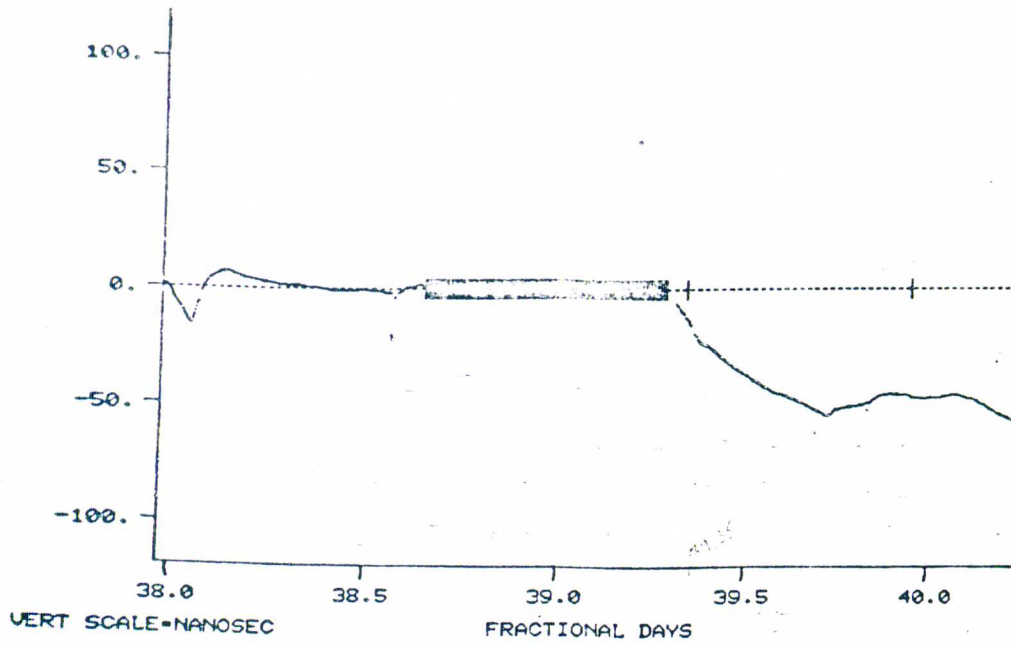
RESIDUALS, FILE: RBTOTG1114 SLOPE FILE: RBDSGB1114  
 CLOCK # 12 US PAPER REF 1, 2, 3, 15, 16,

Rubidium clock 12  
 Flight 3



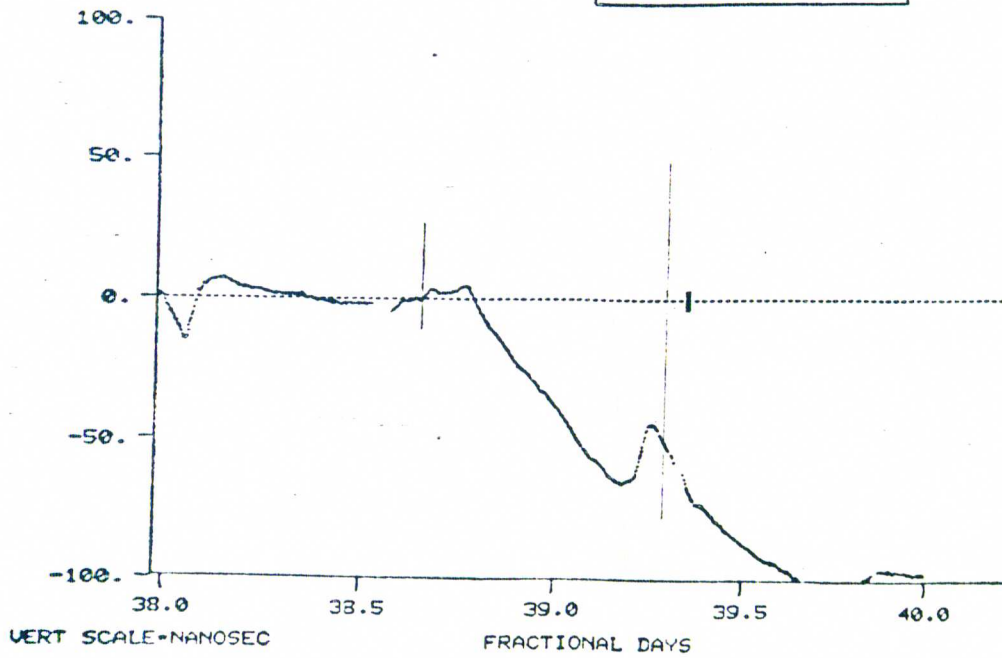
RESIDUALS, FILE: RBTOTA1114 SLOPE FILE: RBPSAB1114  
 CLOCK # 12 US PAPER REF 8,



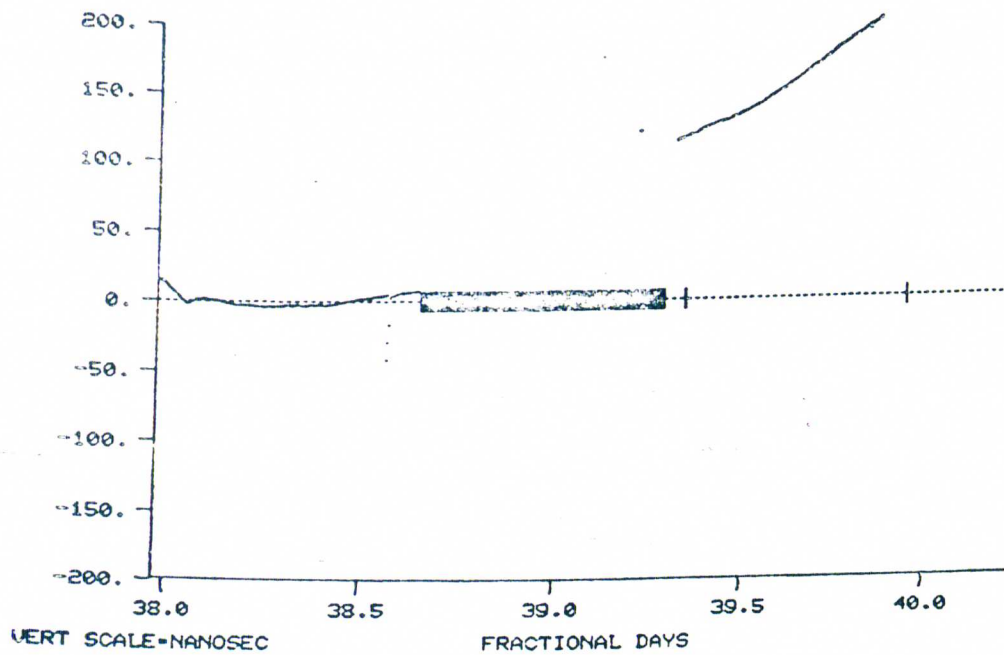


RESIDUALS, FILE: RBTOTG1122 SLOPE FILE: RBDSGB1122  
 CLOCK # 4 US PAPER REF 7, 8, 9, 17,

Rubidium clock 4  
 Flight 4

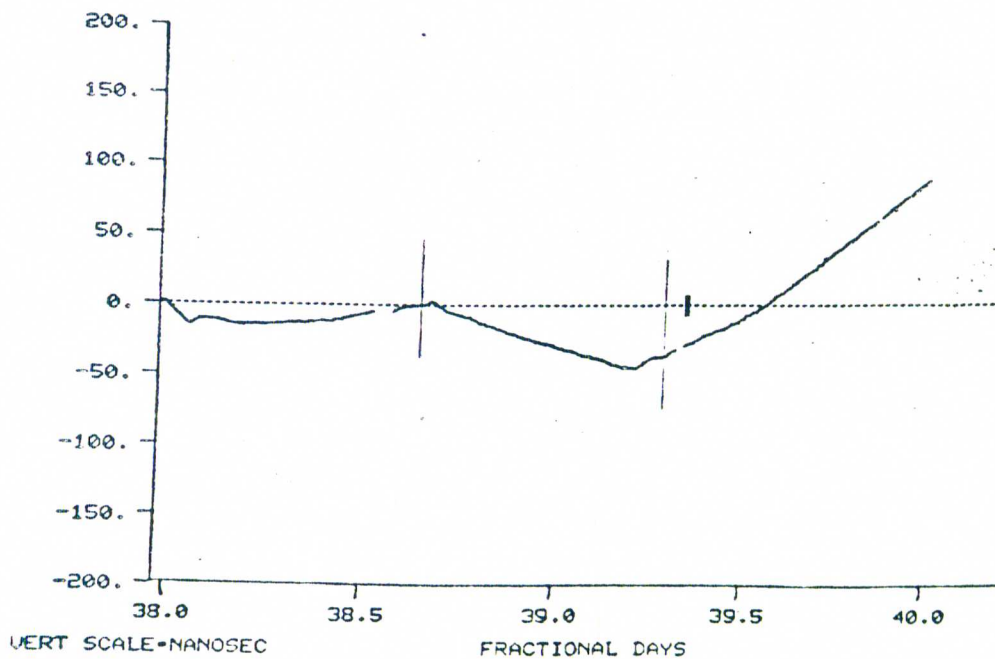


RESIDUALS, FILE: RBTOTA1122 SLOPE FILE: RBPSAB1122  
 CLOCK # 4 US PAPER REF 1, 2, 3,

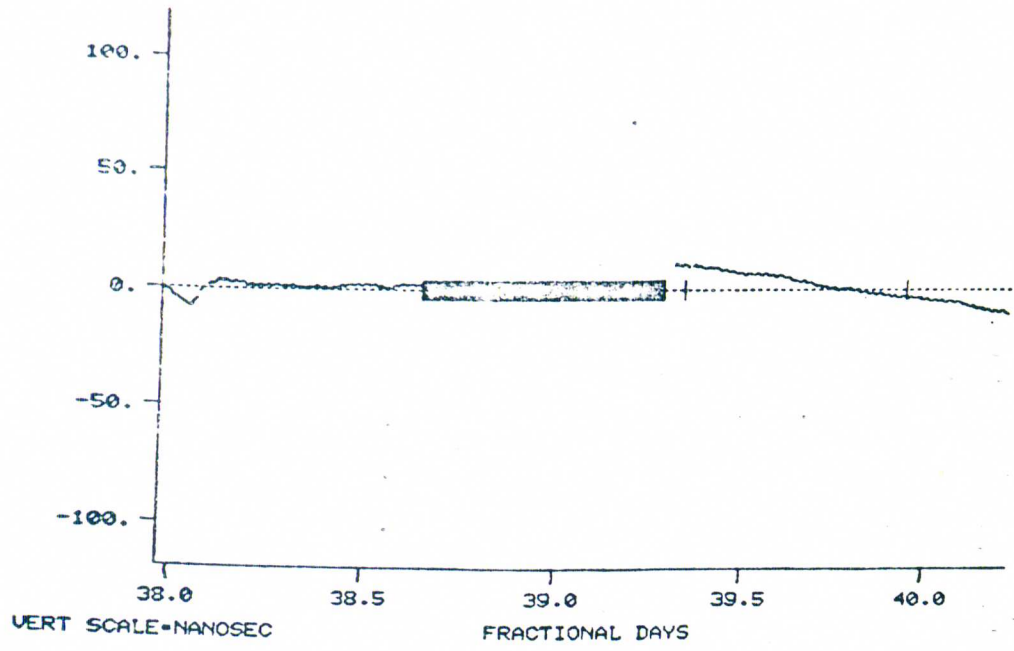


RESIDUALS, FILE: RBTOTG1122 SLOPE FILE: RBDSGB1122  
 CLOCK # 5 US PAPER REF 7, 8, 9, 17,

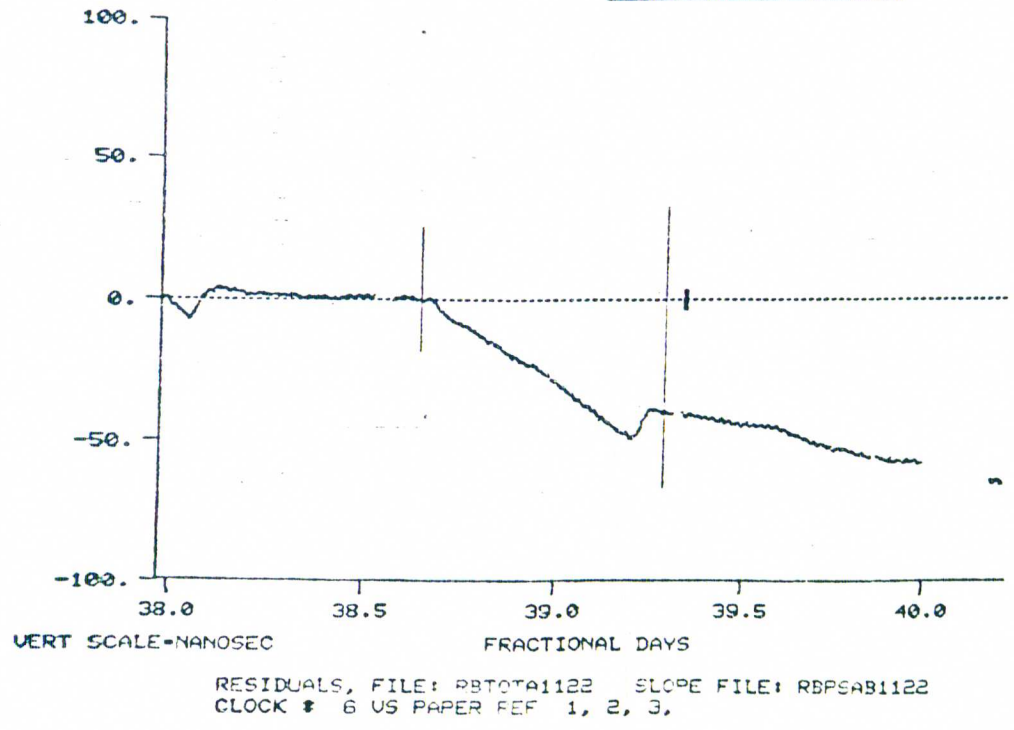
Rubidium clock 5  
 Flight 4

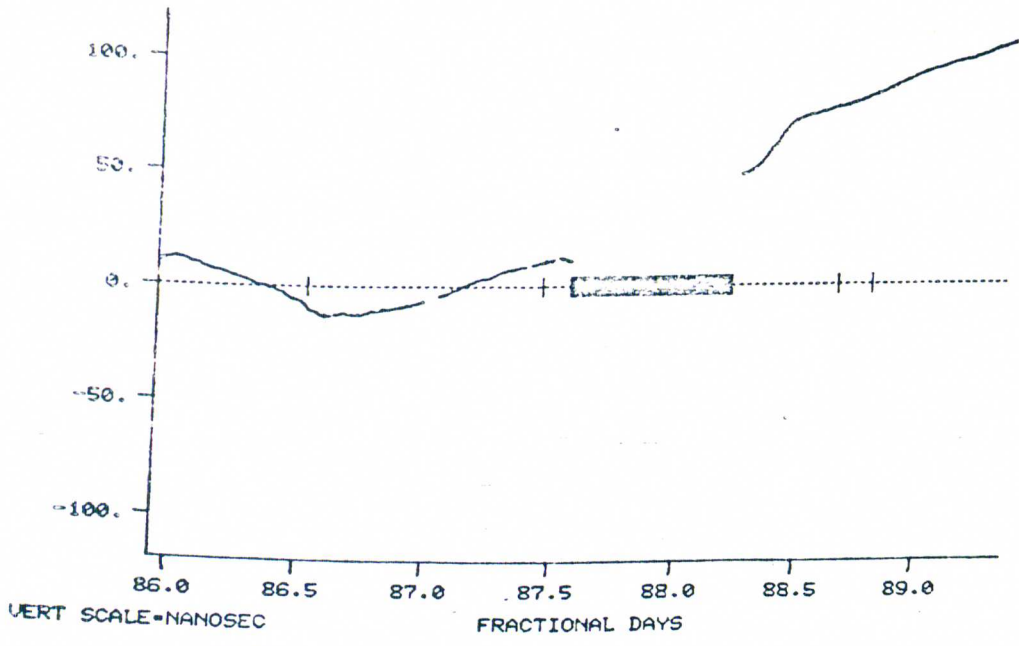


RESIDUALS, FILE: RBTOTA1122 SLOPE FILE: RBPSAB1122  
 CLOCK # 5 US PAPER REF 1, 2, 3,



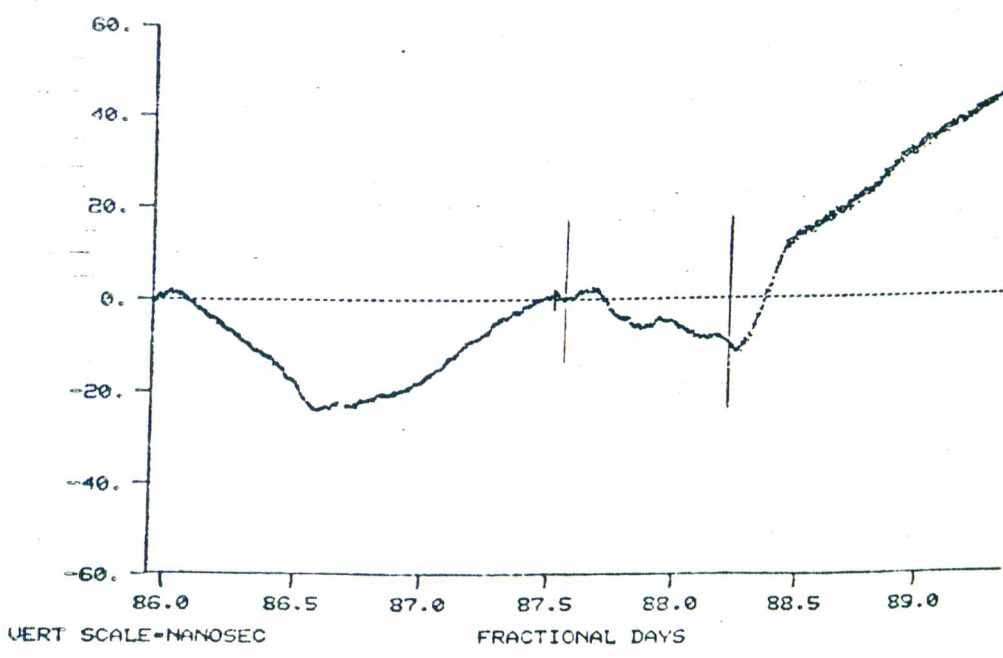
Rubidium clock 6  
Flight 4



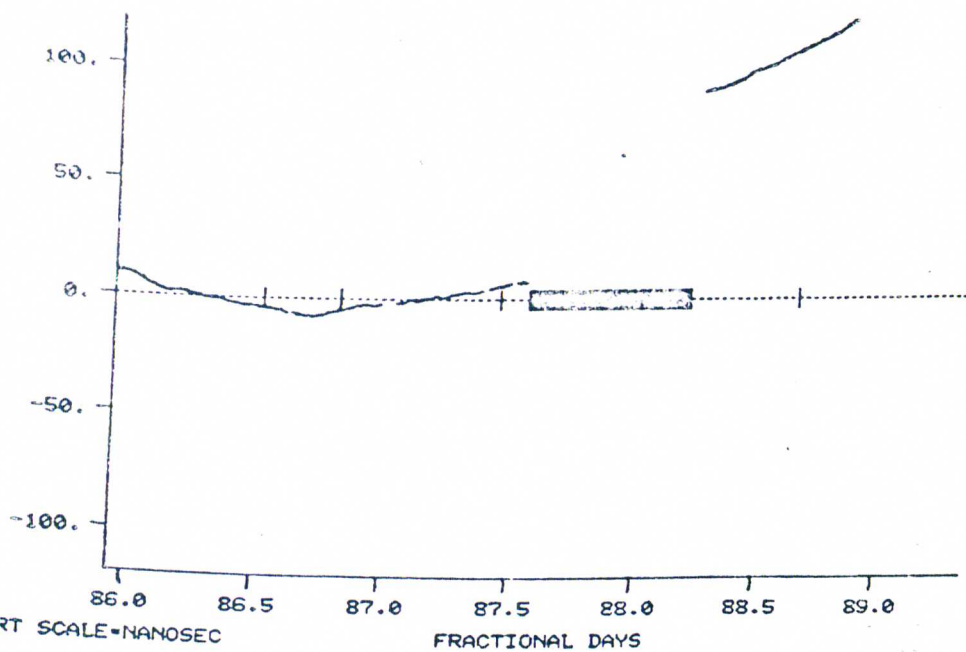


RESIDUALS, FILE: DFTOTG110 SLOPE FILE: GDSGB110  
 CLOCK # 4 US PAPER REF 7, 8, 9,15,17.

Rubidium clock 4  
 Flight 5

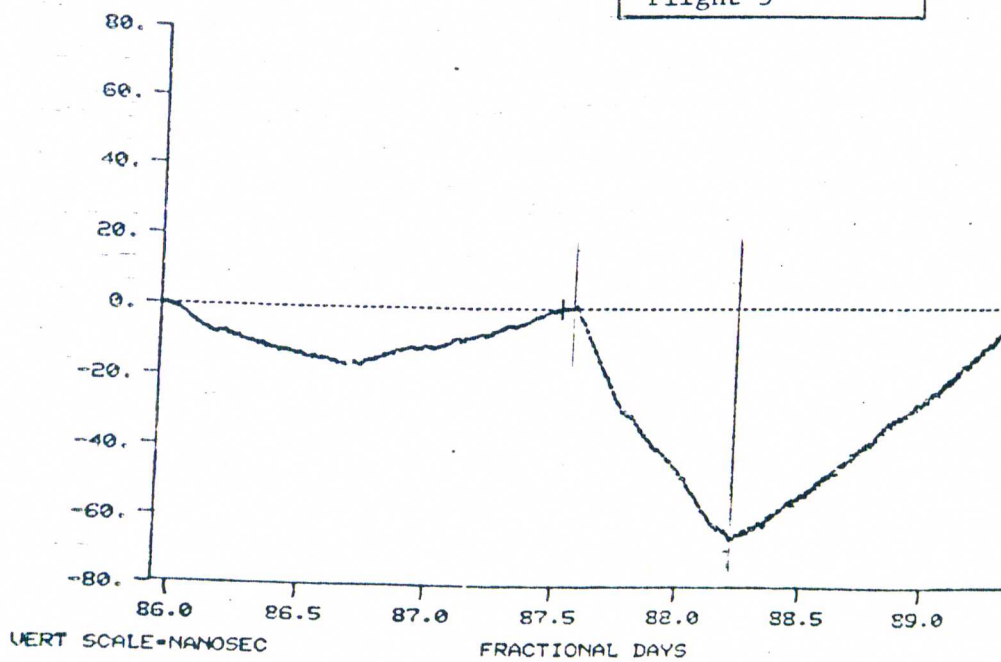


RESIDUALS, FILE: DFTOTA110 SLOPE FILE: PSAB110  
 CLOCK # 4 US PAPER REF 2, 3.

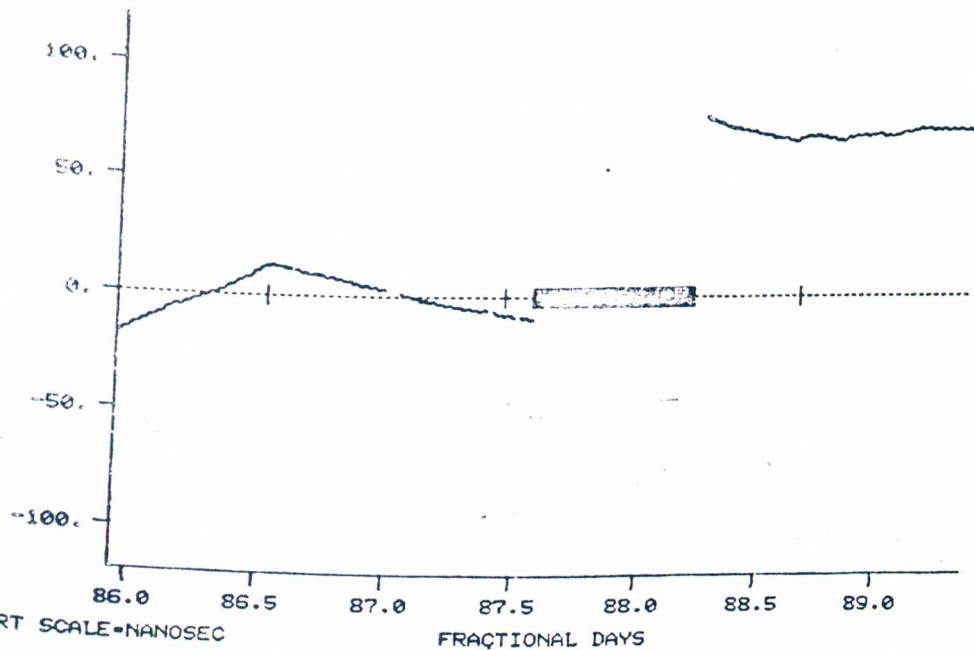


RESIDUALS, FILE: DFTOTG110 SLOPE FILE: GDSGB110  
 CLOCK # 5 US PAPER REF 7, 8, 9,15,17,

Rubidium clock 5  
 Flight 5

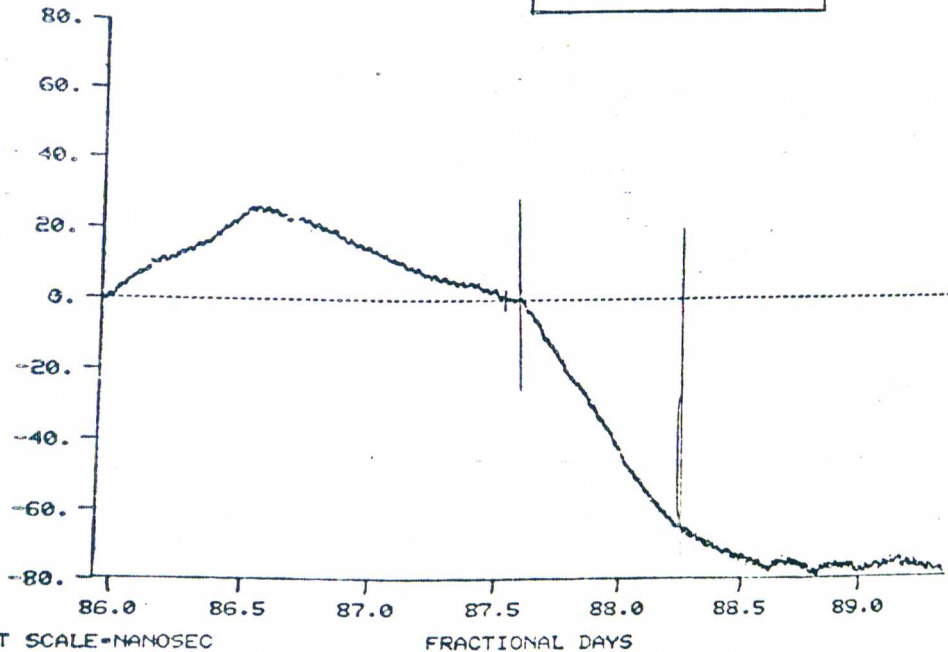


RESIDUALS, FILE: DFTOTA110 SLOPE FILE: PSAB110  
 CLOCK # 5 US PAPER REF 2, 3,



RESIDUALS, FILE: DFTOTG110 SLOPE FILE: GDSGB110  
 CLOCK # 6 US PAPER REF 7, 8, 9,15,17,

Rubidium clock 6  
 Flight 5



RESIDUALS, FILE: DFTOTA110 SLOPE FILE: PSAB110  
 CLOCK # 6 US PAPER REF 2, 3,

## APPENDIX E

### LISTING OF VARIOUS PROGRAMS

This appendix contains several computer programs written in FORTRAN for the Data General NOVA 2 minicomputer. This version of FORTRAN is slightly different from the FORTRAN of larger computers. It should be noted as well that the programs, like the experiment, were often modified in haste when time was short. The result is that a better set of programs doing the same jobs could be written if one were starting from scratch. There has not been the time nor the real need to do this.

TRANSD - The program TRANSD translates the raw digital clock phase data into the new file format.

```

TYPE TRANSD
  INTEGER RTYPE, IBUF(2,1000), INDEX(2,10), FNAME(7)
  REAL BUF(20), TS(20), SAVE(20), YF(20), YL(20), OS(2)
  CALL JFDATA(OFFSET)
  CALL ASG(1)
  WRITE(13,1)
1  FORMAT(' OUT FILE? ',Z)
  READ(11,2) FNAME(1)
2  FORMAT(S13)
  CALL CFILW(FNAME,1,IERR)
  CALL FOPEN(2,FNAME)
  ACCEPT '# CLOCK BOXES(1 OR 2): ',NB
3 INITIALIZE CONSTANTS
  OS(1)=7
  OS(2)=15
  N=0
  DO 4 I=1,20
    YF(I)=-1.E6
    SAVE(I)=50.
    TS(I)=0.
4  DO 5 I=1,6
    INDEX(1,I)=1
    INDEX(2,I)=I+6
5  DO 6 I=7,10
    INDEX(1,I)=0
    INDEX(2,I)=0
6  NCP=7
  IF(NB.EQ.2) NCP=14
  TYPE 'INSERT CLOCK BOX #, CHANNEL FOR THE FOLLOWING:'
  IF(NB.EQ.1) GO TO 12
  ACCEPT 'MASER NP2 ',J,K
  INDEX(J,K)=15
  NCP=NCP+1
13 DO 11 I=1,5
  ACCEPT 'SPARE CLOCK ',J,K
  IF(J.EQ.0) GO TO 12
  INDEX(J,K)=OS(NB)+I
  NCP=NCP+1
11 WRITE BINARY(2) NCP,NCP,N,TS(1),TS(1),TS(1),(TS(J),TS(J),J=1,NCP)
12 READ BINARY(1,END=60) NR,RTYPE,ISEC,JDAY,NN,(IBUF(1,J),J=1,NN)
13 IF((RTYPE.EQ.6).OR.(RTYPE.EQ.7)) GO TO 15
  GO TO 13
15 IF(NB.EQ.1) GO TO 16
  IF(RTYPE.EQ.6) GO TO 200
  DO 150 K=1,10
    IBUF(2,K)=IBUF(1,K)
    IBUF(1,K)=0
150 GO TO 16
200 READ BINARY(1,END=60) NR,RTYPE,ISEC,JDAY,NN,(IBUF(2,J),J=1,NN)
  IF(RTYPE.EQ.7) GO TO 16
  DO 250 K=1,10
    IBUF(2,K)=0
250 GO TO 16
16 IF(N.NE.0) GO TO 15
  TYPE 'FIRST POINT:'
  CALL THEAD(ISEC,JDAY,OFFSET)
  CALL FJDAY(ISEC,JDAY,FJD,FJDS)
  S=FJD-OFFSET
  SFJD=FJDS

```



TRANSD continued

```

18 CALL FJDAY(ISEC,JDAY,FJD,FJDS)
   FJD=(FJD-OFSET-3)+FJDS
   WRITE BINARY(2) FJD
C COMPUTE BUF
   DO 25 J=1,NB
     DO 25 K=1,13
       IF(INDEX(J,K).EQ.2) GO TO 25
       BF=IBUF(J,K)
       IF(BF.GT.3..AND.BF.LT.8003.) GO TO 22
       IF(BF.LT.3.) BF=BF+65536.
       BF=BF/16.
22    BF=(BF-1000.)/12.
       IF(BF.LT.-70.) BF=-1.E6
       BUF(INDEX(J,K))=BF
25    CONTINUE
     DO 39 I=1,NCP
       IF(BUF(I).LT.-.9E6) GO TO 32
       IF((NB.EQ.1).AND.(I.EQ.7)) GO TO 32
       IF((NB.EQ.2).AND.((I.EQ.13).OR.(I.EQ.14))) GO TO 32
       BUF(I)=BUF(I)+TC(I)
       DT=BUF(I)-SAVE(I)
       IF(ABS(DT).LT.55.) GO TO 27
       BUF(I)=BUF(I)-SIGN(120.,DT)
       TC(I)=TC(I)-SIGN(100.,DT)
27    SAVE(I)=BUF(I)
       IF(BUF(I).GT.-.9E6) YL(I)=BUF(I)
       IF(YF(I).LT.-.3E6) YF(I)=BUF(I)
39    CONTINUE
C DO PAPER CLOCKS
   BF=(BUF(1)+BUF(2)+BUF(3))/3.
   IF(BF.LT.-.3E6) BF=-1.E6
   IF(NB.EQ.2) GO TO 35
   BUF(7)=BF
   IF(YF(7).LT.-.9E6) YF(7)=BUF(7)
   IF(BUF(7).GT.-.9E6) YL(7)=BUF(7)
   GO TO 43
35  BUF(13)=BF
   IF(YF(13).LT.-.9E6) YF(13)=BUF(13)
   IF(BUF(13).GT.-.9E6) YL(13)=BUF(13)
   BF=(BUF(7)+BUF(8)+BUF(9))/3.
   IF(BF.LT.-.3E6) BF=-1.E6
   BUF(14)=BF
   IF(YF(14).LT.-.9E6) YF(14)=BUF(14)
   IF(BUF(14).GT.-.9E6) YL(14)=BUF(14)
40  WRITE BINARY(2) (BUF(J),J=1,NCP)
     N=N+1
     GO TO 13
60  TYPE 'LAST POINT:'
     CALL THEAD(ISEC,JDAY,OFSET)
     WRITE(10,70) N
70  FORMAT(1X,/, ' TOTAL POINTS=', I5,/)
     REWIND 2
     WRITE BINARY(2) NCP,NCP,N,S,BFJD,FJD,(YF(J),YL(J),J=1,NCP)
     STOP
     END
R

```

TLIST - Displays the contents of a translated file. It is very flexible in that parts of interest may be examined while ignoring other parts.

```

TYPE TLIST
  REAL SLOPE(15),BUF(20),YF(20),YL(20)
  CALL ASG(1)
  READ BINARY(1) NC,NCP,N,S,BFJD,EFJD,(YF(J),YL(J),J=1,NCP)
  ACCEPT ' EVERY N? ', K
  I=K-1
  WRITE(10,2)
2  FORMAT(' TYPE HEADER? ',Z)
  READ(11,3) NANSW
3  FORMAT(S1)
  IF(NANSW.NE.'Y') GO TO 10
  WRITE(10,5) NC,NCP,N,S,BFJD,EFJD,(J,YF(J),YL(J),J=1,NCP)
5  FORMAT(1X,/, ' # CLOCKS=',I3,5X, 'TOTAL CLOCKS=',I3,5X,
1  'TOTAL POINTS=',I5,/, ' OFFSET=',F6.1,8X, 'FIRST FJD=',F9.6,/,
1  '22X, 'LAST FJD=',F9.6,/,/, ' CLOCK FIRST POINT LAST POINT',/,/,
1  20(1X,I4,2F10.2,/,/,))
  IF(K.EQ.0) STOP
10 READ BINARY(1,END=20) FJD,(BUF(J),J=1,NCP)
  FJD=FJD+S
  I=I+1
  IF(I.NE.K) GO TO 10
  WRITE(10,15) FJD,(BUF(J),J=1,NCP)
15 FORMAT(1X, 'FJD=',F12.6,3(/,8F9.2))
  I=0
  GO TO 10
20 IF(I.EQ.0) GO TO 25
  WRITE(10,15) FJD,(BUF(J),J=1,NCP)
25 WRITE(10,26) N
26 FORMAT(1X,/, ' TOTAL POINTS=',I5)
  STOP
  END
R

```

SLOPES - Prepares a slope file based on a least squares regression line.

SLOPELIST - Displays the contents of a slope file.

```

TYPE SLOPES
  DOUBLE PRECISION SX(20),SXX(20),SY(20),SYY(20),SXY(20)
  DOUBLE PRECISION RN(20),DFJD,Y
  REAL BUF(20),YF(20),YL(20)
  INTEGER NCLK(20),FNAME(7)
  CALL ASG(1)
  TYPE 'REF PAPER CLOCK:'
  CALL CLOCKS(NP,NCLK)
  WRITE(10,3)
3  FORMAT(' SLOPE FILE NAME? ',Z)
  READ(11,4) FNAME(1)
4  FORMAT(S13)
  CALL FOPEN(2,FNAME)
  READ BINARY(1) NC,NCP,N,S,BFJD,EFJD,(YF(J),YL(J),J=1,NCP)
  DO 5 K=1,NCP
    SX(K)=0.
    SXX(K)=0.
    SY(K)=0.
    SYY(K)=0.
    SXY(K)=0.
5   RN(K)=0.
  ICOUNT=0
10  READ BINARY(1,END=15) FJD,(BUF(J),J=1,NCP)
  DFJD=FJD-BFJD
  DO 100 K=1,NCP
    IF(BUF(K).EQ.-1.E6) GO TO 100
    CALL PAPCLOCK(BUF,NP,NCLK,PBUF,S100)
    Y=BUF(K)-PBUF
    CALL SUM(SX(K),SXX(K),SY(K),SYY(K),SXY(K),RN(K),DFJD,Y)
100  CONTINUE
  GO TO 10
15  TYPE '          TOTAL POINTS=',N
  WRITE BINARY(2) NC,NCP,N,S,NP,(NCLK(J),J=1,NP)
  TYPE 'CLOCK      A1          A0          R*R          SX.Y          N'
  DO 200 K=1,NCP
    CALL REG(SX(K),SXX(K),SY(K),SYY(K),SXY(K),RN(K),A1,A0,RR,SSXY)
    A0=A0-A1*BFJD
    SRN=RN(K)
    WRITE BINARY(2) A1,A0,RR,SSXY,SRN
    WRITE(10,20) K,A1,A0,RR,SSXY,SRN
20  FORMAT(1X,13,F13.5,F12.5,F9.4,F10.3,F6.0)
200  CONTINUE
  STOP
  END
R

```

```

TYPE SLOPELIST
  INTEGER NCLK(20)
  REAL A1(20),A0(20),RR(20),SSXY(20),RN(20)
  CALL ASG(1)
  READ BINARY(1) NC,NCP,N,S,NP,(NCLK(J),J=1,NP)
  (A1(J),A0(J),RR(J),SSXY(J),RN(J),J=1,NCP)
  WRITE(10,5) (NCLK(J),J=1,NP)
5  FORMAT(5X,'REF PAPER CLOCK: ',7(12,' ','))
  TYPE 'CLOCK      A1          A0          R*R          SX.Y          N'
  WRITE(10,10) (J,A1(J),A0(J),RR(J),SSXY(J),RN(J),J=1,NCP)
10  FORMAT(20(1X,13,F13.5,F12.5,F9.4,F10.3,F6.0, /))
  STOP
  END

```

PSLOPES - Prepares a slope file based on a "first-last point" line.

```

TYPE PSLOPES
  DOUBLE PRECISION SX(20),SXX(20),SY(20),SYY(20),SXY(20)
  DOUBLE PRECISION FX(20),DFJD,DY
  REAL BUF(20),YF(20),YL(20),Y(2,20),X(2)
  INTEGER NCLK(20),FRAME(7)
  CALL ASS(1)
  ACCEPT 'DEF CLOCK (#,LIST): ', NP,(NCLK(J),J=1,NP)
  WRITE(13,3)
3  FORMAT(' SLOPE FILE NAME? ',Z)
  READ(11,4) FNAME(1)
4  FORMAT(S13)
  CALL FOPEN(2,FNAME)
  READ BINARY(1) NC,NCP,N,S,BFJD,EFJD,(YF(J),YL(J),J=1,NCP)
  ACCEPT '# POINTS IN AVE: ', NUM
  ACCEPT 'START,STOP FJD: ', FJD1,FJD2
  FJD1=FJD1-S-.0001
  IF(FJD2.GT.0.001) FJD2=FJD2-S-.2001
  ICT=3
  NTEST=N-NUM-1
  M=1
8  DO 5 K=1,NCP
    SX(K)=0.
    SXX(K)=0.
    SY(K)=0.
    SYY(K)=0.
    SXY(K)=0.
5  RN(K)=0.
  IC=3
10 READ BINARY(1,END=300) FJD,(BUF(J),J=1,NCP)
  ICT=ICT+1
  IF(FJD.LT.FJD1) GO TO 13
  IF((FJD2.LT.0.001).AND.(ICT.GE.NTEST)) GO TO 12
  IF((FJD2.GT.0.001).AND.(FJD.GE.FJD2)) GO TO 12
  IF(M.EQ.2) GO TO 10
12 IF(IC.EQ.0) X(M)=FJD
  DFJD=FJD
  IC=IC+1
  DO 100 K=1,NCP
    IF(BUF(K).LT.-.7E6) GO TO 123
    CALL PAPCLOCK(BUF,NP,NCLK,PBUF,S100)
    DY=BUF(K)-PBUF
    CALL SUN(SX(K),SXX(K),SY(K),SYY(K),SXY(K),RN(K),DFJD,DY)
130 CONTINUE
  IF(IC.LT.NUM) GO TO 13
  X(M)=(X(M)+FJD)/2.
  DO 14 K=1,NCP
    CALL REG(SX(K),SXX(K),SY(K),SYY(K),SXY(K),RN(K),A1,A3,RP,SSXY)
14 Y(M,K)=A1*X(M)+A3
  IF(M.EQ.2) GO TO 15
  N=2
  GO TO 8
15 WRITE BINARY(2) NUM,NCP,N,S,NP,(NCLK(J),J=1,NP)
  XX1=X(1)+S
  XX2=X(2)+S
  WRITE(13,17) XX1,XX2
17 FORMAT(1X,/,10X,'T1=',F13.5,4X,'T2=',F13.5)
  TYPE '          A1          A3          X1          X2'
  DO 200 K=1,NCP
    A1=(Y(2,K)-Y(1,K))/(X(2)-X(1))
    A3=Y(1,K)-A1*X(1)
    WRITE BINARY(2) A1,A3,Y(1,K),Y(2,K),X(1)
    WRITE(13,20) K,A1,A3,Y(1,K),Y(2,K)
20 FORMAT(1X,13,2F13.5,2F12.4)
200 CONTINUE
330 WRITE BINARY(2) X(1),X(2)
  STOP
  END

```

PSLOPELIST - Displays the contents of a pslope file.

```

TYPE PSLOPELIST
  REAL A(20),B(20),Y(2,20),XX(20)
  INTEGER NCLK(20)
  CALL ASSG(1)
  READ BINARY(1) NUM,NCP,N,S,NP,(NCLK(J),J=1,NP),
1   (A(J),B(J),Y(1,J),Y(2,J),XX(J),J=1,NCP),T1,T2
  T1=T1+S
  T2=T2+S
  WRITE(10,5) NUM,(NCLK(J),J=1,NP)
5  FORMAT(1X,/, ' NUM POINTS/AVE=',I3,/, ' REF CLOCK=',10(12,','))
  WRITE(10,6) T1,T2
3  FORMAT(1X,/,16X,'T1=',F10.5,4X,'T2=',F10.5)
  TYPE '          A1          A3          X1          X2'
  WRITE(10,12) (J,A(J),B(J),Y(1,J),Y(2,J),J=1,NCP)
12  FORMAT(4(6(1X,I3,2F13.5,2F12.4,/,/)))
  STOP
  END
R

```

SIGMATAU - A graphics program that computes and displays  $\sigma(2;\tau)$  using a translated file as source.

```

TYPE SIGMATAU
  DCUOLE PRECISION AVE,SD
  INTEGER NCLK(20),FNAME(7)
  REAL BUF(20),LSIGMA(15),YF(20),YL(20)
  WRITE(10,1)
1  FORMAT(' FILE? ',Z)
  READ(11,2) FNAME(1)
2  FORMAT(S13)
  CALL FOPEN(1,FNAME)
  ACCEPT 'T,DT? (SEC): ',T,DT
  ACCEPT 'PHASE TST (TRY 23): ',ITST
  ITST=ITST**2
  ACCEPT 'CLOCK? ',I
  TYPE 'REF PAPER CLOCK:'
  CALL CLOCKS(NP,NCLK)
C  DRAW & LABEL AXIS
  CALL INITT(0)
  CALL MOVAB(110,110)
  CALL DRWAB(540,110)
  CALL MOVAB(110,110)
  CALL DRWAB(110,779)
  L=130
  DO 3 K=1,9
3  CALL TICX(L,110,15)
  L=L+50
  L=150
  DO 4 K=1,5
4  CALL TICY(110,L,20)
  L=L+150
  L=150
  DO 5 K=1,4
5  CALL TICY(110,L+45,10)
  CALL TICY(110,L+105,10)
  L=L+150

```

## SIGMATAU continued

```

        CALL MOVAB(110,80)
        CALL ANMOD
        WRITE(10,6)
6       FORMAT(1X,'204      816      3264  13056  52224',//16X,'T (SECONDS)')
        CALL MOVAB(2,135)
        LABY=-15
        L=135
        DO 8 K=1,5
            CALL ANMOD
            WRITE(10,7)
7           FORMAT(1X,'10*')
            CALL MOVAB(20,L+12)
            CALL ANMOD
            WRITE(10,233) LABY
233          FORMAT(1X,13)
            LABY=LABY+1
            L=L+150
8           CALL MOVAB(0,L)
            CALL MOVAB(1,750)
            CALL ANMOD
            WRITE(12,9) FNAME(1)
9           FORMAT(32X,'SIGMA(2;T), FILE: ',S13, '//,32X,
1           'TAU(SEC) N      SIGMA LOG SIG SD      DEL')
C COMPUTE
        INTER=1
        INUM=1
10          TAU=T*INTER
            TST=DT*INTER
            READ BINARY(1) NC,NCP,N,S,BFJD,EFJD,(YF(J),YL(J),J=1,NCP)
            N=0
            ND=0
            AVE=0.
            SD=0.
15          READ BINARY(1) S3,(BUF(J),J=1,NCP)
            CALL PAPLOCK(BUF,NP,NCLK,PBUF,S15)
            IF(BUF(1).LT.--7E6) GO TO 18
            T0=BUF(1)
            N=1,INTER
20          READ BINARY(1) S2,(BUF(J),J=1,NCP)
            CALL PAPLOCK(BUF,NP,NCLK,PBUF,S15)
            IF(BUF(1).LT.--7E6) GO TO 15
            T0=BUF(1)-PBUF
25          DO 30 KK=1,INTER
30          READ BINARY(1,END=45) S1,(BUF(J),J=1,NCP)
            T1=-1.E6
            CALL PAPLOCK(BUF,NP,NCLK,PBUF,S40)
            IF(SUF(1).LT.--3E6) GO TO 40
            T1=BUF(1)-PBUF
            DS=(S1-S2)*86400.
            DSS=(S2-S3)*86400.
            IF(AMIN(T1,T0,T3).LT.--3E6) GO TO 40
            IF(ABS(DSS-TAU).GT.TST) GO TO 40
            IF(ABS(DS-TAU).GT.TST) GO TO 40
            SIGMA=(T1-2.*T2+T3)**2
            IF(SIGMA.GT.ITST) GO TO 40
            SIGMA=SIGMA/(2.*DS*DS)
            AVE=AVE+SIGMA
            SD=SD+SIGMA**2
            N=N+1
            GO TO 41
40          ND=ND+1
41          T3=T2
            T2=T1
            S3=S2
            S2=S1
            GO TO 25

```

## SIGMA TAU continued

```

45     IF(N.LT.1) GO TO 99
        SIGMA=AVE/M
        SSD=0.
        IF(N.GT.1) SSD=(SD-AVE**2/N)/(N-1)
        SSD=SQRT(SSD/N)
        SIGMA=1.E-9*SQRT(SIGMA)
        SSD=1.E-18*SSD/(2.*SIGMA)
        LSIGMA(INUM)=ALOG10(SIGMA)
50     WRITE(10,50) TAU,N,SIGMA,LSIGMA(INUM),SSD,ND
        FORMAT(32X,F7.2,I5,E9.2,F7.2,E9.2,I3)
        IF(N.EQ.1) GO TO 99
        REMIND 1
        INUM=INUM+1
        INTER=INTER*2
        GO TO 10
C PLOT RESULTS
99     CALL SWIND(100,400,110,669)
        CALL VWIND(1.,8.,-15.27,4.46)
        LIM=MING(INUM-1,9)
        CALL PNTA(1.,LSIGMA(1))
        DO 110 K=2,LIM
            RK=K
110     CALL DRAWA(RK,LSIGMA(K))
        A1=LSIGMA(1)-2.4082
        A2=LSIGMA(1)-2.4082/2.
        CALL MOVEA(1.,LSIGMA(1))
        CALL DASHA(9.,A1,12)
        CALL MOVRE(3,-25)
        CALL ANCHO(84)
        CALL MOVRE(3,15)
        CALL ANMOD
        WRITE(10,115)
115     FORMAT(1X,'-1')
        CALL MOVEA(1.,LSIGMA(1))
        CALL DASHA(9.,A2,12)
        CALL MOVRE(3,-25)
        CALL ANCHO(84)
        CALL MOVRE(3,15)
        CALL ANMOD
        WRITE(10,116)
116     FORMAT(1X,'-1/2')
        CALL MOVAB(400,30)
        CALL ANMOD
        WRITE(10,120) 1,(NCLK(J),J=1,NP)
120     FORMAT(1X,'CLOCK',I3,' VS REF:',I3,7(' ',I2))
        CALL HENT(1)
        STOP
        END

```

PHASEPLOT - A graphics program that plots the phase of any clock with respect to any choice of reference clock.

```

TYPE PHASEPLOT
  INTEGER NCLK(20), FNAME(7)
  REAL BUF(20), YF(20), YL(20)
  CALL ASGG(1, FNAME)
  ACCEPT 'CLOCK? ', I
  TYPE 'REF PAPER CLOCK: '
  CALL CLOCKS(NP, NCLK)
  READ BINARY(1) NC, NCP, N, S, BFJD, EFJD, (YF(J), YL(J), J=1, NCP)
  ACCEPT 'XMIN, XMAX? ', X1, X2
  IF(X1.NE.0.) GO TO 10
  X1=BFJD-2.*(0023611)
  X2=EFJD+2.*(0023611)
  GO TO 11
10  X1=X1-S
  X2=X2-S
11  ACCEPT 'YMIN, YMAX? ', Y1, Y2
  IF(Y1.NE.0.) GO TO 12
  CALL PAPCLOCK(YF, NP, NCLK, YFF, $10)
  CALL PAPCLOCK(YL, NP, NCLK, YLL, $10)
  YFF=YF(1)-YFF
  YLL=YL(1)-YLL
  Y1=AMINI(YFF, YLL)
  D=ABS(YFF-YLL)
  Y1=Y1-.1*D
  Y2=Y1+1.2*D
12  CALL INITT(0)
C DRAW AXIS
  CALL SWIND(130, 870, 130, 649)
  CALL VWIND(S+X1, X2-X1, Y1, Y2-Y1)
  CALL AXIS(S+X1, S+X2, Y1, Y2)
  CALL MOVAB(0, 70)
  CALL ANMOD
30  WRITE(10, 33) FNAME(1), I, (NCLK(J), J=1, NP)
  FORMAT(1X, 'VERT SCALE=nanosec', 15X, ' FRACTIONAL DAYS'/27X,
  'PHASE PLOT, FILE: ', $13, '/27X, 'CLOCK', I3, ' VS PAPER REF ',
  I2, 7(' ', I2))
  1
  1
C PLOT
  CALL VWIND(X1, X2-X1, Y1, Y2-Y1)
  DO 50 J=1, N
  READ BINARY(1) FJD, (BUF(J), J=1, NCP)
  CALL PAPCLOCK(BUF, NP, NCLK, PBUF, $50)
  IF(BUF(1).EQ.-1.E6) GO TO 50
  Y=BUF(1)-PBUF
  CALL PNTA(FJD, Y)
50  CONTINUE
  CALL NEAT(1)
  STOP
END
R

```



SRESIDUALS - A graphics program the displays the residuals of phase data from a slope line.

```

TYPE SRESIDUALS
  INTEGER NCLK(20),MX(20),MY(20),FNAME(7),SNAME(7)
  REAL BUF(20),A1(20),A3(20),FR(20),SSXY(20),RN(20),YF(20),YL(20)
  CALL ASSG(1,FNAME)
  TYPE 'SLOPE FILE:'
  CALL ASSG(2,SNAME)
  ACCEPT 'CLOCK?' ,I
  ACCEPT 'RANGE(NS)?' ,R
  READ BINARY(2) NC,NCP,N,S,NP,(NCLK(J),J=1,NP),
1    (A1(J),A3(J),FR(J),SSXY(J),RN(J),J=1,NCP)
  READ BINARY(1) NC,NCP,N,S,EFJD,EFJD,(YF(J),YL(J),J=1,NCP)
  ACCEPT 'START,STOP FJD?' ,XMIN,XMAX
  IF(XMIN.NE.0.) GO TO 10
  XMIN=EFJD-5.*(0023611)
  XMAX=EFJD+5.*(0023611)
  GO TO 12
10  XMIN=XMIN-S
    XMAX=XMAX-S
C DRAW AXIS
12  CALL INITT(0)
    CALL SWIND(130,870,175,575)
    SXMIN=S+XMIN
    CALL VWINDO(SXMIN,XMAX-XMIN,-R,R+R)
    CALL AXIS(SXMIN,S+XMAX,-R,R)
    CALL VWINDO(XMIN,XMAX-XMIN,-R,2*R)
    CALL MOVEA(XMIN,0.)
    CALL DASHA(XMAX,0.,12)
C PLOT
30  READ BINARY(1,END=50) FJD,(BUF(J),J=1,NCP)
    IF(BUF(1).EQ.-1.E6) GO TO 38
    CALL PAPCLOCK(BUF,NP,NCLK,PEUF,538)
    Y=BUF(1)-PEUF-A1(1)*FJD-AC(1)
    CALL PNTA(FJD,Y)
    GO TO 40
38  CALL TIC(FJD,20)
40  CONTINUE
    GO TO 30
C WRITE LEGEND
50  CALL MOVAB(0,100)
    CALL ANMOD
    WRITE(10,60) FNAME(1),SNAME(1),I,(NCLK(J),J=1,NP)
60  FORMAT(1X,'VERT SCALE=NANOSEC',15X,'FRACTIONAL DAYS',/,
1    15X,'RESIDUALS, FILE:',S13,'SLOPE FILE:',S13,/,15X,'CLOCK #',
1    13,' VS PAPER REF ',7(12,','))
    CALL NEAT(1)
  STOP
  END
R

```

SHIFTV - A version of several shift programs that generate the  $\Delta x_{fi}$ .

This version allows variable endpoints.

```

TYPE SHIFTV
  REAL T(4,20),TAU(4,20),DTAU(20),DSLOPE(20),SD(20)
  REAL BUF(20),YF1(20),YF2(20),YL1(20),YL2(20)
  INTEGER N(4,20),NCLK(10),FNAME(7),GNAME(7)
  TYPE ' '
  CALL ASGG(1,FNAME)
  CALL ASGG(2,GNAME)
  READ BINARY(1) NC,NCP,N1,S1,BFJD1,EFJD1,(YF1(J),YL1(J),J=1,NCP)
  READ BINARY(2) NC,NCP,N2,S2,BFJD2,EFJD2,(YF2(J),YL2(J),J=1,NCP)
  DO 3 I=1,4
  DO 3 J=1,NCP
    T(I,J)=0.
    TAU(I,J)=0.
3    N(I,J)=0
  ACCEPT 'REF CLOCK? (#,LIST): ', NP,(NCLK(J),J=1,NP)
  ACCEPT '# POINTS IN AVERAGE (UNDER 10): ',KP
  ACCEPT 'T1,T2; T3,T4: ', T1,T2,T3,T4
  TT2=T2
  TT4=T4
  IF(T1.EQ.0.) T1=S1+BFJD1
  IF(T2.EQ.0.) T2=S1+EFJD1
  IF(T3.EQ.0.) T3=S2+BFJD2
  IF(T4.EQ.0.) T4=S2+EFJD2
  TST1=T1-S1-.0009
  TST2=T2-S1-.0009
  TST3=T3-S2-.0009
  TST4=T4-S2-.0009
  TI=(T2-T1)*24.
  TM=(T3-T2)*24.
  TF=(T4-T3)*24.
4  WRITE(10,4) T1,T3,T1,T2,T4,TM,TF
  FORMAT(3X,'T1=',F7.3,4X,'T3=',F7.3,8X,'(T2-T1)=',F6.2,' HRS',
1  /,3X,'T2=',F7.3,4X,'T4=',F7.3,8X,'(T3-T2)=',F6.2,' HRS',
1  /,35X,'(T4-T3)=',F6.2,' HRS')
  ICT=0
5  READ BINARY(1,END=12) FJD,(BUF(J),J=1,NCP)
  ICT=ICT+1
  IF(FJD.LT.TST1) GO TO 5
  DO 10 I=1,NCP
    IF(N(I,1).GE.KP) GO TO 8
    IF(BUF(I).LT.-.9E6) GO TO 8
7    T(I,1)=T(I,1)+FJD
    TAU(I,1)=TAU(I,1)+BUF(I)
    N(I,1)=N(I,1)+1
8    IF((TT2.NE.0.).AND.(FJD.LT.TST2)) GO TO 10
    IF((TT2.EQ.0.).AND.(ICT.LT.(N1+1-KP))) GO TO 10
    IF(N(2,1).GE.KP) GO TO 13
    IF(BUF(I).LT.-.9E6) GO TO 10
9    T(2,1)=T(2,1)+FJD
    TAU(2,1)=TAU(2,1)+BUF(I)
    N(2,1)=N(2,1)+1
10   CONTINUE
  GO TO 5
12   DO 15 I=1,2
  DO 15 J=1,NCP
    T(I,J)=T(I,J)/N(I,J)
15   TAU(I,J)=TAU(I,J)/N(I,J)
  DS=S2-S1
  ICT=0
17  READ BINARY(2,END=20) FJD,(BUF(J),J=1,NCP)
  ICT=ICT+1
  IF(FJD.LT.TST3) GO TO 17
  DO 20 I=1,NCP
    IF(N(3,I).GE.KP) GO TO 18
    IF(BUF(I).LT.-.9E6) GO TO 18

```

## SHIFTV continued

```

16      T(3,1)=T(3,1)+FJD+DS
        TAU(3,1)=TAU(3,1)+BUF(1)
        N(3,1)=N(3,1)+1
18      IF((TT4.NE.3.).AND.(FJD.LT.TST4)) GO TO 23
        IF((TT4.EQ.3.).AND.(ICT.LT.(N2+1-KP))) GO TO 20
        IF(N(4,1).GE.NP) GO TO 23
        IF(BUF(1).LT.-.9E6) GO TO 20
19      T(4,1)=T(4,1)+FJD+DS
        TAU(4,1)=TAU(4,1)+BUF(1)
        N(4,1)=N(4,1)+1
23      CONTINUE
        GO TO 17
22      DO 25 I=3,4
        DO 25 J=1,NCP
25      T(I,J)=T(I,J)/N(I,J)
        TAU(I,J)=TAU(I,J)/N(I,J)
        DO 43 I=1,NCP
        SL2=(TAU(4,I)-TAU(3,I))/(T(4,I)-T(3,I))
        SL1=(TAU(2,I)-TAU(1,I))/(T(2,I)-T(1,I))
        DSLOPE(I)=SL2-SL1
        ETA=(T(3,I)-T(2,I))/(T(4,I)-T(1,I))
        DTAU(I)=(TAU(3,I)-TAU(2,I)-ETA*(TAU(4,I)-TAU(1,I)))/(1.-ETA)
43      SD(I)=4.22E-3*SQRT((T(3,I)-T(2,I))*26422./ (1.-ETA))
        DO 50 I=1,NCP
        DTAU(I)=DTAU(I)-100.*IFIX(DTAU(I)/100.+0.5)
        IF(I.EQ.13) DTAU(13)=(DTAU(1)+DTAU(2)+DTAU(3))/3.
        IF(I.EQ.14) DTAU(14)=(DTAU(7)+DTAU(8)+DTAU(9))/3.
50      CONTINUE
        IF(NP.EQ.3) GO TO 59
        SLP=3.
        TAU1=3.
        DO 54 K=1,NP
        KK=NCLK(K)
        SLP=SLP+DSLOPE(KK)
54      TAU1=TAU1+DTAU(KK)
        SLP=SLP/NP
        TAU1=TAU1/NP
        DO 56 I=1,NCP
        DSLOPE(I)=DSLOPE(I)-SLP
56      DTAU(I)=DTAU(I)-TAU1
59      WRITE(13,60) (J,DTAU(J),SD(J),DSLOPE(J),(N(I,J),I=1,4),J=1,NCP)
60      FORMAT(1X,/, ' CLOCK',3X, 'SHIFT(NSEC)',3X, 'S.D.',5X, 'DSLOPE',3X,
1      'N1,N2 N3,N4',4(6/,14,F13.3,F13.3,F13.2,9X),2(12,',',12,2X)),/)
70      TYPE ' '
        WRITE(13,72) FNAME(1),GNAME(1),KP
72      FORMAT(1X, 'PAGE 2 OF SHIFT: ',S13,',',S13,',',S13,',',S12,' PTS')
        TYPE ' DELTA TAU CALCULATIONS'
        ACCEPT 'MAKE WHICH CLOCK ZERO? ',NZ
        ACCEPT 'BASE CLOCK SET (#,LIST): ',L,(NCLK(J),J=1,L)
        IF(L.EQ.0) GO TO 100
        SX=3.
        SXX=2.
        DO 75 I=1,L
        K=NCLK(I)
        IF(K.EQ.NZ) GO TO 75
        SX=SX+DTAU(K)
        SXX=SXX+DTAU(K)*DTAU(K)
75      CONTINUE

```

## SHIFTV continued

```

      RN=L
      RRM=SX/RN
      RSD=SQRT((SXX-SX*SX/RN)/(RN-1.))
      RSDM=RSD/SQRT(RN)
      WRITE(10,77) RRM,RSD,RSDM
77    FORMAT(5X,'DTAU= ',F7.3,5X,'S.D.= ',F6.3,3X,'S.D.M.= ',F6.3,/)
80    ACCEPT 'CLOCKS (#,LIST): ',L,(NCLK(J),J=1,L)
      IF(L.EQ.0) GO TO 100
      SX=0.
      SXX=0.
      DO 85 I=1,L
        K=NCLK(I)
        IF(K.EQ.NZ) GO TO 85
        SX=SX+DTAU(K)
        SXX=SXX+DTAU(K)*DTAU(K)
85    CONTINUE
      RN=L
      RM=SX/RN
      CSD=SQRT((SXX-SX*SX/RN)/(RN-1.))
      SDM=CSD/SQRT(RN)
      A=RM-RRM
      B=SQRT(RSDM*RSDM+SDM*SDM)
      WRITE(10,87) A,B
87    FORMAT(5X,'DELTA TAU= ',F7.3,3X,'S.D.M.= ',F6.3,/)
      GO TO 80
100   STOP
      END
R

```

SHIFTM - A version of SHIFT that adjusts for two rate changes during flight.

```

TYPE SHIFTM
  REAL A1(20),B1(20),Y1(20),Y2(20),XX(20)
  REAL A2(20),B2(20),Y3(20),Y4(20),Y1(20),Y2(20)
  REAL DYY(20),TDT(20)
  INTEGER NCLK1(20),NCLK2(20),NCLKA(20),NCLKB(20)
  TYPE 'AIR MIDDLE FILE:'
  CALL ASS(1)
  READ BINARY(1) NUN1,NCP1,N1,S,NP1,(NCLK1(J),J=1,NP1),
1    (A1(J),B1(J),Y1(J),Y2(J),XX(J),J=1,NCP1),T1,T2
  ACCEPT 'AIR REF (#,LIST): ',NPA,(NCLKA(J),J=1,NPA)
  ACCEPT 'CLOCK? ',ICLK
  CALL PAPCLOCK(Y1,NPA,NCLKA,PEUF,S100)
  Y1(ICLK)=Y1(ICLK)-PEUF
  CALL PAPCLOCK(Y2,NPA,NCLKA,PEUF,S100)
  Y2(ICLK)=Y2(ICLK)-PEUF
  DY=Y2(ICLK)-Y1(ICLK)
  TT1=T1+S
  TT2=T2+S
  WRITE(10,5) NUN1,TT1,TT2,DY
  FORMAT(1X,/,10,'PT AVE: T1=',F8.4,' T2=',F8.4,/,
1    ' PHASE DIFF=',F7.3,' NS',/)
  TYPE 'GND PRE FILE:'
  CALL ASS(2)
  READ BINARY(2) NUN2,NCP2,N1,S2,NP2,(NCLK2(J),J=1,NP2),
1    (A1(J),B1(J),Y1(J),Y2(J),XX(J),J=1,NCP2),TT1,TT2
  TYPE 'GND POST FILE:'
  CALL ASS(3)
  READ BINARY(3) NUN3,NCP3,N2,S3,NP3,(NCLK3(J),J=1,NP3),
1    (A2(J),B2(J),Y3(J),Y4(J),XX(J),J=1,NCP3),TT3,TT4
  ACCEPT 'GND REF (#,LIST): ',NPA,(NCLK3(J),J=1,NPA)

```

## SHIFTM continued

```

DO 20 I=1,NCP1
  YT1(I)=A1(I)*(T1+S-S1)+B1(I)
  YT2(I)=A2(I)*(T2+S-S2)+B2(I)
DO 25 I=1,NRG
  K=NCLKG(I)
  DELTA=100.*IFIX((YT2(K)-(YT1(K)+A1(K)*(T2-T1)))/100.+5)
  YT2(K)=YT2(K)+DELTA
CALL PAPCLOCK(A1,NRG,NCLKG,SG1,5100)
CALL PAPCLOCK(A2,NRG,NCLKG,SG2,5100)
CALL PAPCLOCK(A1,NEA,NCLKA,SA1,5100)
CALL PAPCLOCK(A2,NEA,NCLKA,SA2,5100)
SLP1=SA1-SG1
SLP2=SA2-SG2
DCLP=SLP2-SLP1
DYP=((SLP1+SLP2)/2.)*(T2-T1)
DYT=DY+DYP
DO 40 I=1,NRG
  K=NCLKG(I)
  DYY(K)=DY+((SA1-A1(K)+SA2-A2(K))/2.)*(T2-T1)
  DIFF=YT2(ICLK)-YT2(K)-YT1(ICLK)+YT1(K)
  TSFT(K)=DIFF-DYY(K)
  TSFT(K)=TSFT(K)-100.*IFIX(TSFT(K)/100.+5)
  IF(TSFT(K).LT.-10.) TSFT(K)=TSFT(K)+100.
CONTINUE
CALL PAPCLOCK(TSFT,NRG,NCLKG,SHIFT,5100)
WRITE(13,50) SLP1,DCLP,DYYT
FORMAT(1X,/, 'SLOPE OF AIR REF WRT GND REF:',F8.3,
  ' (DELTA=',F7.3,')',/, 'CORRECTED PHASE DIFF=',F7.3,/,)
TYPE 'SHIFTS:'
DO 60 I=1,NRG
  K=NCLKG(I)
  WRITE(13,55) K,TSFT(K)
FORMAT(1X,12,F10.3)
CONTINUE
WRITE(13,70) SHIFT
FORMAT('MEAN SHIFT=',F8.3)
STOP
END
R

```

The integration program that computes the predicted result is as follows:

```

P 34
REAL P(3)
INTEGER H,IX(3),IU(3)
DOUBLE PRECISION Q0,GBB40G/A*2.02573D7/C*9.835712D3/
DOUBLE PRECISION U,T,DSQRT(RO-12.),J2*1.08364D-3/
DOUBLE PRECISION W*1.40769D16/R*2.089897D7/
DOUBLE PRECISION CU,CG,UG,UG,FP,GP,DU,DUU,DU1,DUU1
DOUBLE PRECISION T(3),T1,T2,DT
DEFINE Q(R,Q)=(CU/R)*1D0-J2*.5D0*(3D0*DSIN(Q)**2-1D0)*(A/R)**2)
NL=-1
T2=-1
DO 4 I=1,3
4   T(I)=0
   CU=-GM/C**2
   RG=DSQRT(RO-12.)**2+2993.**2+9350.**2)
   QG=Q0+DATAN(-9350./RO-12.)
   UG=J(RG,CG)
   UUG=(U*RG*DCOS(CG))**2/(2.*C**2)
5   WRITE(6,6)
6   FORMAT(' NEXT FILE ')
7   READ(5,7) N
   FORMAT()
   IF(N.EQ.0) GO TO E0
10  READ(N,11,END=5,ERR=10) N1,H,M,SEC,IX,IU
11  FORMAT(I8,1X,2I2,F6.3,3I8,27X,3I6)
   T1=T2
   T2=60*(60*H+M)+SEC
   RP=DSQRT((RO+IX(3))**2-IX(1)**2+IX(2)**2)
   QP=Q0+DATAN(IX(2)/(RO+IX(3)))
   DU=U(RP,QP)-UG
   DUU=((IU(1)+U*RP*DCOS(QP))**2+IU(2)**2+IU(3)**2)/(2.*C**2)-UUG
   IF(T1.LT.0) GO TO 15
   IF(T2+12*60*60.LT.T1) T2=T2+24*60*60
   DT=T2-T1

   P(1)=T(1)+.5D0*(DU+DU1)*DT
   T(2)=T(2)+.5D0*(DUU-DUU1)*DT
   T(3)=T(1)-T(2)
15  DU1=DU
   DUU1=DUU
   IF(M.EQ.NL) GO TO 10
   NL=M
   DO 16 I=1,3
16  P(I)=1D9*T(I)
   WRITE(9,18) H,M,IX,IU,P
18  FORMAT(1X,2I2,2X,3I7,2X,3I6,2X,3F7.3)
   WRITE(6,17) H,M,IX,IU,P
17  FORMAT(1X,I2,1X,J2,2X,3I7,2X,3I6,2X,3F7.3)
   GO TO 10
20  DO 22 I=1,3
22  P(I)=1D9*T(I)
   WRITE(6,17) H,M,IX,IU,P
   END
EOF AT LINE 51
x

```

## BIBLIOGRAPHY

1. A. Einstein, Jarb. Radioakt., 4, p. 411 (1908)
2. For a review of early work (including references 3-6 below) see Theory of Relativity by W. Pauli, p. 153 (1958)
3. K. Schwarzschild, S. B. preuss. Akad. Wiss., p. 120 (1914)
4. C. E. St. John, Astroph. J., 46, p. 249 (1917)
5. J. Evershed and Royds, Bull. Kodaikanal Obs., 39
6. L. Grebe, Phys. Z., 21, p. 662 (1920)
7. W. S. Adams, Proc. Natl. Acad. Sci., 11, p. 382 (1925)
8. D. M. Popper, Astrophys. J., 120, p. 316 (1954)
9. J. Brault, Bull. Am. Phys. Soc., 8, p. 28 (1963)
10. R. V. Pound and G. A. Rebka, Phys. Rev. Lett., 4, p. 337 (1960)
11. R. V. Pound and J. L. Snider, Phys. Rev. Lett., 13, p. 539 (1964)
12. R. V. Pound and J. L. Snider, Phys. Rev. B, 140, p. 788 (1965)
13. More recent red-shift experiments are:
  - F. Roddier, Ann. Astrophys., 23, p. 463 (1965)
  - J. L. Snider, Phys. Rev. Lett., 28, p. 853 (1972)
14. This argument is attributed to A. Schild. For a discussion see Gravitation by Misner, Thorne, and Wheeler, p. 187.
15. S. F. Singer, Phys. Rev., 104, (1956)
16. B. Hoffman, Phys. Rev., 106, p. 358 (1957)
17. S. Refsdal, Phys. Rev., 127, p. 977 (1962)
18. W. J. Cocke, Phys. Rev. Lett., 16, p. 662 (1966)
19. J. C. Hafele and R. E. Keating, Science, 177, p. 166 (1972)
20. R. Reisse, Thesis, Dept. of Physics and Astronomy, University of Maryland (1976)
21. A. O. McCoubrey, Proc. IEEE, 54, p. 116 (1966)

22. I. I. Rabi, J. R. Zacharias, S. Millman, and P. Kush, Phys. Rev., 53, p. 318 (1938)
23. J. G. King and J. R. Zacharias, Advances in Electronics VIII, L. Marten, Ed., New York: Academic (1958)
24. N. Ramsey, Molecular Beams, New York: Oxford, p. 124 (1956)
25. R. C. Mockler, Advances in Electronics and Electronic Physics, vol. 15, No. 1, L. Marton, Ed., New York: Academic (1961)
26. R. E. Beehler, R. C. Mockler, and J. M. Richardson, Metrol., 1, p. 114 (1965)
27. L. Essen and J. Parry, Phil. Trans. Roy. Soc. London, 250, p. 45 (1957)
28. J. H. Holloway and R. F. Lacey, 1964 Proc. Internat'l Conf. on Chronometry, Lausanne, p. 317 (1964)
29. R. H. Dicke, Phys. Rev., 89, p. 472 (1953)
30. M. E. Packard and B. E. Swartz, IRE Trans. on Instrumentation, I-11, p. 215 (1962)
31. H. M. Goldenberg, D. Kleppner, and N. F. Ramsey, Phys. Rev. Lett., 5, p. 361 (1960)
32. D. Kleppner, H. C. Berg, S. B. Crampton, N. F. Ramsey, R. F. C. Vessot, H. E. Peters, and J. Vanier, Phys. Rev., 138, p. A972 (1965)
33. D. Kleppner, H. M. Goldenberg, and N. F. Ramsey, Phys. Rev., 126, p. 603 (1962)
34. R. F. C. Vessot and H. E. Peters, IRE Trans. on Instrumentation, I-11 p. 183 (1962)
35. C. Steggerda, A Precision Event Timer for Lunar Ranging, Tech. Report #74-038, Dept. of Physics, Univ. of Maryland (1973)
36. C. W. Allen, Astrophysical Quantities, The Athlone Press, p. 112 (1973)
37. B. Hoffman, Phys. Rev. Lett., 16 p. 779 (1966)  
This is an errata to reference 16.
38. L. S. Cutler and C. L. Searle, Proc. IEEE, 54, p. 136 (1966)
39. D. W. Allan, Proc. IEEE, 54, p. 221 (1966)
40. J. A. Barnes, et al., IEEE Trans. Instrum. Meas. IM-20, p. 105 (1971)
41. P. Lesage and C. Augoin, IEEE Trans. Instrum. Meas., IM-22, p. 157 (1973)



42. L. S. Cutler, private communication.

43. H. Arzelies, Relativite Generalisee Gravitation (1961)